FLUID DISTURBED K-Ar MINERAL AGES FROM THE DALRADIAN ROCKS OF CONNEMARA, WESTERN IRELAND

by

WILLIAM MACAULEY MILLER

This thesis is submitted for the degree of Doctor of Philosophy.

The University of Glasgow.

June 1990.

ProQuest LLC.
789 East Eisenhower Parkway
P.O. Box 1346
Ann Arbor, MI 48106 – 1346

ACKNOWLEDGEMENTS

Firstly, I wish to give my thanks to my two supervisors, Professor Bernard Leake and Doctor Mitch Macintyre, for giving me the opportunity to undertake this study. They both gave much needed direction and encouragement that did much to bring this research to fruition. I also wish to give my heartfelt thanks to Bernard for introducing me to Connemara, where both the people and the place now mean much to me.

I particularly wish to thank two other people who helped me considerably; Doctor Tony Fallick who, by taking such an interest in my research, helped me to see many of the complexities of the problem with which I was faced, and Professor Tullis Onstott of Princeton University for giving me the chance to work with him and for showing me some of the fine art of ^{40}Ar-^{39}Ar dating. I also thank him for being such a great host on my visit to Princeton.

I wish to express my gratitude to several people for allowing me time on various analytical systems; Professor Chapman of Glasgow University for use of the TEM, Doctor Richard Hinton of Edinburgh University for use of the ion-probe and Doctor Peter Hill also of Edinburgh University for use of the electron-probe.

I acknowledge receipt of an NERC research studentship during the course of my study.

CONTENTS

CHAPTER TWO:
SAMPLING PROCEDURES, PETROGRAPHIC AND GEOCHEMICAL SAMPLE CHARACTERISATION.

CHAPTER THREE:
POTASSIUM-ARGON, ^{40}Ar-^{39}Ar INCREMENTAL STEP-HEATING AND ^{40}Ar-^{39}Ar TOTAL FUSION LASER-PROBE DATING METHODS: RESULTS AND CONCLUSIONS.

CHAPTER FOUR:
HYDROGEN AND OXYGEN STABLE ISOTOPIC RESULTS:
IMPLICATIONS FOR RESETTING OF K-Ar SYSTEMS.

CHAPTER FIVE:
DISCUSSION AND GEOLOGICAL SYNTHESIS, FURTHER RESEARCH AND IMPLICATIONS FOR OTHER GEOCHRONOLOGICAL STUDIES

APPENDICES

FIGURES

ABSTRACT

This thesis is concerned with explaining the cause of a wide range (about 100 Ma) of K-Ar mineral ages in the Connemara Schists, western Ireland. This range was first reported by Elias (1985) and Elias *et al.* (1988) who determined a total of over sixty biotite, muscovite and hornblende K-Ar ages. These authors concluded that the ages were the result of differential uplift and cooling of three, independent 'blocks' within Connemara. Examination of the age data of Elias (1985) and Elias *et al.* (1988) reveals, however, that at best this can only be a partial explanation because some regions within Connemara record mica K-Ar ages significantly older than amphibole K-Ar ages. This is the opposite to the order predicted from commonly accepted closure temperature estimates (Harrison 1981, Harrison *et al.* 1985) and the opposite to the order recorded in many other metamorphic terranes. It was apparent, therefore, that some process other than simple cooling of the rocks was responsible for, at least, some of the K-Ar mineral ages.

Fourteen biotite, twenty muscovite and thirty hornblende K-Ar mineral ages determined during the course of this study exhibited an age range indistinguishable from that of Elias (1985) and Elias *et al.* (1988). Hydrogen isotopic ratios measured on seven biotites and six muscovites showed slight variation and averaged around -66 and -41‰, respectively. Hydrogen isotopic ratios measured on hornblendes showed a larger variation that ranged from -51.5 to -75.1‰. The variation in the hydrogen isotopic ratios from the micas and the hornblendes is attributed to variable, incomplete, exchange between the minerals and a fluid at temperatures about 300 to 350°C. Oxygen isotopic ratios were measured on thirteen of the hornblendes. These showed some variation, from +5.5 to +11‰, which reflects primary compositional variations in the

hornblendes and not partial exchange with the fluid that caused the variation in hydrogen isotopic ratios.

The spread in the K-Ar mineral ages is shown to be neither geographically correlated nor the result of diachronous, slow cooling of the rocks. There is a weak correlation between the hornblende K-Ar age and the Fe/(Fe+Mg) ratio that may indicate some compositional control over the Ar closure temperature. The range of K-Ar mineral ages is shown to be the result of variable, partial resetting of individual K-Ar 'clocks' that had all previously been totally rejuvenated by the intrusion, at 490±1 Ma (Jagger *et al.* 1988), of a large (>80 km x >20 km) metagabbro-gneiss complex. The subsequent, variable and partial resetting occurred at c. 400 Ma and was induced by the intrusion of a suite of Lower Devonian Granites into the Connemara rocks. The resetting was not simply a thermal event as witnessed by the lack of any spatial correlation between sample location and K-Ar mineral age. Instead, the variable and partial resetting was brought about by interaction of the minerals with the fluid identified from the hydrogen isotopic ratio measurements. This fluid was circulating in a hydrothermal system around the granites.

Different mineral species interacted with this fluid in different ways. Muscovite lost Ar where it was in contact with the fluid with a temperature in excess of the muscovite Ar closure temperature, about 350°C, long enough for Ar diffusion to occur. Biotite was reset in a similar way, except that Ar loss would have been enhanced by chloritisation of the biotite. For both micas, a correlation exists between the K-Ar ages and the extent of alteration of the rock indicated by the degree of sericitisation of the plagioclase. Oldest K-Ar mica ages were yielded by samples with little or no visible alteration of the feldspar.

Argon loss from hornblendes was more complicated and was primarily governed by the extent of heterogeneity in the crystal microstructure. TEM investigation revealed that sub-micron scale exsolution and phyllosilicate growth along cleavages existed in some samples. Similiar features have been shown to cause a reduction in the Ar closure temperature of hornblende to about that of biotite (Harrison & Fitz Gerald 1986). Direct evidence of a linkage between Ar loss from hornblendes and interaction with the fluid comes from a correlation between the hornblende K-Ar ages and hydrogen stable isotopic ratios. It is suggested that sometimes Ar loss in hornblende is coupled directly with stable isotopic exchange. In such situations a hornblende could have two Ar closure temperatures; one 'wet', in the presence of a fluid, and one 'dry', in the absence of a fluid.

It is possible to identify samples which yield ages which were not reset and which are consequently, geologically significant as closure ages following emplacement of the metagabbro-gneiss complex. These ages indicate that initially there was rapid cooling, c. 30°C/Ma, immediately subsequent to the intrusion. There was then a hiatus in the uplift history. A second period of slower uplift and cooling started at c. 460 Ma and was related to the ramping of Connemara over an Ordovician terrane, the Delaney Dome Formation, along the Mannin Thrust. This uplift ceased, and all minerals had closed to Ar loss, by the time of last movement along this thrust, 447±4 Ma (Tanner *et al.* 1989). The resetting or partial resetting of the K-Ar mineral ages occurred at c. 400 Ma when the Lower Devonian Granites were intruded and the Connemara Dalradian rocks were buried under a considerable thickness of Silurian sediments (Elias *et al.* 1988).

CHAPTER ONE:

INTRODUCTION TO PROJECT, PREVIOUS GEOLOGICAL AND GEOCHRONOLOGICAL STUDIES IN CONNEMARA AND REVIEW OF RADIOMETRIC AND STABLE ISOTOPE PRINCIPLES.

1.1 Project rationale.

Much is known about the geology of the Connemara Dalradian rocks. It is accepted that they have endured a somewhat different and perhaps more complex deformational history and have reached higher metamorphic grades than most of the Dalradian rocks elsewhere (Leake *et al.* 1983). This is partly because the Connemara Dalradian massif became detached and moved away from the main strike continuation of the Dalradian Supergroup (Leake *et al.* 1983, Hutton & Dewey 1986). Consequently, the conclusions drawn from geochronological studies of the Dalradian rocks of Scotland and Donegal cannot simply be extrapolated to Connemara. The present day metamorphic isograds in Connemara are predominantly due to the intrusion of a large metagabbro-gneiss complex at 490±1 Ma. This intrusion caused intensive heating of the Dalradian rocks and local migmatisation. Geobarometry has shown that metamorphic pressures dropped significantly from 7 kbar to 3 kbar during and soon after intrusion, most probably as a result of uplift and cooling.

It might be expected that following such strong heating and subsequent rapid cooling of the Connemara Schists their K-Ar ages would reflect this and record ages similar to the age of the intrusion. Previous geochronological studies have shown this is far from the case. As highlighted by the two most recent studies (Elias *et al.* 1988, Jagger *et al.*

1988), the K-Ar ages from the Connemara Schists show a range of almost 100 Ma from the zircon Pb-Pb age of the metagabbro-gneiss complex and show no geographical trend or correlation with known geological features. Furthermore, in some localities micas record older ages than hornblende, a feature not expected from closure temperature theory. Elias *et al.* (1988) suggested that the K-Ar ages were tectonically controlled, linked to the major slide zones, and that differential uplift was responsible.

A study of the hydrogen and oxygen isotope systematics of both the metagabbro-gneiss complex rocks and the Connemara Schists by Jenkin (1988) found that the ubiquitous secondary minerals in all the Connemara rocks had formed in the presence of a high δD and low $\delta^{18}O$ fluid. This fluid was supposed to have been at temperatures of about 300°C and to have persisted in the region for some time. It is inferred that this fluid was of meteoric origin and the infiltration event was the result of thermal convection connected with the intrusion of the Galway Granite and its satellite plutons at about 400 Ma.

The need for further geochronological research grew out of the questions posed by the results of Elias (1985) and Jenkin (1988). Particular questions that needed to be addressed were:

1) What role did the slide zones and other major tectonic features have in differential uplift and what was the likely affect on the K-Ar ages? It can be imagined that if uplift of adjacent blocks through the relevant closure temperature isotherms were diachronous, then the K-Ar ages either side of the fault or slide zone could be significantly different and a sharp change in K-Ar ages across the fault or slide should occur.

2) Assuming differential uplift did occur, how many possible 'blocks' were there uplifting in Connemara, and at what rates and at what times? If sharp changes in the K-Ar ages do occur when crossing the major fault zones it should be possible to determine which faults are important in this respect and to constrain the time of movement along them by dating samples collected from traverses across these faults.

3) Is the apparent inverse discordance in the mica and amphibole ages real, and if so what is its cause? From the data of Elias (1985) it appears that a large region in the north west of Connemara shows inverse discordance in the average K-Ar ages for amphibole and mica. This might be purely statistical. In order to test for this, amphibole and micas need to be dated from samples from the same location.

4) What other factors, not previously considered could have had a significant control over the ages? Jenkin (1988) showed that warm fluid infiltration occurred over the whole region. It is known that one way in which K-Ar ages can be disturbed is by releasing Ar from, or introducing Ar to, minerals by way of fluids. This can occur at low temperatures if chemical reaction occurs.

5) What are the implications from geochronological research in Connemara to similar projects elsewhere? This depends on whether the conditions affecting the K-Ar systems in the Connemara rocks are geologically common or are unique in some way to this region. In the former case it would be necessary to consider extrapolating conclusions reached in Connemara to other areas.

In the following pages these questions have been addressed and in some cases answered. Although this study is similar in several respects to that of Elias (1985) the conclusions reached are significantly different.

1.2 The geology of Connemara.

1.2.1 Tectonic position.

Since the work of Kilburn *et al.* (1965) it has been recognised that the Dalradian rocks of Connemara occupy an anomalous position to the south of the strike continuation of the main Dalradian Supergroup (Leake *et al.* 1983). The Connemara rocks are separated from the nearest other Dalradian rocks of northern Mayo and Donegal by the South Mayo Trough, figure 1.1. To the south the contact between the schists and the lower Ordovician South Connemara Group is obscured by the Galway Granite and Galway Bay.

Both the Connemara massif and the South Mayo Trough are thought to occupy a position in the strike continuation of the Midland Valley of Scotland. Magnetic mapping (Max & Inamadar 1983) reveals two linear features which are considered to be extensions of the Southern Uplands Fault (SUF) and the Highland Boundary Fault (HBF). The HBF is generally thought to correlate with the Fair Head-Clew Bay line on the north side of Clew Bay (Max & Riddihough 1975; Max & Inamadar 1983). An alternative proposal extends the HBF along the south side of Clew Bay (Bailey & Holtedahl 1938). The SUF is thought to correlate either with the Skird Rocks Fault (Leake 1963; Max & Ryan 1975) which separates the Connemara metagabbro-gneiss complex from the South Connemara Group (to the south). An alternative suggestion projects the SUF across Co. Clare to a point SE of Galway City (Phillips *et al.* 1983). Regardless of which interpretation is correct the Connemara massif lies wholly within the Midland Valley extension. This is significant as the Connemara Dalradian rocks are the only undoubted substantial outcrop of Dalradian rocks to lie south of the HBF. In Tyrone there is a small exposure of high grade rocks that may relate to the Dalradian. These may be a continuation

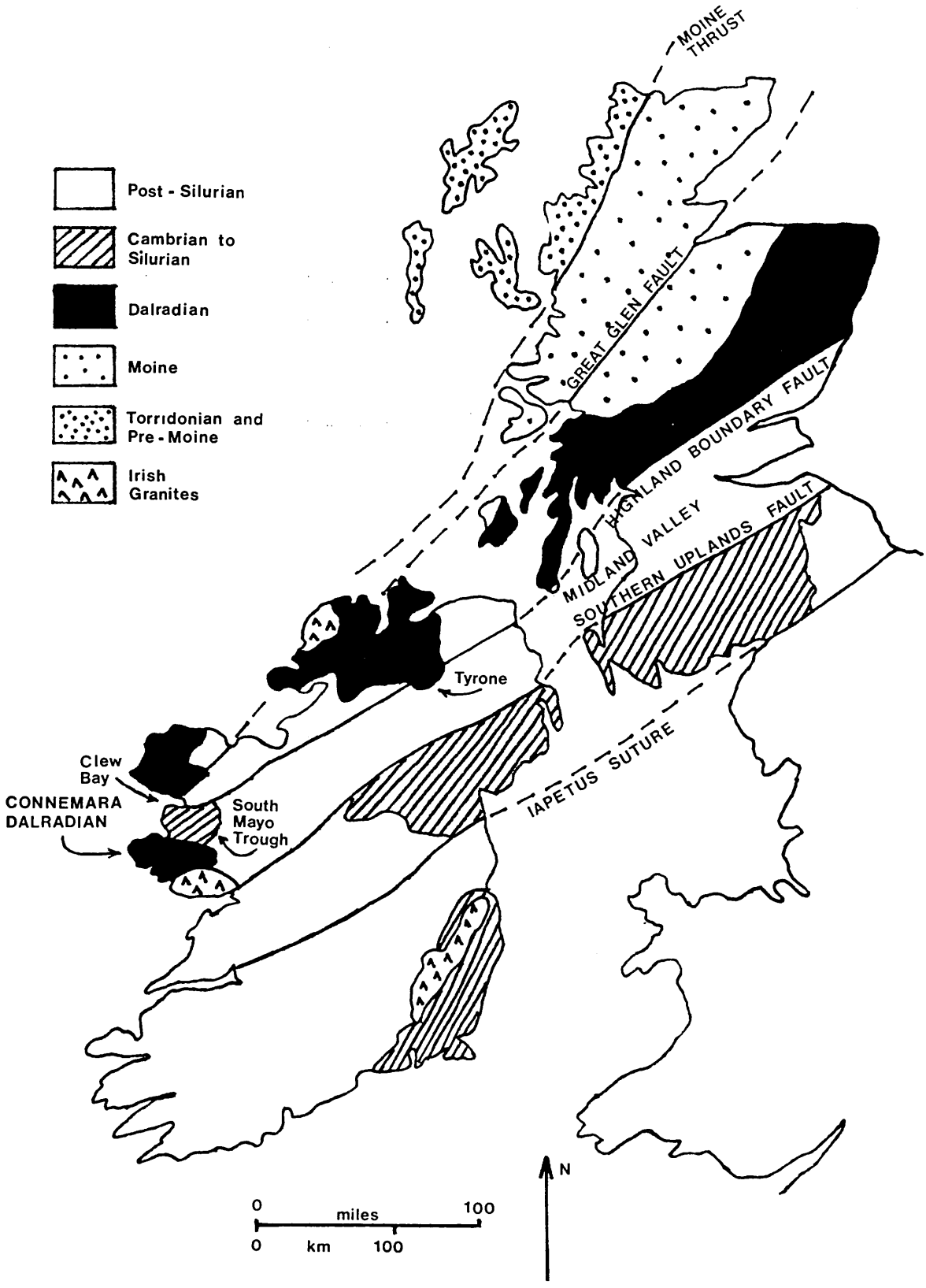

Figure 1.1. Sketch geological map of the British Isles showing the geographical position of Connemara. The principal geological features discussed in the text are indicated.

along strike of the Connemara Dalradian rocks (Leake *et al.* 1983). Little is known about early movements (Ordovician-Silurian) on the HBF and what structures and lithologies lie within the Midland Valley. Recent work (Bluck 1984) has shown that the Highland Boundary Complex may be an amalgamation of mainly Ordovician suspect terranes.

Hutton & Dewey (1986) identified Connemara as an exotic terrane and used internal stratigraphy and Grampian structure to constrain the original location of Connemara with respect to the strike continuation of the Scottish-Donegal Dalradian belt. They suggest Connemara originated outboard but slightly to the south (because of its higher Barrovian metamorphic grade) of SW Donegal between Ireland and Newfoundland. They propose that Connemara was detached by a curved and braided sinistral strike-slip system from the belt of Dalradian rocks prior to docking against the South Mayo Trough in Llanvirn-Llandeilo time. Dewey (1961, 1962) claimed to have recognised detrital staurolite and sillimanite from the South Mayo Trough. It was further suggested (Dewey *et al.* 1970) that an inverted succession of metamorphic mineral zones is recognisable in the Ordovician sediments. It has therefore been claimed that eroded material from Connemara has been deposited in the South Mayo Trough (Dewey 1961, 1962; Dewey *et al.* 1970; Yardley *et al.* 1982; Hutton & Dewey 1986). Bluck and Leake (1986) gave evidence to show that some 25km of erosion of the Dalradian rocks would have occurred in the Ordovician yet claim that the Ordovician basins flanking the Dalradian rocks ie. the South Mayo Trough, do not contain any undoubted Dalradian rock fragments. The authors conclude that docking of Connemara with the South Mayo Trough must have occurred in the Late Ordovician-Early Silurian ie. Taconic, after the major Connemara

uplift and erosion event. This view is supported by Graham (1987) who concludes that while much of the debris in the South Mayo Trough has a south-easterly origin this is unlikely to be present day Connemara.

Regardless of the fine detail it is generally accepted that at some time Connemara rifted off and migrated away from the main Dalradian Supergroup and at some time docked with the South Mayo Trough. The only certain evidence of the time of docking of these terranes is that it took place pre-Upper Llandovery since sediments of this age unconformably overlie both the Connemara Dalradian rocks and the South Mayo Ordovician rocks. This strongly suggests an Ordovician docking age.

1.2.2 The regional geology.

The Connemara massif consists of schists belonging to the Dalradian Supergroup which extend for over 50 km east-west along strike in the central portion of the inlier, figure 1.2. To the south of these lie an array of syn-metamorphic intrusive rocks which range from ultra-basic bodies through to acidic ortho-gneisses all of Arenig age. Intruded into these meta-igneous rocks is a suite of post-orogenic calc-alkaline granites of Lower Devonian age, the largest being the Galway Granite. To the north of the Connemara Schists lies the South Mayo Trough, a sedimentary basin consisting of early to middle Ordovician sequences, in which the rocks have only been weakly metamorphosed. The structural contact between the Connemara Schists and the South Mayo Trough is hidden by an overlapping sequence of Silurian (Upper Llandovery) age. The Connemara Schists consist of a sequence of well-bedded quartzites, psammites, pelites, marbles, amphibolites and pebble beds. The

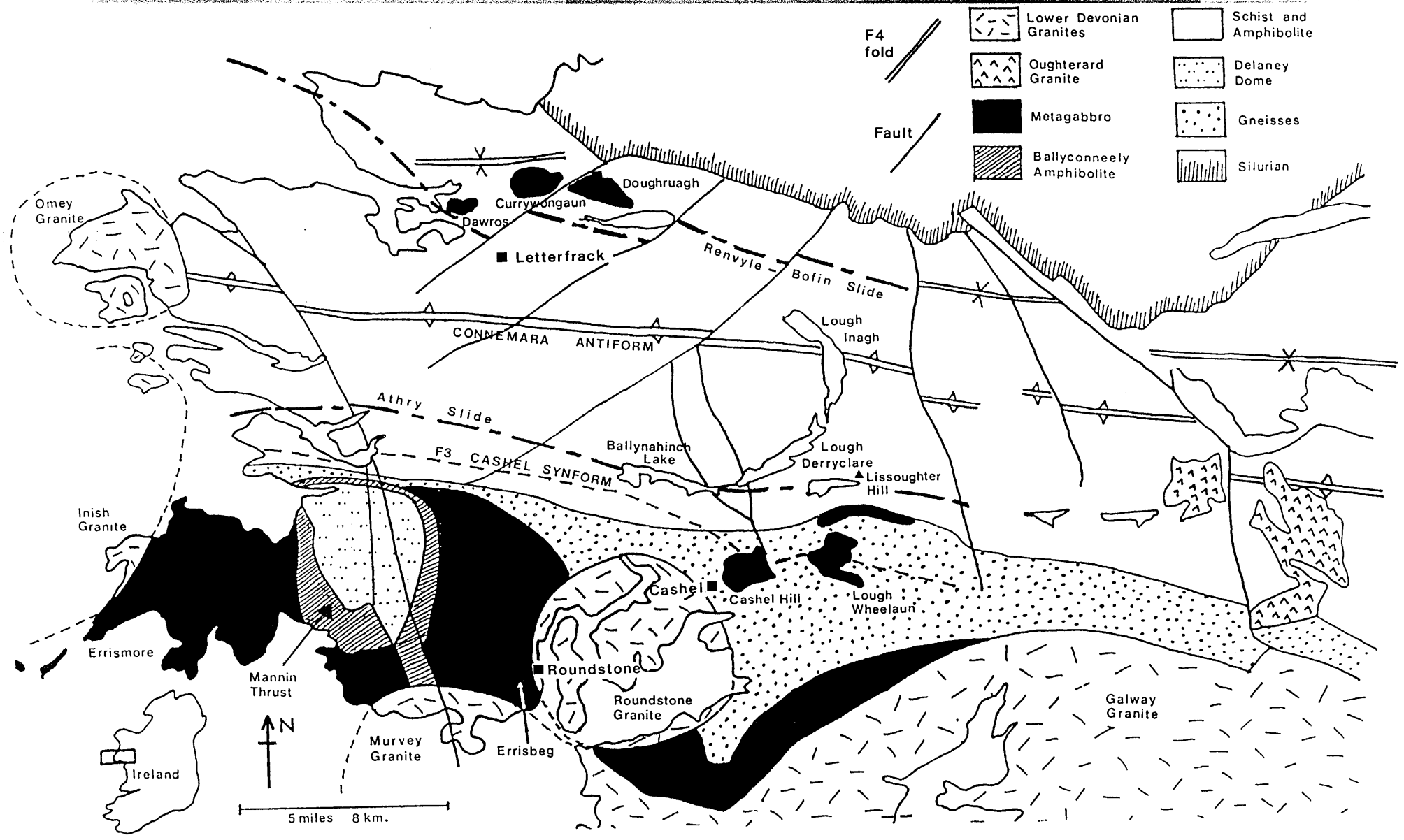

Figure 1.2. Geological sketch map of Connemara showing the principal geological features and locations discussed in the text.

Connemara marble, boulder bed and Bennabeola quartzite were correlated with the Islay succession in Donegal and Scotland by Kilburn *et al.* (1965) which established the Dalradian nature of the schists. A more general correlation was made by Harris & Pitcher (1975). Like the Scottish and Donegal Dalradian rocks those of Connemara can be subdivided into the Appin, Argyll and Southern Highland Groups. Only a brief description of the lithologies will be given here but detailed accounts of lithology and structure can be found in Tanner & Shackleton (1979) and references therein. The Cashel district (see figure 1.2) displays most of the rock types and detailed accounts of the mineralogy found here are given in Leake (1969). The psammites are of two main types; siliceous granulites (50-70% quartz) and quartzites (>75% quartz). These types are distinct in their field occurrence, the siliceous granulites are interbedded with the pelite and semipelites. They contain quartz (~70%), plagioclase (~25%), biotite (~5%) plus accessory minerals. The impure quartzite contains amounts of plagioclase + muscovite ± K-feldspar ± biotite and accessory minerals. The pelites and semipelites contain variable amounts of quartz, chloritised biotite, sericitised plagioclase (An_{30}-An_{40}), garnet, cordierite, sericitised sillimanite with lesser amounts of K-feldspar and accessory minerals. Following Leake (1969) pelite denotes an assemblage of <33% quartz + feldspar and semipelites contain more than this. The calcareous and magnesian metasediments range from nearly pure calcite marbles to calc-silicate rocks and para-amphibolites. These were originally limestones and calcareous and dolomitic pelites. These rocks have a diverse mineralogy. The precursors to the striped amphibolites were syn-depositional lava flows, dykes or sills. These rocks commonly are schistose and comprise hornblende and calcic oligoclase or andesine ± quartz ± biotite. They may sometimes contain up to 25% diopside segregated into diopside rich layers with plagioclase and sphene.

The diverse stratigraphy has allowed detailed structural study (eg. Badley 1976; Yardley 1976 and Tanner & Shackleton 1979) and three important deformation phases have been recognised; D2, D3 and D4. The major structure evident in the Connemara Schists is the D4 Connemara antiform striking east-west and plunging at a low angle to the east. The north and south limbs of this antiform form the two steep-belts which mark two major slide zones. No complementary synform is known to the south although there is one to the north, figure 1.2. The antiform refolds earlier D3 folds which can be seen from repetitions in the stratigraphy, the best example being the Glen Coaghan antiform. The first F2 fold to be positively identified passes through Lough Derryclare and on to Lissoughter Hill (see figure 1.2). This Derryclare (Lissoughter) fold contains the Connemara Marble Formation in its core at Lissoughter Hill. D2 deformation was responsible for the present day dominant fabric in the metasediments.

The syn-metamorphic intrusive rocks (the metagabbro-gneiss complex) in the south are of two main types A) the metagabbro suite comprising basic and ultra-basic rocks and B) the associated, but slightly later, orthogneisses. The metagabbro-gneiss complex rocks form the fairly flat areas from Errismore to Roundstone (see figure 1.2) but they also comprise the high standing Errisbeg and Cashel Hill as well as the large fault divided Currywongaun-Doughruagh intrusion in the north of Connemara. These metamorphosed basic-ultrabasic intrusions have variable mineralogy but they all originate from the same magma (Leake 1969 & 1989). Typically these rocks contain igneous and metamorphic hornblende (~50%), relic clinopyroxene (~5%), sericitised and saussuritised labradorite or bytownite (~40%), quartz (~5%) and accessory minerals. In some areas these rocks exhibit original igneous layering. From this layering and from geochemical studies it has been shown

(Singh 1984) that much of the metagabbro-gneiss complex in the south is inverted. The bodies in the north, Dawros, Currywongaun and Doughruagh show a differentiation series (Kanaris-Sotiriou & Angus 1976) and it is thought that these bodies were separated from the main metagabbro melt during the syn-deformation injection of magma. The orthogneisses form a series of quartz-diorite gneisses and trondjhemites with some K-feldspar granite gneiss. These are not in-situ differentiates of the metagabbro rocks but are thought to be co-genetic. These orthogneisses were injected after the metagabbro rocks and can be seen to be intruding and agmatising them (Leake 1989).

The injection of both the metagabbro rocks and the gneisses was accompanied by a marked increase in temperature. In the south, close to the injected rocks, some metasediments have been altered to paragneiss while others further away have been partially melted to form migmatites. The regional metamorphic grade increases southwards, across the strike direction, towards the injected rocks which were the major controlling factor on the present day metamorphic pattern. The metamorphic zones, moving north away from the injected rocks are: migmatite zone; sillimanite, K-feldspar zone; sillimanite, muscovite zone; staurolite zone and garnet zone (Barber & Yardley 1985).

1.2.3 Geological history.

The geological evolution of the Connemara massif began with the deposition of the Dalradian sediments as a bedded sequence of muds, sands and limestones with some volcanic ash and lavas on shelves and in extensional basins (Anderton 1982). The duration and timing of sedimentation has caused debate. Anderton (1982) in a review of the early

history of the Iapetus Ocean concluded that the Appin Group sediments were first deposited in the late Riphean, ie c. 650 Ma, and that deposition of the Dalradian continued through the Vendian and into the Cambrian, until the source regions had subsided below sea level. Rogers *et al.* (1989) produced a U-Pb zircon age of 590±2 Ma for the Ben Vurich Granite. This granite was intruded into the Dalradian rocks of Perthshire *after* the deposition and the D1/D2 deformation of the whole Scottish Dalradian. Consequently the authors conclude that all Dalradian deposition was Precambrian. Rogers *et al.* (1989) also question the general belief that Dalradian deposition is connected with the Laurentian margin. Instead they tentatively suggest that the whole Dalradian Supergroup is allochthonous and might have originally belonged to the Gondwanaland margin. Halliday *et al.* (1989) dated the Tayvallich Volcanics in the Dalradian rocks of the SW Scottish Highlands by the U-Pb method on zircons. These authors obtained an age of 595±4 Ma, close to the age of the Ben Vurich Granite (Rogers *et al.* 1989). The 595±4 Ma age for the Tayvallich Volcanics further suggests that all or most of the Dalradian sedimentation is Precambrian. Elias (1985) concludes, from whole rock Rb-Sr isochrons, that the diagenesis within the Connemara Dalradian rocks occurred between 687±65 and 542±5 Ma.

The Connemara Dalradian sediments were intruded by minor dolerite sills and dykes (now amphibolites) prior to the onset of the first phase of deformation, D1. This deformation is now only recognised from microscopic fabric details, trailing inclusions in garnet and plagioclase porphyroblasts (Badley 1976). The second phase of deformation, D2, resulted in the F2 folds of nappe-like dimensions, for example the Derryclare (Lissoughter) fold, and isoclinal minor folds. The main penetrative fabric in the Dalradian rocks developed through D2 and was accompanied by, or followed by, Barrovian style regional metamorphism,

reaching staurolite grade. The third deformation, D3, followed D2 in quick succession with the peak metamorphic pressures being reached pre- or syn- D3. Yardley *et al.* (1987) and Barber & Yardley (1985) indicate that this metamorphic pressure was greater than 7 kbar, comparable to the Dalradian rocks of Donegal.

It has generally been believed (Leake 1969) that the intrusion of the large metagabbro-gneiss complex was intruded syn-D2. Re-interpretation of the field evidence, however, has led to a change of view. It is now thought that this metagabbro-gneiss complex was intruded pre- or syn- D3 (P.W.G. Tanner *pers. comm.*, Leake 1989). Progressive D3 deformation caused folding of the basic rocks themselves and intrusion of the quartz-diorite gneiss agmatised and partially converted to gneiss the metagabbro rocks. Some of the metasediments were also altered to paragneiss while others suffered partial melting to form migmatites. This phase ended with the formation of the K-feldspar granite gneiss. The heat source for the orthogneiss formation and the migmatisation was almost certainly the injected rocks themselves. This stage also marked the peak of thermal metamorphism. In the southern area near to the injected basic rocks sillimanite grade assemblages were formed whilst elsewhere at least garnet grade assemblages grew. Treloar (1985) shows that temperatures approaching 900°C were reached in the metasediments close to the contact with the metagabbro-gneiss complex, and that even in the further away migmatised schists temperatures were up to 700°C. The probable plate tectonic setting during which the metagabbro rocks and the gneisses were intruded is that of a continental magmatic arc or a continental-island arc above a subduction zone. The injected rocks represent the roots of a now eroded batholith (Leake 1989).

Barber & Yardley (1985) and Treloar (1985) show that the metamorphic assemblages resulting from the intrusion of the metagabbro-gneiss complex rocks and the gneisses record metamorphic pressures of around 4 to 5 kbar. This indicates that during the period from just pre- to just post-intrusion a significant pressure decline from 7 to 5 kbar had occurred and this most likely relates to uplift. Barber & Yardley (1985) suggest that the pressure declined still further with time. From the evidence of CO_2 rich fluid inclusions and andalusite occurrences in leucosomes that must have formed during injection of the metagabbro-gneiss complex, crystallisation of the leucosomes did not happen until pressures as low as 3 kbar had been reached, although melting to form them was at higher pressures.

The third deformation, D3, and the injection of the magmas was followed by the fourth deformation, D4, which is responsible for the Connemara antiform. All these events are believed to be over by the late Ordovician because the 459±7 Ma Oughterard Granite (Leake 1978a & 1989) can be seen to cut the Connemara antiform (Bradshaw *et al.* 1969).

The main penetrative fabric in the Connemara Schists developed during D2, however new fabric growth, recognisable in the field, occurred during D3 in regions of high metamorphic grade. The high temperatures associated with D3 would have effectively ensured total resetting of the K-Ar 'clocks' of all D2 grown minerals. Consequently both the D2 and D3 mineral generations will have started to accumulate Ar at the same time and thus both generations would record D3 ages if all else were equal. No new fabric development occurred during D4 and so the the K-Ar mineral ages can confidently be said not to be the result of 'mixing' between two, or more, generations of minerals.

The translation of the Connemara massif to its present position thrust over the Delaney Dome Formation is post- D3 and probably pre-D4. The movement along the Mannin thrust resulted in mylonitization of the overlying Ballyconneely amphibolite, the fabric of which cross cuts the D3 fabric. Numerous ductile thrusts and slides were developed post-D3 (Leake *et al.* 1983). The Delaney Dome Formation is exposed because of interference between the D4 fold structures and the later, minor, D5 folds creating small dome and basin structures (Leake *et al.* 1983). Last movement on the Mannin Thrust was over by 447±4 Ma ie. Late Ordovician (Tanner *et al.* 1989).

The major orogenic episodes were over by this time. The post-orogenic Galway Granite and its satellite plutons were injected at c. 400 Ma (Leggo *et al.* 1966). Minor magmatic events are marked by Carboniferous and Tertiary dykes in Connemara and South Mayo.

1.3 Previous radiometric dating and interpretation in Connemara.

In this and all subsequent chapters referring to radiometric dating all the ages quoted have been (re-)calculated using the decay constants and isotopic ratios from Steiger & Jager (1977).

Radiometric dating in Connemara began in the early 1960's, soon after the development of both the Rb-Sr and K-Ar techniques. The early workers compared ages obtained from Connemara and from the Scottish Dalradian as a test for the supposed contemporaneity of the metamorphisms in the two regions.

The first radiometric dates from Connemara were reported by Giletti *et al.* (1961) who gave Rb-Sr mineral ages for two samples from the schists and one sample from the Galway Granite. Micas from the schists yielded an age of c. 490±15 Ma while biotite from the Galway Granite gave an age of 377±10 Ma. The ages from the schists are equivalent to those the authors obtained from the Scottish Dalradian and they suggested that the Scottish Dalradian and Connemara metamorphisms are contemporaneous and represent the same event. They further concluded that this event is different to the last metamorphism to affect the Moinian rocks of Scotland which they believed to have occurred c. 430-440 Ma. It is important to note that these authors interpreted these ages as representing cooling ages from a metamorphic thermal peak through to the temperature below which Ar is retained in biotite.

Muscovite from the same two schist samples dated by Giletti *et al.* (1961) was redated, again by the Rb-Sr mineral age method, by Long & Lambert (1963). The latter authors used a different spike, one enriched in ^{84}Sr and ^{86}Sr, than before. This resulted in their revised ages being c. 10 Ma younger than those of Giletti *et al.* (1961) but are the same within experimental error. Long & Lambert (1963) interpreted these ages in the same manner as Giletti *et al.* (1961) as cooling ages.

It should be noted that both Giletti *et al.* (1961) and Long & Lambert (1963), like other workers at that time, calculated Rb-Sr ages assuming a fixed ^{87}Sr abundance in the mineral at the time of metamorphism, expressed as the initial $^{87}Sr/^{86}Sr$ atom ratio. A value of 0.710 was used, about the same as for present day sea-water. It is now known that this assumption is usually not justified for *single* mineral Rb-Sr ages. Moorbath *et al.* (1968) estimate that this results in the ages of

Giletti *et al.* (1961) and Long & Lambert (1963) being some 20-30 Ma too high.

Fitch *et al.* (1964) reviewed the then current geochronological data for the British Caledonides and presented some data, including 2 K-Ar ages for the Connemara Schists from Miller & Brown (1965). In their reappraisal of the data the authors rejected the view of Giletti *et al.* (1961) that the Moinian and Dalradian rocks recorded different metamorphic peak ages. Fitch *et al.* (1964) conclude that the ages obtained for these two different supergroups, including Connemara, could best be explained as "resulting from a combination of partial and complete 'overprinting' of older metamorphic rocks by a (430-420) ± 10 Ma main Caledonian orogenic/magmatic/metamorphic event which was contemporaneous throughout Britain."

K-Ar ages from Connemara Schists were reported by Miller & Brown (1965) in a paper presenting K-Ar ages from mainly Scottish rocks ranging in age from Lewisian to Tertiary. The authors produced repeat ages for two schist samples, one on muscovite the other on biotite, of 428±19 Ma and 392±16 Ma respectively. These are the ages listed by Fitch *et al.* (1964). In this paper the authors also reported many K-Ar ages from the Moinian and Dalradian rocks of Scotland. The authors noted the similarity in the Connemara ages with those from the Moine and tentatively suggested a late Caledonian event was responsible for partially overprinting the radiometric ages.

Leggo *et al.* (1966) published whole rock Rb-Sr isochron ages on the Connemara granites and also the K-feldspar gneisses. The ages are: Galway Granite, 398±1 Ma; Omey Granite, 388±17 Ma; Roundstone Granite, 409±80 Ma; Inish Granite, 418±8 Ma and the potash feldspar gneisses, 751±175 Ma and the Oughterard Granite 528±35 Ma. A second

isochron for the Oughterard Granite indicated that it had been metamorphosed at 460±7 Ma. This is close to the average of three K-Ar ages on hornblende from the K-feldspar gneisses of 444±17 Ma. Leggo *et al.* (1966) concluded that these two ages are 'overprinted' onto older ages, as suggested by Fitch *et al.* (1964).

The results from the first larger scale geochronological investigation of Dalradian schists to be restricted to the west of Ireland were presented by Moorbath *et al.* (1968). They presented five hornblende, twelve muscovite and eight biotite K-Ar ages, some of which represented mica pairs, from Connemara. These samples were collected from both the schists and the metagabbro-gneiss complex. Included in these were yet another redate of the schist samples previously dated by Giletti *et al.* (1961) and Long & Lambert (1963). Moorbath *et al.* (1968) also presented nine Rb-Sr mineral ages for the schists and one for the metagabbro-gneiss complex. The authors' intention was to date the main metamorphic event, in their conclusions they show that this aim was not realised. Of the twenty-five K-Ar ages twenty-two fell in the range 445 to 475 Ma, with an average age from all the samples of 456 Ma. Moorbath *et al.* (1968) postulate that some event occurred at this time and that Ar had been retained from this point. The two principal possibilities that they suggested are either uplift of the Connemara massif at 450-470 Ma and, or, a widespread retrogressive metamorphism at this time. Moorbath *et al.* (1968) suspected that the probable retrogressive event at this time was responsible for the ubiquitous chloritisation in Connemara and was the same event that caused the resetting of the Oughterard Granite (Leggo *et al.* 1966).

U-Pb ages on zircons from two samples from the schists, one from the metagabbro-gneiss complex and one from the Carna (Galway) Granite

were published by Pidgeon (1969). Results from the schist samples could not be interpreted unequivocally but the author suggested that the detrital zircons were derived from a source region of Laxfordian age, possibly the Lewisian. The metagabbro-gneiss complex sample was taken from the Lough Wheelaun part of the Cashel-Lough Wheelaun intrusion. The zircon U-Pb age was calculated as 510±10 Ma. The author believed this to be the primary crystallisation age of this intrusion and that this age represents the age of the main Dalradian metamorphism, then called M1. The calculated zircon U-Pb age for the Carna Granite is 420±20 Ma and the author claims good agreement with the Leggo *et al.* (1966) Rb-Sr isochron age of 398±1 Ma for the Galway Granite. In a later paper (Pankhurst & Pidgeon 1976) the authors indicate that the zircon U-Pb ages from Pidgeon (1969) may have been overestimated by as much as 20 Ma.

Dewey *et al.* (1970) reviewed the radiometric data of Moorbath *et al.* (1968) in the light of four new K-Ar ages on mica from the Connemara Schists and the field evidence. Dewey *et al.* (1970) consider the best interpretation of the isotopic ages from the Connemara Schists to be that "they are related to the pre-Llandoverian cooling of the Connemara region to temperatures below the threshold temperature for argon diffusion from biotite." They further used the isotopic data to suggest that a trough-cordillera pair existed in Ordovician times. In this model material eroded from Connemara is deposited in the South Mayo Trough.

The first attempt to determine the time of thrusting of Connemara over the Delaney Dome Formation along the Mannin thrust was made by Leake *et al.* (1983). The authors constructed a whole rock Rb-Sr isochron from samples collected from the Delaney Dome Formation.

Two samples were rejected from the analysis because of probable alteration. The remaining 9 samples gave an isochron corresponding to an age of 460±25 Ma. The authors could not be certain if this was a crystallisation age or a mylonitization (thrusting) age. Leake *et al.* (1984) further confined the age of movement along the Mannin thrust by dating 8 lineated hornblendes from the Ballyconneely Amphibolite by the K-Ar method. The ages produced range from 384±12 to 469±20 Ma with an average of 454 Ma. This average age Leake *et al.* (1984) shows overlaps with the 460±25 Ma Rb-Sr age of Leake *et al.* (1983) and is therefore thought to confirm the latter age as the time of thrusting. The 460±25 Ma Rb-Sr isochron of Leake *et al.* (1983) was criticised by Kennan & Murphy (1987) who used all 11 of the original isochron points of Leake *et al.* (1983) to construct two isochrons defining ages of 425±31 and 426±10 Ma. The authors conclude that 426±10 Ma represents the time of mylonitic homogenisation and therefore thrusting. The rationale behind this approach has been strongly criticised (Tanner & Dempster 1988). Tanner *et al.* (1989) resampled from the Delaney Dome Formation and produced a mineral-whole rock isochron corresponding to an age of 443±4 Ma. This together with new muscovite-whole rock Rb-Sr ages of 448±4 and 451±4 Ma yield an average of 447±4 Ma which the authors consider to represent the last movement on the Mannin thrust.

The age of the Oughterard Granite has provoked continuing debate. The first published Rb-Sr isochron ages were reported by Leggo *et al.* (1966) who claim the youngest possible age is 528 Ma but that the granite has been metamorphosed at 460 Ma. Leake (1978a) recalculating and reinterpreting the data of Leggo *et al.* (1966) suggests 459±7 Ma represents a true minimum age of intrusion. In contrast Kennan *et al.* (1987) present new data and another Rb-Sr isochron age of 407±23 Ma.

Jagger *et al.* (1988) redated the Cashel-Lough Wheelaun metagabbro-gneiss complex intrusion and also an associated K-feldspar granite gneiss from Lettershinna Hill. The metagabbro-gneiss complex sample was collected from the Lough Wheelaun part of the intrusion from the same location as that studied by Pidgeon (1969). Jagger *et al.* (1988) obtained an age of 490±1 Ma and, as there were no apparent inherited characteristics, this age is believed to be very close to the age of intrusion of this metagabbro-gneiss complex. Note that this age is in close agreement with the revision of the age from Pidgeon (1969) by Pankhurst & Pidgeon (1976). The sample of the K-feldspar granite gneiss yielded a lower intercept age of 454 +6/-14 Ma and the upper intercept indicated evidence of a possible Laxfordian precursor. The authors suggested that the lower intercept age indicated a period of lead loss and is not the age of crystallisation.

The minor intrusions have received some study and several have been dated by the K-Ar and ^{40}Ar-^{39}Ar methods: Doon Hill, 61 Ma (Macintyre *et al.* 1975); Tertiary dolerite dykes, 25 to 70 Ma (Mitchell & Mohr 1986); Carboniferous dolerite dykes, 305 Ma (Mitchell & Mohr 1987). In the case of the Tertiary dykes the authors (Mitchell & Mohr 1986) suspect Ar loss causes the large spread of ages, most of which do not reflect the age of intrusion.

The most recent radiometric study (before the present investigation) is detailed in Elias (1985). In this work K-Ar ages are reported on twenty-six hornblendes, twenty-six muscovites and twenty-six biotites from the Connemara Schists, metagabbros and gneisses. These are supplemented by nineteen whole rock-mica Rb-Sr ages and four ^{40}Ar-^{39}Ar incremental heating ages on micas. The average K-Ar mineral ages are: hornblende, 466 Ma; muscovite, 455 Ma and biotite, 435 Ma. The

author tested for correlation between age and elevation, grain size and chemical composition and found none. Elias (1985) plotted thermochron maps for these ages and from these concluded that an irregular increase in the K-Ar mineral ages is apparent towards the south. Using the average mineral ages and the thermochrons the author constructed a cooling and uplift history for Connemara. In this model initial uplift was rapid, with temperature falling from 700°C (probable maximum metamorphic temperature) to 550°C (closure temperature for amphibole to Ar diffusion) in 10 Ma, this was followed by a period of slower uplift indicated by the mica ages. This model is based mainly on the K-Ar ages. The mineral-whole rock Rb-Sr results were considered of doubtful reliability. The ^{40}Ar-^{39}Ar results on the micas (3 biotites and 1 muscovite) were used by Elias (1985) to demonstrate that there is no sign of an overprinting event.

The ideas of Elias (1985) were summarised and refined in Elias *et al.* (1988). This work was based on the same data as Elias (1985). The same initial conclusion is drawn; that older ages in the south indicate that the higher grade rocks there cooled through the temperature of Ar retention in amphibole before those in the north. The authors developed the rapid uplift model invoking the two major slide zones to divide the Connemara massif into three blocks that uplifted at different times and at different rates. Movement on these slide zones and the rapid uplift is considered to be related to the thrusting of Connemara over the Delaney Dome Formation along the Mannin Thrust. The widespread c. 440 Ma ages, in both Connemara and Scotland, are thought to reflect the late Ordovician docking of the Dalradian block against the Ordovician rocks of the South Mayo Trough and the Midland Valley.

1.4 Review of K-Ar and ^{40}Ar-^{39}Ar radiometric dating of metamorphic micas and amphibole.

1.4.1 Closure temperature estimates for micas and amphibole.

The K-Ar and ^{40}Ar-^{39}Ar radiometric dating techniques are now well established but the interpretation of the dates obtained by these methods is, however, far from straightforward. Since the inception of the K-Ar and later the ^{40}Ar-^{39}Ar methods hundreds of papers have been published arguing and counterarguing the actual geological significance of K-Ar and ^{40}Ar-^{39}Ar dates determined on many different minerals sampled from a wide variety of geological settings. For dating metamorphic rocks by the K-Ar and ^{40}Ar-^{39}Ar methods muscovite, biotite and hornblende are the most useful. These minerals are common, have significant amounts of K, and are usually retentive of the radiogenic Ar. It is generally agreed that K-Ar ages are cooling ages, not crystallisation ages, and that different minerals record different ages. The best early evidence for this came from K-Ar ages patterns for muscovite and biotite from the central Alps (Jager 1965; Armstrong *et al.* 1966 and Jager *et al.* 1967) which were interpreted as recording post-metamorphic cooling. It is normally supposed that K-Ar dates record the time since minerals last cooled below their Ar diffusion closure temperature and that this closure temperature is mineral specific. Closure temperature theory was defined mathematically by Dodson (1973) who derived an equation for the calculation of closure temperatures:

$$E / RT_C = \ln [ART_C^2 D_O / a^2 E(dT/dt)] \qquad \text{(Eqn 1.1)}$$

where R is the real gas constant, E the activation energy, T_C the closure temperature, A is a numerical constant describing the diffusion geometry, D_O is the diffusion coefficient and 'a' is the characteristic

diffusion radius and dT/dt is the cooling rate. A consequence of this mathematical treatment was the conclusion that closure temperatures are not only mineral specific but are affected by the cooling rate of the mineral. Dodson (1973) calculated that a change in the cooling rate by a factor of 10 changes the closure temperature by 11%. This theory does not allow simple calculation of closure temperatures for minerals because the activation energy and the diffusion coefficient have to be determined experimentally. Consequently, there has been much debate on what closure temperatures to adopt. The following account reviews the most important issues raised in the literature concerned with interpretation of K-Ar and ^{40}Ar-^{39}Ar dates on biotite, muscovite and hornblende from metamorphic regions.

The important closure temperature estimates from the account below have been summarised in diagrammatic form in figure 1.3. Estimates of closure temperatures were first determined empirically from K-Ar mineral ages disturbed by thermal metamorphism or from studying patterns of mineral ages obtained in metamorphic regions from samples taken from a range of metamorphic grades. Hart (1964) showed that K-Ar dates on hornblende in the country rock intruded by a Tertiary stock are undisturbed beyond the first 30 - 40m away from the contact while biotite was disturbed within the first 3 km. Hart (1964) concluded that the hornblende retains Ar at higher temperatures than biotite. A similar investigation was performed by Hanson & Gast (1967) who found Ar to diffuse from biotite over the temperature ranges 720 to 450°C in country rock adjacent to a Wyoming dyke and 500 to 350°C in country rock near the Duluth gabbro. The corresponding range of activation energies was calculated to be 50 - 75 kcal/mol. The loss of Ar in the hornblende was found to be at higher temperatures and activation energies but was variable. Purdy & Jager (1976) in a study of the central Alps compared the

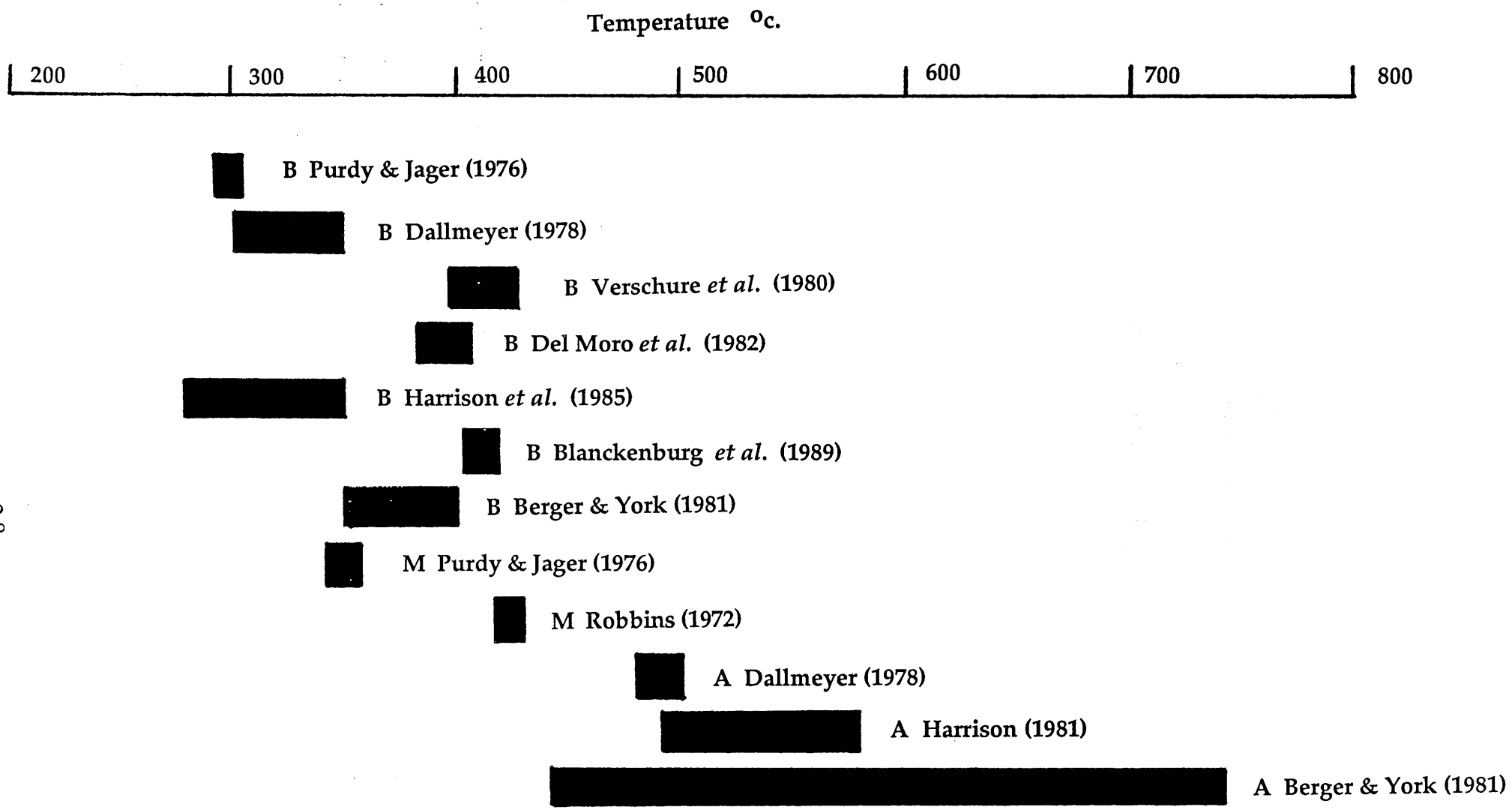

Figure 1.3. Diagram showing the comparison between the most important estimates of argon closure temperatures in amphibole (A), biotite (B) and muscovite (M).

transition from pre-Alpine to Alpine mica Rb-Sr ages to metamorphic isograds and derived Rb-Sr blocking temperatures for biotite and muscovite. The K-Ar ages were then compared to the Rb-Sr ages to derive K-Ar blocking temperatures of 350°C for muscovite and phengite and 300°C for biotite. It has been indicated (Del Moro *et al.* 1982) that these closure temperature estimates are too low because the metamorphic isograd calibration of Purdy & Jager (1976) is based on a value for the upper stability of stilpnomelane of about 300°C whereas Nitsch (1970) has found stilpnomelane to be stable up to 460°C and Brown (1971) has found it stable up to 480°C. Dallmeyer (1978) dated biotite and hornblende from the Georgia Inner Piedmont, which has undergone late Palaeozoic regional metamorphism, by the ^{40}Ar-^{39}Ar step-heating method. He estimated from metamorphic isograds that the closure temperature for biotite was between 345 and 300°C and that the closure temperature for hornblende was likely to have been in excess of 480°C. Contradicting the mica closure temperature determinations of Purdy & Jager (1976) and Dallmeyer (1978) was the discovery that biotites can retain Ar even at temperatures in excess of 400°C. Verschure *et al.* (1980) dated samples from SW Norway and showed that Sveconorwegian (pre-Caledonian Orogeny) biotites maintain Sveconorwegian ages c. 870 Ma despite the fact that during the Caledonian Orogeny temperatures of up to 400°C would have been reached in this region. This is indicated by the growth of a Caledonian generation of biotite that records Caledonian ages. Del Moro *et al.* (1982) have demonstrated that six biotites taken from the bottom of two 2km wells in the Larderello Geothermal Field in Italy record non-zero ages despite the fact that down hole temperatures are 290 and 380°C. In fact these biotites plus two muscovites and one hornblende give K-Ar ages that cluster around 2.5 to 3.7 Ma. This date is thought to mark the onset of the geothermal field. Note the temperatures

recorded by Verschure (1980) and Del Moro *et al.* (1982) are significantly higher than the mica closure temperatures determined by Purdy & Jager (1976) and Dallmeyer (1978).

After the publication of Dodson's theory for slow cooling researchers began to perform laboratory experiments to determine activation energies and diffusion coefficients and hence to calculate closure temperatures for specific mineral samples. For the two most commonly dated minerals, biotite and hornblende, a large range of activation energies were published. These data showed a large spread in values that apparently indicated a possible range of closure temperatures for biotite and hornblende of several hundred degrees. However according to Giletti (1974) and Harrison (1981) most of these experimental determinations of activation energies and diffusion coefficients violate the requirement that the mineral phase remain stable during the experiment. It was demonstrated that this is a necessary requirement by Gaber *et al.* (1988) who conducted SEM imaging of biotite and amphibole following intermediate steps in an *in vacuo* step-heating experiment. The authors proved conclusively that these hydrous minerals suffer weight loss and irreversible structural changes in the range 600 to 800°C. The biotite and muscovite suffered significant splitting along the basal cleavage. The authors showed that during step-heating experiments Ar loss is not controlled by volume diffusion and therefore it is inappropriate to calculate diffusion coefficients and closure temperatures from ^{40}Ar-^{39}Ar data. A range of isothermal-hydrothermal heating experiments have been performed by Harrison (1981) and Harrison *et al.* (1985). These techniques are not thought to violate the important criteria of mineral stability. Harrison (1981) performed isothermal-hydrothermal experiments on hornblende to determine activation energies and diffusion coefficients and, assuming spherical geometry, applied the

equations of Dodson (1973) to obtain closure temperatures of 578 to 490°C for cooling rates of 500 to 5°C/Ma. Harrison *et al.* (1985) performed similar experiments on biotite and concluded that the closure temperatures for this mica are 345, 310 and 280°C for cooling rates of 100°C/Ma, 10°C/Ma and 1°C/Ma respectively. These closure temperatures are often quoted (eg. Anderson 1988) as being the most reliable available. However, it should be noted that even the highest biotite Ar closure temperature estimate (345°C) of Harrison *et al.* (1985) is below the down hole temperature recorded in the Larderello geothermal field in which Del Moro *et al.* (1982) recorded non-zero biotite ages. Isothermal-hydrothermal experiments do not necessarily give low estimates of closure temperatures. Blanckenburg *et al.* (1989) used the the activation energy and diffusion coefficient of biotite determined from these types of experiments (Giletti 1974) to determine the closure temperature (Dodson 1973) and obtained a value of 410°C. Robbins (1972) performed a hydrothermal experiment on muscovite and obtained a closure temperature of c. 420°C, which is significantly higher than the estimate of Purdy & Jager (1976).

Berger & York (1981) dated several different minerals, from a high grade metamorphic terrane in Ontario, by the *in vacuo* ^{40}Ar-^{39}Ar step-heating method. The authors determined K-Ar apparent ages from the ^{40}Ar-^{39}Ar age spectra and Ar isotopic closure temperatures from rate parameters that were derived from the same experiments and these were then combined with the closure temperature theory of Dodson (1973). The calculated closure temperatures for hornblende cover a wide range, from 443 to 747°C but with five out of six samples having calculated closure temperatures in excess of 600°C. The calculated closure temperatures for biotite from this experiment range from 350 to 400°C. Berger & York (1981) acknowledge that they violate the requirement for

mineral stability by performing the experiment *in vacuo* but they point out that the maximum calculated hornblende and biotite closure temperatures of about 700°C and 400°C are reasonable insofar as they correspond to independent mineral geothermometers.

It is worth asking if field and laboratory determinations of closure temperatures are necessarily directly comparable as the two methods require different assumptions to be made. Field based determinations require estimates of maximum temperatures reached ie. Purdy & Jager (1976). Calculations based on laboratory determinations of rate parameters assume that the experiments mimic nature in a systematic manner and also assume a cooling rate. Perhaps more importantly these calculations require a value for the characteristic diffusion radius. Little effort appears to have been made to determine this value precisely. Is it the actual grain size? or is it the domain size bounded by cleavages? Layer *et al.* (1987) from laser-probe ages of individual grains and Kelley (1988) from bulk K-Ar ages both show a grain size dependence on the ages. This implies that the characteristic diffusion radius, if not the actual grain size, is related to it. Most calculations (ie. Harrison 1981) assume spherical geometry for Ar diffusion in hornblende. However, Farver & Giletti (1985) show that oxygen diffusion is 10 times faster along the c-axis than along a or b. If this is also true for Ar diffusion then it may have a significant affect.

1.4.2 Physico-chemical effects on closure temperatures.

It has been recognised in much of the literature that factors other than just the cooling rate may potentially affect the closure temperature. This arose from a realisation that many factors affect the activation energy and diffusion coefficients and therefore indirectly the closure

temperature from the slow cooling theory of Dodson (1973). If other factors are important it may also be true that the opening temperature of a mineral is not the same as its closure temperature as suggested by Chopin & Maluski (1980). It has been hard to prove conclusively, from field evidence, that other factors can affect the closure temperature because major factors, such as changes of cooling rate, tend to mask any effect.

As the closure temperature concept is closely related to diffusion theory the latter is reviewed briefly in section 1.6. The most important potential effect is that due to variable composition. The potential importance of composition was first proposed by Gerling *et al.* (1965) who found that the Fe/Mg ratio controlled the activation energy for the loss of Ar from hornblende. This idea found some support from Hanson & Gast (1967) who proposed that the variation in calculated activation energies for partially reset amphiboles in the vicinity of the Duluth Gabbro might be due to the variation in the Fe/Mg ratios. Later O' Nions *et al.* (1969) showed an apparent compositional dependence on hornblende K-Ar ages from a high-grade, slowly-cooled metamorphic terrane in South Norway. These authors show that the oldest ages are derived from amphiboles in which the 'Y' sites are filled with small positive cations, ie. Mg^{2+}, while the youngest ages are the most Fe^{2+} rich. These conclusions can be criticised because the samples were collected from a large part of South Norway and consequently it is difficult to rule out the influence of differential uplift and variable cooling rates. Berry & McDougall (1986) determined K-Ar and ^{40}Ar-^{39}Ar ages on amphiboles from the zoned metamorphic complex at Aileu, East Timor. These authors found that Mg-rich hornblendes lost most of their pre-existing radiogenic Ar and Fe-rich hornblendes were completely reset, during a retrogressive metamorphic event of amphibolite grade. At lower grades of

retrogression the Mg-rich hornblendes retained appreciable radiogenic Ar while the Fe-rich hornblendes lost most of their accumulated radiogenic Ar even at upper green-schist facies.

Despite the apparent field evidence the possibility of compositional control over the closure temperatures of amphibole was contested by Harrison (1981) who during isothermal-hydrothermal heating experiments showed that the calculated activation energies for both Fe and Mg rich hornblendes were the same. According to the equations of Dodson (1973) the closure temperatures should be identical.

The effect of composition on the closure temperatures of micas has received less study but there is evidence to suggest that the affect is real. Harrison *et al.* (1985) compiled hydrothermal diffusion data for the annite-phlogopite series from Norwood (1974) and Giletti (1974) and showed that the activation energy drops significantly with increasing mole percent of annite. Harrison *et al.* (1985) reported results of isothermal-hydrothermal experiments on biotites with differing compositions. The authors concluded that the activation energy and consequently the closure temperatures are strongly dependent on the Fe/Mg ratio.

A second potentially important effect on the closure temperatures of minerals is their variable structure, this includes; twinning, exsolution, alteration products, solid and fluid inclusions etc. The affect of exsolution was demonstrated by Harrison & Fitz Gerald (1986) who dated hornblende and biotite from a single amphibolite exposure in Vermont by ^{40}Ar-^{39}Ar step-heating. They found that the biotite gave a flat plateau with an age of 345 Ma but the hornblende gave a complex spectra and a total fusion age of 259 Ma. This represents an inversion of the normally expected age pattern. In addition it was found that the K/Ca

ratio varied antipathetically with the hornblende age spectra. TEM investigation of the hornblende showed it to contain up to 2.5% of exsolution lamellae, each no more than 4 microns wide. The authors conclude that the exsolved components (cummingtonite and hornblende) have different Ar retentivities and that small scale exsolution structures control Ar loss causing the unusually low closure temperature for this hornblende sample. The existence of patches of variable Ar retentivity within single hornblende crystals was discovered by Kelley & Turner (1987) by laser microprobe ^{40}Ar-^{39}Ar studies.

The affect of later generations of mineral inclusions has been shown by several authors. Sisson & Onstott (1986) dated by ^{40}Ar-^{39}Ar a Na-bearing amphibole, crossite, from Alaska. The K content estimated from the ^{39}Ar release was incompatible with the microprobe determinations. The discrepancy was found to be the result of fine grained inclusions of phengite in the crossite grains. These fine grained phengites were thought to be susceptible to Ar loss and so cause the total fusion (K-Ar) ages to be unreliable. Onstott & Peacock (1987) dated hornblende from samples of amphibolite and granitic gneiss from the same outcrop in the Adirondacks. These two samples must have been through the same P-T cycle. The two samples gave significantly different ^{40}Ar-^{39}Ar plateau ages of 948 and 907 Ma respectively. TEM investigation of the samples showed that both samples contained zones of fibrous phyllosilicates no more than 2 microns wide. The authors suggest that the phyllosilicate zones may act as channels for Ar escape and may influence the closure temperature by partitioning the grains into diffusion domains of varying size. By measuring the apparent domain sizes and assuming this to be the characteristic diffusion radius and using the activation energy and diffusion coefficients from Harrison (1981) Onstott & Peacock (1987) calculated effective closure temperatures of 412

and 451°C for the granitic gneiss and the amphibolite samples. These authors also calculated that if the samples were homogeneous (ie. the characteristic diffusion radius was the grain diameter) then the closure temperatures would be 503 and 562°C. Phyllosilicate inclusions have also been reported in 'low age' hornblendes by Ross & Sharp (1988) who have dated by ^{40}Ar-^{39}Ar three samples from the Franciscan Complex, California. These three samples give discordant total gas (K-Ar) ages of 147 to 161 Ma but the same plateau age of 162 Ma. The discordant total gas ages were caused by K-rich phyllosilicate inclusions. These phyllosilicates degas during step-heating at lower temperatures than the hornblende and so consequently are not thought to have affected the hornblende plateau age. These phyllosilicates were estimated to contain 50 to 100 times more K than the hornblende.

The effect of twin planes on amphibole closure temperatures has not been tested but it has for feldspar. Parsons *et al.* (1988) during a combined ^{40}Ar-^{39}Ar dating and TEM study concluded that feldspar twin boundaries are normally coherent and so do not provide channels for Ar loss. However the authors note that those feldspars that appear most turbid give the most disturbed ^{40}Ar-^{39}Ar spectra and this the authors ascribed to large numbers of micropores that allow Ar leakage. These general conclusions may have a bearing on other mineral types. Evidence to indicate this is not necessarily the case comes from a study (Krishnaswami & Seidemann 1988) of Ar leakage in amphibole and other minerals. These authors measured the leakage of radiogenic ^{222}Rn and ^{40}Ar and reactor produced ^{39}Ar and ^{37}Ar to assess the role of nanopores in minerals on gas transport. It was found that the leakage of all the Ar isotopes was barely measurable suggesting that no extensive nanopore network intersecting the grain boundaries exists in these samples.

The slow cooling theory of Dodson (1973) assumes that no initial Ar was present and that when a mineral has closed to Ar diffusion no Ar is added to, or lost from the system. This is often not so when dealing with natural minerals from metamorphic terranes. These minerals are frequently subjected to periods of reheating, tectonic movement, fluid migration etc. which could add to or subtract from the Ar, or even the K, budget of the minerals concerned. Excess Ar has long been recognised as an important potential source of error when dating poly-metamorphic terranes and has been demonstrated to cause geologically meaningless dates eg. Harrison (1983). The ^{40}Ar-^{39}Ar step-heating method is particularly useful in identifying samples that contain excess Ar. There is often sufficient excess Ar to cause the K-Ar (total fusion) age to be significantly older than the plateau age. This implies that the excess Ar is held in specific lattice sites other than those which hold radiogenic Ar (Harrison & McDougall 1980). Phillips & Onstott (1988) were able to contour the Ar content of a single phlogopite grain by multiple ^{40}Ar-^{39}Ar laser-probe age dating. They showed that excess Ar was held in significant quantities in the core of the mineral in contrast to the rims. Blanckenburg & Villa (1988) dated amphibole from the Western Alps. They found that an obviously later generation of cummingtonite rimmed hornblende and yielded ages of 120 Ma while the hornblendes scatter between 17 and 37 Ma. They showed that excess Ar in the cummingtonite was responsible and that this Ar might be located in fluid inclusions that mark the locations of healed microfractures in the mineral. Rama & Hart (1965) showed that most minerals, with the possible exception of the phyllosilicates, commonly contain fluid inclusions. The authors indicate that these often contain Ar and so act as a possible source of error when dating low K minerals by the K-Ar method.

It is now apparent that no single, universal Ar diffusion closure temperature can be adopted for any of the common rock forming minerals. The absolute closure temperatures are potentially sensitive to many physico-chemical factors such that it may be pointless to speculate only on the affect of, say, Fe/Mg ratio without considering all of the other likely factors. With this in mind it is worth considering the caution expressed by Harrison & Fitz Gerald (1986) who stated "Prior to assigning a variable as sample intensive as closure temperature, it would be prudent to fully characterise metamorphic amphiboles..." It would seem that this characterisation should ideally include calculation of sample specific closure temperatures based on isothermal-hydrothermal determinations of activation energies and diffusion coefficients together with measurement of the diffusion radius. This closure temperature is then only applicable to chemically similar samples collected from a field area in which other geological constraints indicate that the whole area has been affected by the same P, T and P_{H2O} conditions. Furthermore it would appear that minerals, and especially hornblende, do not always exhibit constant closure temperatures on the subgrain scale. Blanckenburg & Villa (1988) propose that metamorphosed mineral grains display undegassed patches tightly adjacent to rejuvenated patches. They suggest that these minerals should not be considered as uniform, isotropic spheres but as patchy aggregates of leaky and retentive allotropes.

Consideration of the recent literature reviewed above must cast doubt on the validity of uplift conclusions based on geochronological syntheses of metamorphic terranes based on simple open or shut, closure temperature models. Indeed, it has been argued that closure temperature theory is not sufficient to model complex metamorphic geochronologies. Chopin & Maluski (1980) in attempting to determine the uplift history of

the Western Alps by ^{40}Ar-^{39}Ar dating of micas found that their data could not be explained in terms of a simple closure temperature model. These authors found that for micas that had experienced the same P-T history some had remained as closed systems while others had opened during heating. This they explain as resulting from deformation enhanced diffusion and was not primarily a thermal affect and consequently the authors question the relevance of the closure temperature theory. Chopin & Maluski (1980) suggest that a distinction may exist between an opening and a closing temperature. In a subsequent comment Desmons *et al.* (1982) claim to be able to explain all the ages of Chopin & Maluski (1980) by closure temperature theory but while apparently criticising the views of Chopin & Maluski (1980) they state that "many other factors than temperature" are involved in opening a system. Deutsch & Steiger (1985) when dating amphiboles from the Central Alps came to the same conclusion as Chopin & Maluski (1980), namely that "the K-Ar systematics in amphiboles of the Central Alps is mainly governed by recrystallisation induced by pervasive deformation; thermal activated diffusion processes play a subordinate role." It seems likely that at least in some cases the ages recorded by minerals in metamorphic regions signify the periods of deformation while the rocks are at high temperature and not a cooling or uplift phase following high temperatures.

To conclude it would appear that the slow cooling and closure temperature theory as outlined by Dodson (1973) is only a first approximation to natural events. When applied to some relatively simple situations, ie. cooling following one period of heating, either from contact or regional uplift and cooling, then geologically significant results can be obtained. However, when applied to polymetamorphic terranes or heterogeneous mineral samples, a multitude of factors may be

influencing the K-Ar or ^{40}Ar-^{39}Ar ages to the extent that they become geologically indecipherable.

1.5 Review of oxygen and hydrogen stable isotope principles.

1.5.1 Introduction.

Only a brief review will be given here, for a more complete account the reader is referred to Faure (1986) which covers all the basic theory.

It is normal practice to report the stable isotopic composition of a sample using the δ notation. This is defined as:

$$\delta_{sam} = [(R_{sam} - R_{std}) / R_{std}] \times 1000 \text{ ‰} \qquad \text{(Eqn 1.2)}$$

where R is the atomic ratio of the heavy to light isotope for the sample (sam) and the standard (std). For hydrogen isotopes this ratio is D/H where D denotes deuterium and H hydrogen, for oxygen it is $^{18}O/^{16}O$. The δ value is measured directly by the mass spectrometer but is usually recalculated with reference to international standards. For oxygen and hydrogen this standard is SMOW (Standard Mean Ocean Water) or V-SMOW (Vienna-Standard Mean Ocean Water) which has the same value.

To report isotopic fractionation the α notation is used, where α (the fractionation factor) is given by:

$$\alpha_{A-B} = R_A / R_B \qquad \text{(Eqn 1.3)}$$

where R_A and R_B are the absolute isotopic ratios in phases (minerals or fluids etc.) A and B respectively. The values α and δ are related by the equation:

$$\alpha_{A-B} = [(\delta_A + 1000) / (\delta_B + 1000)] \qquad \text{(Eqn 1.4)}$$

In some texts the fractionation of a species is expressed as the 'permil fractionation' which is $10^3 \ln \alpha$ as this often provides more convenient numbers to use. In many cases the approximation:

$$\Delta_{A-B} = \delta_A - \delta_B \approx 10^3 \ln \alpha_{A-B} \qquad \text{(Eqn 1.5)}$$

which tells us that the permil fractionation is approximately equal to the difference in δ values.

1.5.2 Isotopic fractionation.

During natural processes the isotopes of oxygen and hydrogen tend to become fractionated because of variations, however small, in their physical and chemical properties. As a result of their low atomic masses these effects can be significant, for instance D is almost twice the mass of H. The fractionation mechanisms are of two types, kinetic and equilibrium. The former case, kinetic fractionation, occurs in fast, one way processes such as evaporation and diffusion and is the result of mass differences in the isotopes. It is generally thought that kinetic fractionation processes are insignificant in high temperature geological processes and so they will not be discussed further. The latter case, equilibrium fractionation, occurs during isotopic exchange reactions and is the result of the different isotopes having different bonding energies. It has been demonstrated (O' Neil 1986) that molecules with the heavier isotopes are generally the more stable, at least in non-organic

environments. Equilibrium fractionation is important in geological conditions involving the partitioning of the isotopes of oxygen and hydrogen.

1.5.3 Factors affecting the fractionation factor under geological conditions.

Several factors can have an influence on the fractionation factor, α, the most important for geological consideration is temperature. In the range of temperatures of geological interest it has been observed (Javoy 1977) that an approximation to a straight line relationship exists between ln α and T^{-2}. On the other hand Graham *et al.* (1980, 1984) have shown from experimental evidence that the isotope fractionation of hydrogen in amphibole-water systems and epidote-water systems is not temperature dependent between 400 to 500°C.

The dependence of the isotope fractionation of oxygen on pressure has been shown empirically by Clayton *et al.* (1975) to be insignificant. This seems to be true for mineral-fluid and for mineral-mineral systems. Little experimental work has been published on the dependence of hydrogen isotopic fractionation on pressure, most workers supposing the effect to be insignificant as with oxygen. Jenkin (1988) in re-examining the data from several authors has tentatively concluded that pressure may have a significant affect on hydrogen isotopic fractionation in mineral-fluid systems in the temperature range 200 to 400°C.

In many cases a dependence of oxygen and hydrogen isotopic fractionation on the chemistry of both mineral and fluid in mineral-fluid systems has been shown to be significant, although subordinate to the affect of temperature.

1.5.4 The influence of mineral chemistry on isotopic fractionation factors.

a) Oxygen. For oxygen isotopic fractionation a general trend is apparent in which those minerals containing Si-O bonds are more ^{18}O rich than those with Al-O bonds which in turn are more ^{18}O rich than those with Fe-O bonds. This is due to the decreasing ionic potential, charge and increasing mass of the Si^{4+}, Al^{3+} and Fe^{2+} ions. Consequently measurable (1.3 to 2.3 ‰) oxygen isotope fractionation occurs between the end members (albite - anorthite) of the plagioclase series (Matsuhisa *et al.* 1979). On the other hand no observable oxygen isotopic fractionation occurs for the muscovite - paragonite series. Although no known experimental data exist it is likely that some observable affect would occur within the amphibole group.

b) Hydrogen. For hydrogen isotopic fractionation conflicting experimental and theoretical data have been published. Suzuoki & Epstein (1976) determined experimentally the following relationship for the hydrogen isotopic fractionation between mica-water and amphibole-water systems which incorporates the temperature and composition:

$$10^3 \ln \alpha_{min\text{-}water} = -22.4\,(10^6\,T^{-2}) + (2X_{Al} - 4X_{Mg} - 68X_{Fe}) + 26.3 \qquad \text{(Eqn 1.6)}$$

where X is the mole fraction of the cation in the octahedral site. It should be noted that there was a mistake in the original equation published by Suzuoki & Epstein (1976) which has been pointed out by Kuroda *et al.* (1986), the original factor of 28.2 should be replaced by 26.3, as above. This amendment is carried through all calculations in this study and the equation will be referred to in this text as the amended Suzuoki & Epstein equation. This relationship has been strongly

criticised. Graham *et al.* (1984) showed that the one hornblende used by Suzuoki & Epstein (1976) was in fact an actinolite. Graham *et al.* (1984) performed detailed experiments into the nature of hydrogen isotopic fractionation in amphibole-water systems using a variety of amphiboles including hornblende. These authors found that the relationship proposed by Suzuoki & Epstein (1976) did not hold for the amphiboles they examined. Graham *et al.* (1984) found that in the temperature range 350 to 650°C no difference could be measured between the permil fractionation factors of the hornblende-water and the tremolite-water systems. The authors produced the following relationships:

for tremolite; $1000 \ln \alpha_{min\text{-}wat} = -21.7 \pm 2$ (Eqn 1.7)

for hornblende; $1000 \ln \alpha_{min\text{-}wat} = -23.1 \pm 2.5$ (Eqn 1.8)

At temperatures in the range 650 to 850°C Graham *et al.* (1984) found hydrogen isotopic fractionation to be a function of temperature. The authors tentatively suggested this was the result of Na substitution into the 'A' site. No conflicting evidence against the amended Suzuoki & Epstein (1976) equation is known for the hydrogen isotopic fractionation of micas.

1.5.5 The influence of fluid chemistry on isotopic fractionation factors.

Graham & Sheppard (1980) measured the hydrogen isotopic fractionation between epidote-pure water and epidote-saline water. The authors found that between 250 and 450°C the saline solutions all concentrated H as opposed to D, with a maximum difference of 12‰. Above 500°C this fractionation was insignificant. Truesdell (1974)

measured the difference in the oxygen isotopic activity (effectively the oxygen isotopic fractionation factor) between pure water and various saline solutions over the temperature range 25 to 275°C. The author found measurable variations with temperature, up to 2‰. If this fractionation effect is widespread it may have important implications as a wide range of 'brines' can occur in geological conditions. Without knowledge of the chemistry of a hydrothermal solution complete interpretation of hydrogen and oxygen isotopic data may not be possible.

1.6 Review of isotopic exchange mechanisms and geologically important diffusion principles.

For both loss of radiogenic Ar from a mineral, and stable isotopic exchange between a mineral and a fluid, the process can occur by one or more of three mechanisms; diffusion, recrystallisation and chemical reaction. For chemical reaction to occur the species involved must be in chemical disequilibrium, on the other hand both diffusion and recrystallisation can occur while the mineral and the fluid are in chemical equilibrium. Cole *et al.* (1983) termed recrystallisation and chemical reaction surface reaction processes. It is obvious that very different geological conditions are necessary if radiogenic isotope loss and/or stable isotope exchange is to proceed by diffusion rather than surface reaction processes. In the latter case, surface reaction processes, the geological environment is likely to be 'active', possibly with progressive regional metamorphism providing strain for mineral recrystallisation and thermal and pressure changes for mineralogical (chemical) reaction. In the former case with diffusion, the environment is more likely to be 'passive', in a steady state. When opening or closing of the K-Ar system is considered it is often thought that simple thermally driven diffusion

controls the loss or retention of the Ar, but it is becoming clear that surface reaction processes within an 'active' environment may play an important, but complex role. However, for many geological considerations, ie. for radiogenic Ar loss and stable isotope exchange, diffusion processes are more important than surface reaction processes.

1.6.1 Diffusion mechanisms and factors affecting diffusion rates in minerals.

The subject of diffusion mechanisms is reviewed in detail by Manning (1974) and only a short summary is given here. In practice, within a rock mass, diffusion occurs by volume diffusion through regions of homogeneous crystal structure and by short-circuit diffusion along paths of easy migration. These paths are surface or line defects such as dislocations or grain boundaries. Volume diffusion mechanisms occur via point defects such as vacancies or interstitial atoms. This is displayed in diagrammatic form in figure 1.4. The diffusion coefficient, D, depends on the activation energy, Q, and the absolute temperature, T, by the equation:

$$D = D_0 \exp(-Q / RT) \qquad \text{(Eqn 1.9)}$$

where R is the universal gas constant and the pre-exponential quantity D_0 is temperature independent. When two or more diffusion mechanisms operate each supplies a separate contribution to D. At low temperatures short-circuit diffusion can normally operate more readily than volume diffusion; in this case short circuit diffusion is dominant. However, at high, geologically relevant, temperatures the effective multitude of possible paths and greater temperature dependence makes

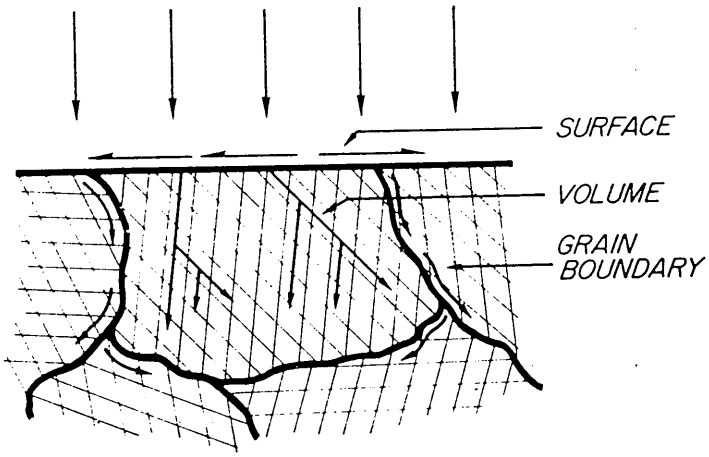

Figure 1.4. Pathways for volume diffusion and short circuit diffusion (grain boundary and surface diffusion). From Manning (1974).

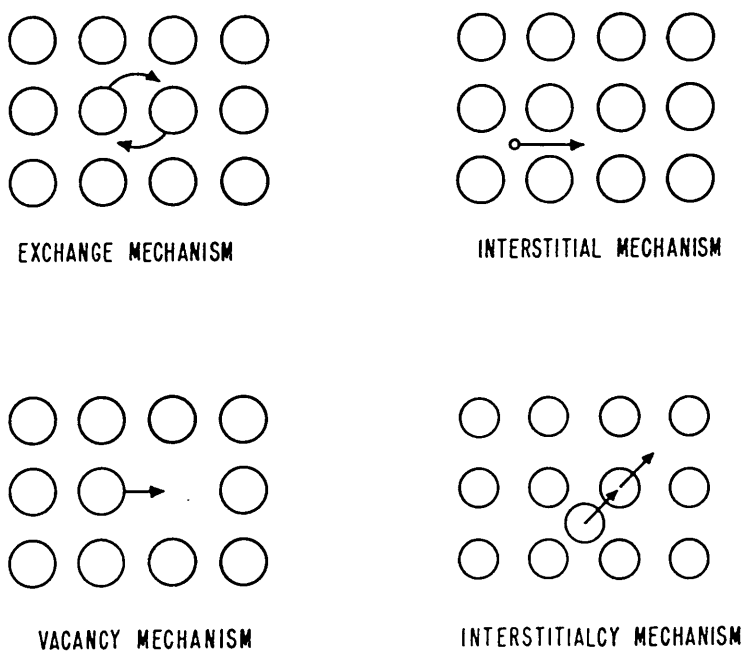

Figure 1.5. Elementary atomic jumps in the four main possible mechanisms for volume diffusion. From Manning (1974).

volume diffusion dominant. However, it must be noted that at any temperature as volume diffusion provides the migrating species from areas of good crystal structure to the surface and line defects for short-circuit diffusion, then volume diffusion will always be the rate limiting step. Consequently for most geological considerations volume diffusion is the most important process. Four types of volume diffusion mechanisms can occur, these are explained below and shown diagrammatically in figure 1.5. Which of these mechanism(s) are dominant for a particular system depends on the nature of both the diffusant, the lattice structure and the temperature:

a) exchange mechanism. This is simply the swapping of the positions of two neighbours, therefore requiring no crystal defect. A variation is the ring mechanism which can involve a larger number of atoms. As both these mechanisms have a large activation energies they are unlikely to be geologically important.

b) interstitial mechanism. Small interstitial atoms can jump between interstitial sites without much affect on the lattice. In this case the interstitial atom is the point defect. Because of the small size of hydrogen atoms it is possible that the interstitial mechanism is one way in which hydrogen isotopes diffuse through a silicate lattice.

c) vacancy mechanism. This depends on point vacancy defects in the lattice, a common feature of natural minerals. Neighbouring atoms can diffuse by jumping into the vacancy possibly invoking a 'domino' effect where many atoms can jump. This mechanism requires less activation energy than the exchange mechanism and is possibly the dominant mechanism for diffusion in geological systems.

d) interstitialcy mechanism. In this case an interstitial atom moves by pushing a lattice atom out into an interstitial site and itself moving into the vacancy created.

Several physical parameters have been proposed to affect the rate of diffusion, and these are discussed below.

a) Temperature. The equation relating the diffusion coefficient to activation energy and temperature has already been given (Eqn 1.9). In this relationship both the pre-exponential factor, D_O, and the activation energy, E, are independent of temperature. The temperature dependence can be explained simply by considering that as the temperature increases more thermal energy can be used to overcome the activation energies for the various diffusion processes and diffusant species. As implied by the relationship (Eqn 1.9) the diffusion rate increases exponentially with increasing temperature. This relationship is often shown graphically in the form of Arrhenius plots, which are; log D v. 1/T. These normally give a straight line, intercepting the log D axis at D_O and with a slope equal to -E/2.303 R.

b) Pressure. It is generally thought that any affect on the diffusion rate to changing pressure is insignificant, a less than measurable affect. Two experimental studies have been published with results purporting to show measurable changes in diffusion rate with pressure: the first, Yund & Anderson (1978) who measured oxygen diffusion in andularia in saline solution and recorded an order of magnitude increase in their diffusion rate with a pressure increase of 125 to 4000 bars; the second, Giletti & Yund (1984) observed an order of magnitude increase in the oxygen diffusion rate in quartz in water over a pressure range of 250 to 3500 bars. These results have not been confirmed by other workers and it is

generally thought that that these results are the consequence of some other spurious parameter not controlled in the experiments.

c) Grain size. The actual diffusion rate is not dependent on the grain size. However, for a diffusant with a concentration gradient in a silicate lattice the time taken by that diffusant to become distributed homogeneously is dependent on the size of the grain. This is true for either diffusion of radiogenic Ar out of a mineral grain or for exchange of oxygen or hydrogen between a mineral and fluid in isotopic disequilibrium. Most natural minerals contain line and surface defects and once a diffusant has reached these by volume diffusion then short-circuit diffusion can be considered to rapidly take that diffusant out of the system. Consequently, the actual grain size may be unimportant, rather the effective grain size determined by cleavages, dislocations etc. is the dominant factor. Dodson (1973) incorporated into his mathematical treatment of closure temperatures the effective grain size.

d) Grain shape. Due to the fact that natural minerals normally have lattices that are constructed differently along the 'a', 'b' and 'c' crystallographic axis the diffusion coefficient shows anisotropy within these lattices. Giletti & Yund (1984) show that oxygen diffusion in quartz proceeds 2 to 3 times faster parallel to the 'c' axis than normal to the 'c' axis. It is generally supposed that the same is true for diffusion of radiogenic Ar out of many mineral species. For modelling diffusion throughout silicate lattices three basic shapes are considered which can be related to crystal lattice anisotropy. These models are shown diagrammatically in figure 1.6.

Plate (sheet) model: In this case diffusion is thought to occur in only one dimension, normal to two parallel infinite plates. This model is

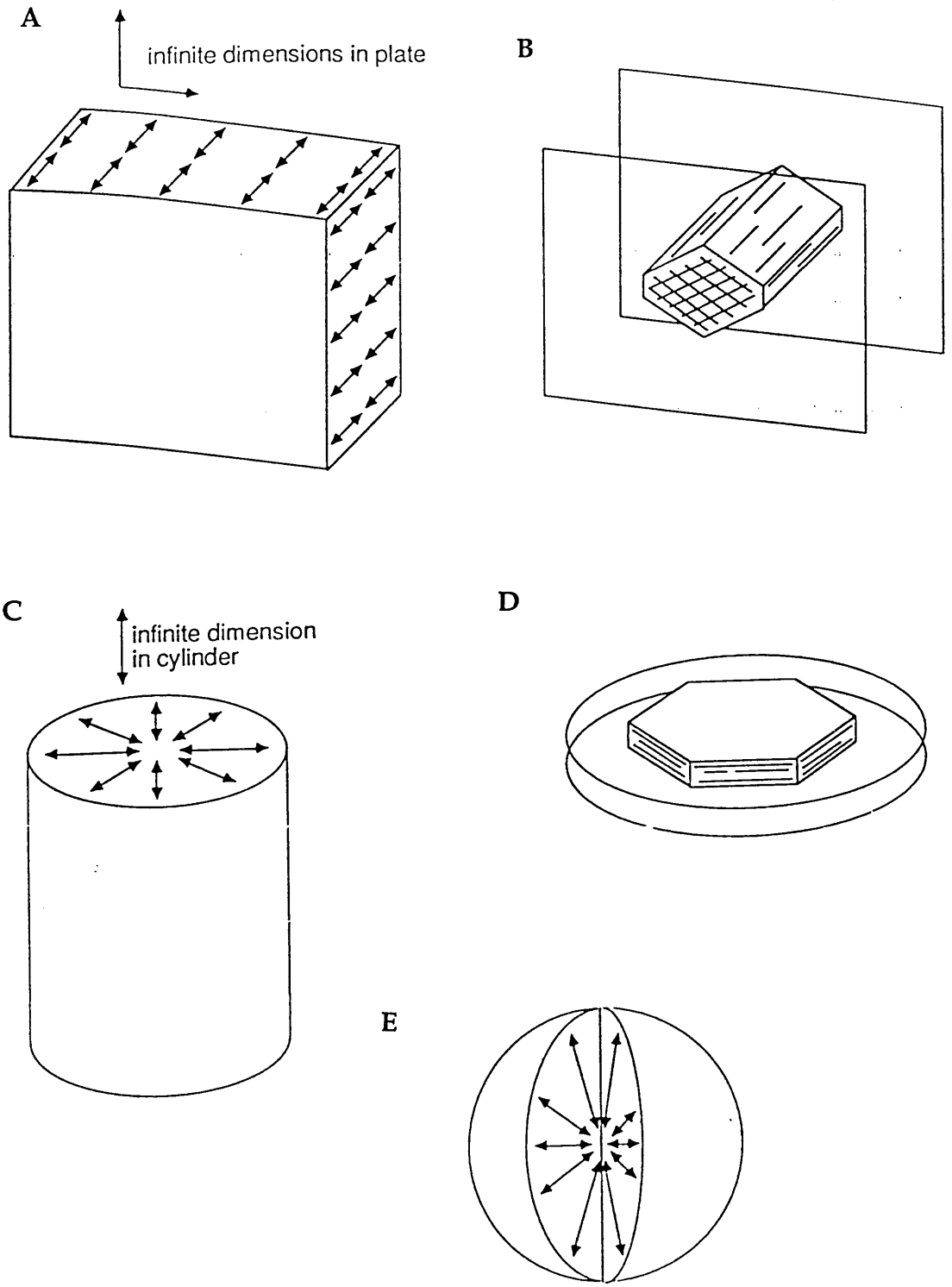

Figure 1.6. The three models of volume diffusion geometry. The double headed arrows show the net diffusion paths. A) Plate model. B) Plate model applied to amphibole. C) Cylinder model. D) Cylinder model applied to mica. E) Spherical model. After Jenkin (1988).

thought appropriate to describe diffusion in amphibole, where the transport direction is predominantly parallel to the twin chains.

Cylinder model: In this case diffusion takes place radially from the axis of a cylinder to the curved surface or the other way around. This model describes diffusion in micas where the transport direction is parallel in all directions to the mica sheets.

Spherical model: This is the simplest model which assumes that diffusion is equally rapid in all directions. Although this may not be directly analogous to natural mineral systems this model is often used to describe natural processes because of the simpler mathematics required.

e) Other factors that have been proposed that may have an effect on the diffusion rate include: the impurity content of the lattice, (impurities act as point defects which enhance volume diffusion) and radiation damage where crystal lattices are disrupted by impact of α particles from natural decay of U etc. in neighbouring or enclosed zircons, apatites etc. These two factors while they may be important in certain, unusual, geological conditions are not thought to be generally significant. It must be stressed, however, that this has not been quantitatively proved.

CHAPTER TWO:

SAMPLING PROCEDURES, PETROGRAPHIC AND GEOCHEMICAL SAMPLE CHARACTERISATION.

2.1 Introduction.

The first section of this chapter describes the rock sampling programme in relation to the aims of the overall project (section 1.1). The following two sections detail the petrographic and geochemical information acquired during sample analysis. The geochemical data that are given in this chapter have been obtained using a range of techniques including; electron-probe analysis, ion-probe analysis and transmission electron-microscopy (TEM). This information is described prior to the isotopic data given in chapters three and four because it was concluded in section 1.4.2 that full geochemical characterisation of samples is necessary before any meaningful interpretation of isotopic data can be performed.

2.2 Sampling programme.

Samples were collected in a pattern and from sites that were most likely to help fulfil the aims of the project, listed in section 1.1. All the sample locations with grid references are given in appendix A.1. and are indicated on a map, figure 2.1. Also shown on this map are two areas labeled A and B, which have greater sample density. These areas are discussed in detail in section 3.1.1. In general, samples were taken from any rock type if it contained biotite, muscovite or hornblende. Where possible, several samples from different lithologies were collected from

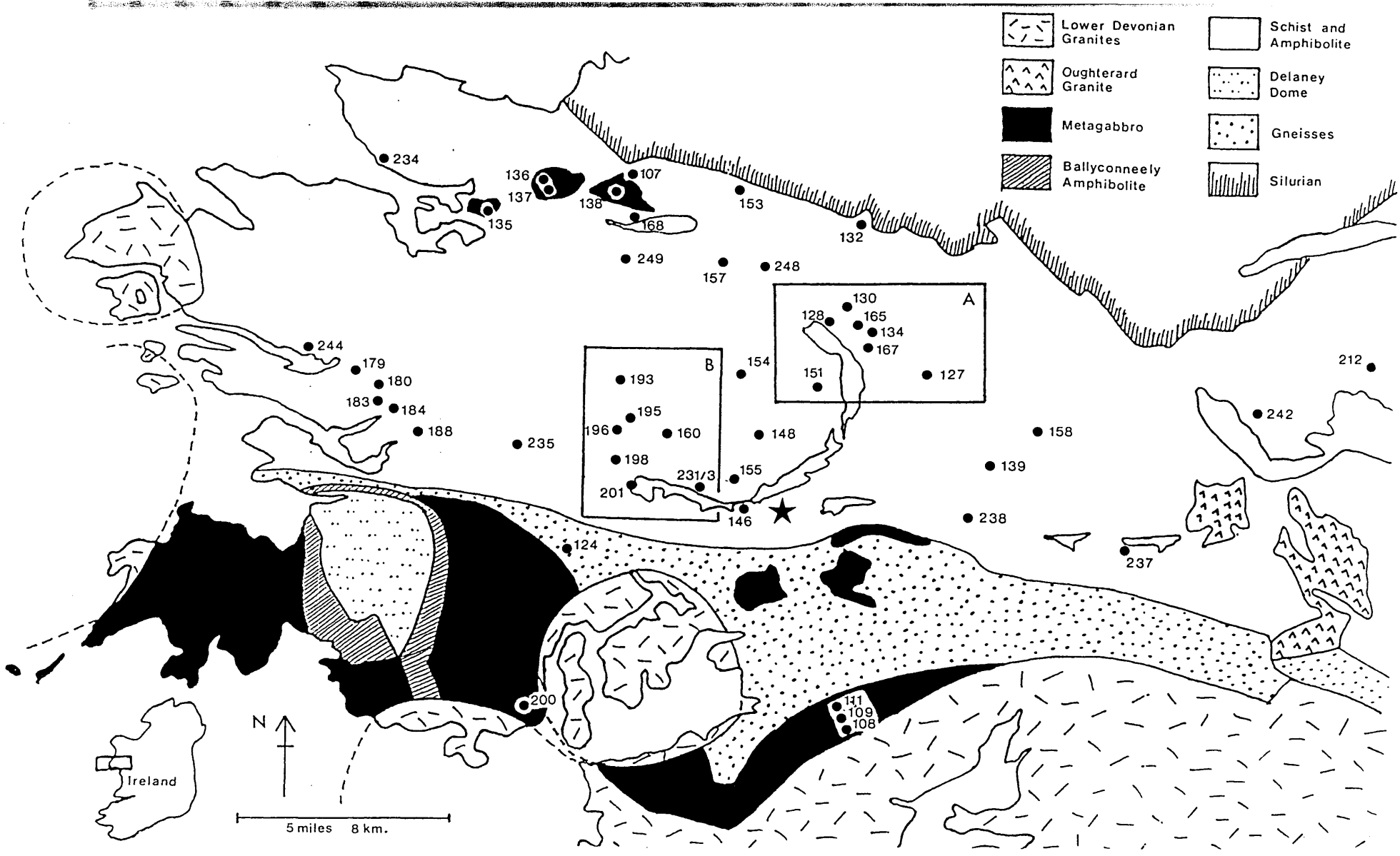

Figure 2.1. Sketch geological map showing all the sample locations. All sample numbers are prefixed by WM. The exact grid references are given in appendix A.1. The star marks the location of the quarry from which samples 119 and 220 to 228 were collected. Areas A and B are discussed in detail in section 3.1.1.

the same location to obtain mica and amphibole. Some of the schist samples contain both muscovite and biotite. Unfortunately, although amphibolites do exist that contain both hornblende and biotite the latter is generally too chloritised to be worth dating. The sampling procedure can best be considered in five parts:

1) General sampling of a large number of widely spaced sites from the whole of Connemara. These samples would be expected to reveal (possibly with consideration of the data from Elias (1985)) any geographical trend to the ages or correlation with geological features that has not been seen in the data of previous workers because of their smaller number of samples. In some cases samples were collected from the same locations sampled and dated by Elias (1985), this repetition was deliberate in order to assess the comparability of ages from the two studies. For the most part areas adjacent to the Oughterard Granite and the Galway Granite and its satellite plutons were avoided because of potential problems with thermal resetting.

2) Closely spaced sampling from sites in a traverse near to the Athry Slide, area B on figure 2.1. A specific aim of the project was to assess the importance of the slide zones and their potential for tectonic influence on the K-Ar ages. This traverse roughly followed the road to Barnanoruan and the road to Ballynahinch Castle. Mostly mica schists were sampled but some amphibolites were also collected. The closest sample in the traverse (WM 201) to a granite is c. 2.5 km away from the contact and this is considered distant enough to avoid any potential effects from thermal resetting.

3) Closely spaced sampling from within one small (<30m wide) quarry, to assess the variability of the chemistry of micas and amphibole

and their K-Ar ages at the outcrop scale. A particular quarry was chosen in the southern part of the Connemara Schists that contained both mica schist and amphibolite horizons so that fresh hornblende, muscovite and biotite could be sampled. The quarry is sufficiently distant from the large granites, c. 5 km, to avoid any problems associated with thermal resetting. This quarry is marked by a star on figure 2.1.

4) Samples were collected from the metagabbro-gneiss complex rocks at Dawros-Currywongaun-Doughruagh, in the north of Connemara, and at Errisbeg in the south for comparison with the ages obtained from other parts of the metagabbro-gneiss complex by other workers as a test for the contemporaneity of the whole complex.

5) Three metagabbro-gneiss complex rocks were collected close to the contact with the Galway Granite in an area some 5 km SE of Cashel to determine the extent to which the K-Ar 'clocks' in hornblende were thermally disturbed by the intrusion of the Galway Granite and its satellite plutons.

In all cases the areas around the sample sites were scouted to ensure no dykes or other complicating features that could affect the ages were present. Generally several kilograms of rock were taken from each location and the weathered rim trimmed off in the field. Sample preparation procedures adopted in the laboratory are given in appendix A.3.1

2.3 General sample petrography.

No attempt is made here to give a full account of each individual sample. Brief petrographic descriptions of each sample are given in

appendix A.2, only general observations are made here. Photomicrographs of representative samples of each rock type are displayed in figures 2.2 to 2.5.

1) Metasediments: These are the Connemara Schists. The metasediment nomenclature is that of Leake (1969) which uses the following classifications. Semi-pelites (more than 33% quartz and feldspar), pelites (less than 33% quartz and feldspar), siliceous granulites (with 50 to 75% quartz) and quartzites (more than 75% quartz). The semi-pelite, pelites and siliceous granulites can be found grading into each other in the field and so this classification is purely arbitrary. The quartzites on the other hand can be mapped separately, these belong to the Bennabeola Quartzite Formation, and they do not grade into any other lithology. The mineralogy of all these rock types is as follows: Semi-pelites; 30 to 40% quartz, 25 to 35% plagioclase (oligoclase-andesine), 10 to 25% biotite, 10 to 30% muscovite with variable amounts of accessory orthoclase, garnet, zircon, apatite, epidote, sillimanite, cordierite, calcite and opaque minerals. Pelites; 20 to 30% quartz, 20 to 40% plagioclase (oligoclase-andesine), 10 to 40% biotite, 10 to 30% muscovite with variable amounts of accessory orthoclase, garnet, zircon, apatite, epidote, sillimanite (up to 10%), tourmaline, graphite and opaque minerals. A typical pelitic schist is shown in figure 2.2. Siliceous-granulites; 50 to 60% quartz, 15 to 20% plagioclase, 15 to 20% biotite, 0 to 30% muscovite with variable amounts of accessory zircon, apatite, garnet, tourmaline and opaque minerals. Quartzites; 75% or more quartz, 5 to 20% plagioclase (oligoclase-andesine), 5 to 15% muscovite with variable amounts of accessory orthoclase, biotite, zircon, apatite, haematite, rutile and opaque minerals. In all these rock types the feldspar is ubiquitously sericitised and saussuritised to varying degrees, sometimes completely altered. The

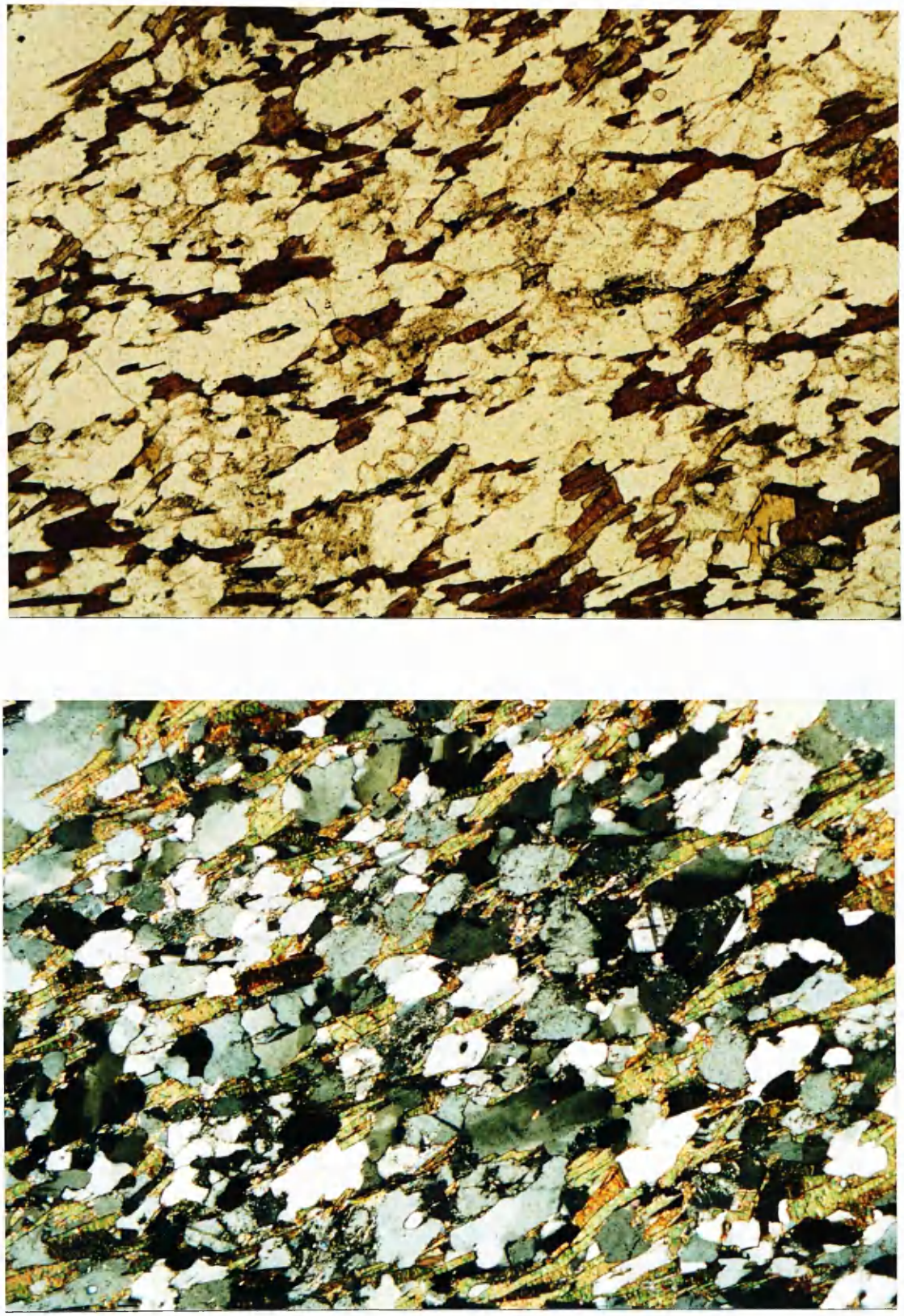

Figure 2.2. Pelitic schist, WM 227. Top view in plane polarised light, lower view in crossed polarised light. Note the biotite is slightly chloritised and the feldspar is partly sericitised and saussuritised. The long axis is 1 cm.

biotite frequently shows varying degrees of chloritisation, sometimes completely altered, often with accompanying leucoxene. In some samples epidote is seen growing along the cleavages of the biotite. There is a general correspondence between the degree of alteration of the feldspar and the biotite in each sample. The alteration of these minerals is evident in the photomicrographs. The muscovite in some samples, particularly those from the quartzite, has a pale green colour in plane polarised light and this is even more noticeable in the mineral separates. This colour is likely to be caused by the high concentration of FeO in the mineral. Often the biotite and muscovite occur together as 'fish'. The cordierite found in some of the pelites and semi-pelites is usually heavily altered to pinite which makes identification difficult. The sillimanite shows varying degrees of alteration to sericite.

2) Amphibolites: These rocks are usually found in association with the Lakes Marble Formation and occur more frequently in the southern part of the Connemara Schists. These are the striped amphibolites of Evans & Leake (1960) to which the reader is referred for more detailed accounts of the amphibolite petrography and chemistry. This striping is a result of syn-metamorphic movement but in some cases the amphibolites are 'massive' with little or no apparent striping. These rocks contain 10 to 70% amphibole, 20 to 40% plagioclase (andesine), 0 to 20% quartz with variable amounts of accessory biotite, apatite, epidote, sphene, carbonate and opaque minerals. Amphibolites are shown in figures 2.3 to 2.5. The striping in the amphibolites is composed of alternate 'amphibolite' layers, described above, and amphibole poor layers containing up to 20% diopside. The amphibole is commonly 'hornblende' but cummingtonite and actinolitic amphibole do occur (see section 2.4.2 for electron-probe analyses and corresponding nomenclature

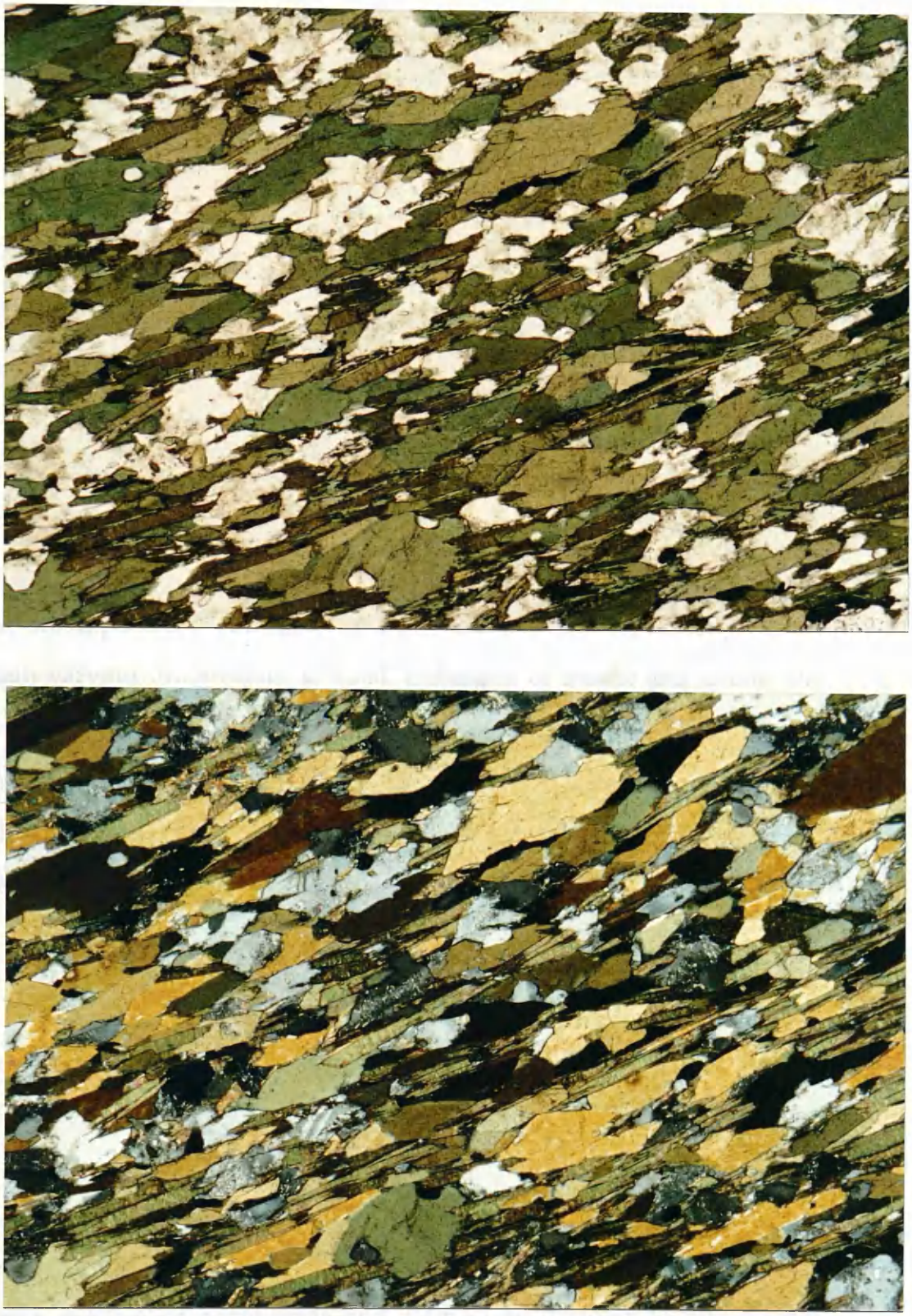

Figure 2.3. Amphibolite, WM 235. Top view in plane polarised light, lower view in crossed polarised light. Note the good alignment of the hornblende and the biotite. The biotite is noticeably chloritised and the feldspar is partly sericitised. The long axes are 1 cm.

of samples). In some samples hornblende and cummingtonite co-exist. This seems to be most common in samples from an area to the north-east of Lough Inagh and is seen in samples WM 128, WM 165 and WM 167. The amphibole grains are usually sub- to euhedral and in most samples display a strong schistosity. Grain size is commonly from 1/4 to 2mm, but a few grains up to 6mm occur. The amphibole in some samples shows 'patchy' and 'streaky' birefringence, the latter occurs as fine zones along the cleavages which can not be put to extinction under the microscope. This is thought to result from the alteration of the amphibole to fine grained biotite which is sometimes seen better developed elsewhere in the slide and is usually partly chloritised. Epidote often accompanies biotite growth along the cleavages. The amphiboles contain varying proportions of small inclusions of quartz and zircon, the latter causing obvious pleochroic haloes. In some samples partial recrystallisation of the amphibole has occurred. The plagioclase is usually partly sericitised, sometimes it is completely altered. When biotite occurs in the amphibolites it is strongly chloritised, often completely so, figure 2.3.

3) Metagabbro-gneiss complex rocks: A review of current understanding of the metagabbro-gneiss rocks was published by Leake (1989). For a detailed account of the petrography the reader is referred to this and references therein. These rocks are a sequence of meta-igneous rocks ranging from ultrabasic through intermediate rocks to acid ortho-gneisses and trondjhemites. The metagabbros are principally hornblende gabbros, containing hornblende and plagioclase (bytownite-labradorite) with accessory chloritised biotite, epidote, quartz, zircon and opaque minerals. The hornblende is partly igneous, partly metamorphic replacing olivine, orthopyroxene, clinopyroxene and plagioclase. In most

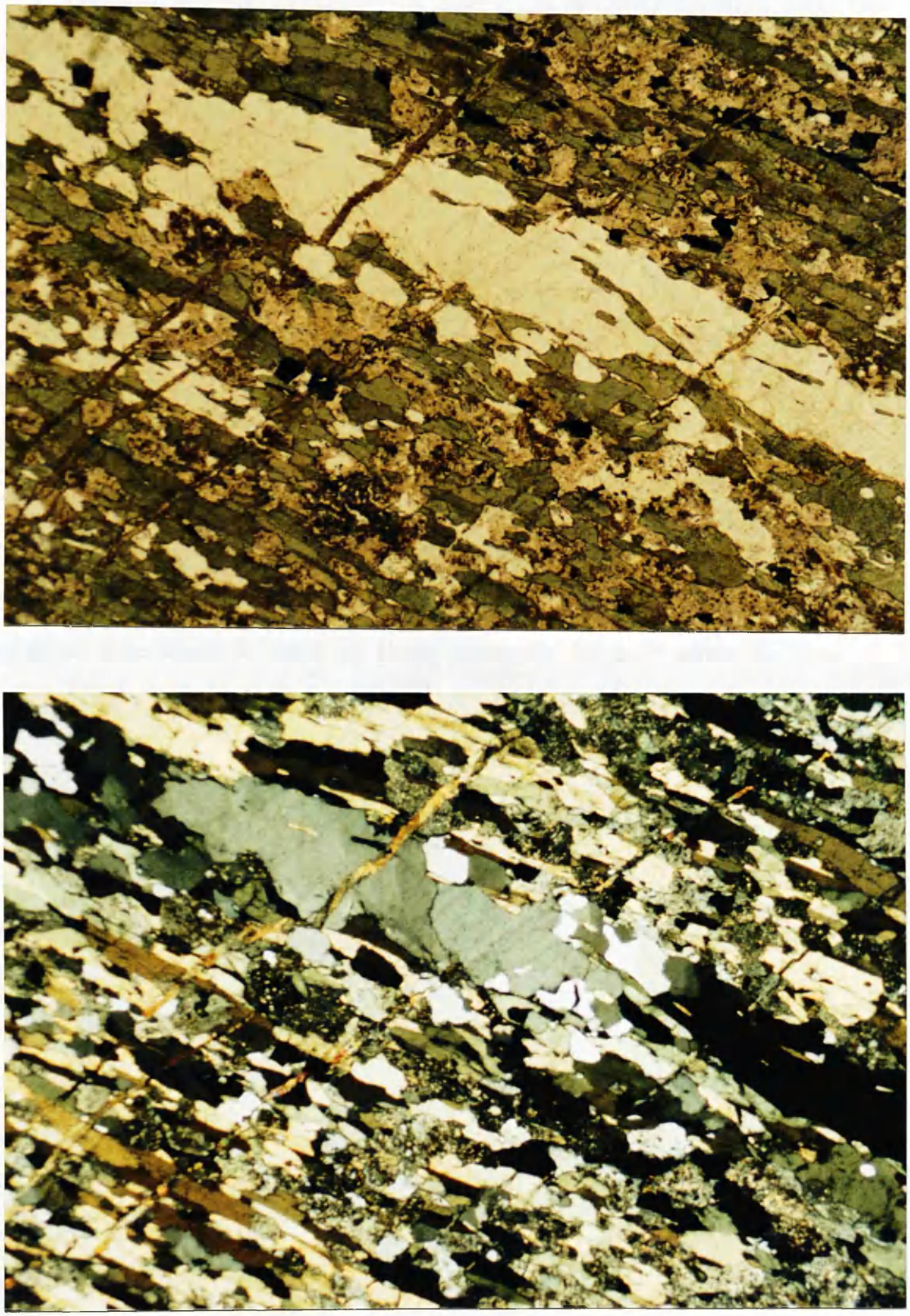

Figure 2.4. Amphibolite, WM 139. Top view in plane polarised light, lower view in crossed polarised light. The infilled microcracks contain mostly calcite with lesser quartz and epidote. The long axes are 1 cm.

samples the hornblende is partly altered to biotite (variably chloritised) and epidote. The plagioclase is also extensively altered to sericite and saussurite, generally the plagioclase in the amphibolites is more altered than the plagioclase in the schists. This alteration of hornblende and plagioclase is due to a later event than the one which caused replacement of olivine to form the metamorphic hornblende.

From the petrography of all the Connemara samples it becomes abundantly clear that significant retrogressive hydrous alteration of all of the rock types has occurred. Mineralogically the evidence for this is alteration of biotite to chlorite, hornblende to chlorite and epidote, plagioclase and orthoclase to sericite and saussurite, cordierite to pinite and sillimanite to sericite. There is a rough correlation between the degree of alteration of each of these minerals in each sample. This suggests all the retrogressive reactions occurred at the same time.

Frequent sealed microcracks indicate that significant net movement of fluid has occurred throughout these rocks. The microcracks seen in thin section are quite narrow, normally less than 1 mm wide, although much wider veins are seen in the field. The infilling minerals include quartz, calcite, epidote and minor feldspar and amphibole. In thin sections exhibiting filled microcracks the retrogressive alteration of the whole slide is more pronounced. Normally plagioclase is extensively altered for about 2 cm either side of microcracks, figures 2.4 and 2.5. On the other hand, when an amphibole grain is cut by a microcrack only a narrow (1 to 2 mm) reaction rim exists, beyond this the grain appears, optically, to be unaltered, figure 2.5. Microcracks sometimes parallel each other, a few centimetres apart. In some thin sections and in the field, veins and microcracks are seen to cross cut each other, but this is not common. This may imply that all the veining is coeval, occurring during

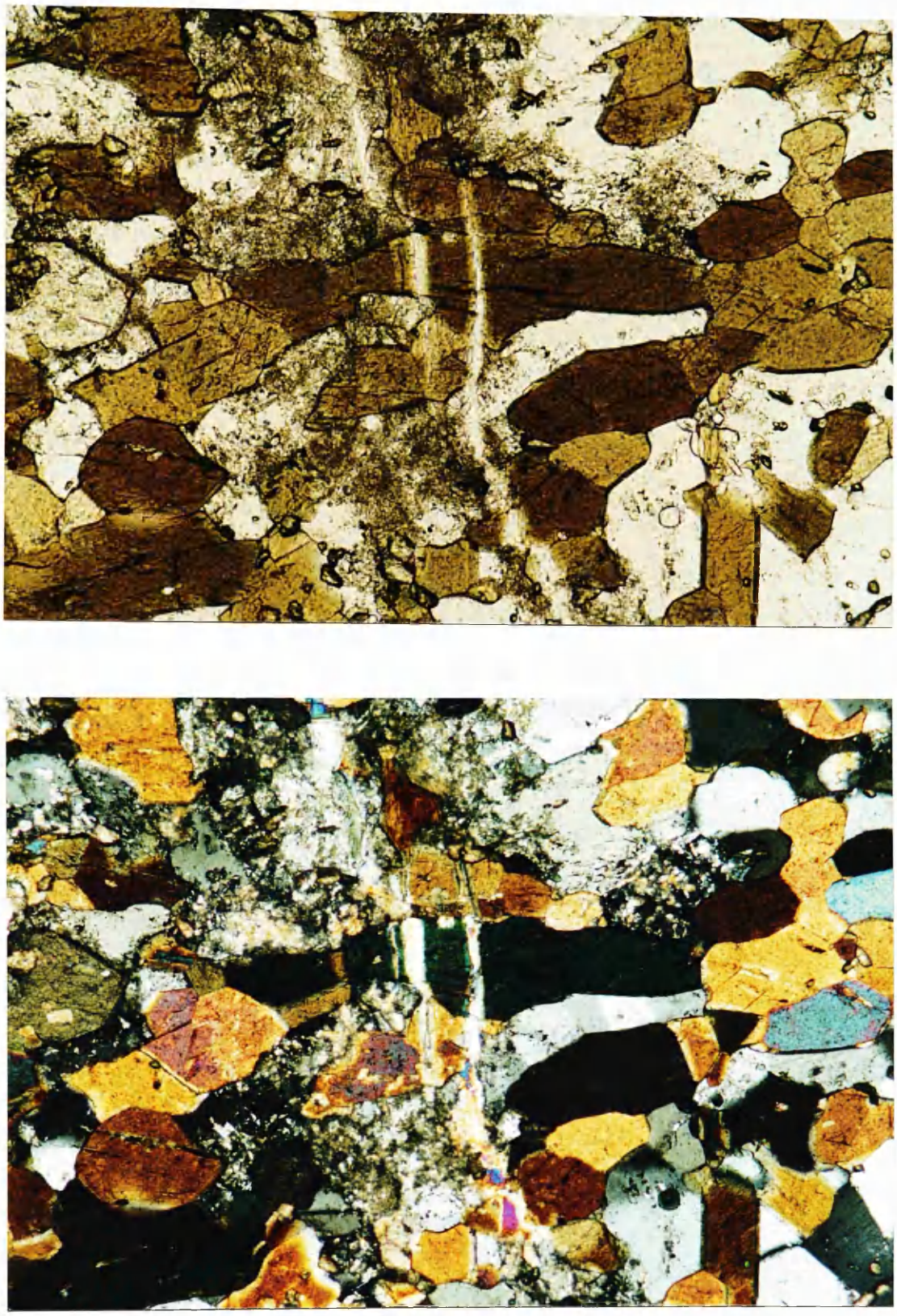

Figure 2.5. Amphibolite, WM 237. Top view in plane polarised light, lower view in crossed polarised light. Note the considerably increased sericitisation along the length of the veins and the apparently unaltered hornblende. The vein infilling material is epidote, chlorite with some amphibole. The long axis is 0.5 cm.

the imposition of a single stress event. Although veins and microcracks occur in all the rock types they are more common in the amphibolites within the Lakes Marble Fm, which suggests that fluid flow was lithologically controlled. Independent evidence that the Lakes Marble Formation was an important aquifer comes from Yardley (1989 and *pers. comm.*) who shows, from whole rock $^{87}Sr/^{86}Sr$ and $\delta^{18}O$ values, that these rocks "focussed massive water flow". Yardley (1989) followed, isotopically, a marble aquifer for more than 10 km and showed that fluid flow was essentially along beds, although some breakouts did occur.

The degree and abundance of retrogressive alteration and infilled microcracks in each sample is indicated in the following table (table 2.1) which gives a subjective alteration index for the feldspar and biotite and lists any infilling vein minerals. This exercise obviously can only give a rough approximation to the abundance of alteration and veining in the outcrop from which the samples were acquired because only one or two thin sections were examined per sample; however the following list will hopefully indicate the relative degree of alteration between samples.

Table 2.1. Plagioclase and biotite alteration indexes. The numbers in the table under plagioclase (PLAG) and biotite (BIOT) are the alteration indexes and indicate the degree of alteration: 0 = fresh to slight alteration; running to 3 = strongly to completely altered. The Y or N under epidote (EPI) indicates the presence or otherwise of epidote in the thin section. MS = mica schist, Q = quartzite, A = amphibolite, MGS = metagabbro-gneiss complex. Vein minerals: q = quartz; epi = epidote; cal = calcite; chl = chlorite; amph = amphibole.

	ROCK	DATED	ALT. INDEX			VEIN
SAMPLE	TYPE	MINERAL	PLAG	BIOT	EPI	MINERAL
WM 107	A	BIOT	1	0	N	-
WM 108	MGS	AMPH	2	-	Y	-
WM 109	MGS	AMPH	1	-	N	-
WM 111	MGS	AMPH	2	-	Y	q, epi

WM 119	no thin section, pegmatitic mica books collected.					
WM 124	A	AMPH	2	-	Y	epi
WM 127	MS	MUSC	3	2	Y	-
WM 128	A	AMPH	2	2	N	Fe
WM 130	MS	BIOT	1	0	N	-
WM 132	MS	MUSC	1	3	N	-
WM 134	Q	MUSC	2	-	N	-
WM 135	MGS	AMPH	3	-	Y	epi, amph
WM 136	MGS	AMPH	1	-	Y	q, epi, cal
WM 137	MGS	AMPH	2	-	Y	epi
WM 138	MGS	AMPH	2	-	Y	-
WM 139	A	AMPH	3	-	N	q, cal
WM 146	A	AMPH	1	2	Y	q, cal
WM 148	MS	BIOT	2	2	Y	-
WM 151	MS	MUSC	3	3	N	-
WM 153	MS	MUSC	1	2	N	-
WM 154	Q	MUSC	2	2	N	-
WM 155	A	AMPH	3	3	Y	-
WM 157	Q	MUSC	3	-	N	-
WM 158	MS	BIOT	2	1	Y	-
WM 160	Q	MUSC	3	-	N	-
WM 165	A	AMPH	1	-	Y	q, epi, Fe
WM 167	A	AMPH	3	-	N	-
WM 168	MS	MUSC	2	3	N	-
WM 179	MS	BIOT	2	2	N	-
WM 180	Q	MUSC	0	-	N	-
WM 183	A	AMPH	3	-	Y	q, epi, Fe
WM 184	MS	BIOT	3	3	Y	-
WM 188	MS	BIOT, MUSC	2	3	N	-
WM 193	MS	BIOT, MUSC	0	1	Y	-
WM 195	Q	MUSC	2	-	N	-
WM 196	MS	BIOT, MUSC	3	3	N	-
WM 198	MS	MUSC	1	1	Y	Fe
WM 200	MGS	AMPH	1	2	Y	q, chl
WM 201	A	AMPH	3	-	Y	q, cal
WM 212	MS	BIOT	1	1	N	-
WM 220	A	AMPH	2	-	Y	epi, cal, chl
WM 221	MS	MUSC	3	3	Y	cal
WM 222	MS	MUSC	1	1	Y	-
WM 223	MS	MUSC	1	2	N	q, cal
WM 224	A	AMPH	3	-	N	q, epi
WM 225	A	AMPH	1	-	N	-
WM 226	MS	MUSC	0	1	Y	q, epi
WM 227	MS	BIOT	1	0	Y	epi
WM 228	A	AMPH	2	3	Y	-
WM 231	MS	BIOT	2	2	Y	-
WM 232	A	AMPH	2	3	Y	-
WM 233	MS	BIOT	1	1	Y	-
WM 234	A	AMPH	3	3	Y	q, epi, amph
WM 235	A	AMPH	0	2	N	-
WM 237	A	AMPH	2	-	Y	q, epi, amph

WM 238	A	AMPH	2	2	N	-
WM 242	A	AMPH	2	3	Y	-
WM 244	A	AMPH	2	1	Y	-
WM 248	A	AMPH	3	3	Y	epi
WM 249	A	AMPH	2	-	N	-

2.4 Geochemical sample characterisation.

2.4.1 X-ray diffraction (XRD) analysis.

For both K-Ar radiometric dating and stable isotopic analysis mineral separates need to be as pure as possible. In general, for K-Ar studies, researchers aim to produce separates that are better than 99% pure. Simple optical examination of the mineral separates, using a binocular microscope, is the standard way of determining sample purity but this is not ideal because it may not reveal minor impurities that are intergrown with the sample. As an additional check of purity aliquots of all the mineral separates were analysed by XRD.

In several of the biotite separates XRD analysis revealed some chlorite impurity that was not seen during optical examination with the binocular microscope even though some chlorite was evident in the thin section. The reason for this is simply that the chlorite and biotite are intergrown, with the chlorite replacing the biotite. Under examination with the binocular microscope the dark brown of the biotite masks the light green colour of the chlorite. An example of a biotite XRD trace showing some chlorite contamination is given in figure 2.6. When XRD analysis of biotite revealed substantial chlorite contamination the separate was recrushed and passed through the separation procedures again. Both chlorite and biotite are similar intensity X-ray emitters, consequently small concentrations of chlorite in a chlorite-biotite mixture

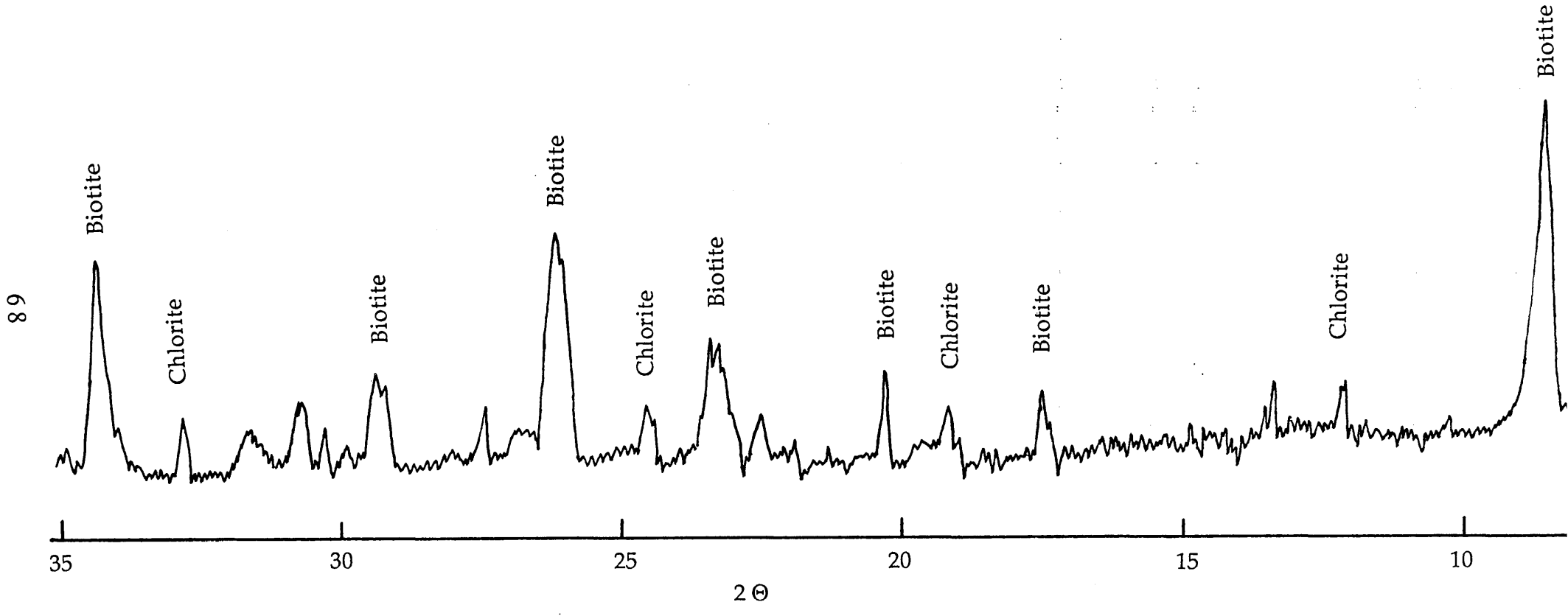

Figure 2.6. Line copy of a photographically reduced XRD trace of a biotite mineral separate from WM 179. There are some chlorite peaks in this trace.

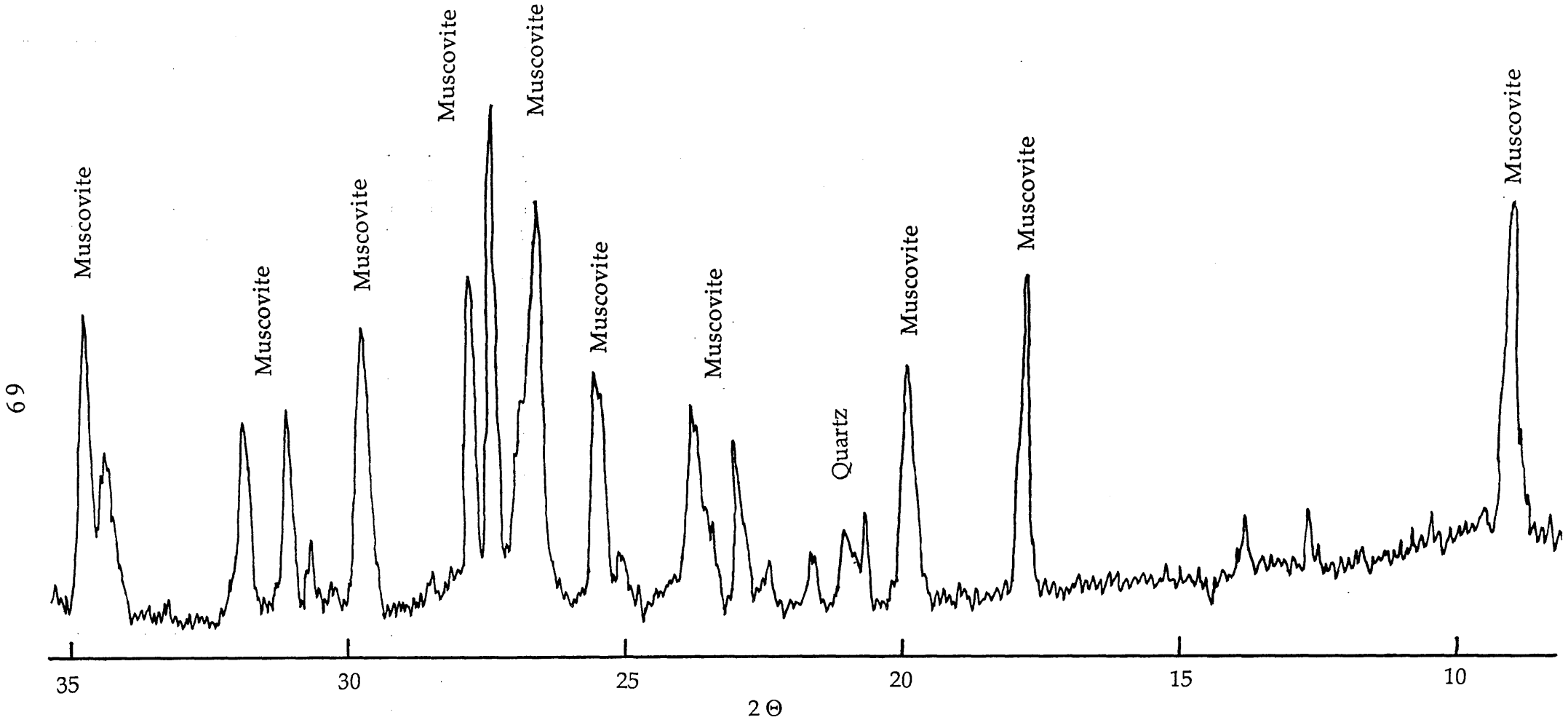

Figure 2.7. Line copy of a photographically reduced XRD trace of a muscovite mineral separate from WM 127. There is a small quartz peak in this trace.

will be detected by XRD. Although no investigation of the lower detection limit was made it is usually taken by XRD workers to be 1 to 2 wt.% chlorite. Even after recrushing, some biotite samples still showed chlorite contamination when re-analysed by XRD. This contamination could not be realistically removed; this would require crushing the sample so fine as to be useless for further analysis. Consequently, some of the biotite samples that were later dated by the K-Ar method did contain measurable amounts of chlorite, the likely effect of this on the K-Ar ages is discussed in section 3.1.6.

XRD analysis of muscovite mineral separates revealed that the only contaminant was fine quartzo-feldspathic grains that occurred in only a few samples. In most cases this contaminant was then either removed or reduced by further passes through the magnetic separator. In all cases the final muscovite separates were 99% pure or better. An example of a muscovite XRD trace is given in figure 2.7.

Analysis of the amphibole separates by XRD was less useful than for the micas. It has already been mentioned (section 2.3) that thin section examination revealed that in some samples the amphibole has fine biotite, chlorite and epidote growth along cleavages. Only in a few cases did XRD analysis of the amphibole separates indicate either chlorite or biotite contamination. It was generally found that chlorite occurred more frequently in the hornblendes from the metagabbro-gneiss complex while hornblendes from the amphibolites contained more biotite. An example of an amphibole sample with biotite contamination is shown in figure 2.8. In these cases the samples were recrushed and passed through the separation procedure again. It is known that amphibole is a strong X-ray emitter in comparison to chlorite or biotite by virtue of the different crystalline structures, consequently much more chlorite can reside in a

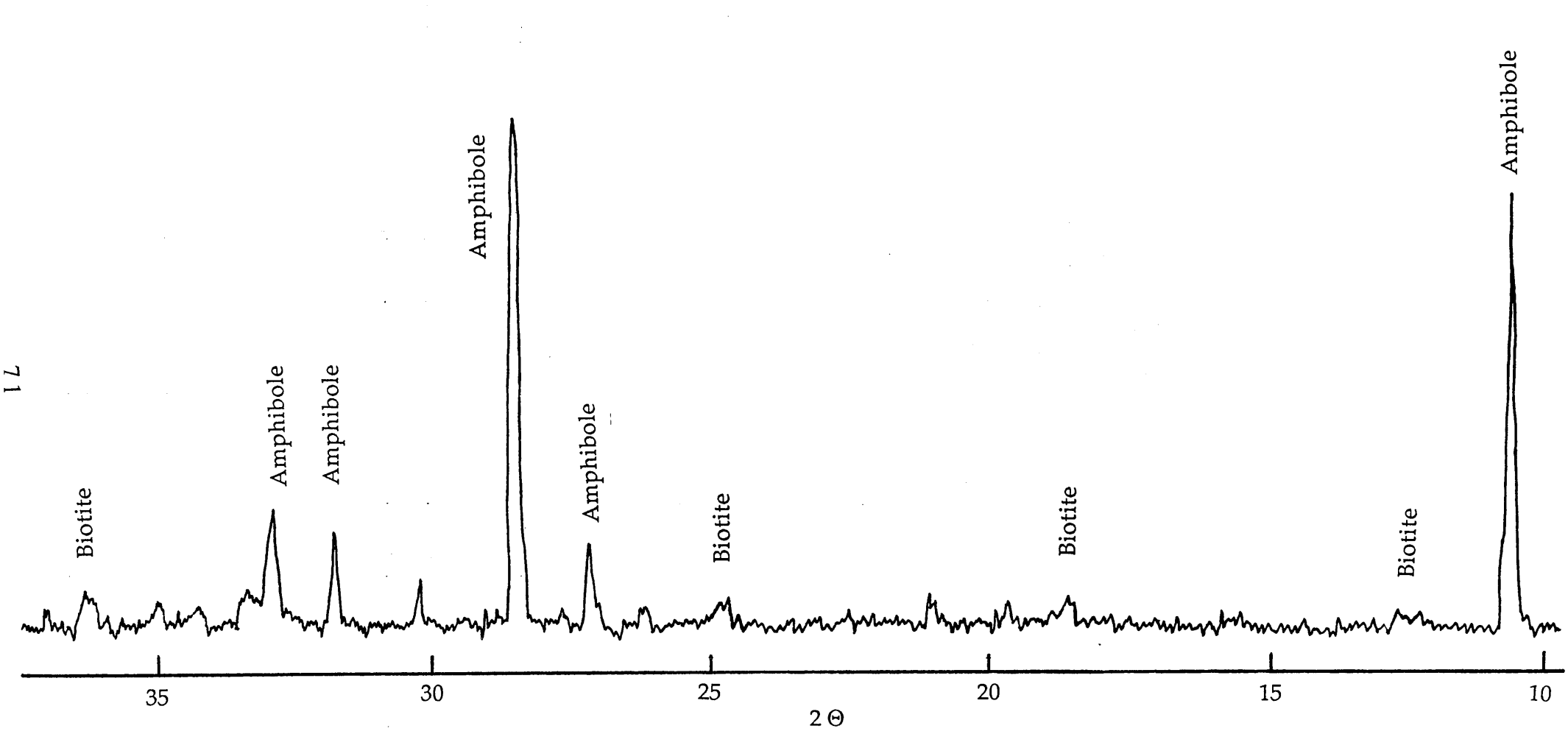

Figure 2.8. Line copy of a photographically reduced XRD trace of an amphibole mineral separate from WM 220. There are small biotite peaks in this trace.

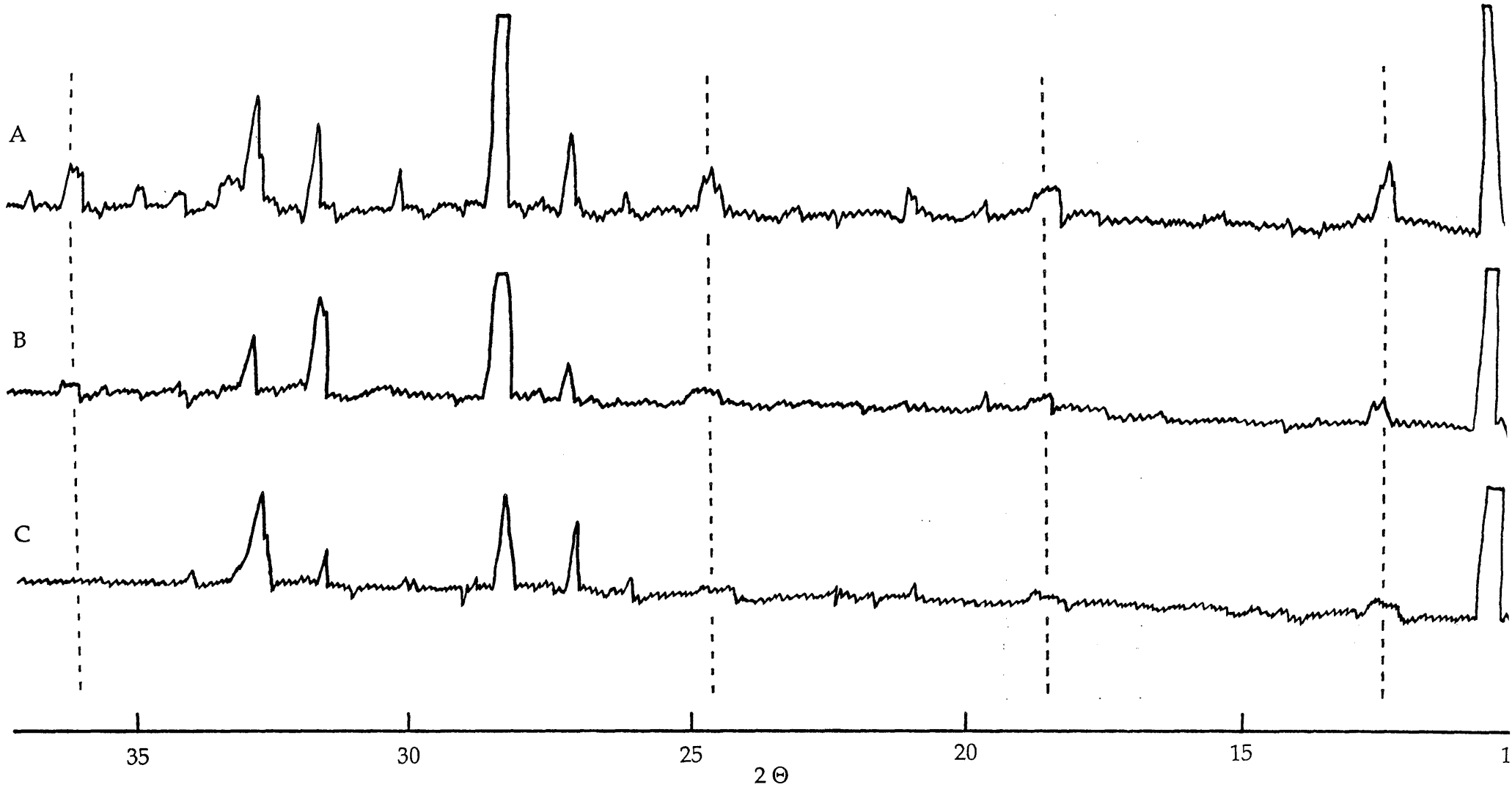

Figure 2.9. Line copies of photographically reduced XRD traces of hornblende-chlorite mixtures. A) 7 wt.%. chlorite, B) 5 wt.%. chlorite, C) 2 wt.%. chlorite. The dashed lines indicate the 2 Θ angles for the characteristic chlorite peaks. All other peaks are amphibole.

chlorite-amphibole mixture without detection than in a chlorite-biotite mixture. To estimate the lower detection limit of chlorite in amphibole, mixtures of 2wt.%, 5wt.% and 7wt.% chlorite were prepared from standard mineral separates. No chlorite peaks were seen in the 2wt.% sample, small peaks seen in the 5wt.% sample and obvious peaks in the 7wt.% sample. Line drawings of the XRD traces of these standard mixtures are given in figure 2.9. Assuming the intensity of the X-ray emissions of the standard minerals are similar to the Connemara samples it is concluded that the lower detection limit of chlorite in a chlorite-amphibole mixture is 4 to 5wt.%. This lower detection limit will also apply to biotite-amphibole mixtures as biotite and chlorite are similar intensity X-ray emitters. As 5% alteration of the amphibole would be detected during thin section examination the upper purity limit is not indicated by XRD but by optical examination and this is taken to be 98% pure or better in most cases. Only 98% is quoted because 1 to 2% contamination might not be seen in the thin section if it was finely disseminated along the cleavages.

2.4.2 Electron-probe analysis.

Electron-probe analyses were used to determine the extent to which each mineral species is chemically heterogeneous, as chemical heterogeneity is an important factor in comparative interpretation of K-Ar ages and stable isotopic data. The sample preparation and analysis procedures for the electron-probe are given in appendix A.3.3. Several analyses were performed on a number of individual grains from each sample. These analyses have been combined to give an average analysis for each sample and these average analyses are listed in appendix A.5.1

together with the standard deviations calculated during the averaging process as an indication of the chemical heterogeneity within each sample. It might be argued that this averaging procedure is not geochemically legitimate, however the point was to derive some indication of the bulk chemistry of the samples analysed, as it was bulk samples that were used for radiometric and stable isotopic study. In the case of the amphibole analyses FeO was determined by wet chemical means and Fe_2O_3 calculated as the difference between Fe_{total} from the electron-probe and FeO from wet chemistry. In the case of the micas no attempt was made to determine FeO by wet chemical methods and the Fe_{total} from the electron-probe is reported as FeO.

Amphibole analyses:

The average amphibole analyses were used to calculated chemical formulae and to assign names to samples according to the amphibole nomenclature procedure recommended by the International Mineralogical Association (Leake 1978b). The chemical formulae for the amphiboles are calculated on the basis of 23 (O), all the chemical formulae and the names are listed in appendix A.5.2.

All the amphiboles analysed belong to the calcic amphibole group and are all 'hornblendes'. The variation in the amphibole compositions is shown graphically in figure 2.10. which shows the compositional fields for the various calcic amphiboles from Leake (1978b). As a group the amphibole samples show significant compositional variation. Most of the amphibolite hornblendes show a trend from ferro-tschermakitic hornblende to ferro-hornblende with a few plotting as magnesio-hornblende. This may possibly represent a primary igneous

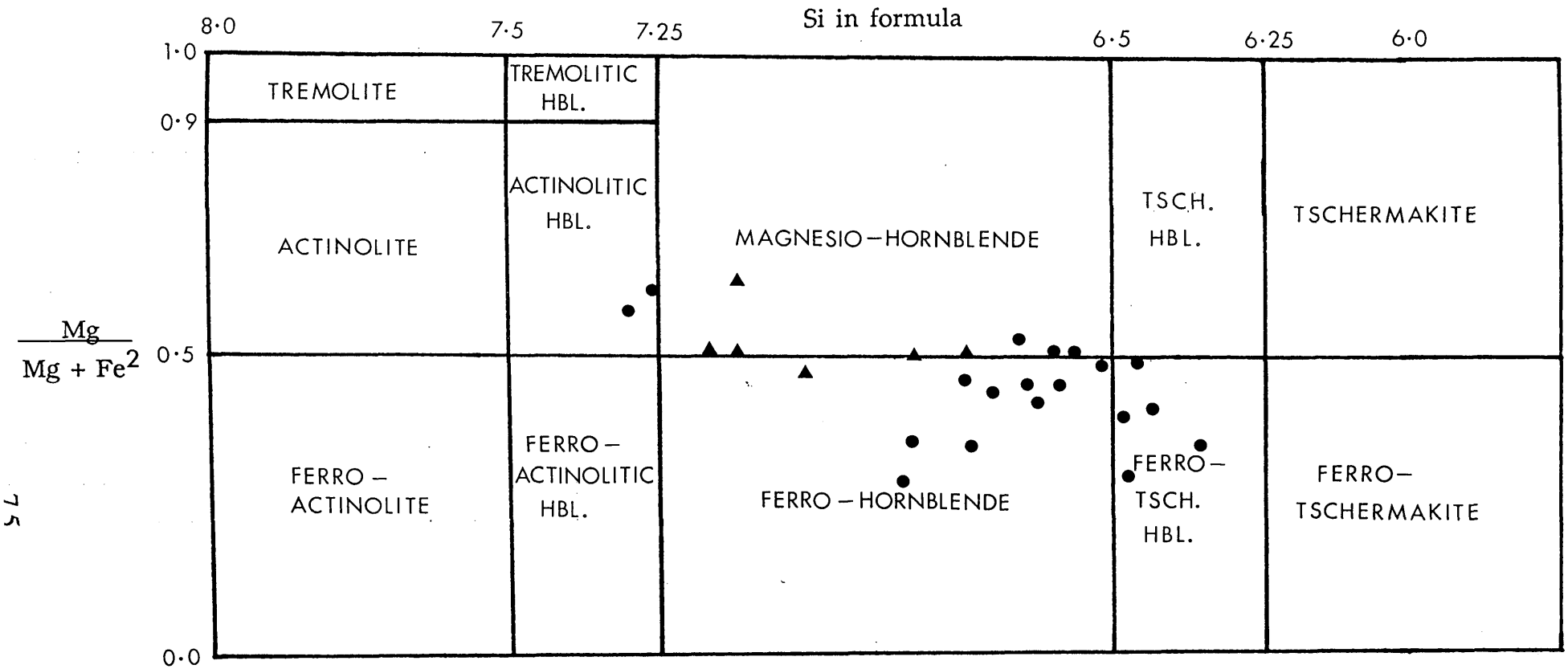

Figure 2.10. Amphibole sample compositions plotted on the calcic amphibole diagram of Leake *et al.* (1978b). The circles are Dalradian amphibolite samples and the triangles are metagabbro-gneiss complex samples. The actual chemical compositions of these samples are given in appendix A.5.1 and the chemical formulae are given in appendix A.5.2.

differentiation sequence. Two amphibolite hornblendes (WM 139 and 183) lie off this trend and plot as actinolitic hornblendes. This geochemical trend is not represented by any pattern in the geographical position of the samples. Generally individual amphibolite hornblende samples are homogeneous with only minor chemical variations occurring between and within grains of the same sample. This is reflected by the low standard deviations given in appendix A.5.1. What variation exists is most probably due to the zoning seen in some samples in thin section. The elements that do show the greatest intra-sample variation are Mg. Fe, Ca, Na and K. The two actinolitic hornblende samples show considerably more intra-sample chemical heterogeneity than the rest of the amphibolite hornblendes. The same elements listed above are again the most variable, but in these two samples considerably more so. An example of the increased chemical heterogeneity of these two samples is the Ca/K ratios. For most of the amphibolite hornblende samples this ratio is constant between and within grains and is typically about 15±5. The actinolitic hornblendes show Ca/K ratios that range from 10 to 60. These two samples show more alteration of the hornblende to chlorite and biotite in thin section than the others and it seems likely that the increased chemical heterogeneity is caused by mobilisation of the more incompatible elements and is not a primary igneous characteristic. At this point it should be noted that invariably electron-probe analyses are performed on areas of grains that appear to be fresh and well polished. This introduces a systematic bias towards grain centres because the edges of grains and areas around cleavages are often poorly polished, the result of 'plucking' of the less secure parts of grains during sample polishing. In addition these areas are often not horizontal or form a hollow in the grain surface, both of these factors will cause a reduction in the X-ray counts and subsequent low analysis totals. It is likely that any alteration of

the hornblende will be most pronounced at grain margins and in cleavages and therefore the systematic bias in the analyses will generally underestimate the heterogeneity of the samples. Some attempt was made to obtain analyses directly from cleavages of three samples; WM 225, WM 234 and WM 235. The average analyses are given in table 2.2. All the analyses from cleavages are analytically suspect because the totals are low, in the range 80 to 90%.

Table 2.2. Comparison of electron-probe analyses from fresh hornblende and cleavages of hornblende with likely alteration. Number indicates the number of individual analyses averaged to obtain this average.

	WM 225		WM 234		WM 235	
	fresh	cleavage	fresh	cleavage	fresh	cleavage
Number	11	4	9	5	10	4
SiO_2	43.96	36.05	44.07	37.32	42.79	39.17
TiO_2	1.09	0.92	0.45	0.39	1.27	1.23
Al_2O_3	11.50	9.20	14.14	12.04	10.91	9.23
FeO	14.38	14.23	13.53	13.42	16.91	16.90
MnO	0.31	0.27	0.23	0.22	0.37	0.37
MgO	12.17	10.10	11.04	10.45	10.48	9.31
CaO	11.18	10.61	11.63	10.56	11.54	11.17
Na_2O	1.39	1.17	1.19	0.99	1.50	1.39
K_2O	0.31	0.35	0.36	0.39	0.98	1.07
sum	96.29	82.90	96.64	85.78	96.52	89.84
Ca/K	30.9	26.0	27.7	23.2	10.1	8.9
Fe/Mg	1.5	1.8	1.6	1.7	2.1	2.4

However, comparison *vis-a-vis* analyses of the fresh hornblende and the cleavage areas does show apparent differences in some elemental ratios, most significantly Ca/K and Fe(total)/Mg. In all three samples the cleavages give lower Ca/K and higher Fe(total)/Mg ratios than the fresh hornblende. The changes in these two elemental ratios is consistent with some biotite being included in the analyses of the hornblende, although

these analyses are not of biotite. The poor analytical quality of the cleavage analyses is recognised but it is believed that, even though *absolute* elemental abundances may be inaccurate, *relative* elemental abundances (in the form of ratios) are still meaningful. Even if this is an incorrect belief, the data still suggests that biotite exists in the cleavages because K shows an absolute increase in the cleavages for each sample. Potassium is the only element that does show an absolute increase in the cleavages.

The hornblendes from the metagabbro-gneiss complex samples lie apart from the amphibolite hornblendes on figure 2.10, but they do not show any distinct within-group trend. All but one metagabbro-gneiss hornblende plot as magnesio-hornblende, but as the $Mg/(Mg+Fe^2)$ ratios are all close to 0.5 this does not have any significance. The metagabbro-gneiss hornblendes show noticeably greater intra-sample chemical heterogeneity than the amphibolite hornblendes. This either reflects original igneous or metamorphic zoning or a later elemental mobilisation event. The electron-probe data are not sufficient to indicate which is the most likely. However as metagabbro-gneiss amphiboles are usually partly altered in thin section this heterogeneity probably relates to the alteration.

The totals for the average electron-probe analyses range from about 95 to 99% (excluding those analyses from amphibole cleavages). Water contents determined gravimetrically during hydrogen isotopic analysis (appendix A.5.7) for some of the amphiboles are typically 2 to 2.5 wt.%. This implies a shortfall in the totals for some of the samples. The likely reason for this is high concentrations of elements unaccounted for, eg. Cl or F. Volatilisation of the alkali elements during electron-probe analysis can sometimes cause a measurable total loss when analysing

calcic amphiboles on an electron-probe using a high beam current and accelerating voltage (Potts 1987) but this could only account for a small proportion of the shortfall.

Muscovite analysis:

The average muscovite electron-probe analyses are given in appendix A.5.1 and average muscovite compositions have been calculated from the electron-probe analyses and these are given in appendix A.5.2. Muscovite shows less chemical heterogeneity than either amphibole or biotite. The most variable element between individual samples is Fe which ranges from 1.06 to 4.13%, averaging about 3.5%. The Fe in the muscovites is most likely to exist as FeO, which gives rise to the characteristic green colour of some of the muscovite samples. The other major elements in muscovite show only small variations between samples. Using the average electron-probe analysis for each muscovite sample the compositional formulae have been determined and these are given in appendix A.5.2. It can be seen that Ca is present in sufficient quantities to be included in the formulae of some samples, where it is most likely replacing K. The alkali element Na is present in all the compositional formulae, but not in sufficient quantities to warrant calling these minerals paragonites. All these white micas are therefore true muscovites.

Muscovite exhibits complete solid solution with phengite with octahedral Al being replaced by Mg and Fe. The muscovite to phengite range of the average compositions of the sample muscovites is indicated by the octahedral, Al / (Fe + Mg) ratio which shows a range from 3.96 to 12.41 in the Connemara samples. Whether this variation is the effect of

hydrothermal alteration is not certain. There is no apparent correlation between Al / (Fe + Mg) and the alteration index of coexisting plagioclase, table 2.1. There is no significant chemical heterogeneity between grains and within grains of the same sample with only Mg and Na showing up to 2% variation.

The totals for the calculated average muscovite electron-probe analyses range from 94.46 to 96.63%, with an average about 95%. Water contents determined gravimetrically during hydrogen isotopic analysis average about 4.5% (appendix A.5.7). There is therefore a small shortfall in the analysis totals. This may be caused by volatilisation of the alkali elements during electron-probe analysis.

Biotite analysis:

The average biotite electron-probe analyses are given in appendix A.5.1. and the biotite compositional formulae calculated from the average electron-probe analyses are given in appendix A.5.2. The composition of the biotite samples are indicated graphically in figure 2.11 which shows the compositional fields of biotite and phlogopite which exhibit complete solid solution (Deer *et al.* 1966). There is some variation between the sample compositions with a small but significant variation in Mg / (Mg + Fe) which ranges from 0.3 to 0.5. The elements Ti, Al and Si show the most variation between samples. Some chemical heterogeneity is apparent between and within grains of individual samples. The biotite samples that show the greatest chemical heterogeneity are WM 130, 196, 212 and 233. Within these samples the element that shows the most variability is K, but Al, Mg, Na and Ti are also changeable. This variability may simply be chemical zoning within grains, but is more likely to be due

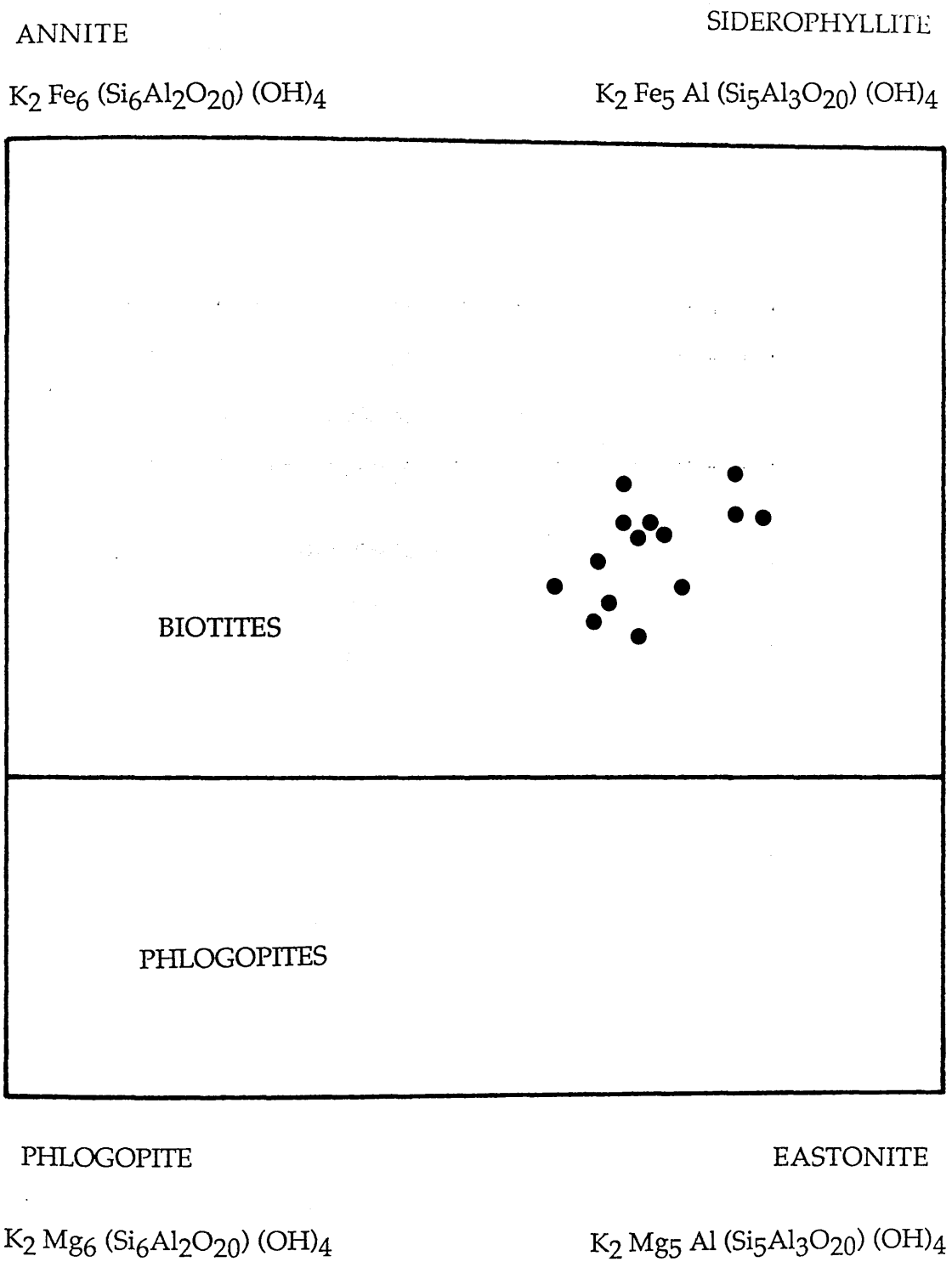

Figure 2.11. Biotite sample compositions plotted on the biotite-phlogopite diagram of Deer *et al* (1966). The actual chemical compositions of these samples are given in appendix A.5.1 and the chemical formulae are given in appendix A.5.2.

to mobilisation of these elements during partial chloritisation of the biotite. The variability of Ti is indicative, as it is the first element to be expelled from biotite at the onset of chloritisation (Deer *et al.* 1966). All four of the samples indicated above show some degree of chloritisation of biotite in thin section, see table 2.1. There is not, however, any apparent correlation between the degree of chloritisation of the biotite and the variability of K in the samples. The lowest value of K_2O in the calculated average compositions is 7.77% which shows that chloritisation of these mineral separates is, at most, only partial.

The totals for the calculated average biotite electron-probe analyses range from 93.85 to 95.73%, with an average about 94%. These low totals are possibly caused by the incorporation of volatile rich chlorite components in the analyses. Determination of water content of the biotites during hydrogen isotopic analysis indicated an average of about 4% (appendix A.5.7). There is therefore a shortfall in the analysis totals, but less than in the case of the amphiboles. This shortfall may be caused by volatilisation of the alkali elements during electron-probe analysis.

2.4.3 Ion-probe analysis.

Five hornblende samples from amphibolites were analysed using the Cameca IMS 4f ion-probe (Edinburgh University, Geology Department). Analyses were performed at the centre of each of five grains from different samples. The ion-probe sample preparation and analysis methods are given in appendix A.3.4. and the analytical data are given in appendix A.5.3. The major element concentrations agree well with the average compositions determined from the electron-probe analyses. In addition to the major elements the ion-probe gave concentrations of F

and several trace elements. The concentration of F ranged between samples from 0.06 to 0.23%. The trace elements showed larger variations in concentration between samples; for instance, Cr ranged from 0.0 to 793ppm while Sr ranged from 16 to 454ppm.

In addition to the spot analysis the ion-probe was used to obtain profiles from the centre to the edge of one grain from each of two samples, WM 201 and 225. These profiles are obtained by 'stepping' the beam at 15 micron intervals. During these profiles several major and trace elements were analysed for; although note that this is not the full range of elements analysed for in the spot analyses using the ion-probe. These profiles are shown in figures 2.12 and 2.13. The relative concentrations are shown on these figures as ion-counts. Profiles such as these should reveal any chemical heterogeneity in the grains such as zoning or secondary mineral growth in cleavages provided such features are larger than 15 microns. It is clear from from figures 2.12 and 2.13 that the major elements show no variation across either grain. On the other hand, the trace elements show significant fluctuations that may be due to primary igneous zoning. The homogeneous major element pattern indicated by the ion-probe is consistent with the insignificant intra-grain variations revealed by the electron-probe for these samples.

It must be stressed that it does not follow that because the two grains profiled with the ion-probe showed no significant within grain heterogeneity that this is necessarily true for other samples or even other grains of the two samples analysed in this manner.

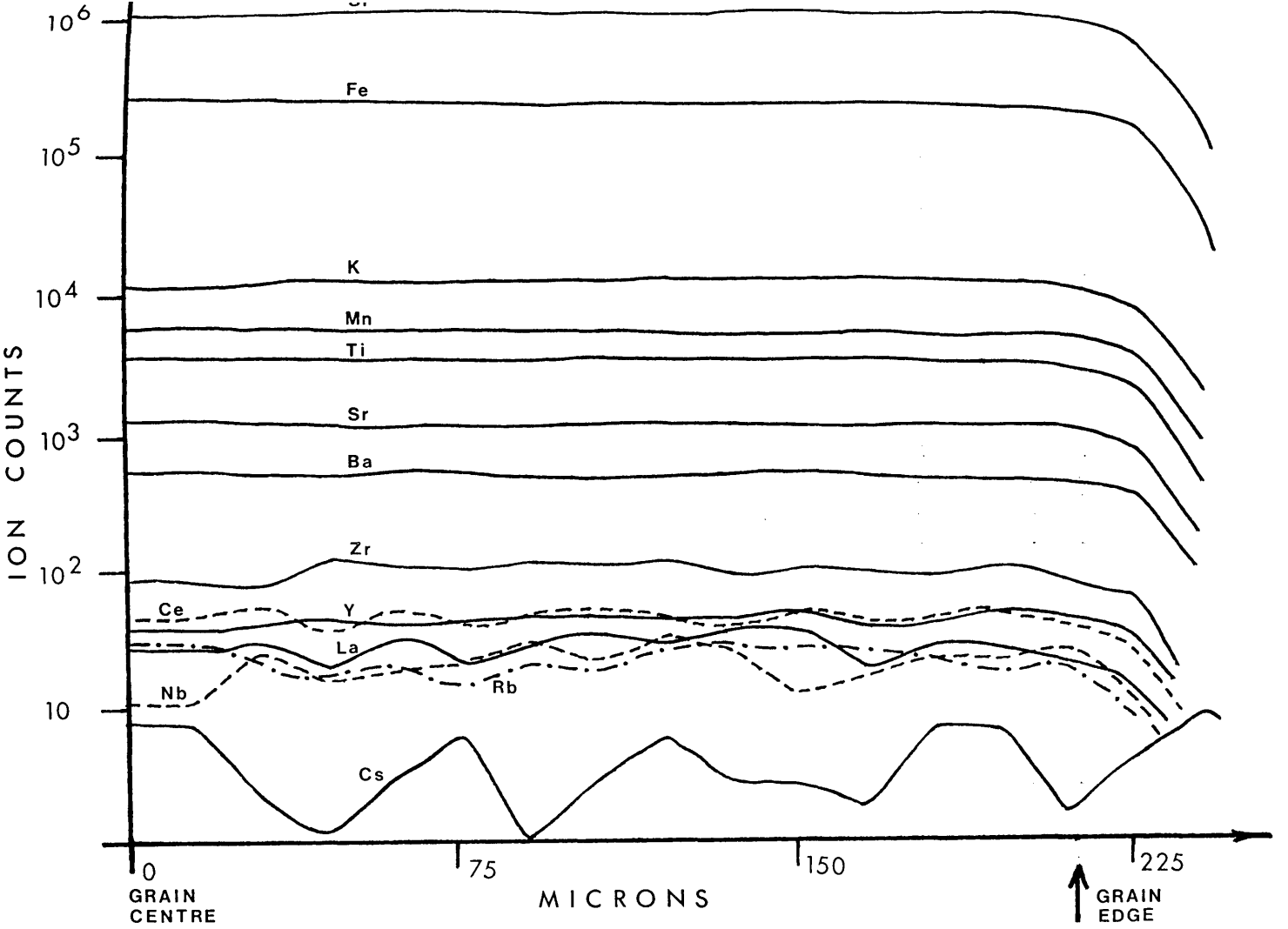

Figure 2.12. Ion-probe step-scan across a hornblende grain from WM 201 in 15 micron steps. The vertical axis is relative, in ion-counts, not absolute elemental abundances. Elemental concentrations for the centre of this grain are given in appendix A.5.2.

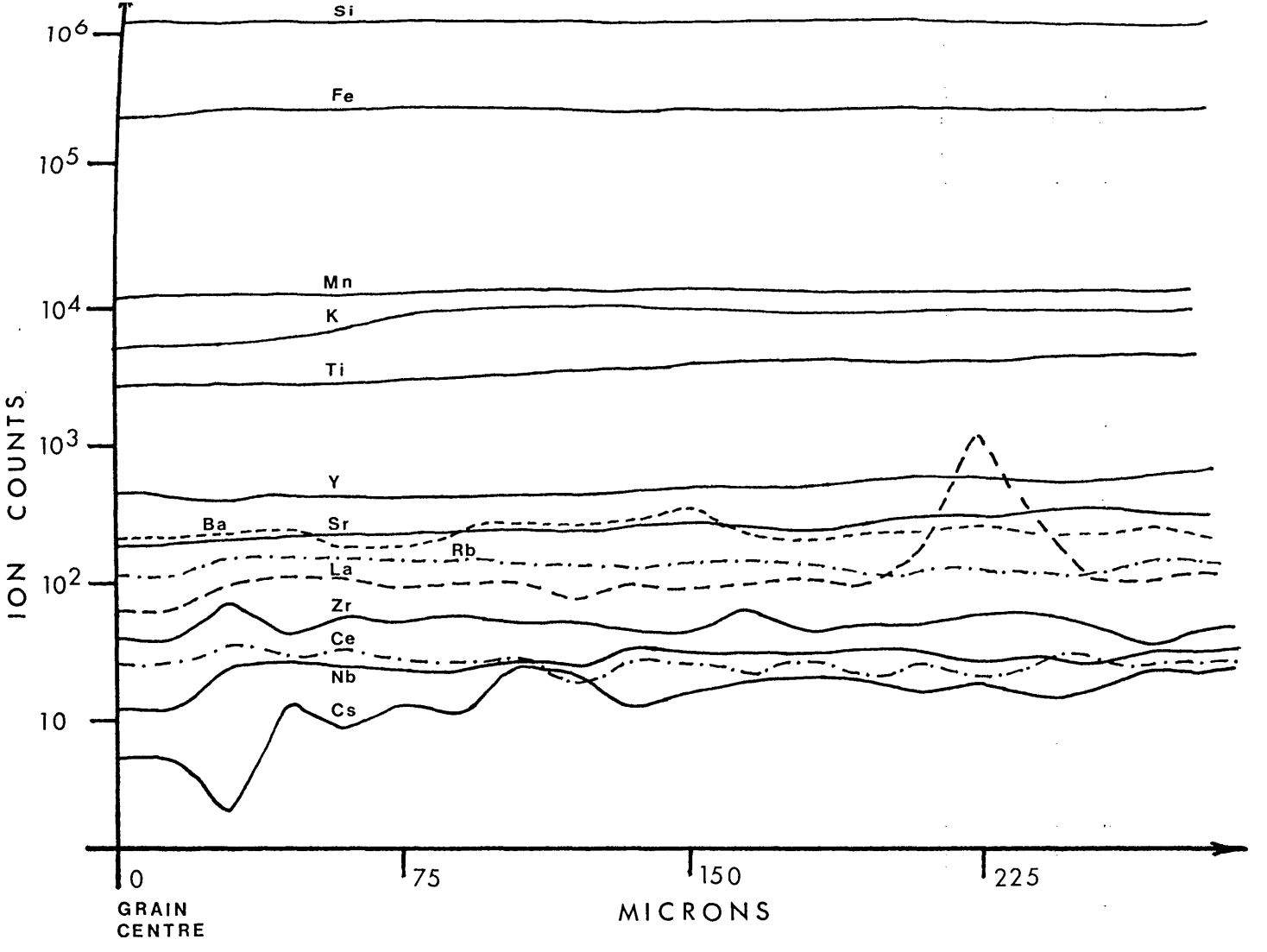

Figure 2.13. Ion-probe step-scan across a hornblende grain from WM 225 in 15 micron steps. The vertical axis is relative, in ion-counts, not absolute elemental abundances. Elemental concentrations for the centre of this grain are given in appendix A.5.2. Note that this profile does not go right to the edge of this grain.

2.4.4 Transmission electron microscopy (TEM).

The TEM analysis undertaken was mostly qualitative, with emphasis placed on imaging and photographing microstructures within amphibole grains. Only two amphibole samples were examined in this manner because the whole procedure was extremely time consuming. The preparation of TEM samples and their analysis is described in appendix A.3.5. The two samples WM 165 and 225 were chosen because of the large contrast in their K-Ar ages which are 479±10 and 397±8 Ma respectively. The K-Ar ages are discussed in detail in the following chapter. The TEM analysis was undertaken because it has become recognised in the literature that sub-grain microstructure can potentially have a significant affect on the closure temperature of amphibole (see section 1.4.2 for an overview of the physico-chemical factors affecting amphibole closure temperatures).

Thin section study of sample WM 225 shows that it contains some 20% chloritised biotite, in addition some minor chlorite/biotite growth occurs on the rims and in the cleavages of the amphibole. Following mineral separation XRD analysis of the separate indicated no chlorite peaks and no chlorite was visible in the separate with the binocular microscope. Thin section examination of WM 165 reveals two co-existing amphiboles; 40% hornblende and 10% cummingtonite. There is a slight suggestion that the cummingtonite might be exsolving from the hornblende in some grains. Amphibole exsolution has been recognised in other Connemara amphibolites (B.E. Leake *pers. comm.*).

Examination of the photomicrographs obtained from TEM imaging shows that substantial heterogeneity exists at the sub-microscopic level in both samples. Two distinct types of feature were

observed and these are described below along with the preferred interpretation of these features. Unambiguous identification of these features was attempted using the energy dispersive X-ray facility (EDX) on the TEM. Unfortunately this was unsuccessful because during the sample preparation procedure (appendix A.3.5) a layer of copper was deposited on the sample. Consequently, the EDX spectra from the sample was swamped by large Cu α and β peaks. As a result the interpretation of the features in the Connemara samples has to be done on a comparative basis with the results of TEM investigations on amphibole by other workers.

1) The first type of feature is seen in figure 2.14 (a) and in the line drawing, figure 2.14 (b), from WM 225. This feature forms areas that are long and thin with an unknown third dimension. In this photomicrograph these features are about 1 micron long and 0.1 microns wide and three of these features run parallel to each other about 0.2 microns apart. Their orientation is apparently controlled by the crystallography of the host hornblende. These features show some apparent internal heterogeneity, although this is not well resolved in the photomicrograph. It is proposed that these features are fine grained precipitates of a phyllosilicate mineral whose growth occurs within and parallel to the cleavage direction of the hornblende. The internal heterogeneity is thought to be individual platelets of the phyllosilicate. The exact nature of the phyllosilicates cannot be ascertained from the TEM investigation, but as both biotite and chlorite are observed in thin section and the presence of biotite has been inferred from electron-probe analysis in the cleavages of the amphibole it seems most likely that the phyllosilicates imaged by TEM are either biotite or chlorite. The presence of fine grained phyllosilicates in the cleavages of hornblende has been revealed in TEM studies before (Onstott & Peacock 1987) and has been inferred from combined ^{40}Ar-^{39}Ar and electron-probe studies by Sisson

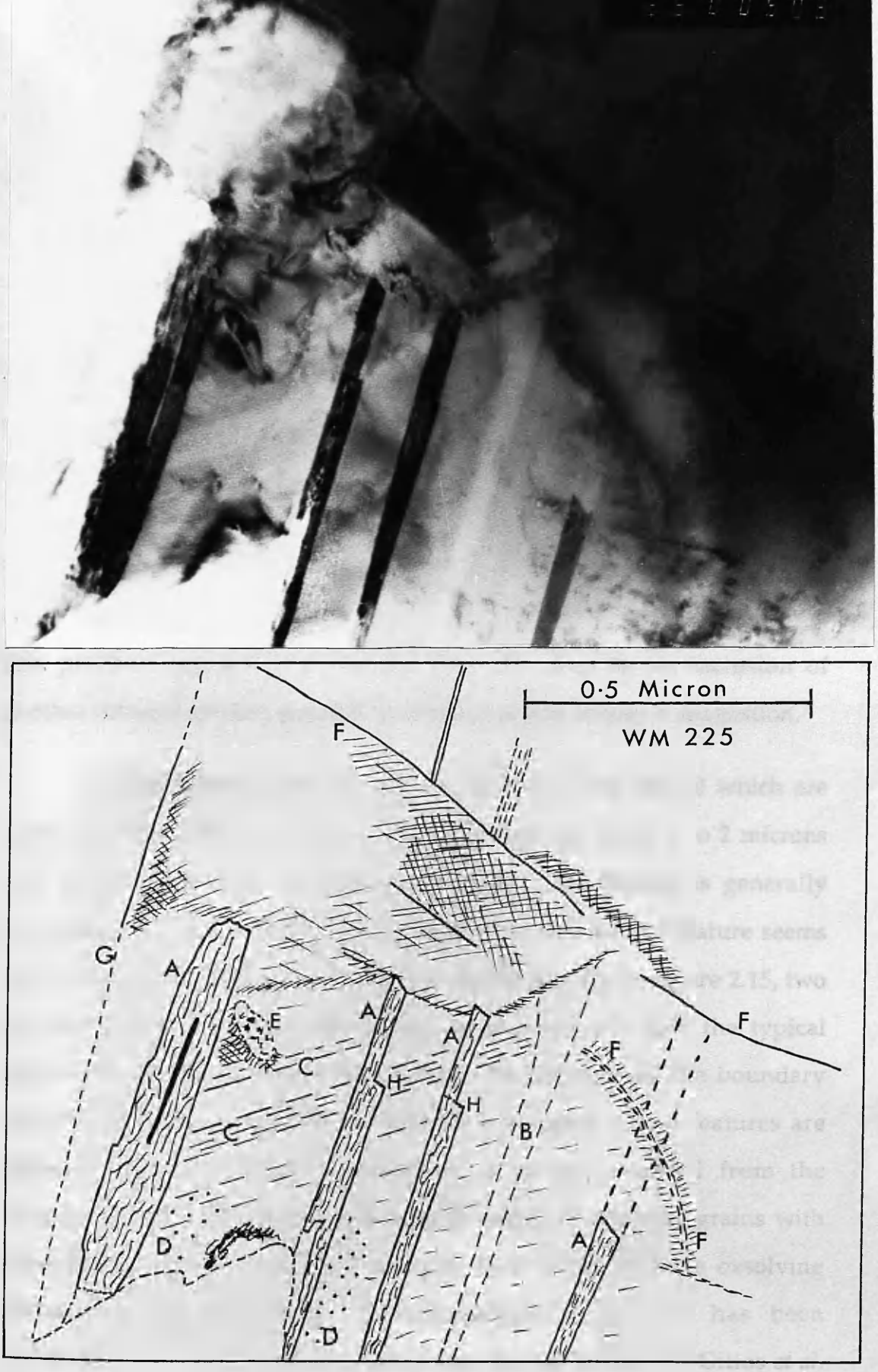

Figure 2.14. Top view. A TEM image of part of a hornblende grain with phyllosilicate inclusions, from WM 225. Lower view. A line drawing of the TEM image. A = phyllosilicate inclusions along the cleavages. B = 'ghost' cleavage without any inclusions. C = Growth lines of the crystal. D = Ablation pits, formed during ion-thinning of the sample. E = other inclusion? F = Fractures, dislocations in the crystal. G = outline of grain. H = Growth ledges on the phyllosilicate.

& Onstott (1986) and Ross & Sharp (1988). In addition to the phyllosilicate inclusions some other features can be seen in figure 2.14 and these are highlighted in the line drawing of figure 2.14 (b). The small depressions on the sample surface are erosion pits caused by the ablation of the sample by Ar ion bombardment during sample thinning. The fine lines that are cross cut by the phyllosilicates are crystal growth lines, and as such show the orientation of the crystal faces. The angle between these growth lines and the phyllosilicates (which sit in the cleavages) is approximately 60°. Parallel to the phyllosilicates is a lighter zone that is a 'ghost' cleavage, one that has not been occupied by inclusions. Growth ledges are clearly visible on the phyllosilicates. In the upper central part of this photomicrograph is a discrete area that may be an inclusion of another mineral species, possibly epidote?, but this is only a suggestion.

2) The second feature is seen in figures 2.15 (a and b) which are from WM 165. This feature has dimensions typically about 1 to 2 microns and can be seen to be intergrown. Internally this feature is generally homogeneous. Like feature 1, the orientation of this second feature seems to be controlled by the host hornblende crystallography. In figure 2.15, two sets of these features are intersecting at an angle of c.60°, the typical intersection angle of amphibole cleavages. In some cases the boundary between the feature and the hornblende is stepped. These features are believed to be exsolution lamellae of a second material from the hornblende. As cummingtonite is seen to coexist as separate grains with hornblende in thin section it is thought most likely that the exsolving material is cummingtonite. Cummingtonite-hornblende has been reported several times in TEM studies (see review articles by Gittos *et al.* 1976 and Ghose 1981). Exsolution (immiscibility) between two amphiboles is expected when the following two rules are met (Ghose

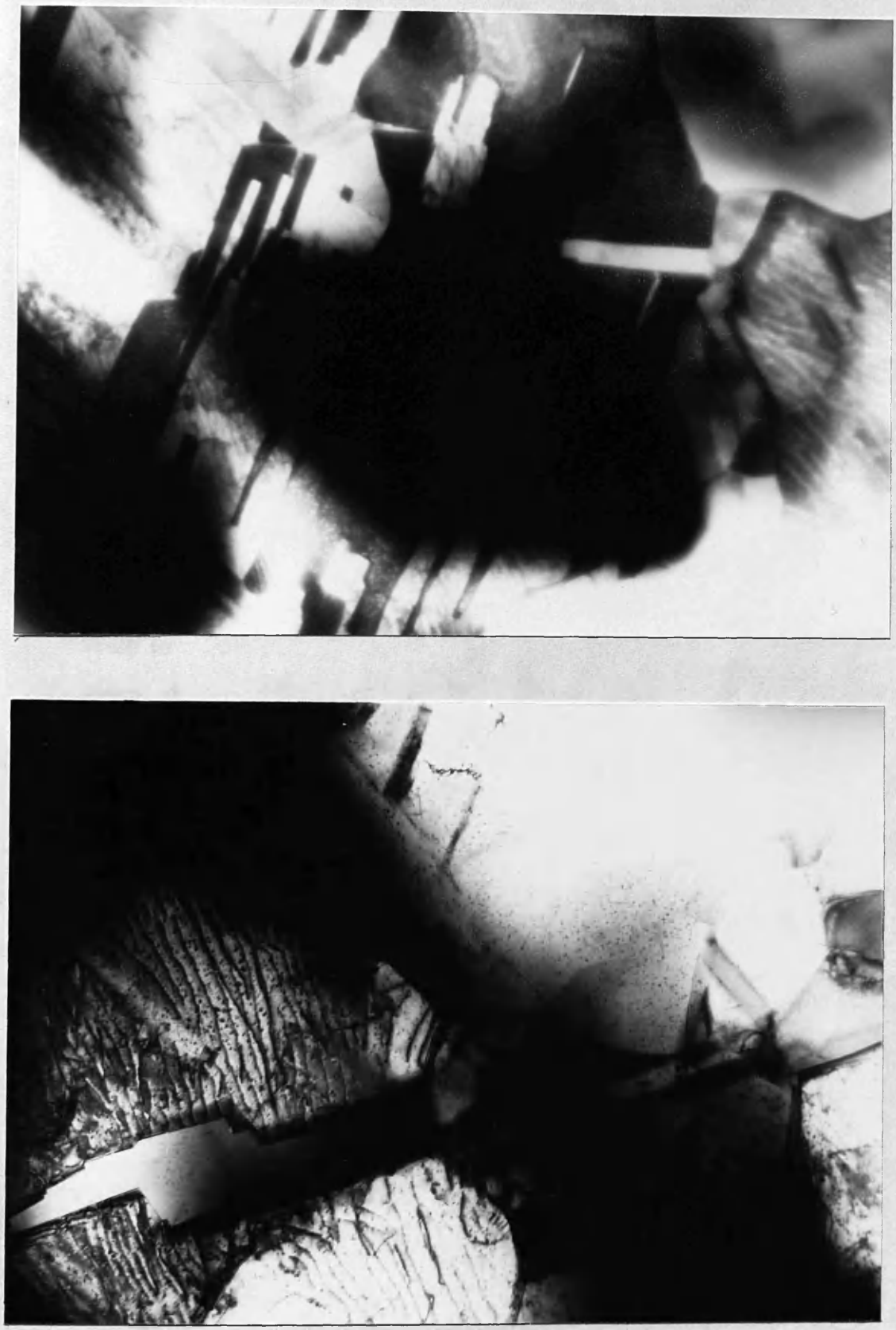

Figure 2.15. TEM images of parts of hornblende grains from WM 165 showing complex exsolution. In the upper view growth ledges are apparent. In the lower view the 'fish scale' pattern is due to grinding during sample preparation. The long axis of the upper image is 9 microns and in the lower image it is 4.5 microns.

1981); a) the 'M4' site is filled with large cations, Ca^{2+}, in one amphibole and small cations, Fe^{2+} and Mg^{2+}, in the other, and b) the 'A' site is fully or partially occupied in one and empty in the other. Both these rules are met by cummingtonite-hornblende. It is generally believed (Ghose 1981) that the exsolution in amphiboles occurs via a nucleation and growth mechanism. Similar ledges to those seen in figures 2.14 and 2.15 have been reported by Gittos *et al.* (1974 & 1976) in amphiboles and by a variety of workers (see Champness and Lorimer 1976) in pyroxenes and feldspars. These ledges are interpreted as a growth mechanism whereby the thickening of the exsolution precipitate perpendicular to the boundary proceeds by migration of the boundary along the boundary plane. It is normal for exsolution of cummingtonite from hornblende to parallel (101) although finer intergrowths parallel to (100) have been observed (Ghose 1981). In the Connemara sample, however, two sets of lamellae are apparent, both with the same dimensions. The black areas in figure 2.15 are not a feature of the sample but is an anomaly in the photographic exposure. The undulating ripple features are caused by the grinding down of the sample during preparation.

It has to be stressed that only two samples were examined by TEM and although complex and possibly influential to Ar retention features were imaged in both this is not a sufficient condition to definitely conclude that all the other amphibole samples analysed in this study also show such features. However, having said this, as the hornblende with exsolution came from a sample in which coexisting cummingtonite and hornblende were seen in thin section and that this is characteristic of a number of other amphibolite samples, especially from an area to the north-west of Lough Inagh, it seems likely that exsolution might be present in all the

Connemara samples with coexisting amphiboles. The other hornblende sample, with phyllosilicate inclusions, is likely be more typical of the majority of hornblendes than the sample with exsolution. This is because many of the amphibolites when examined in thin section were seen to have minor zones of alteration at grain rims and along cleavages. The phyllosilicates seen with the TEM in the second sample are, most likely, alteration products of the same type formed by the same process, as the alteration products visible in thin section. Consequently many of the other hornblende samples could contain these sub-microscopic inclusions. The different sub-microscopic structures seen in these two samples could allow for varying degrees of Ar loss from the hornblendes and therefore could be responsible for the difference in their K-Ar ages. This idea is discussed more fully in section 4.3.3. However, it is very interesting to note that the sample that showed the exsolution features, WM 165, yielded one of the older ages, 479±10 Ma. This age is almost identical, within error, to the age of the metagabbro-gneiss complex and cannot therefore have suffered significant resetting. Furthermore, for the age to be this old the samples effective closure temperature must be high. This is in contradiction to the conclusion of Harrison & Fitz Gerald (1986) who found that a hornblende with exsolved cummingtonite had an apparent closure temperature some 200°C below that of 'normal' hornblende. It would seem that the effect exsolution has on the closure temperature of hornblende is far from clear. It may be analogous to the situation in feldspars where exsolution boundaries are semi-coherent and in some cases may allow Ar loss while in other cases Ar is held securely. However exsolution along with phyllosilicate growth will be considered in later discussions, chapter four, as a potential mechanism for Ar loss.

CHAPTER THREE:

POTASSIUM-ARGON, ^{40}Ar-^{39}Ar INCREMENTAL STEP-HEATING AND ^{40}Ar-^{39}Ar TOTAL FUSION LASER-PROBE DATING METHODS: RESULTS AND CONCLUSIONS.

3.1 K-Ar ages from the Connemara Schists and amphibolites.

The interpretation of the K-Ar mineral ages depends on whether or not these ages are simply cooling ages resulting from a steady temperature decline through hornblende, muscovite and then biotite closure temperatures or whether they are the result of some other process. If these K-Ar mineral ages can be shown to be cooling ages then a wealth of temperature-time information could be obtained if the relevant closure temperatures are known. Before conclusions are drawn on the cooling age question the K-Ar mineral ages are described firstly in terms of the geographical positions of the samples and then in terms of the range of K-Ar ages obtained for each mineral species. Considering the geographical position of the samples the whole of Connemara is considered first and then smaller areas which have higher densities of K-Ar mineral ages. A combined analysis of both the geographical distribution of the ages and the range of ages helps to constrain the likely interpretation. On the question of whether or not the K-Ar ages are cooling ages the physico-chemical factors that can potentially influence closure temperatures are considered before a final conclusion is drawn as to the nature of the K-Ar mineral ages.

3.1.1 Correlation between K-Ar mineral ages from the Connemara Schists and geography and sample proximity to geological features.

A total of fifty-five K-Ar mineral ages have been determined on samples of the Connemara Schists and amphibolites. This total is made up of fourteen biotite K-Ar ages, twenty muscovite K-Ar ages and twenty one hornblende K-Ar ages. The sample locations together with the respective ages are shown on figures 3.1, 3.2 and 3.3 for biotite, muscovite and hornblende. In these figures the stars represent the location of a quarry which will be discussed in detail later.

Examination of these figures reveals no distinct geographic trend to the K-Ar ages of any mineral species. This is consistent with the findings of Elias *et al.* (1988) for the micas but not for hornblende because these workers reported an irregular increase in hornblende ages towards the south. The two sets of data, Elias *et al.* (1988) and the present study, should be directly comparable because the K-Ar ages have been determined on the same equipment, in the same laboratory, and using the same decay constants. It is likely, therefore, that the discrepancy in the findings for hornblende is the result of sampling and statistical variations. In figure 3.4 the two sets of hornblende ages have been combined. Examination of this figure does not reveal any obvious geographical trend in the ages. Although several old ages do exist in the south there are many young ages also. If there is a pattern in the hornblende K-Ar ages in the south then it is complicated and the combined total of 45 hornblende K-Ar ages is insufficient to reveal it. The lack of any obvious north-south or east-west trend in the data for either mineral species also suggests that there is no relationship between the mineral ages and sample proximity to either the metagabbro-gneiss complex in the south or to the Ordovician rocks of the South Mayo Trough to the north as both these rock units have well defined

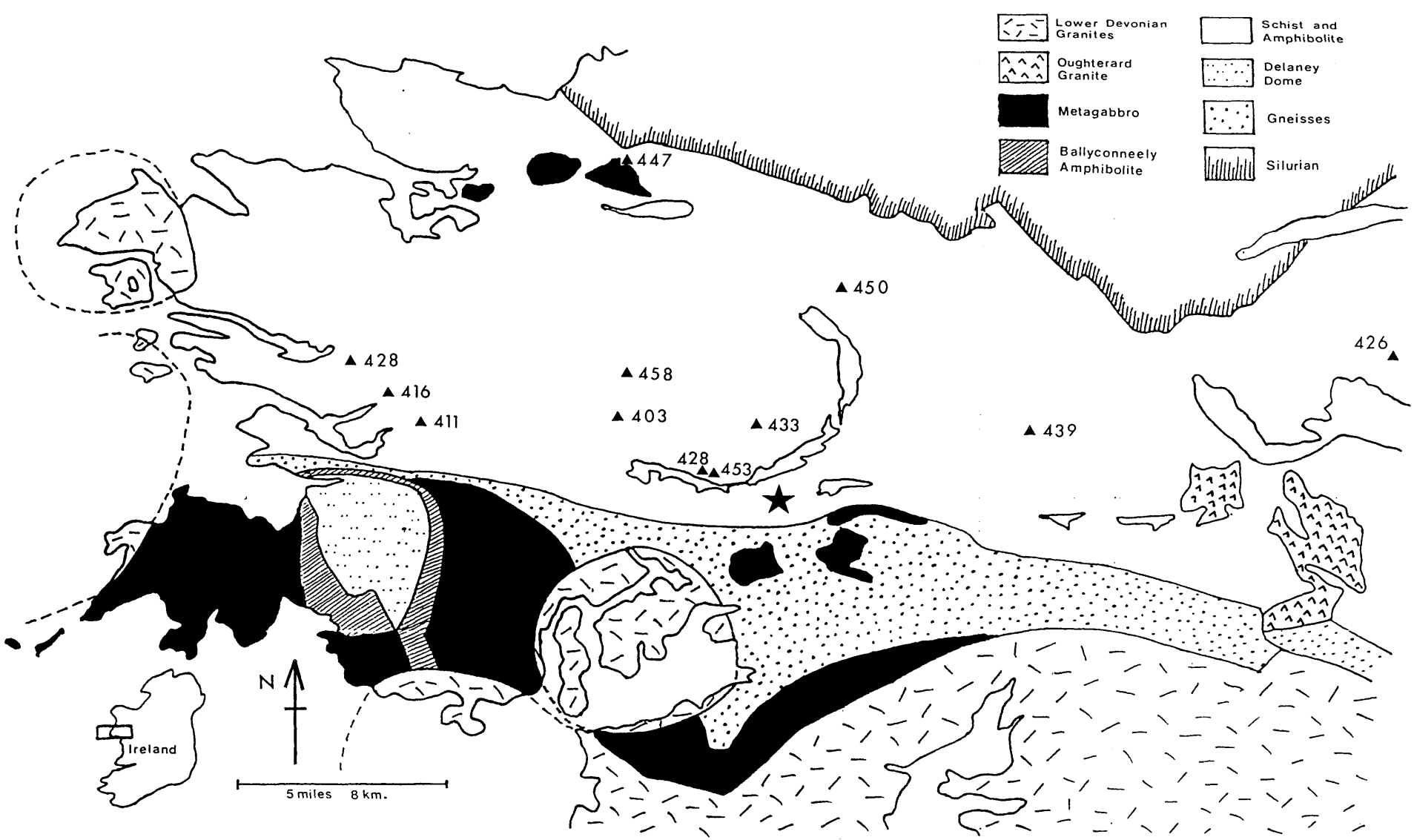

Figure 3.1. Map showing locations and ages, in Ma, of all the biotite samples dated by the K-Ar method in this project. The sample numbers can be read from figure 2.1. The exact grid references for all these samples are given in appendix A.1. The star shows the location of the quarry from which samples were collected which yielded biotite K-Ar ages of 447 and 454 Ma.

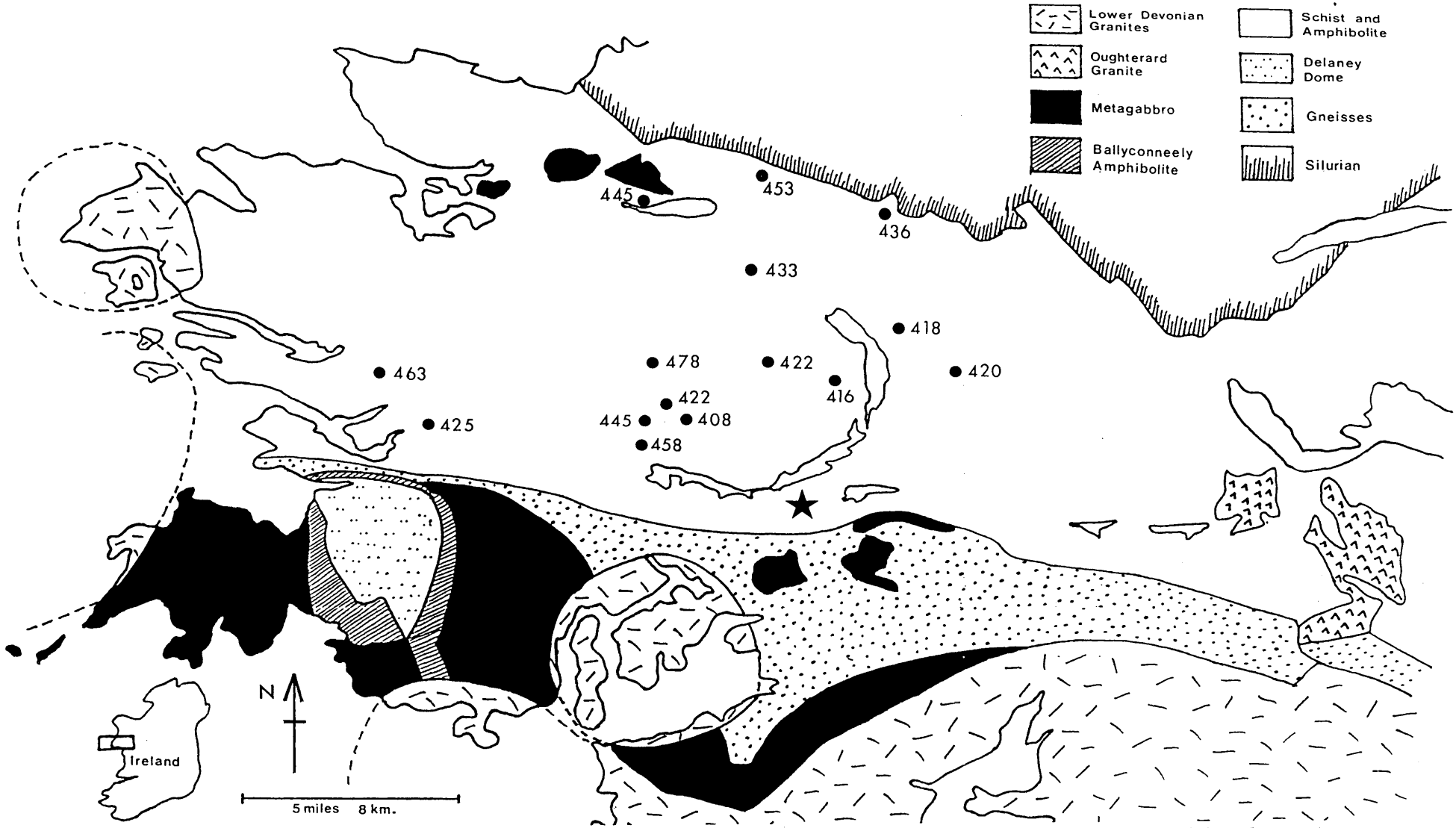

Figure 3.2. Map showing locations and ages, in Ma, of all the muscovite samples dated by the K-Ar method in this project. The sample numbers can be read from figure 2.1. The exact grid references for all these samples are given in appendix A.1. The star shows the location of the quarry from which samples were collected which yielded muscovite K-Ar ages of 415, 438, 444, 461 and 464 Ma.

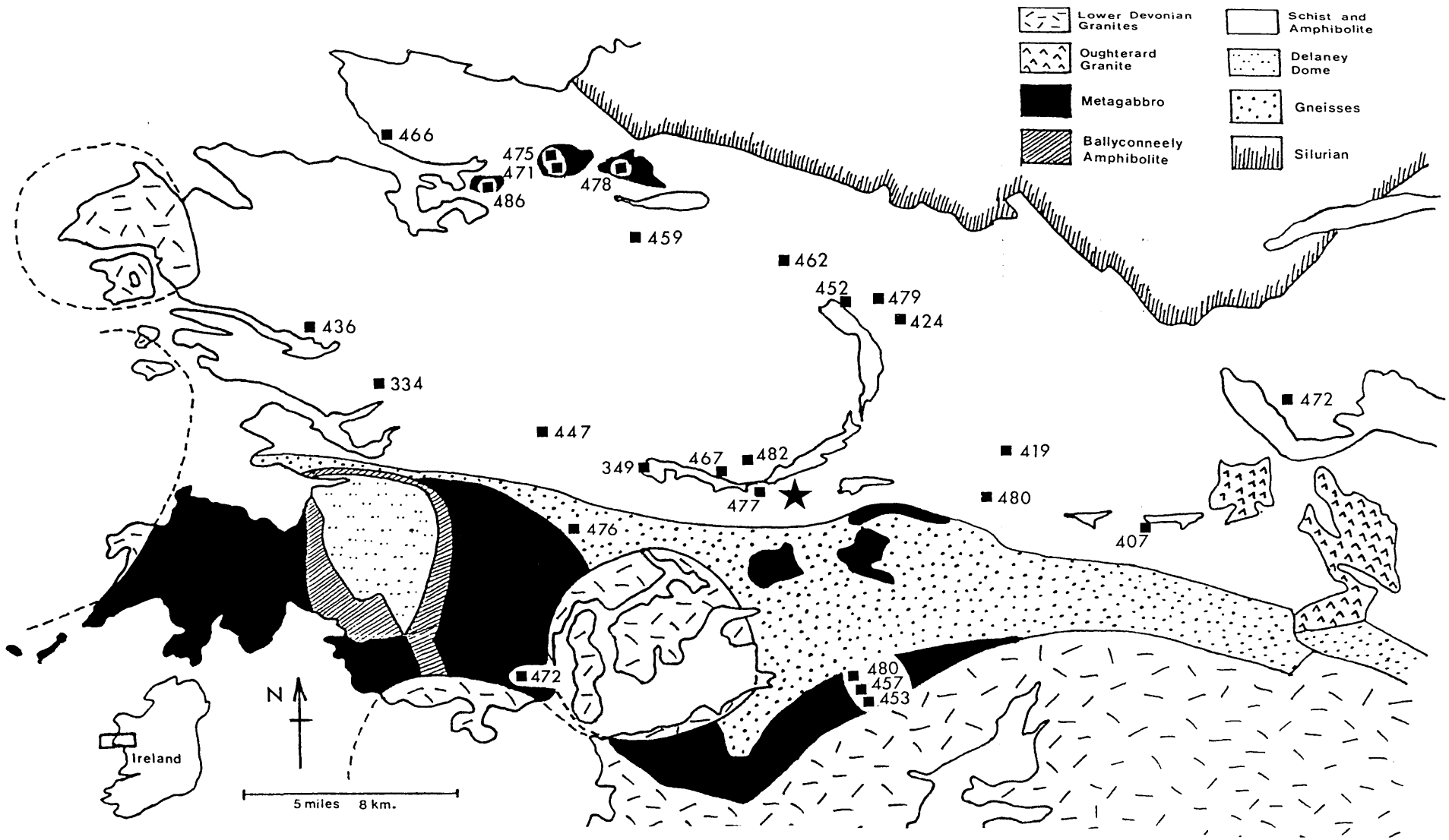

Figure 3.3. Map showing locations and ages, in Ma, of all the hornblende samples dated by the K-Ar method in this project. The sample numbers can be read from figure 2.1 and the grid references are given in appendix A.1. The star marks the location of the quarry from which samples were collected which yielded hornblende ages of 397, 406, 452 and 481 Ma.

contacts, striking roughly east-west, with the Connemara Schists. It is interesting to note, however, that two of the oldest (480 and 481 Ma) amphibolite hornblendes dated by Elias (1985) come from locations in the south of Connemara very close to the Cashel Hill body of the metagabbro-gneiss complex. This cautions against completely disregarding the possibility that there might be some relationship between amphibolite K-Ar age and proximity to the metagabbro-gneiss complex. Also shown on figure 3.4 are eight hornblende K-Ar ages determined on samples of the Ballyconneely Amphibolite (Leake *et al.* 1984). These average 454±11 Ma which is identical, within error, to the 447±4 Ma age of last movement on the Mannin Thrust determined by Tanner *et al.* (1989).

It is more problematic to determine if any relationship existed between the mineral ages and sample proximity to the Silurian or Carboniferous rocks that once unconformably overlay the Connemara Schists and are now eroded away. The dissected pre-Carboniferous peneplain that controls the topography in the South Mayo Trough is roughly horizontal and lies about 1000m higher than the present day Connemara erosional surface over which it once extended. As most of the Connemara samples were collected from within a small range in elevation it seems likely that there would not have been much variation in the separation distance between them and the unconformable sedimentary sequences and therefore little probability of a relationship existing.

It is rather more difficult to rule out a relationship between the mineral ages and sample proximity to the Lower Devonian Granites. The largest granite, the Galway Granite, is intruded into the metagabbro-gneiss complex. Consequently, because there is no apparent relationship between mineral age and sample proximity with the metagabbro-gneiss complex there can be no relationship with the Galway Granite. However, the

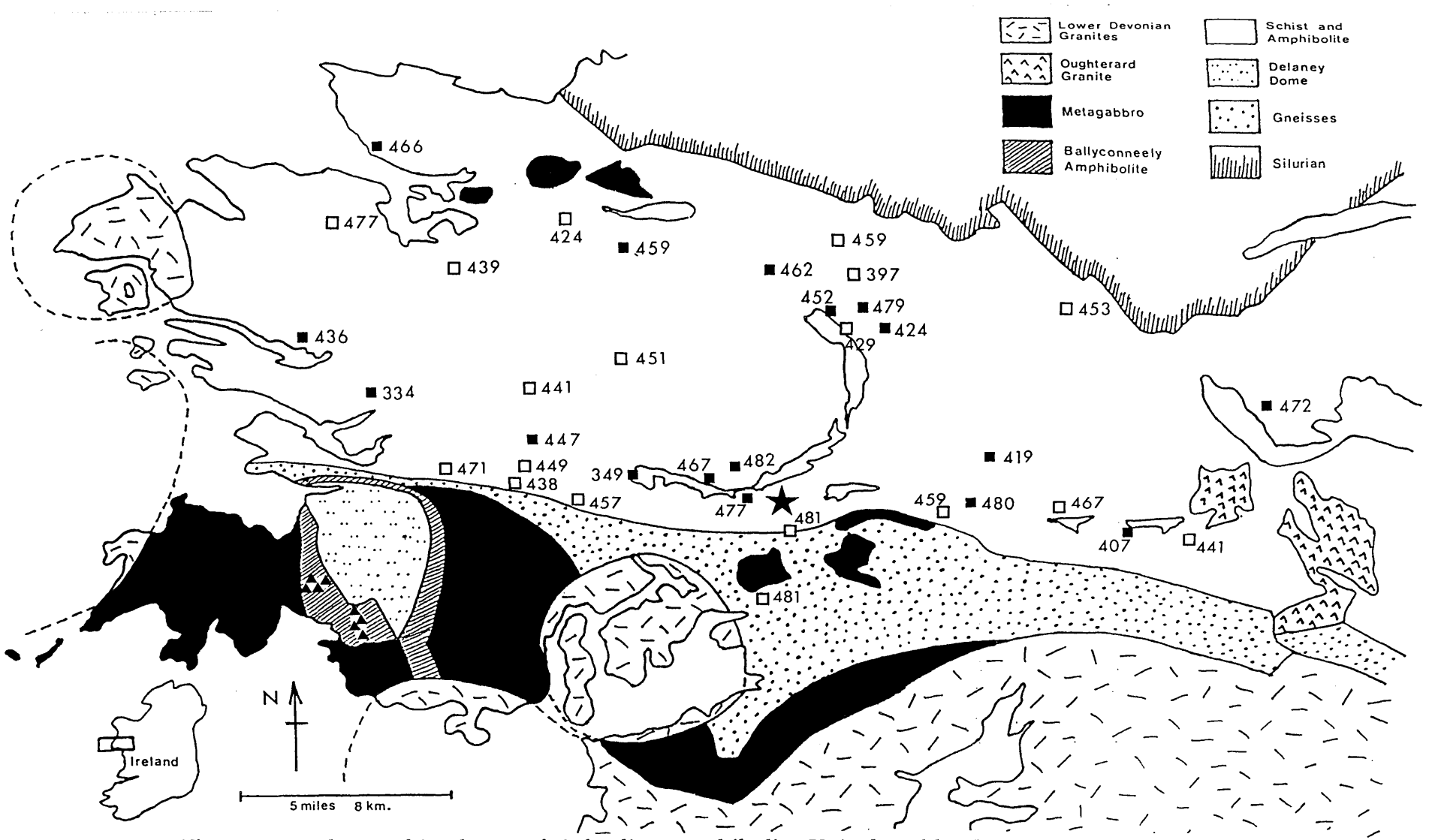

Figure 3.4. The combined sets of Dalradian amphibolite K-Ar hornblende ages, in Ma, from Elias *et al.* (1988), open squares and the present study, solid squares. The star marks the location of the quarry from which samples were collected, in this study, that yielded hornblende K-Ar ages of 397, 406, 452 and 481 Ma. The triangles mark the locations of Ballyconneely Amphibolite hornblende K-Ar ages from Leake *et al.* (1984) of 437, 451, 384, 468, 469, 455, 443 and 464 Ma.

satellite plutons, particularly the Inish and Omey Granites, lie to the west and are intruded, in part, into the Connemara Schists. These granites could have had some influence on the mineral ages. Elias *et al.* (1988) considered that three samples, giving c.410 Ma ages, had been partially reset during intrusion of the Inish Granite. The matter is further confused for three reasons;

a) There may be one or more large granite bodies, unexposed, close to the surface. In the area around Letterfrack (see figure 1.2) there are some small granite exposures which may be the top of a much larger granite body. There does appear to be a lowering of mineral ages in this region. Also throughout much of Connemara, pods and dykes of Oughterard Granite type rock occur. These may all be connected by larger intrusions to the main exposure but without geophysical evidence this must be conjecture.

b) There is disagreement over the age of the Oughterard Granite. This may be another c. 400 Ma granite (see section 1.3). Even if the age of the Oughterard Granite is 459±7 Ma as Leake (1978a) suggests it could still have had a significant controlling influence on the mineral ages from the schists, especially if it does have many shallow underground extensions.

c) There is uncertainty regarding how far the thermal influence of the granites would have extended. The samples identified by Elias *et al.* (1988) as being thermally reset were 2 to 3 km from the contact with the Inish Granite. Ferguson & Al-Ameen (1985) found thermal biotite growing up to 2 km away from the contact with the Omey Granite.

To further understand the variation in ages from the whole of Connemara it is useful to examine smaller areas in more detail. Two areas

are examined both of which have a high density of K-Ar mineral ages. These areas are:

1) To the north-east of Lough Inagh (area A on figure 2.1).

2) To the south of Barnanoruan (area B on figure 2.1). This area includes a section of the Athry Slide (see figure 1.2).

Sketch geological maps of these two areas showing the sample locations and respective mineral ages are shown in figures 3.5 and 3.6.

The first area, the region to the north-east of Lough Inagh, figure 3.5, contains ten K-Ar mineral ages, eight of which come from a smaller 3 km^2 district. Included in this discussion, and shown on figure 3.5, are three hornblende K-Ar ages from Elias *et al.* (1988) which are; 397±7, 429±8 and 459±8 Ma. The hornblende ages from this study are 424±9, 452±9 and 479±10 Ma. All the hornblende ages come from samples of amphibolite. There are three muscovite ages which show identical ages, within error, of 416±8, 418±8 and 420±8 Ma. These three samples are from different formations and lithologies; the Streamstown (semi-pelite), Lakes Marble (pelite) and Bennabeola Quartzite (quartzite) Formations respectively. Only one biotite sample occurs in this area, this has an age of 450±10 Ma and is from a pelitic schist from the Ballynakill Formation. It is clear that in area A, hornblende gives both the youngest and oldest K-Ar ages. The two samples that yielded these ages are only little more than 1 km apart. There is no geographical trend to the ages from area A, either for individual mineral species or combined. There is no correlation between sample age and rock type, or correlation with any geological features, such as proximity to faults. There are no granite exposures in this area. In short all the observations from area A are consistent with observations from the whole of Connemara but on a smaller scale.

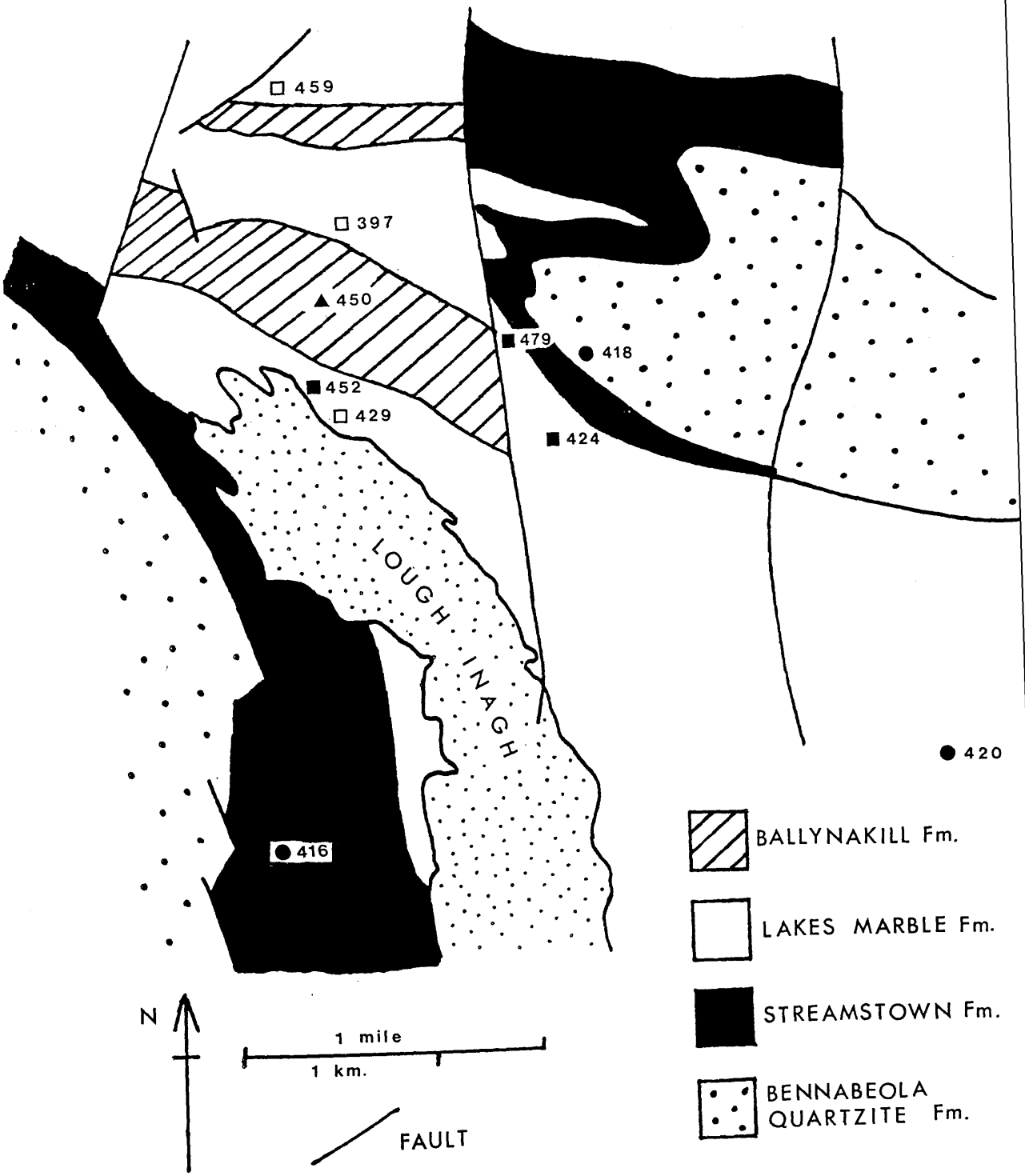

Figure 3.5. Sketch geological map with K-Ar ages, in Ma, from the region to the north of Lough Inagh, area A on figure 2.1. Squares represent hornblende samples, circles muscovite and triangles biotite. Solid symbols represent sample locations from this study, open symbols are locations from Elias (1985); EL 38, EL 75 and EL 76. The geology is based on Leake *et al.* (1981).

The second area, to the south of Barnanoruan, figure 3.6 contains thirteen K-Ar mineral ages. This includes three muscovite ages from Elias *et al.* (1988). In contrast to the first area, the muscovite ages from this area do not show any consistency. The three muscovite ages from Elias *et al.* (1988) are; 429±8, 457±9 and 461±9 Ma. The four muscovite ages from this study are; 408±8, 422±8, 445±9 and 458±10 Ma. All three muscovite samples from Elias *et al.* (1988) and the two youngest samples from this study are quartzites from the Bennabeola Quartzite Formation. The other two muscovites are from pelites of the Cleggan Boulder Bed and Streamstown Formations. There are four biotite ages in area B of; 403±7, 428±9, 438±9 Ma and 453±9 Ma. The youngest biotite age comes from the same Cleggan Boulder Bed sample that gave a muscovite age of 445±9 Ma. The 438±9 Ma biotite age was obtained on a pelitic sample of the Barnanoruan Formation. The remaining two biotite ages of 428±9 and 453±9 Ma came from different semi-pelite samples collected from the same large road cutting in the Streamstown Formation. It is important to note that even though these samples were collected only some 30m apart the ages are different even considering the errors. There are two hornblende ages from area B of 349±7 and 467±9 Ma. These come from amphibolites from two different locations. The youngest hornblende sample was collected from the Lakes Marble Formation close to the shore of Ballynahinch Lake. The second hornblende sample was collected from an amphibolite horizon at the same road cutting as two of the biotite samples. It is clear that consistent with the whole of Connemara, and area A, the ages from area B show no systematic variations. There are no geographical trends apparent, either for each mineral species or collectively as a group. The Athry Slide cuts through the southern part of area B, following roughly the southern shore of Ballynahinch Lake. The lack of any geographical trend to the ages in this area also implies that there is no correlation between the ages and sample

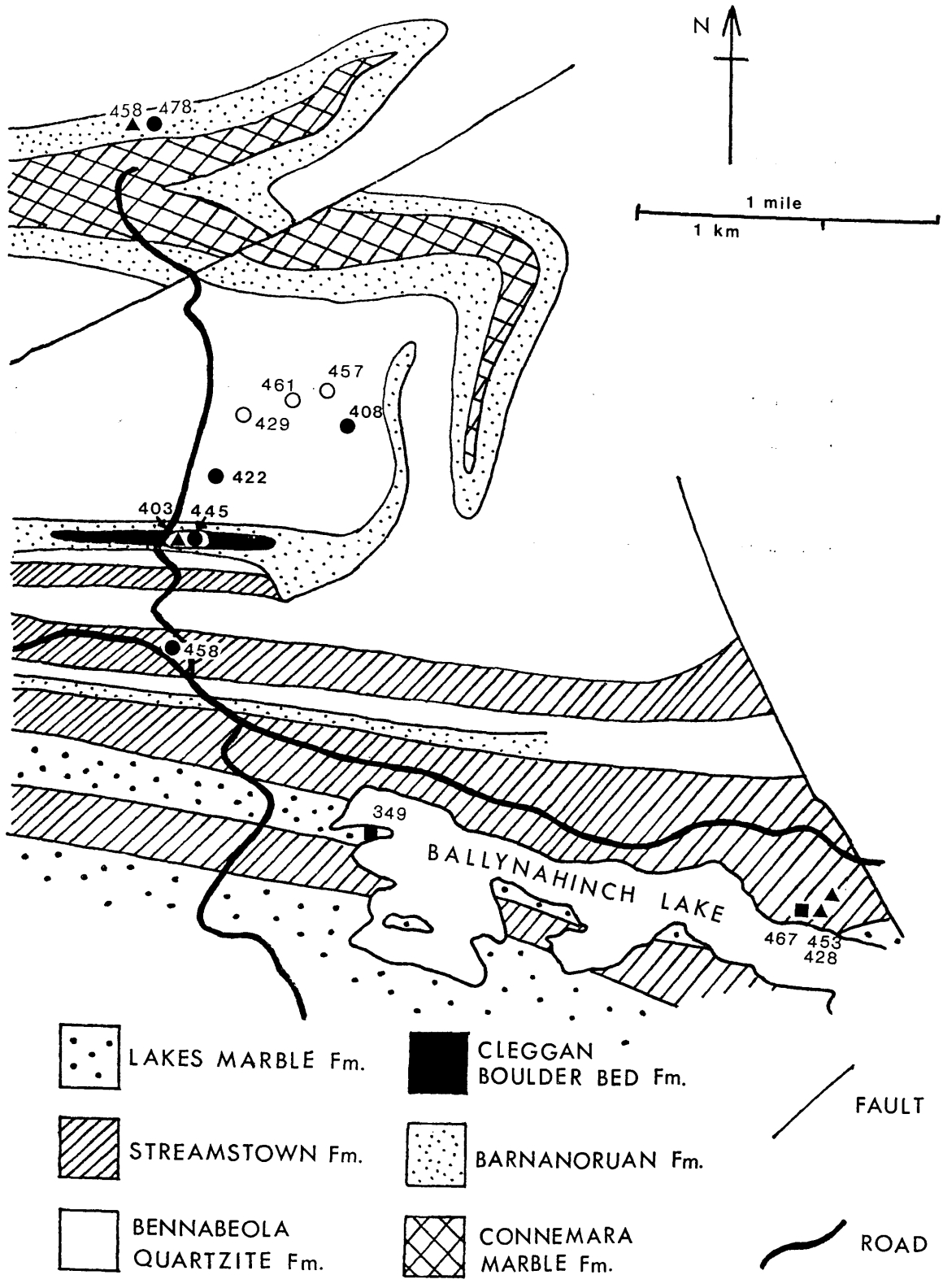

Figure 3.6. Sketch geological map with K-Ar ages, in Ma, from the region to the west of Ballynahinch Lake, area B on figure 2.1. Squares represent hornblende samples, circles muscovite and triangles biotite. Solid symbols represent sample locations from this study, open symbols are locations from Elias (1985); EL 71, EL 72 and EL 73. The geology is based on Leake *et al.* (1981).

proximity to this slide. There is also no correlation between sample age and rock type. There are no granite exposures in area B.

To understand the unexpectedly large variation in the two biotite ages and the one hornblende age from the road cutting in area B is obviously important because this should help to identify the process(-es) which have controlled the K-Ar mineral ages. To fully characterise the possible range in ages from one locality, many K-Ar ages for each mineral species were required. The road cutting in area B was limited in this respect because little muscovite was present in the rocks there. Another site, a quarry, was therefore chosen for detailed sampling. This quarry was along strike from the road cutting, in the Streamstown Formation, and consequently was at the same metamorphic grade. The quarry was in the migmatite zone and had exposure of both amphibolite, and muscovite and biotite-rich semi-pelite, and as the quarry was recently worked fresh material was easily obtained. The amphibolite in the quarry had a very well developed east-west schistosity. The quarry was about 40m wide and was cut out of a sloping hillside. The back wall was some 25m high with the side walls somewhat lower. This meant that samples could be collected from effectively three dimensions. The location of this quarry is marked by a star on figures 3.1 to 3.4.

Eleven K-Ar mineral ages were obtained from samples from different sites in the quarry. These mineral ages consisted of four hornblende ages; five muscovite ages and two biotite ages. The four hornblende ages were; 397±8, 406±8, 452±9, and 481±10 Ma. The five muscovite ages were; 415±8, 438±9, 444±9, 461±9 and 464±9 Ma. The two biotite ages were 447±9 and 454±9 Ma. All the mica ages were from samples of semi-pelite except one biotite and one muscovite, ages 447±9 and 438±9 Ma respectively. These two mica samples came from a pegmatitic

leucosome which had very large (1 to 2 cm) 'books'. It is clear that consistent with areas A and B, hornblende yielded both the youngest and oldest ages obtained in this quarry. In fact the the total range of ages for each mineral species is similar to the overall range of ages from the whole of Connemara. Within the quarry there is no apparent spatial trend to the ages, either for individual mineral species or for all the ages as a group. No major dislocations cross the quarry and so there is no case for arguing that the different samples were obtained from different tectonic 'blocks'. There are no igneous intrusions in or near the quarry. The nearest c. 400 Ma granite is the Roundstone Granite which is about 5 km distant. The small size of this quarry means that all these samples must have undergone the same P-T cycle.

When comparing the observations from Connemara as a whole, areas A and B, and the quarry it is clear that the K-Ar ages, both for each mineral species and collectively, show a wide range of ages of over 100 Ma and these ages are apparently geographically random. The same large ranges in the mineral ages, with hornblende always showing the greatest range, is recognisable down to areas of only 10's m square. At no locality, except for perhaps within a few kilometres of the contact with the granites, are there any apparent relationship between mineral ages and sample proximity to geological features. Particularly, there was no relationship between the ages and sample proximity to the Athry Slide in area B.

It is clear that because of the large range in K-Ar mineral ages that have been obtained from within a few metres within the quarry no direct comparison between the data of Elias (1985) and the present study can be made unless exactly the same outcrops as those collected from by Elias can be sampled again. The locations given by Elias (1985) are not precise enough to enable this. A direct comparison of age dates could however be

made if the mineral separates dated by Elias (1985) were available but unfortunately this is not the case. However, the very similar overall range in ages for each mineral species obtained by the two studies suggests that the two data sets should be comparable. Without any evidence to the contrary it is assumed that the two data sets are in fact complementary, however it is stressed that all the conclusions in this thesis can be arrived at by consideration of the ages obtained during this study alone. The data of Elias (1985) serve only to strengthen those conclusions.

3.1.2 The range of K-Ar mineral ages and correlation with major geological events in Connemara.

The range of K-Ar ages for each mineral species from the whole of Connemara is best understood in the form of histograms, figure 3.7. Also marked on these histograms are the currently accepted ages of the main geological events in Connemara. These events and their ages have been discussed in sections 1.2.3 and 1.3. Figure 3.7 shows clearly that each of the three different mineral species shows a continuous spread of ages from a maximum to a minimum, with the exception of two apparently anomalously young hornblende ages. The maximum age in the age ranges for each mineral species are significantly different and follow the order; hornblende (480 to 490 Ma) > muscovite (460 to 470 Ma, with one older) > biotite (450 to 460 Ma). This is the same order of mineral species predicted by the closure temperature theory if the ages are uplift-cooling ages. This does not imply that these ages *are* uplift-cooling ages, however, and this point will be discussed in the next section. The youngest ages in the continuous age ranges for each mineral species are the essentially same (c. 400 Ma), ignoring for the moment the two young hornblende ages. The shape of the histograms for biotite and muscovite are similar from their

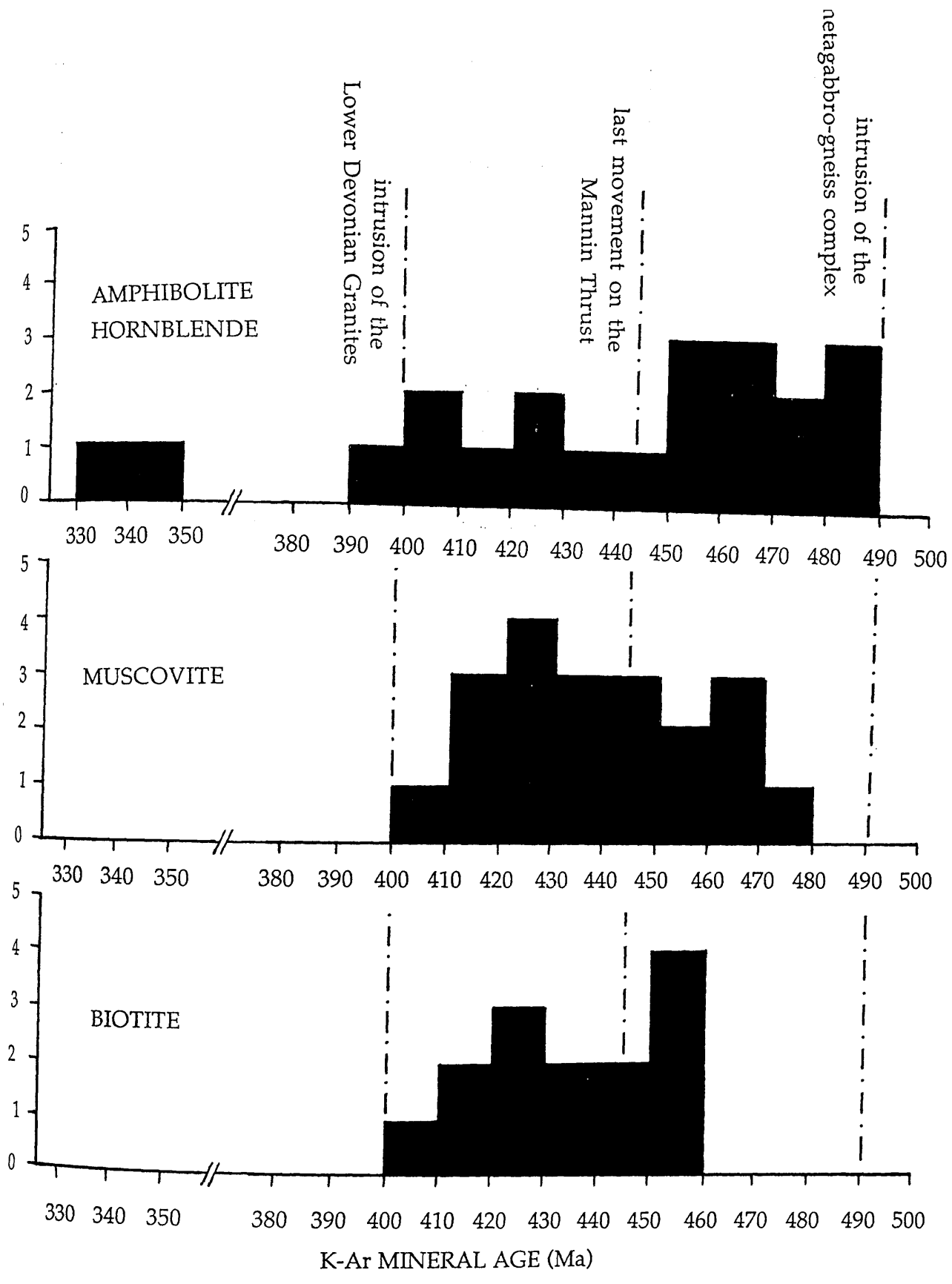

Figure 3.7. Histograms showing the range of K-Ar ages for biotite, muscovite and hornblende. Also shown are the dates for the intrusion of the metagabbro-gneiss complex and the intrusion of the Lower Devonian Granites. There is some suggestion that these two intrusive events are responsible for the spread in the K-Ar ages. In addition the date for the last movement on the Mannin Thrust is shown.

respective maximum ages there are peaks at 430 to 420 Ma and then a stepped decrease in frequency to 400 Ma. The c. 420 Ma peak is more pronounced in the case of muscovite. This pattern is noticeably different from the histogram for the hornblende ages which shows half of the recorded ages occur in the age range 450 to 490 Ma and little sign of a peak at 430 to 420 Ma.

These histograms suggest that there could be some relationship between K-Ar mineral ages and geological events in Connemara. Taking the hornblendes first, the oldest hornblende ages are identical to, within error, or are only slightly younger than the zircon Pb-Pb age of 490±1 Ma for the metagabbro-gneiss complex (Jagger *et al.* 1988). Very clearly the corresponding minimum age for each mineral species (c. 400 Ma), excluding the two anomalously young hornblende ages, corresponds with the intrusion ages for the Lower Devonian Granites. This strongly suggests that the two c. 350 Ma age amphibolite hornblendes are not recording the same geological processes that caused the other K-Ar mineral ages. One possible explanation for these two low hornblende ages is that these samples were collected from close to one, or more, of the Carboniferous dykes that occur in Connemara (Mitchell & Mohr 1987). Although the area around each sample location was scouted to ensure no obvious dykes were present it is possible that some were hidden by the extensive blanket bog covering. In the case of WM 201 the sample location was on a lakeshore and so it is possible that a dyke could go unnoticed in the water.

3.1.3 Implications for the interpretation of the K-Ar mineral ages from the Connemara Schists and their geographical distribution and age ranges.

Considering the geographical distribution of the samples and the large range in the K-Ar ages for each mineral species, especially from small areas, it is clear that these ages cannot represent cooling through invariant, mineral specific closure temperatures. If this were to be the case then all the minerals of one species, from one small locality, would be expected to give the same age. The same would be true of the ages from the whole of Connemara if it uplifted in one block, without tilting, all else being equal. If on the other hand Connemara had lifted as separate blocks, possibly at different times and at different rates with each block perhaps tilting, as suggested by Elias *et al.* (1988) then some geographical relationships should exist between the K-Ar mineral ages and the sample localities. Such geographical trends due to tilted uplift and cooling have been recorded in many regions, the best examples are the Alps (Wagner *et al.* 1977) and the Grenville Orogenic belt, Canada (Anderson 1988). Furthermore, because in this type of uplift situation no differential cooling should occur between samples from the *same* locality, all the K-Ar mineral ages would be the same for each mineral species from the same place. This is clearly not the case in Connemara. Even despite the uncertainty over the relationship between mineral ages and sample proximity to the Lower Devonian Granites and the likely influence of these granites on the K-Ar mineral ages (3.1.1) it is reasonable to conclude that the K-Ar mineral ages do not represent uplift and cooling of Connemara, as either one or more blocks, through mineral specific closure temperatures.

Considering only the range of K-Ar mineral ages and their correlations with geological events in Connemara it is tempting to

construct a model that would explain the majority of the K-Ar mineral ages in terms of hornblende closure to Ar loss following intrusion of the metagabbro-gneiss complex, and biotite and muscovite closure to Ar loss occurring later. To do this, however, is premature because this model implies that the majority of ages were initially cooling ages and this is inconsistent with conclusions drawn from the lack of any geographical trend to the K-Ar mineral ages. There is, therefore, a dichotomy between the apparent correlation between the *range of ages* and geological events on one hand and the lack of correlation between the *geographical distribution of ages* and geological features on the other. There are at least three optional alternative explanations for the K-Ar mineral ages.

1) The K-Ar mineral ages are cooling ages, but they are not the result of cooling through invariant, *mineral* specific closure temperatures but are the result of cooling through *sample* specific closure temperatures. It has been clearly shown that the concept of mineral specific closure temperatures is an oversimplification in many geological environments because the closure temperatures can be sensitive to a variety of physico-chemical factors (see section 1.4.2). If these factors could cause a great enough dispersion in the closure temperatures of each mineral species then this might explain the K-Ar mineral ages. However, if this is the case it is hard to understand the apparent correlation between the K-Ar mineral ages and geological events in Connemara.

2) The K-Ar mineral ages are not simply the result of cooling through mineral specific closure temperatures but represent 'mixed ages' between an original cooling event and one or more later partial resetting events. Clearly this type of process could result in a very complicated set of K-Ar mineral ages. There is a suggestion in the correlations apparent between the range of mineral ages and geological events in Connemara

that this type of process might explain the K-Ar mineral ages. The oldest hornblende ages could represent the original cooling event following the intrusion of the metagabbro-gneiss complex and the corresponding minimum ages for each mineral species at c. 400 Ma represents the younger, partial, resetting event synchronous with the intrusion of the Lower Devonian Granites.

3) The large range in K-Ar mineral ages reflects variable amounts of excess Ar in the samples. This alternative is not favoured for the following reasons. During emplacement of the metagabbro-gneiss complex extensive baking of the Connemara Schists occurred. It is proposed that this heating was sufficiently intense and long lived to cause total rejuvenation of all the K-Ar mineral systems. The oldest K-Ar ages from the Connemara Schists are the same age as or slightly younger than the age of the metagabbro-gneiss complex. The lack of any K-Ar mineral ages older than the geological maximum possible age (ie. the age of the metagabbro-gneiss complex) suggests that no significant excess Ar component occurs in the samples. As it is considered that excess Ar is not important to the problem of the K-Ar mineral ages it will not be discussed any further.

The most reliable way to distinguish between the first two alternative models outlined above is to demonstrate beyond all doubt that the K-Ar mineral ages are, or are not, the result of uplift and cooling through sample specific closure temperatures. To do this would require the actual closure temperatures for each mineral sample be calculated and, from the range of actual closure temperatures, to show if these are compatible or incompatible with the range and order of the K-Ar ages. To do this would be a huge undertaking because to calculate closure temperatures it is necessary to measure activation energies and diffusion coefficients and these are difficult and time consuming quantities to

measure. No such attempt has been made. Instead the various physico-chemical factors known to influence closure temperatures such as Fe/Mg ratios are compared to the K-Ar mineral ages for each mineral species. If the range of K-Ar mineral ages are simply and only cooling ages related to highly variable closure temperatures then a correlation should exist between the K-Ar mineral ages and that relevant physico-chemical factor controlling the closure temperature, if all else is equal. The following sections detail the various factors that could influence closure temperatures and therefore K-Ar mineral ages.

3.1.4 Relationship between mineral chemistry and K-Ar age.

There has been much disagreement over the extent of the influence composition can exert on closure temperatures, see section 1.4.2 for a review. The Fe/Mg ratio has been claimed to affect the closure temperature of hornblendes (O' Nions *et al.* 1969; Berry & McDougall 1986), and the same ratio has been claimed to affect the closure temperature of biotite (Harrison *et al.* 1985). The Na content of muscovite has also been inferred to affect its closure temperature by Chopin & Maluski (1980) who claim that paragonite has a higher closure temperature than muscovite. Elias (1985) tested comprehensively for compositional dependence on K-Ar mineral ages for hornblende, biotite and muscovite and found none but in view of the importance of this possibility further tests were carried out.

It has been shown in section 2.4.2, from electron-probe analyses, that there is some chemical variation in hornblende, biotite and muscovite samples. To test for compositional influence on the K-Ar mineral ages four different measures of mineral chemistry have been selected for each mineral species, these are, for hornblende; $Fe^2/(Fe^2+Mg)$, K_2O, Ca/K and

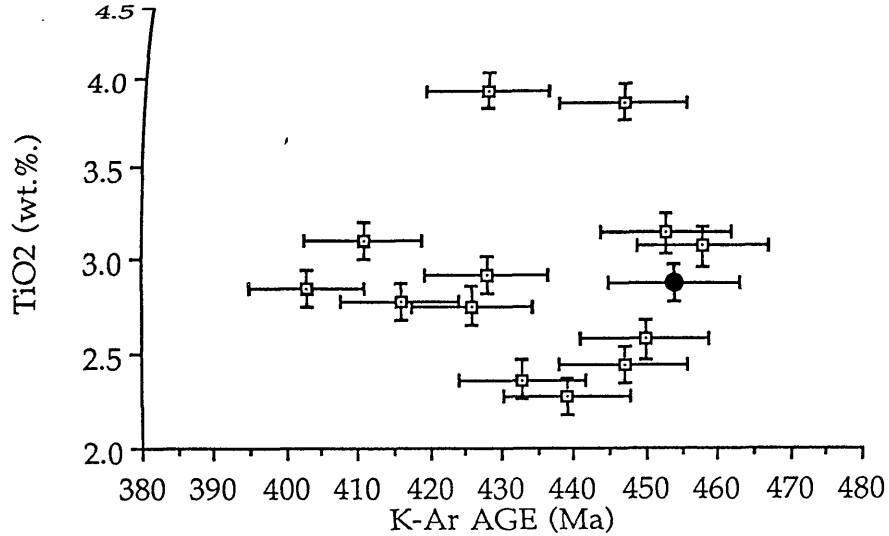

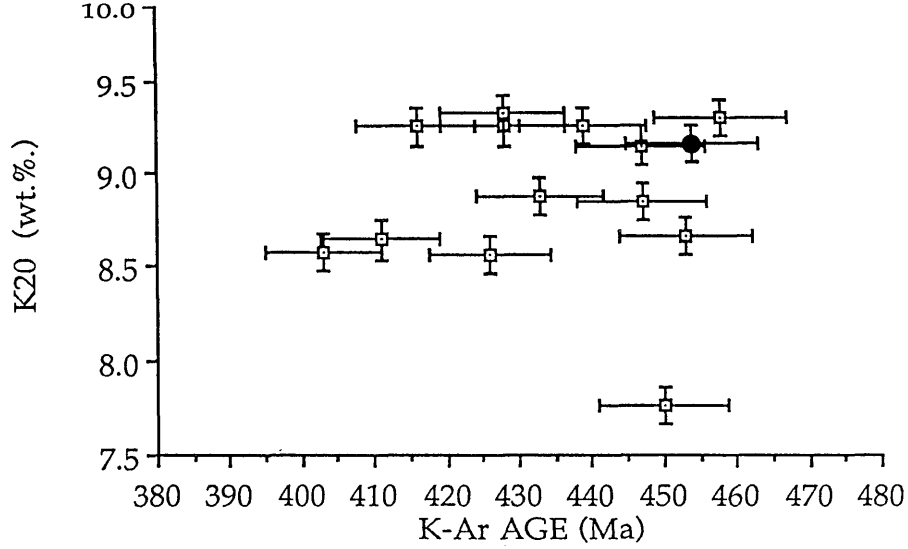

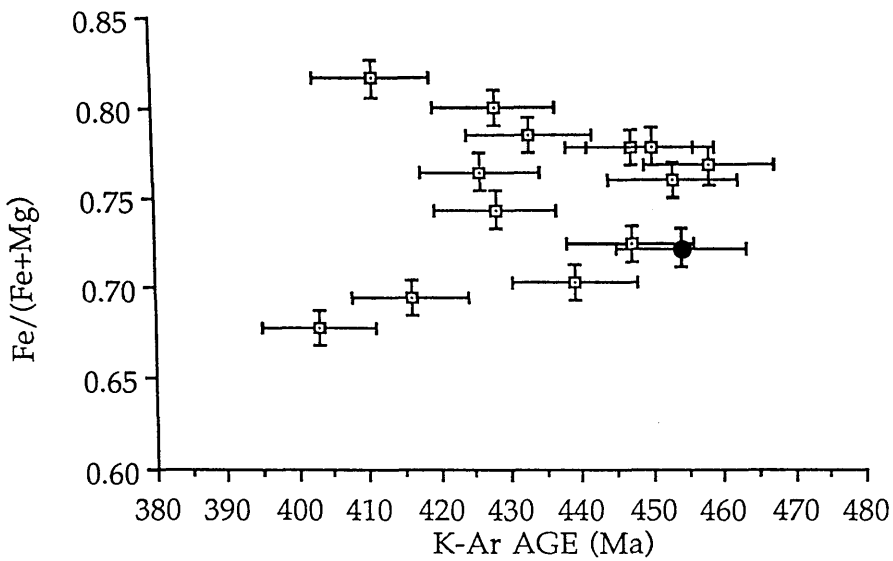

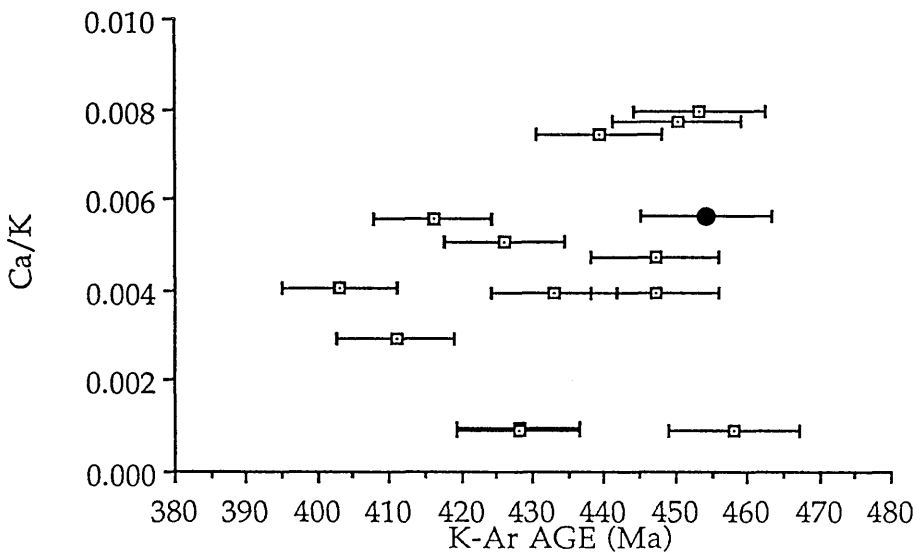

Figure 3.8. Correlation diagrams of biotite K-Ar ages v. various measures of hornblende chemistry. Circles mark samples from quarry, figure 2.1.

'A' site occupancy, for biotite; TiO_2, K_2O, Fe/(Fe+Mg) and Ca/K, and for muscovite; K_2O, Fe/(Fe+Mg), Ca/K and Na/K. These measures of mineral chemistry have been chosen because they reflect either standard compositional fields of the minerals eg. Fe/(Fe+Mg) for hornblendes or some degree of alteration eg. Ti and K expulsion in biotites. The correlation diagrams between these measures of mineral chemistry and K-Ar mineral age for biotite, muscovite and hornblende are shown in figures 3.8, 3.9 and 3.10, respectively.

The correlation diagrams for biotite, figure 3.8, show no obvious relationships in any case except for a slight suggestion that the decrease in K-Ar age is accompanied by a decrease in the Ca/K ratio. The lack of a relationship between K_2O and the K-Ar age, and TiO_2 and the K-Ar age, suggests that the low biotite K-Ar ages are not caused by progressive chloritisation because this process involves expulsion of both K and Ti from the mineral. This is important because the widespread chloritisation in the Connemara Schists could be wrongly used to infer that the wide range of biotite K-Ar ages is simply the result of retrogressive alteration. The recognition that this is not the case confines the cause of the biotite K-Ar ages to either diachronous closure to Ar diffusion, or to Ar loss by some process other than simple chemical reaction.

The correlation diagrams for muscovite, figure 3.9, show no obvious relationships between Ca/K and K-Ar age and Na/K and K-Ar age. There is a slight suggestion that decreasing K-Ar ages might be accompanied by an increase in K_2O and a decrease in the Fe/(Fe+Mg) ratio. The relationships are not sufficiently clear to be reliable, they may be no more than artifacts resulting from the small number of samples. If these relationships are real it *may* be the result of dating two different

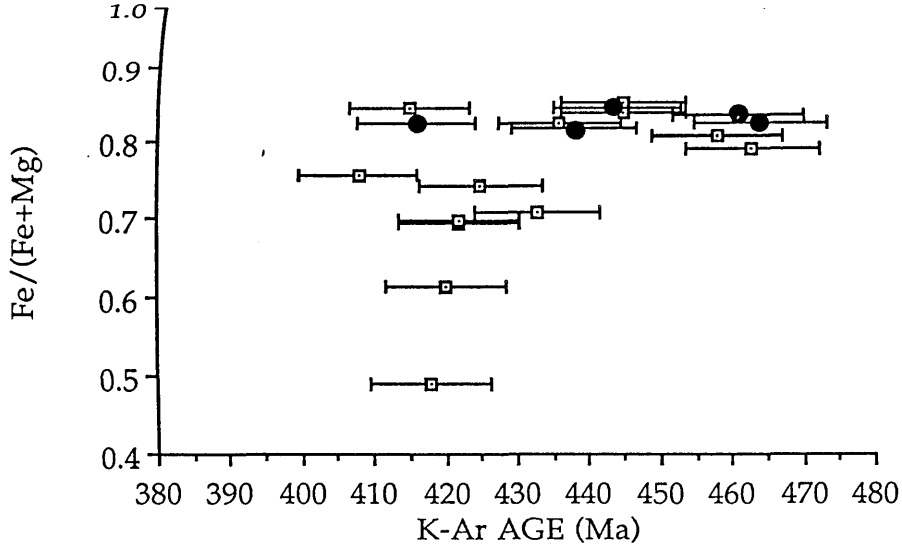

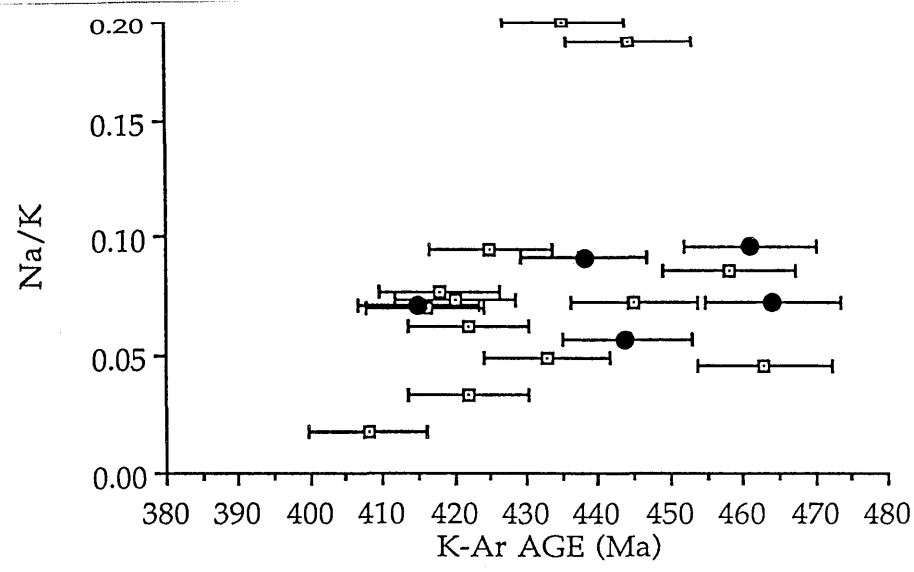

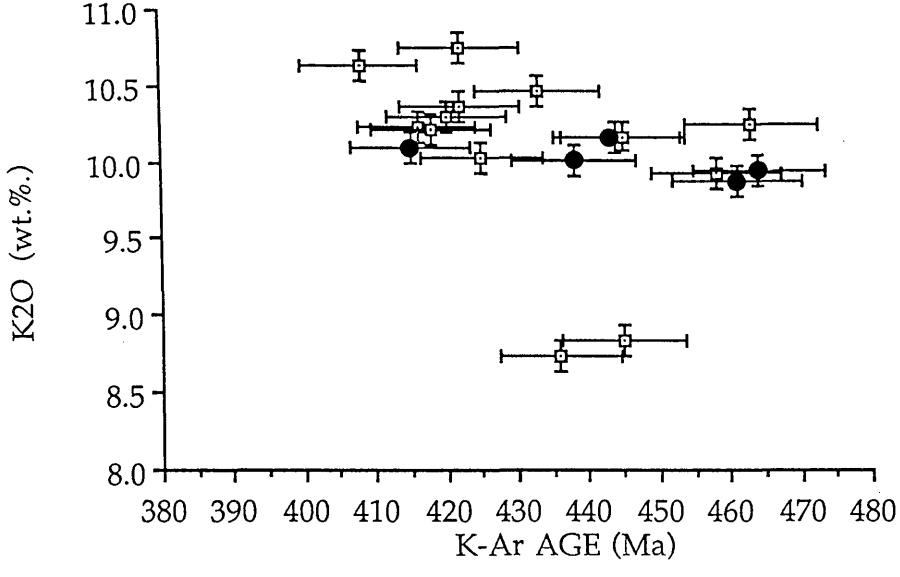

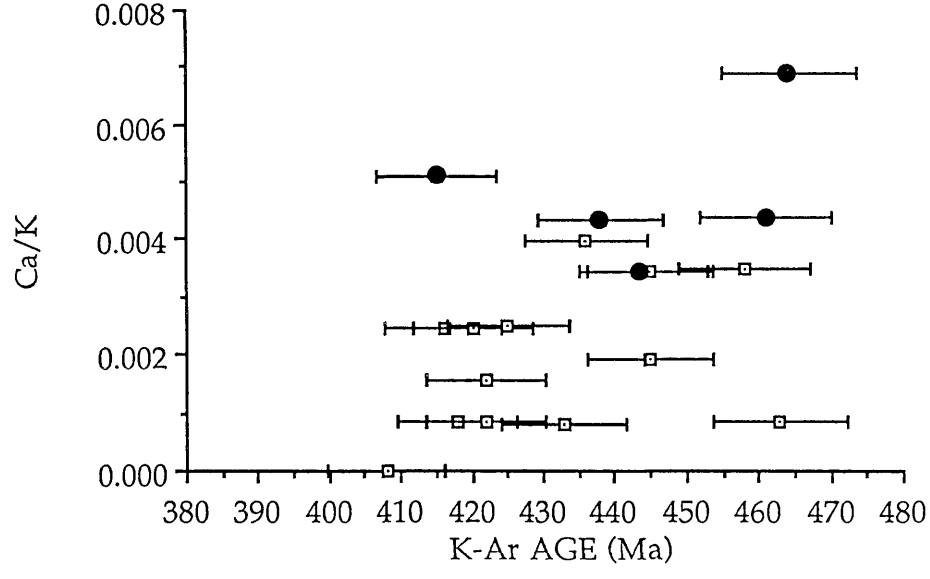

Figure 3.9. Correlation diagrams of muscovite K-Ar ages v. various measures of hornblende chemistry. Circles mark samples from quarry, figure 2.1.

generations of muscovite, an older K and Fe rich generation and a younger K and Fe poor generation.

The correlation diagrams for hornblende, figure 3.10, show no relationships between either Ca/K, K_2O or 'A' site occupancy and K-Ar age. There is, however, a trend between the $Fe^2/(Fe^2+Mg)$ ratios and the K-Ar age which implies that lower K-Ar ages are associated with Mg rich hornblendes. This is the complete reverse of the relationships between Ar retentivity and the Fe/Mg ratios of hornblendes demonstrated by O' Nions *et al.* (1969) and Berry & McDougall (1986). Why this should be the case is not at all clear. It was suggested in section 2.4.2 from the electron-probe analyses that variation in the $Fe^2/(Fe^2+Mg)$ ratios of the hornblendes might reflect either an igneous differentiation trend or, alternatively, alteration. If the former explanation is correct then what is the controlling factor over Ar retention, if it cannot simply be Fe/Mg, consistent with the results of previous workers? If the second explanation is correct then it would be expected that samples more heavily altered would give the lowest ages. Electron-probe analyses of the altered cleavages of hornblendes give high Fe/Mg ratios and yet the lower age hornblendes have low $Fe^2/(Fe^2+Mg)$ ratios. This seems to suggest that whatever the process that caused the variation in the hornblende K-Ar ages, it is not simply retrogressive alteration of the hornblende to biotite. At this point it should be recalled that Elias (1985) did not find any relationship between Fe/Mg ratios and K-Ar ages for hornblende. The probable reason for this apparent discrepancy between the two studies is that Elias, for his analyses, did not measure FeO by direct wet chemical means. The Fe/(Fe+Mg) ratios given by Elias in the diagrams are really $Fe_{(total)}/(Fe_{(total)}+Mg)$ and not $Fe^2/(Fe^2+Mg)$ as reported in this study. Examination of the hornblende

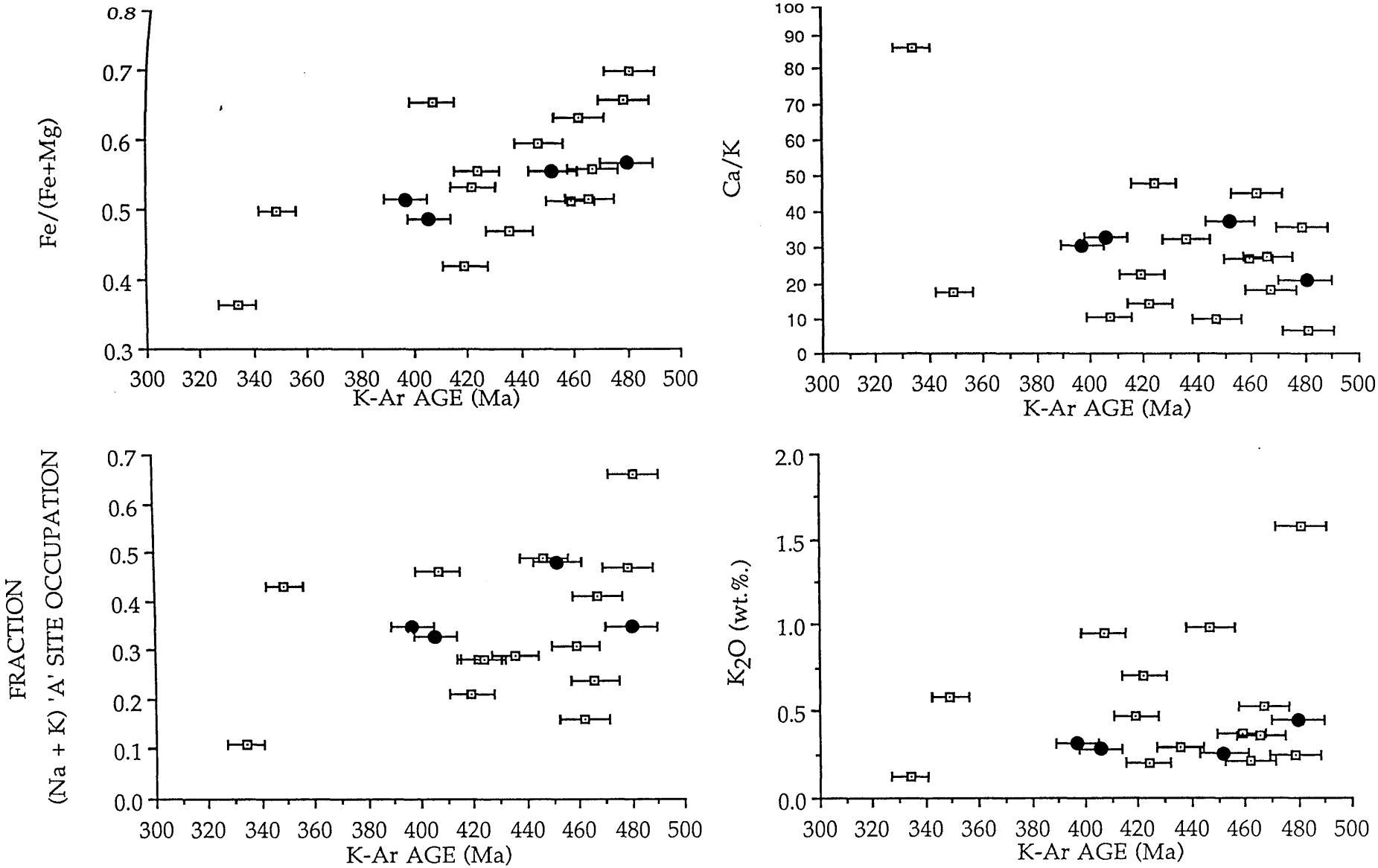

Figure 3.10. Correlation diagrams of amphibolite hornblende K-Ar ages v. various measures of hornblende chemistry. Circles mark samples from quarry, figure 2.1.

chemical analyses performed for this study, appendix A.5.1, show that in some hornblende samples significant amounts of Fe are present as Fe^3.

The lack of any correlation between the mica K-Ar ages and chemistry shows that the ages are not controlled by chemistry and therefore the mica K-Ar ages cannot be caused by cooling through chemistry-dependent closure temperatures. The trend between hornblende K-Ar ages and $Fe^2/(Fe^2+Mg)$ being the opposite to previously published relationships sounds a cautionary note especially with the lack of any correlation between K-Ar age and the other chemical measures. Probably the hornblende K-Ar ages are not the result of cooling through chemistry dependent closure temperatures but it remains possible that the $Fe^2/(Fe^2+Mg)$ ratio does exert some control.

3.1.5 Relationship between crystal microstructure and K-Ar age.

This heading covers a multitude of different features that are all related to crystal heterogeneity or defects. A review of the literature dealing with the affect on closure temperatures by crystal heterogeneity is given in section 1.4.2. The two most common features of this type are exsolution and secondary mineral intergrowths or inclusions and most of the research to date had dealt with the affect of these features on the closure temperature of hornblende (eg. Harrison & Fitz Gerald 1986; Onstott & Peacock 1987; Blanckenburg & Villa 1988). Two of the hornblendes dated in this study were examined by TEM (see section 2.4.4). It was found that one sample showed micron-scale exsolution features, probably cummingtonite exsolving out of hornblende, and the other sample contained sub-micron, probable, phyllosilicate inclusions.

The hornblende sample with exsolution was seen to contain coexisting cummingtonite and hornblende when examined in thin section. This is characteristic of a number of other amphibolite samples from an area to the north-west of Lough Inagh and it seems likely that exsolution would be present in all the Connemara samples with coexisting amphiboles. It must be stressed, though, that this has not been shown to be true. It is difficult to quantify the affect this exsolution might have on the K-Ar ages. Harrison & Fitz Gerald (1986) showed that exsolution in a hornblende had resulted in a lowering of its closure temperature, from about 500°C, to less than the closure temperature of biotite, ie to less than about 300°C. The actual difference a change in closure temperature such as this would have on the K-Ar ages depends on the cooling rate. The slower the rate of cooling the larger the possible range in the K-Ar ages. Furthermore it is intuitively reasoned that the degree of exsolution and the size of the exsolved component will also affect the closure temperature and the resulting K-Ar ages. It is possible, therefore, that varying degrees of exsolution in some of the hornblende samples *could* be responsible for some of the low K-Ar ages, as low or lower than mica ages. However, without sure knowledge of which samples do have exsolution and without being able to quantify the affect this exsolution has on the K-Ar ages it is impossible to be more precise.

The second hornblende sample with probable phyllosilicate inclusions might be more typical of most of the hornblende samples than the sample with exsolution. This is because many of the amphibolites when examined in thin section were seen to have minor zones of alteration at grain rims and along cleavages. The phyllosilicates seen with the TEM in the second sample are most likely to be alteration products of the same type, and from the same process, as the alteration visible in thin section. Consequently many of the other hornblende samples could contain

these sub-microscopic inclusions. As with the exsolution it is very difficult to quantify the affect on the K-Ar ages inclusions such as these might have. Onstott & Peacock (1987) examined two hornblendes, from the same location, that gave different ^{40}Ar-^{39}Ar total fusion ages of 906±5 and 949±4 Ma. The sample yielding the lower age was found to contain significant amounts of sub-microscopic phyllosilicates. The authors calculated that this difference in the ages, if all else were equal, corresponds to a difference in the closure temperatures of between 40 and 200°C for cooling rates of 1 to 5°C/Ma. They further measured the separation distance between the phyllosilicate zones and called this the effective diffusion dimension ('a' in equation 1.1) and calculated the closure temperature to be 412°C for the low age sample, assuming a 1°C/Ma cooling rate. What this means for the Connemara hornblende samples is not clear because so many unknowns persist. However, assuming that some of the hornblendes do contain variable amounts of sub-microscopic phyllosilicates, it *could* be possible that this explains the range in the hornblende K-Ar ages.

To summarise this, exsolution in hornblendes has been shown to be capable of reducing the closure temperature from about 500 to 300°C. Phyllosilicate inclusions in hornblendes have been shown to be capable of reducing the closure temperature to about 400°C. The actual affect on the K-Ar mineral ages depends not only on the degree of exsolution or alteration but also on the size of the components and on the cooling rate. There has been no similar work to determine the affect on closure temperatures of micas from alteration products or inclusions. Micas do not exhibit exsolution so this is not relevant. No TEM investigation of any of the micas dated in this study has been performed and so it is not possible to comment on the crystal heterogeneity. The result of all this, is that it is unknown if there is any likelihood that the closure temperatures of micas could have been, or infact have been, influenced by crystal microstructure.

It is possible that exsolution and phyllosilicate inclusions together *could* cause the range of the hornblende K-Ar ages by lowering the closure temperature, but *this has not been proved.* Indeed it seems unlikely that all the hornblende ages from the whole of Connemara would be affected in this manner to such a large extent. It must be stressed that only a few studies have been published that document such low hornblende K-Ar closure temperatures, but this in itself indicates the rarity of the process especially when this is balanced against the large number of hornblende K-Ar and ^{40}Ar-^{39}Ar ages that are apparently consistent with the 'normal' values of hornblende closure temperatures. The same argument can be used to suggest that the range of mica K-Ar ages is unlikely to be the result of unusual crystal microstructures. There is a second point to consider when discussing the exsolution and the phyllosilicates, and this refers to the time these features formed. If these features existed before the mineral had cooled they could affect the closure temperature. If on the other hand they formed after the mineral had already cooled and closed then they obviously could not cause a retrospective change in closure temperature. Nonetheless, it is likely that the formation of exsolution patterns would cause the loss of retained Ar so exsolved minerals could have disturbed K-Ar ages even if exsolution occurred after closure. In the case of the phyllosilicate inclusions a similar argument can be used. If no phyllosilicates were present before cooling and closure, then the closure temperature would initially be unaffected. If the phyllosilicates formed after closure then Ar might be lost because the characteristic diffusion dimension would be changed. Another point is that if the phyllosilicates were K rich then the apparent K content of the hornblende (which is measured in bulk) would be increased causing anomalously young K-Ar ages.

Considering all these factors, no definite conclusions can be drawn regarding the affect the microstructure has had on the K-Ar ages of hornblende because of the larger number of unknowns, ie. the number of samples affected and the time of formation. For the micas however, it is concluded that the lack of any previous reports of microstructure control on ages is sufficient to conclude that there is probably no such affect in the Connemara biotites or muscovites.

3.1.6 Relationship between rock alteration and K-Ar age.

The Connemara Schists have suffered extensive retrogressive alteration with ubiquitous chloritisation of biotite, and sericitisation and saussuritisation of plagioclase. In table 2.1 (section 2.3) a subjective alteration index for the plagioclase and biotite in each sample was assigned. Alteration of the rock, although not affecting the closure temperature of minerals directly, can potentially cause disturbances in the K-Ar mineral ages. Correlation diagrams have been plotted, figure 3.11, to test for any relationship between the K-Ar mineral ages and the degree of rock alteration. Relationships are apparent between both the biotite K-Ar ages and muscovite K-Ar ages with the alteration index of co-existing feldspar. This suggests that the range of the mica K-Ar ages is related to the hydrous alteration of the rock and therefore occurred during fluid movement. However, reduction in the biotite K-Ar ages cannot simply be the result of alteration of the biotite because no correlation exists between biotite K-Ar age and the biotite alteration index. This conclusion was also reached from the lack of a correlation between the biotite K-Ar ages and K_2O and TiO_2 contents, these being sensitive indicators of alteration. Similarly it is proposed that the reduction in the muscovite K-Ar ages, although occurring during the fluid migration phase, was not the direct result of

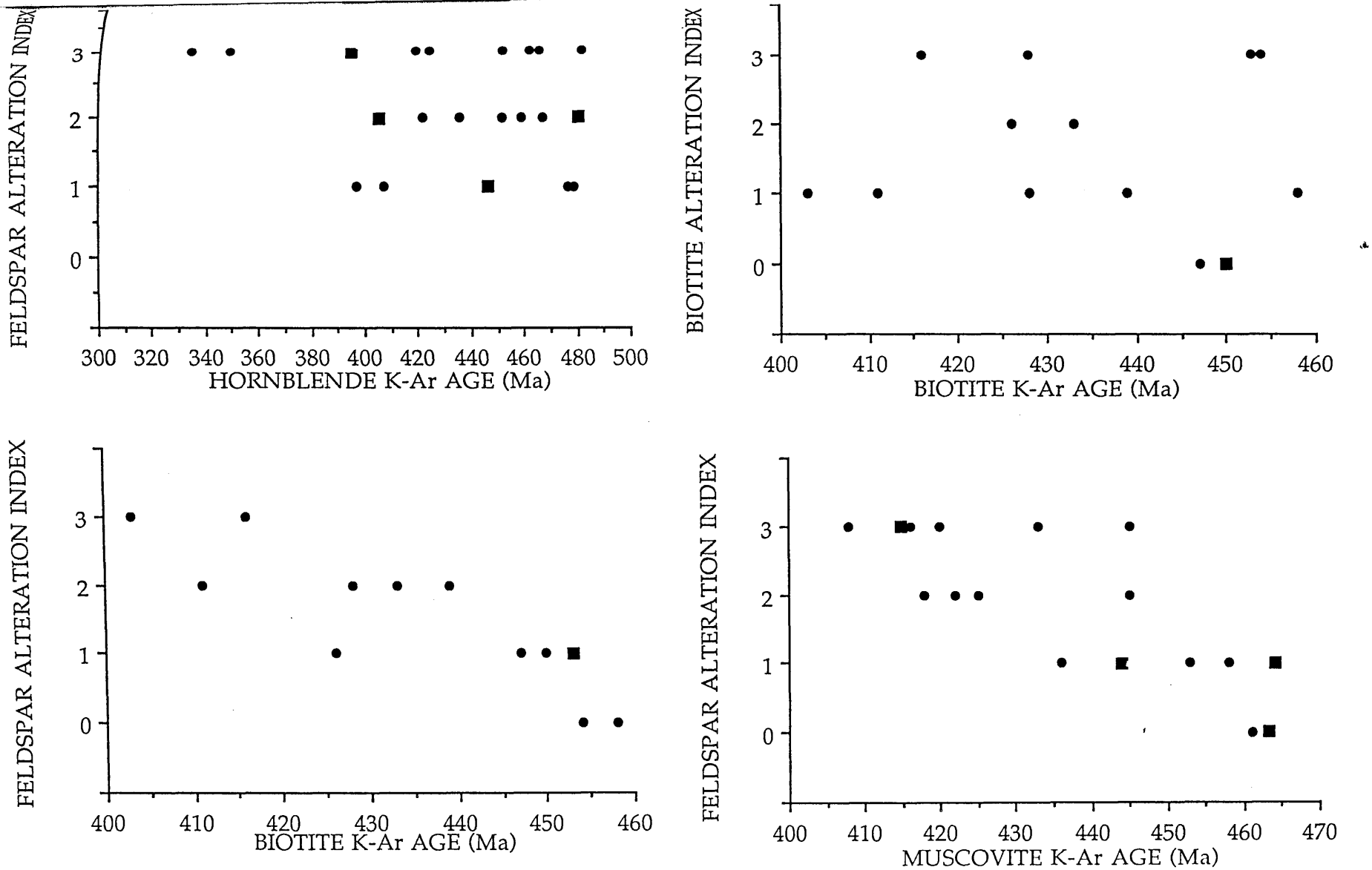

Figure 3.11. Correlation diagrams of biotite, muscovite and amphibolite hornblende K-Ar ages v. co-existing feldspar alteration indexes. Plus, correlation diagram of biotite K-Ar age v. biotite alteration index. Alteration index scale runs from 0 = no alteration to 3 = complete alteration. Squares mark samples from quarry, figure 2.1.

alteration of the muscovite and must therefore the result of some other process. This other process cannot be identified from this information alone but a possible explanation would be that the fluid was at or near the closure (opening) temperature of the micas and for that reason caused partial thermal resetting of the micas it came into contact with. No correlation exists between hornblende K-Ar ages and co-existing feldspar alteration index. That some low hornblende K-Ar mineral ages occur in samples with little feldspar alteration suggests that either the reduction of hornblende K-Ar ages proceeds by a different process than for micas or, if it is the same process, at a different rate.

Fluid involvement in the process that caused the large range of K-Ar mineral ages is an attractive option because the very heterogeneous nature of fluid movement along faults, fractures, veins etc. allows for differing degrees of fluid-mineral interaction and is thus consistent with the variation in the K-Ar mineral ages recorded in samples collected from small areas.

3.1.7 Relationship between grainsize and K-Ar age.

Dodson (1973) showed that the characteristic diffusion dimension affects the closure temperature of minerals, see section 1.4.2 for review. In some cases the actual size of the grains approximates to the characteristic diffusion dimension and in this case a relationship will exist between grain size and K-Ar ages, if these ages are simply cooling ages (eg. Kelley 1988). In many cases there is simply no correlation between the grain size and the K-Ar ages. This implies that either the K-Ar ages are not simple cooling ages, or if they are, that the characteristic diffusion dimension is not the absolute

grain size, but some smaller sub-grain region perhaps bounded by the cleavages.

The grain sizes of both the micas and hornblende are relatively uniform for samples collected all over Connemara. Biotite grains typically range from about 1/4 to 2mm, muscovite from 1/4 to 3mm and hornblende range from 1/4 to 2mm. An average grain size for each mineral species is about 1/2mm. In some of the pelitic samples micas grew to about 3 to 5mm, with finer mica in between. Two such samples were chosen and different size fractions of biotite and muscovite separated and dated by the K-Ar method. The results are given in table 3.1 below.

Table 3.1. The affect of grain size on mica K-Ar ages

SAMPLE	MINERAL	SIZE	AGE
WM 188	M	125-250 microns	425±9 Ma
WM 188	M	500-2000 microns	431±9 Ma
WM 196	B	125-250 microns	403±8 Ma
WM 196	B	500-1000 microns	402±8 Ma

M=muscovite, B=biotite.

It is clear that the ages for each size fraction, from the same sample, are identical within error. There is an inbuilt assumption with this technique and that is that the majority of the grains in the smaller size fractions are actually smaller grains from the rock matrix and not crushed fragments of larger grains. Obviously if this were not a true assumption then the same material would be dated for each size fraction. This assumption is thought to be valid because the elastic nature of the micas tends to prevent the larger grains from being crushed if the whole process is not too vigorous. Elias (1985) measured the actual grain size of each of the samples dated in that study and found no correlation between these

and the K-Ar ages for either biotite, muscovite or hornblende. The results of the present study are consistent with the findings of Elias (1985). It is concluded that the variation in the grain sizes of any of the mineral species in Connemara could not cause the large range of K-Ar mineral ages.

3.1.8 Relationship between sample elevation and K-Ar age.

The structural elevation of samples does not affect the closure temperatures of the minerals but it can influence K-Ar cooling ages. All of the Connemara samples were collected from a small range of elevation, from about 40 to 200m above sea level. Assuming a relatively slow uplift rate of 1km every 10Ma and that the K-Ar ages are cooling ages and all else is equal, this range in elevation translates into an age differential of 1.6 Ma. A typical error on the K-Ar ages is ±9 Ma; this means that any elevation effect on the K-Ar ages is unlikely to be resolved with the accuracy of the methods employed. Consistent with this conclusion are the results of Elias (1985) who plotted the structural elevation against the K-Ar ages for all his samples and found no correlation. It is concluded that the range in elevation of the Connemara samples cannot be responsible for the large range in K-Ar mineral age for any mineral species.

All but one of the factors discussed have been concluded not to have had any affect on the closure temperature of the different mineral species and therefore the K-Ar mineral ages. The outstanding factor to be considered is crystal microstructure and then only its potential affect on hornblende K-Ar ages. The correlation between the rock alteration and the mica K-Ar ages does not indicate a reduction of the closure temperature but rather reduction of the K-Ar ages after closure. This means that the second of the two possible models outlined earlier to explain the biotite and

muscovite K-Ar ages (the 'mixed ages' model) is more consistent with the data. As some uncertainty remains over the possible influence of crystal microstructure on the hornblende K-Ar ages a combination of the first two models is preferred to explain these ages.

It is concluded that the mica ages reflect initial cooling through *mineral* specific closure temperatures and subsequent partial resetting during a later Ar loss event in the presence of a fluid. The hornblende ages reflect initial cooling through an unknown range of *sample* specific closure temperatures and subsequent partial resetting during a later event, at a time of fluid mobility. At this stage the particular geological events corresponding to these cooling and resetting stages are not discussed, the overall geological synthesis will be discussed in chapter five.

3.2 K-Ar ages from the metagabbro-gneiss complex.

Nine hornblende K-Ar ages have been determined on samples of the metagabbro-gneiss complex. The sample locations are indicated on figure 2.1 and table 3.2, together with their respective ages. Also included on the table are the four hornblende K-Ar ages reported by Elias *et al.* (1988). All but one of the samples from this study and two of the samples from Elias *et al.* (1988) were metagabbro rocks, the others were orthogneiss. There is no statistical difference between the hornblende K-Ar ages from the two rock types, consistent with the field evidence which shows that although the orthogneiss is a later intrusion than the metagabbro it was only slightly later. In fact the metagabbro was still plastic when the orthogneiss was intruded into it forming the characteristic agmatite. The two youngest K-Ar hornblende ages, 453±10 and 457±10 Ma, come from less than 200m from the contact with the Galway Granite.

Table 3.2. K-Ar ages from the metagabbro-gneiss complex.

SAMPLE	TYPE	AGE (Ma)	LOCATION
WM 108	M	453±9	Contact with Galway Granite
WM 109	M	457±9	" "
WM 111	M	480±10	" "
WM 124	O	476±10	North of Roundstone
WM 135	M	486±10	Dawros
WM 136	M	475±10	Currywongaun
WM 137	M	471±10	Currywongaun
WM 138	M	478±10	Doughruagh
WM 200	M	472±10	Errisbeg
EL 44	M	481±9	
EL 94	M	486±9	
BL 1248	O	478±10	
GJ 60	O	478±10	

M=metagabbro, O=orthogneiss, WM samples from present study, others from Elias *et al.* (1988).

A third sample only about 700m from the contact gives an age of 480±10 Ma. These results indicate that only minimal thermal heating of the metagabbro-gneiss complex rocks occurred during intrusion of the Galway Granite; considering the batholithic proportions of this granite, this result is surprising. This can be contrasted to the findings of Elias *et al.* (1988) who show that micas in the schists are thermally affected up to 3 km away from the contact with the Inish Granite. A possible explanation for the lack of heating of the metagabbro-gneiss complex rocks by the Galway Granite comes from (B.E. Leake *pers. comm,*) who suggests that the Murvey Granite, which is a late stage differentiate of the Galway Granite, was emplaced around its rims and assimilated the original thermal aureole. Excluding the two samples that have been thermally reset the range of the hornblende K-Ar ages is 471±9 to 486±10 Ma, giving an average age of 478

Ma. The similarity between the ages from different parts of the metagabbro-gneiss complex lends support to the hypothesis of Leake (1970, 1989) who claimed that all these metagabbro-gneiss rocks, including Dawros, Currywongaun and Doughruagh in the north, are all co-magmatic and therefore coeval.

The age range for the metagabbro-gneiss hornblendes is significantly less than the age range for the hornblendes from the amphibolites in the Connemara Schists, although the maximum ages in both cases are identical within error. It was concluded that the amphibolite hornblende K-Ar ages represent a two stage process, initial cooling and later resetting. The initial cooling must have followed the intrusion of the metagabbro-gneiss complex and so the equivalence in the maximum ages from the schists and the metagabbro-gneiss rocks is understandable. It is less obvious why the metagabbro-gneiss complex hornblendes did not suffer the resetting event to the same great extent as the amphibolite hornblendes. This is not simply a geographical artifact because c. 400 Ma amphibolite ages occur close to the contact with the metagabbro-gneiss complex in the south and also the metagabbro-gneiss complex bodies in the north also record old ages. None of the metagabbro-gneiss hornblendes were examined with the TEM so it is not possible to comment on the actual presence or otherwise of exsolution or phyllosilicate inclusions in these minerals. However, the small range in the K-Ar ages suggests that there is unlikely to be substantial exsolution or inclusions in these minerals. Figure 3.12, shows that there is no correlation between the K-Ar ages and the composition of these hornblendes, unlike the amphibolite hornblendes which showed some relationship between K-Ar age and $Fe^2/(Fe^2+Mg)$. No other factors are likely to have had significant influence over the hornblende K-Ar ages from the metagabbro-gneiss complex because the range of ages is small. The grain sizes are typically in the range 2 to 5mm;

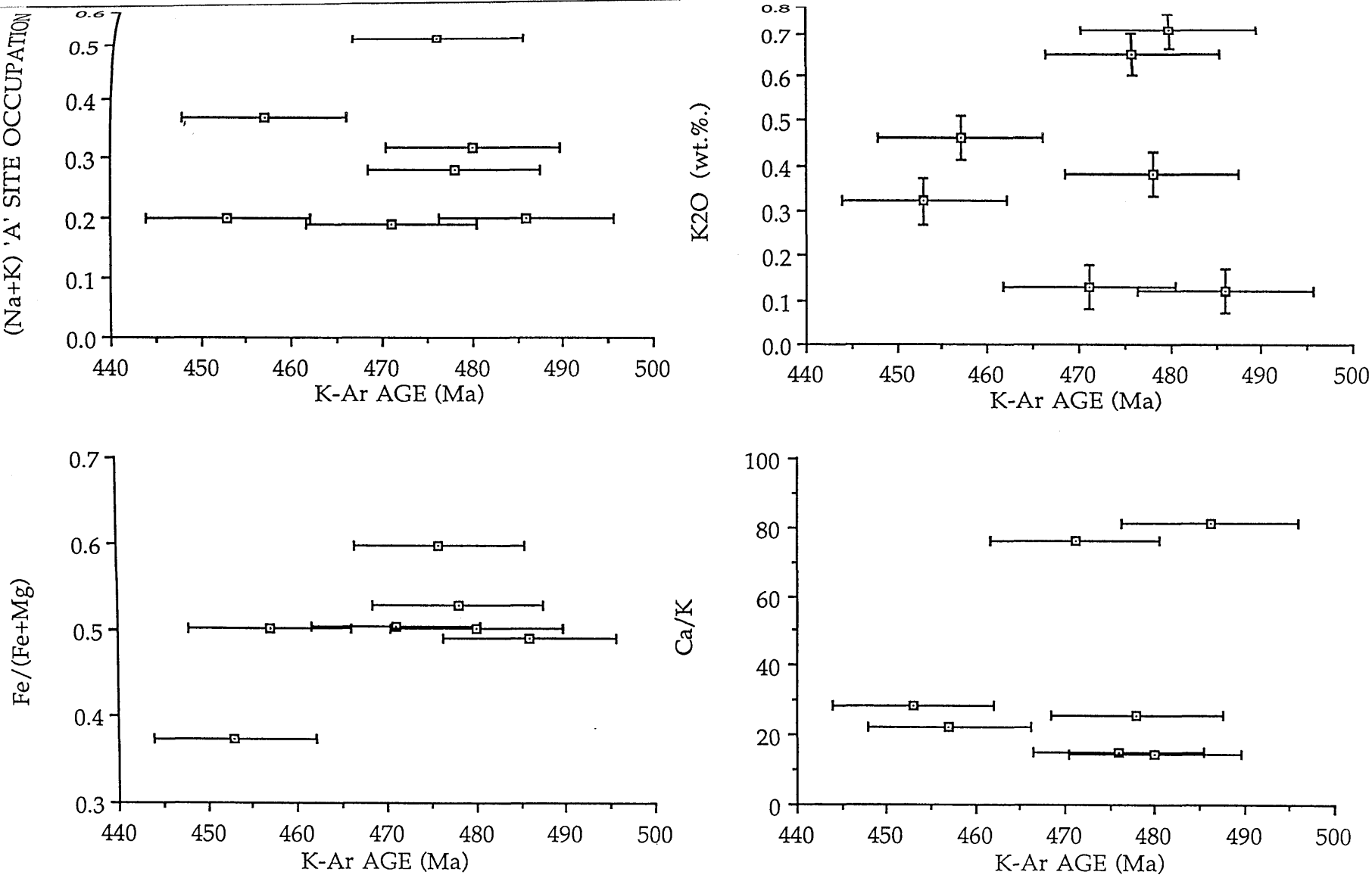

Figure 3.12. Correlation diagrams of metagabbro-gneiss complex hornblende K-Ar ages versus various measures of metagabbro-gneiss complex hornblende chemistry.

although much larger grains sizes do occur in some parts of the complex they were not sampled. The metagabbro-gneiss samples were collected from a greater range in elevation than the amphibolites because this rock type tends to form isolated hills, but this elevation difference is not thought to be significant because there is no correlation between age and elevation.

3.3 ^{40}Ar-^{39}Ar incremental step-heating ages of hornblende.

Five hornblende samples from the amphibolites in the Connemara Schists were dated by the ^{40}Ar-^{39}Ar incremental step-heating method. These samples were chosen because they yielded a wide range of K-Ar mineral ages and because some doubt persisted over the possibility that exsolution or phyllosilicates inclusions had influenced the K-Ar ages. These five samples are WM 167, WM 201, WM 225, WM 228 and WM 232 and they all came from amphibolites within the Lakes Marble and Streamstown Formations. The sample localities are indicated on figure 2.1. Two of the samples came from the quarry locality described in section 3.1.1. All the sample irradiation procedures plus the ^{40}Ar-^{39}Ar incremental step-heating methods are described in appendix A.4.3.

The ^{40}Ar-^{39}Ar incremental step-heating method allows the Ca/K ratio of the gas from each heating step to be calculated by way of $^{37}Ar_{(Ca)}$-$^{39}Ar_{(K)}$. The Ca/K ratios when compared to the hornblende electron-probe analyses indicate which gas releases are likely to be from hornblende and which are from secondary phases such as phyllosilicates contaminating the sample. In addition to the Ca/K ratios, the Cl/K ratios can also be calculated for the gas from each heating step by way of $^{37}Ar_{(Cl)}$-$^{39}Ar_{(K)}$. Chlorine is a useful indicator of hydrous alteration because the fluid involved with

alteration is generally a brine and as such has a higher chlorine content than pristine minerals. This is significant because in section 3.1.3 it was concluded that the hornblende K-Ar ages represent a two stage process, initial cooling and later resetting event with some fluid involvement.

The raw ^{40}Ar-^{39}Ar incremental step-heating results are listed in appendix A.5.5 but in the following discussion these results are presented as standard age spectra, Ca/K release spectra, Cl/K release spectra, % ^{39}Ar and ^{40}Ar release profiles and isochrons ($^{40}Ar/^{36}Ar$ v. $^{39}Ar/^{36}Ar$). From inspection of the results it is clear that the different samples show very different and complex behaviour and it is clear that no simple unambiguous interpretation is possible for the group of five samples as a whole. The results for each sample will be described individually and then the results compared and contrasted. In these discussions the total fusion ages are calculated from the ^{40}Ar-^{39}Ar step-heating data and the K-Ar ages are those measured directly by the conventional K-Ar method (section 3.1). These two ages are effectively measures of the same thing and the ages should be identical. The % ^{39}Ar and ^{40}Ar release profiles are generally used to show at what temperatures the maximum gas release occurred but they can also be used as an indicator of relative ^{40}Ar excess or deficiency over ^{39}Ar. Note all the data are air corrected.

WM 167. K-Ar age = 424±9 Ma, Total fusion age = 436±6 Ma.

Only eight heating steps were performed on this sample because only a small amount of material was available. The first three steps, giving 14% of the ^{39}Ar release, gave discordant ages of 504±63, 414±22 and 410±16 Ma respectively, figure 3.13 (a). The following five steps, with the remaining 78% of the ^{39}Ar release, gave a concordant plateau with an age of 437±6 Ma. The high age first step is indicative of small amounts of, loosely bound, excess ^{40}Ar possibly on the grain boundaries. The total fusion age (integrated age) is 435.5±5.5 Ma which is the same, within error, as the K-Ar age of 424±9 Ma. The Ca/K release spectrum, figure 3.13 (b), varies sympathetically with the age spectrum. Only the Ca/K ratio from the second step is inconsistent with the electron-probe Ca/K ratio. This step gave a Ca/K ratio lower than the other steps. The Cl/K release diagram, figure 3.13 (c), shows an order of magnitude higher Cl/K in the first step than the others. This is the same step that gave the oldest age. The % ^{39}Ar and ^{40}Ar release patterns, figure 3.14 (a), indicate that most of the gas release occurred at c. 900°C. These release patterns also show a slight excess of ^{40}Ar over ^{39}Ar at 600°C, then a slight deficiency of ^{40}Ar compared to ^{39}Ar until 950°C. This corresponds to the second and third steps which gave lower ages. After 950°C the % ^{39}Ar and ^{40}Ar release patterns mutually correspond. All the gas release steps form an isochron, figure 3.14 (b), with an age corresponding to 430.5±68 Ma with a $^{40}Ar/^{36}Ar$ intercept of 302±20, very close to the atmospheric value of 295.5. The isochron age is the same within error as the total fusion age, the plateau age and the K-Ar age.

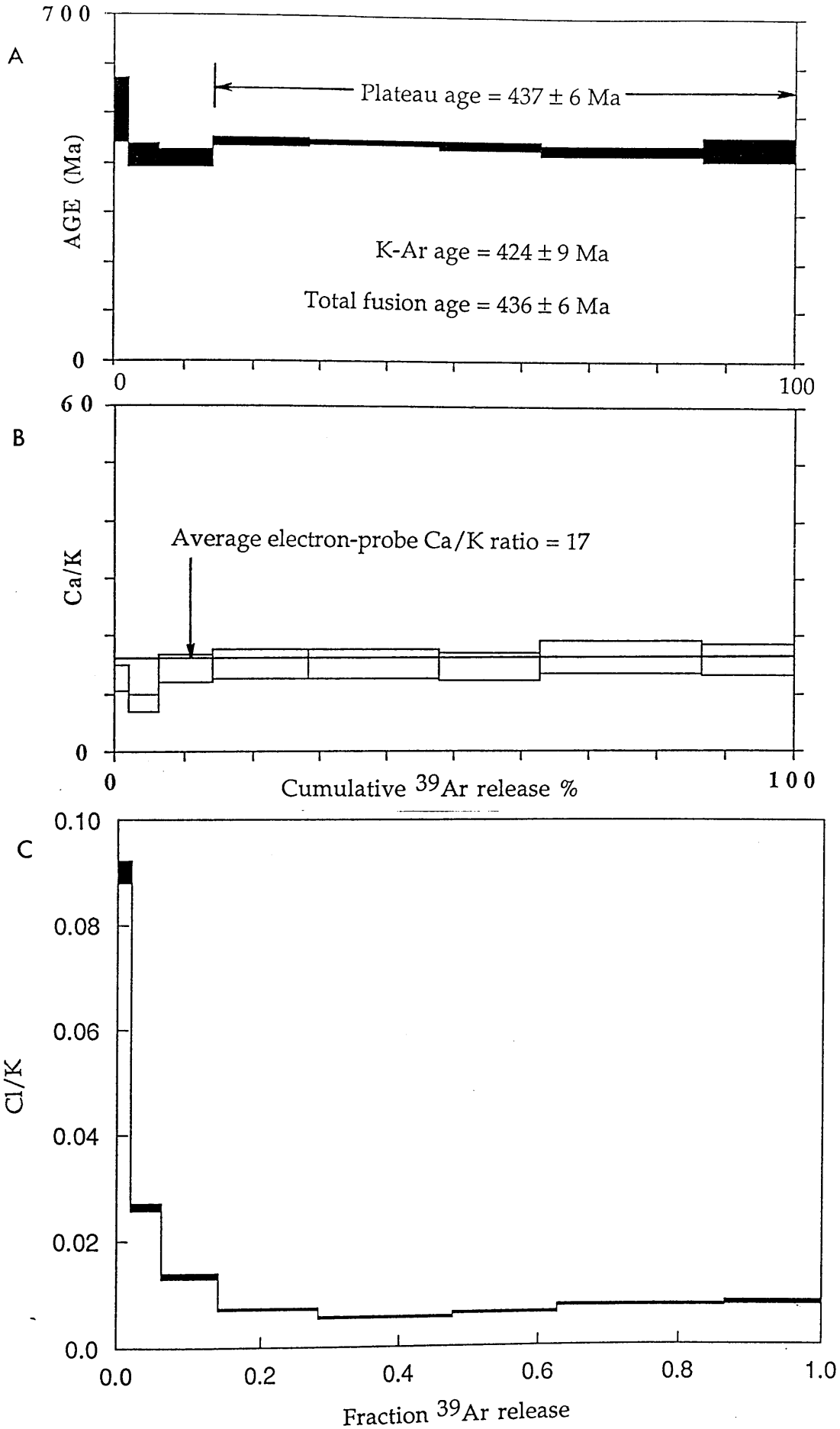

Figure 3.13. WM 167. A) Age spectrum, B) Ca/K release spectrum with the average electron-probe Ca/K ratio indicated, C) Cl/K release spectrum.

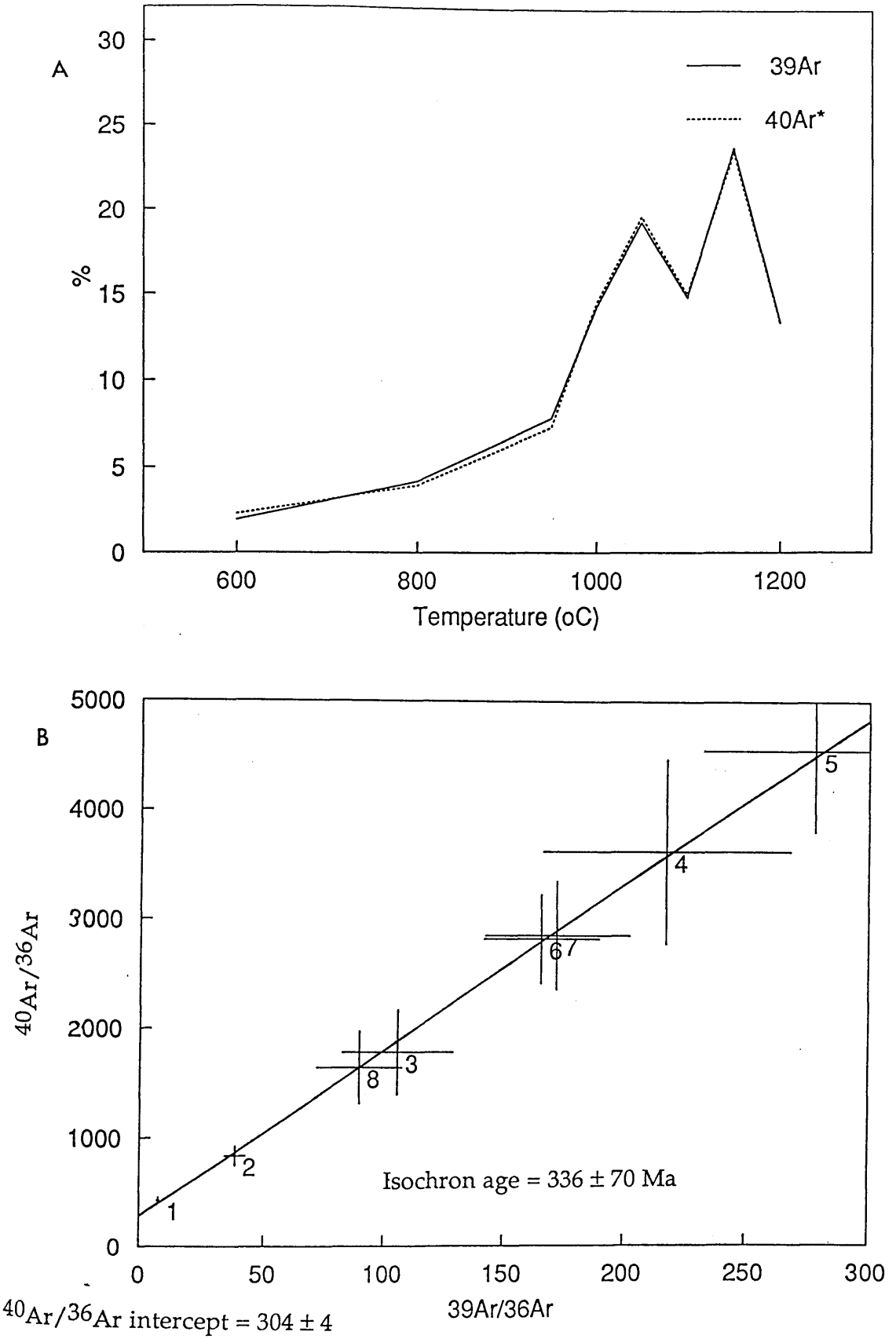

Figure 3.14. WM 167. A) Comparative ^{40}Ar and ^{39}Ar release patterns, B) Isochron diagram.

This excess ^{40}Ar is likely to have been introduced by surface derived water because this is consistent with the corresponding high Cl/K ratio for this step.

WM 201. K-Ar age = 349±8 Ma, Total fusion age = 353±3 Ma.

Fourteen heating steps were obtained from this sample. The age spectrum, figure 3.15 (a), is unusual with 47% of the ^{39}Ar release occurring in the first three steps. These steps are concordant and gave an age of 335 Ma. The fourth step, at 970°C, gave a significantly higher age of 386 Ma. The fifth step gives an age similar to the first three. The heating steps then show a gradual increase in age until step twelve at 415 Ma. The final two steps gave lower ages but with an increased error. The Ca/K spectrum, figure 3.15 (b), shows an almost continuous, staircase like, increase from about 5 to 45. The Ca/K ratios obtained from electron-probe analyses were extremely variable and ranged from 15 to 55. All the steps except the first three, therefore, give Ca/K ratios in agreement with the electron-probe results. The great range of Ca/K ratios makes it uncertain if the first three steps represent degassing of hornblende, with a Ca/K ratio not sampled with the electron-probe, or if it represents degassing of a secondary, contaminating, phase. Thin section examination of this sample, appendix A.2, reveals some alteration in the cleavages but it is not thought likely that the small volume of alteration product could give rise to such a large gas release. The Cl/K release spectrum, figure 3.15 (c), shows an irregular increase with temperature that is similar to the Ca/K release pattern. The % ^{39}Ar and ^{40}Ar patterns, figure 3.16 (a), show that gas was released predominantly at two temperatures, c. 1050 and 1150°C. These patterns also indicate that a ^{40}Ar deficiency occurs up to 900°C after which the ^{39}Ar and ^{40}Ar curves

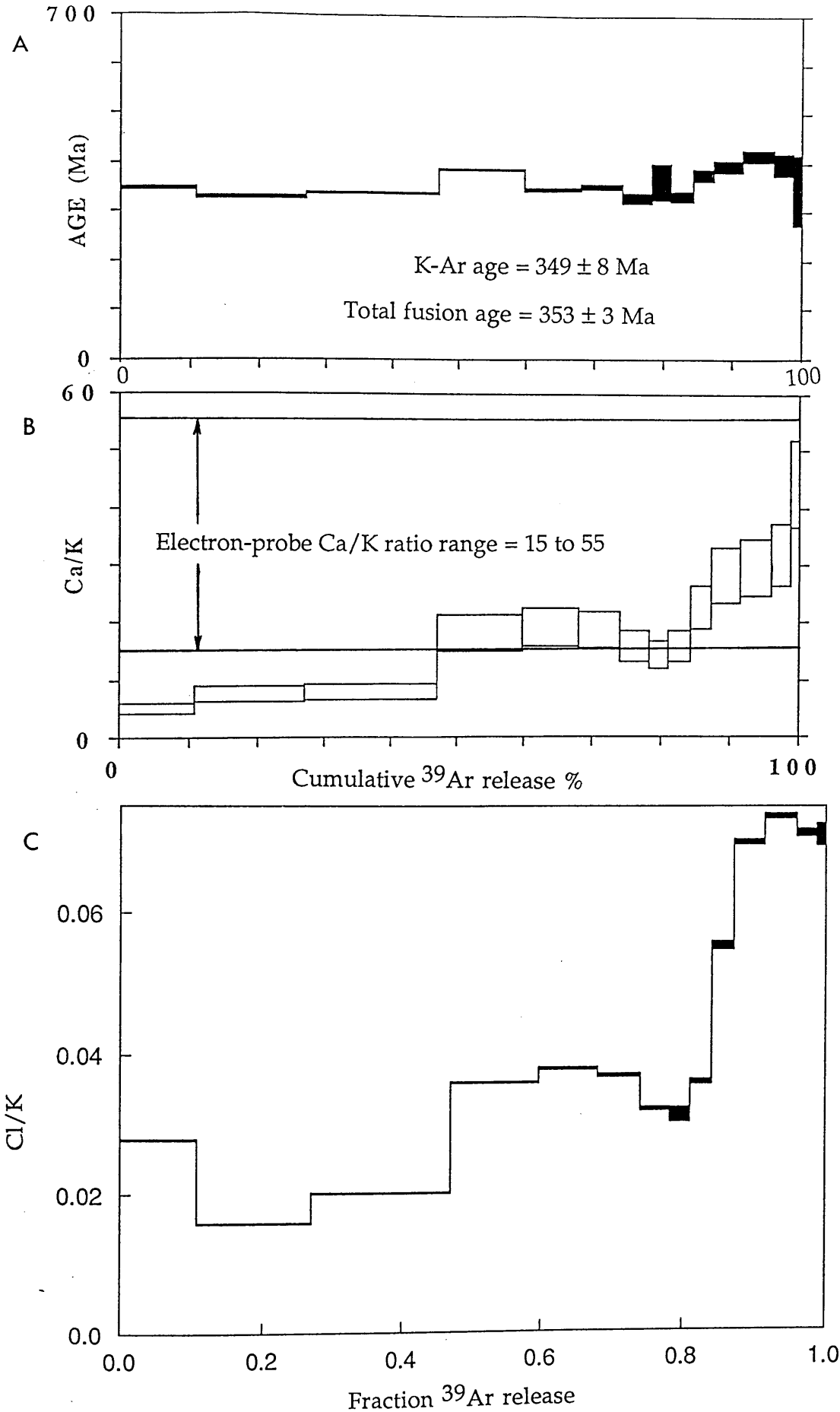

Figure 3.15. WM 201. A) Age spectrum, B) Ca/K release spectrum with the electron-probe Ca/K ratio range indicated, C) Cl/K release spectrum.

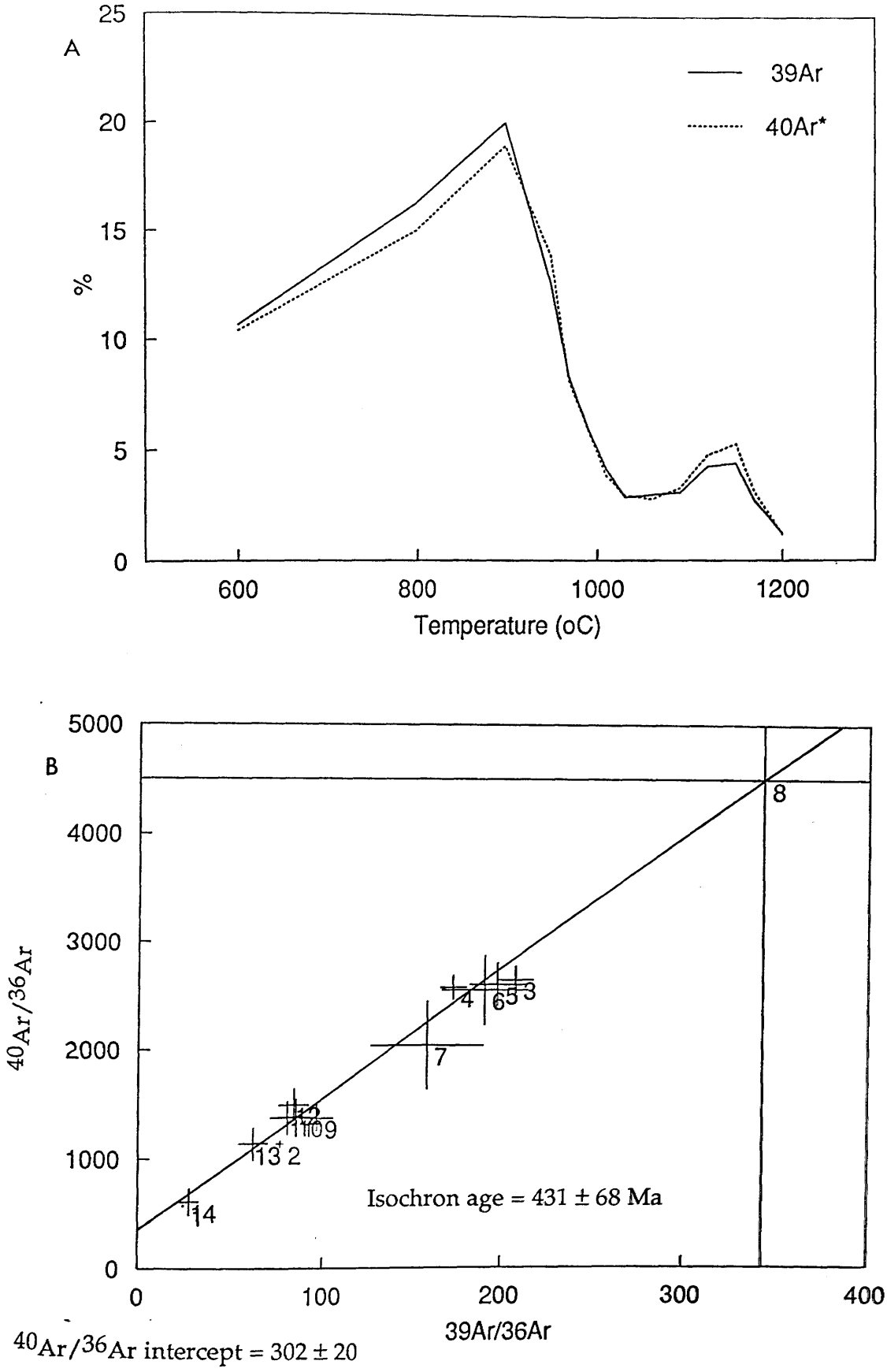

Figure 3.16. WM 201. A) Comparative ^{40}Ar and ^{39}Ar release patterns, B) Isochron diagram.

match except for the 1150 and 1170°C steps which have an apparent excess of ^{40}Ar. These two steps also have the highest Cl/K ratios. The total fusion age for this sample is 353.1±2.7 Ma which is the same, within error, as the K-Ar age which is 349±8 Ma. This is one of the two anomalously low age hornblendes that do not form part of the continuous K-Ar hornblende age range. It is suspected that these two low age hornblendes were reset by local high temperature events, such as dyke emplacement. All the heating steps can be fitted to an isochron, figure 3.16 (b), which gives an age of 336.1±69.5 Ma and a $^{40}Ar/^{36}Ar$ intercept ratio of 304.4±4. The age is the same, within error, as the total fusion and the K-Ar ages by virtue of its large error. This error comes from a scatter in the isochron which in itself suggests a disturbed thermal history.

WM 225. K-Ar age = 452±9 Ma, Total fusion age = 463±4 Ma.

Sixteen heating steps were obtained from this sample and the age spectrum is again complicated. The first five steps of the age spectrum, figure 3.17 (a), show a gradual step-wise increase in age from 196 to 423 Ma, but together they only represent 7% of the ^{39}Ar gas release. The sixth step is slightly younger at 403 Ma. The seventh step gave an age of 467 Ma and this step represents 34% of the total ^{39}Ar release. The next four steps show complicated behaviour, with the tenth step giving an age of 564 Ma. The last five steps show a progressive step down in age from 534 to 413 Ma. It should be noted that the tenth, twelfth and thirteenth steps give ages older than the age of the metagabbro-gneiss complex (490±1 Ma) which is considered to have totally reset the hornblendes. The Ca/K release spectrum, figure 3.17 (b), shows a trend generally sympathetic with the age spectrum. All but the first five steps give Ca/K ratios that agree with the

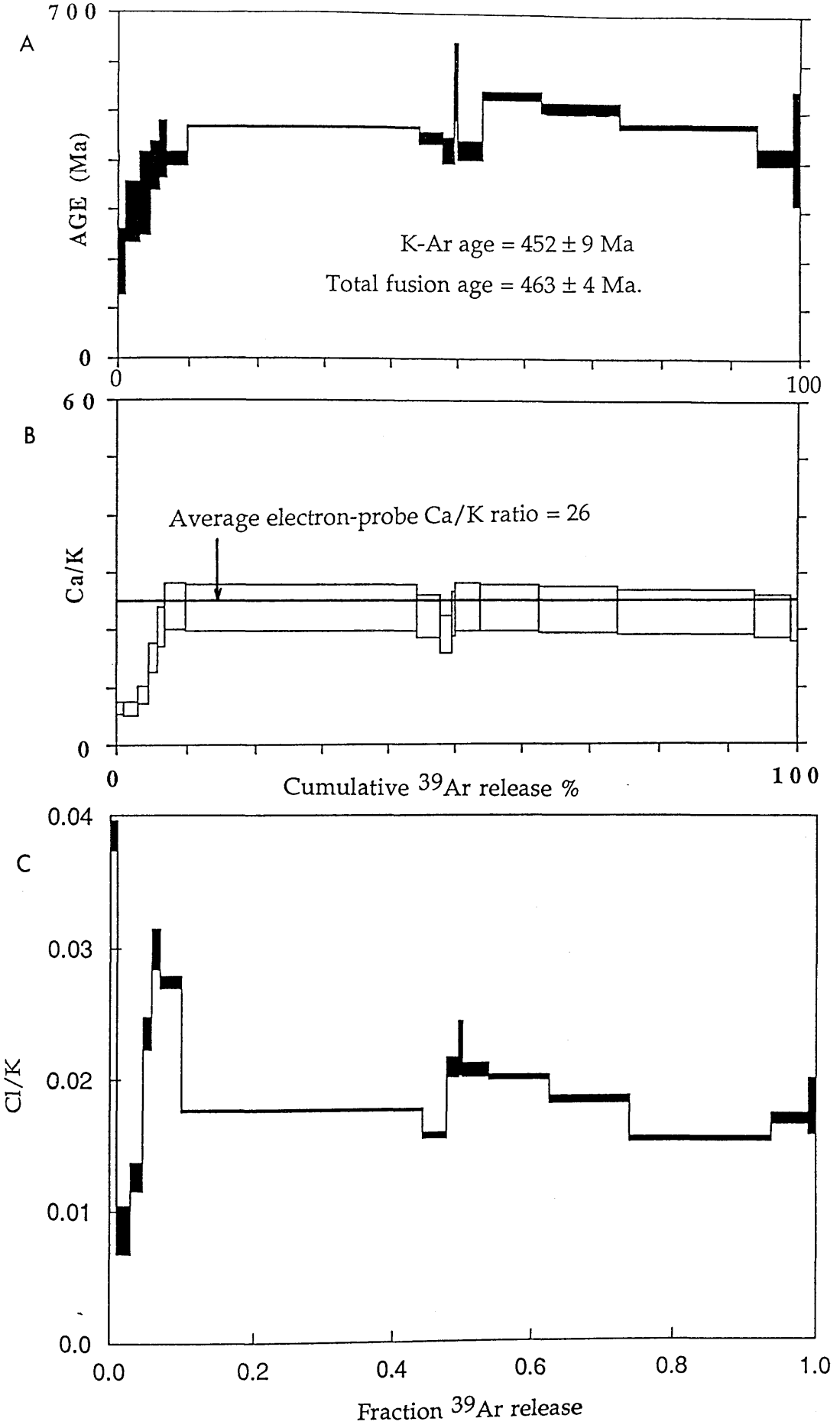

Figure 3.17. WM 225. A) Age spectrum, B) Ca/K release spectrum with the average electron-probe Ca/K ratio indicated, C) Cl/K release spectrum.

electron-probe Ca/K ratios and these five steps give Ca/K ratios lower than the others. There is a drop in the Ca/K ratios at steps eight, nine and ten, but these are still in agreement with the electron-probe data. These are the steps that gave the odd, complicated behaviour in the age spectrum. This complicated gas release is also shown on the Cl/K release spectrum, figure 3.17 (c). The first step has the highest Cl/K ratio, but the second step has the lowest. The Cl/K spectrum does not directly follow either the age spectrum or the Ca/K spectrum and so it is difficult to know if the Cl contents relate to excess Ar or not. The % ^{39}Ar and ^{40}Ar release patterns, figure 3.18 (a), show that the gas was released in two very discrete pulses at temperatures of c. 1000 and 1150°C. Figure 3.18 (a) also indicates apparent ^{40}Ar loss up to 1000°C, corresponding to the first six, low age, steps. After this temperature the ^{39}Ar and ^{40}Ar patterns correspond with each other except for slight excess ^{40}Ar at 1120 to 1140°C. These are the twelfth and thirteenth steps that give ages older than the metagabbro-gneiss complex. Note that the tenth step which also gave an age older than the metagabbro-gneiss complex gave such a small amount of gas that it is not seen on this diagram. The total fusion age is 463.1±4.1 Ma which is identical, within error, to the K-Ar age of 452±9 Ma. The discordant nature of the age spectrum means that no plateau age can be ascribed. When all the steps are plotted on an isochron, figure 3.18 (b), the corresponding age is 457±167 Ma and the $^{40}Ar/^{36}Ar$ intercept ratio is 232±24. The large error on the age is due to the scatter on the isochron which reflects the complex nature of this sample. This also means that the $^{40}Ar/^{36}Ar$ intercept ratio is likely to be unreliable.

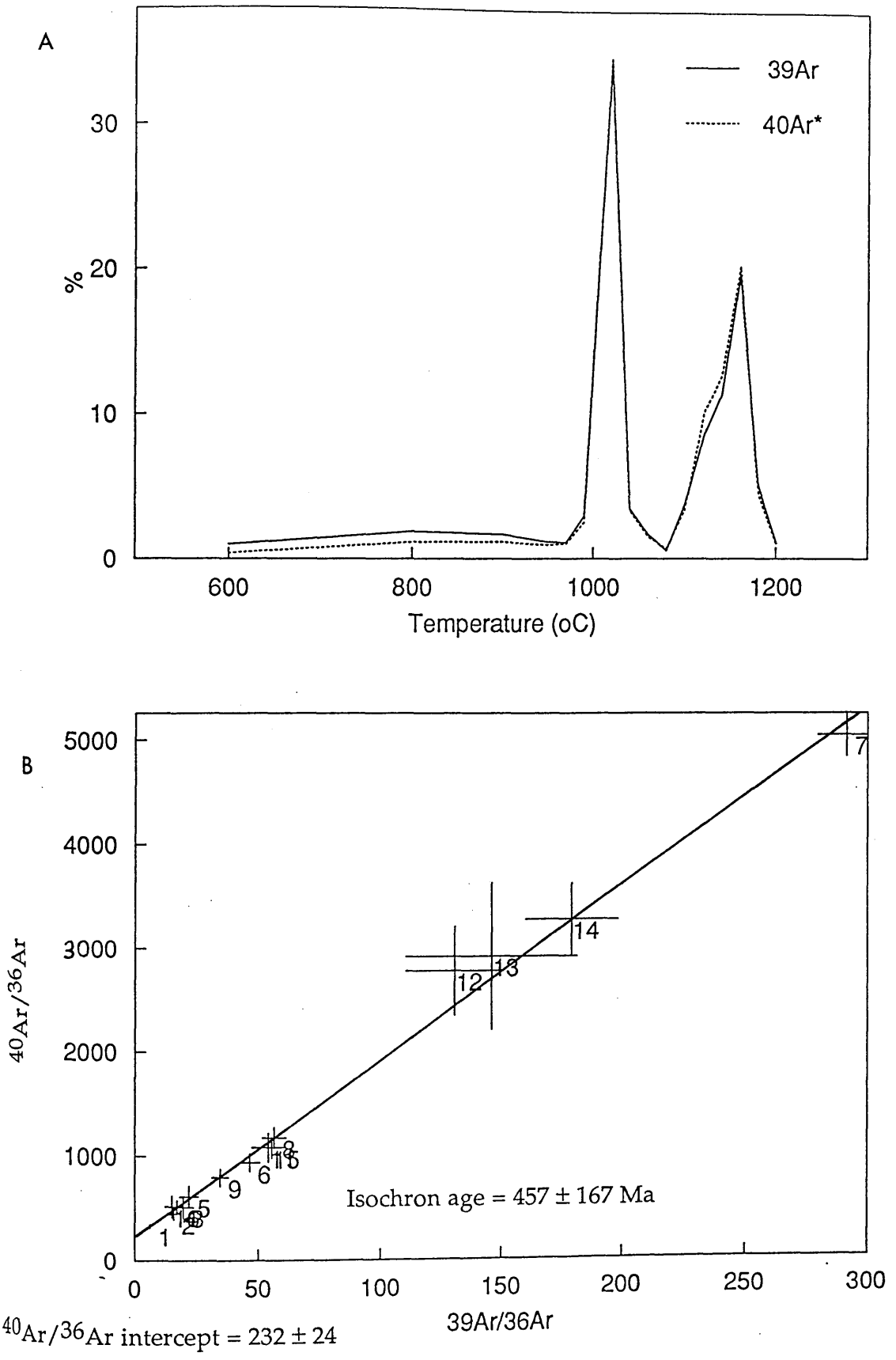

Figure 3.18. WM 225. A) Comparative ^{40}Ar and ^{39}Ar release patterns, B) Isochron diagram.

WM 228. K-Ar age = 481±10 Ma, Total fusion age = 449±2 Ma.

Sixteen heating steps were obtained from this sample. Unlike some of the other samples, this age spectrum, figure 3.19 (a), is relatively simple. The first two steps give low ages, 364 and 335 Ma, and together they represent 8% of the ^{39}Ar release. The third step gives an age of 432 Ma. Steps four to thirteen form an irregular plateau which gives an age of 455±2 Ma. Steps fourteen and sixteen give ages older than the plateau. The age of step sixteen is 529 Ma, which is older than the age of the metagabbro-gneiss complex. The Ca/K release spectrum, figure 3.19 (b), is sympathetic with the age spectrum, with all but steps one, two and sixteen having Ca/K ratios in agreement with the electron-probe Ca/K ratios. Steps one and two gave Ca/K ratios lower than the others while step sixteen gave a Ca/K ratio which is higher. There is a slow but steady drop in the Ca/K ratios of all the steps that represent the age spectrum plateau. Although only the Ca/K ratio of step sixteen is above the electron-probe value steps thirteen to sixteen show a gradual step-wise increase. The Cl/K release spectrum, figure 3.19 (c), is sympathetic with the Ca/K pattern but is exaggerated. The % ^{39}Ar and ^{40}Ar release patterns, figure 3.20 (a), show that most of the gas was released over a broad range of temperatures from 900 to 1200°C, with a peak at 1050°C. Figure 3.20 (a) also shows a significant ^{40}Ar deficit with respect to ^{39}Ar for steps from 600 to 900°C. After 900°C the ^{39}Ar and ^{40}Ar release patterns are in agreement except for slight ^{40}Ar excesses at 1000°C and 1200°C, the later step giving the oldest age of 529 Ma. The total fusion age is 448.5±2.2 Ma which is about 7 Ma younger than the plateau age. All the heating steps form an isochron, figure 3.20 (b), giving an age of 462±12 Ma and a $^{40}Ar/^{36}Ar$ intercept ratio of 287±7. The isochron age is in agreement with the total fusion age but these two ages are not consistent with the K-Ar age of 481±10 Ma. It is not immediately clear why there is this

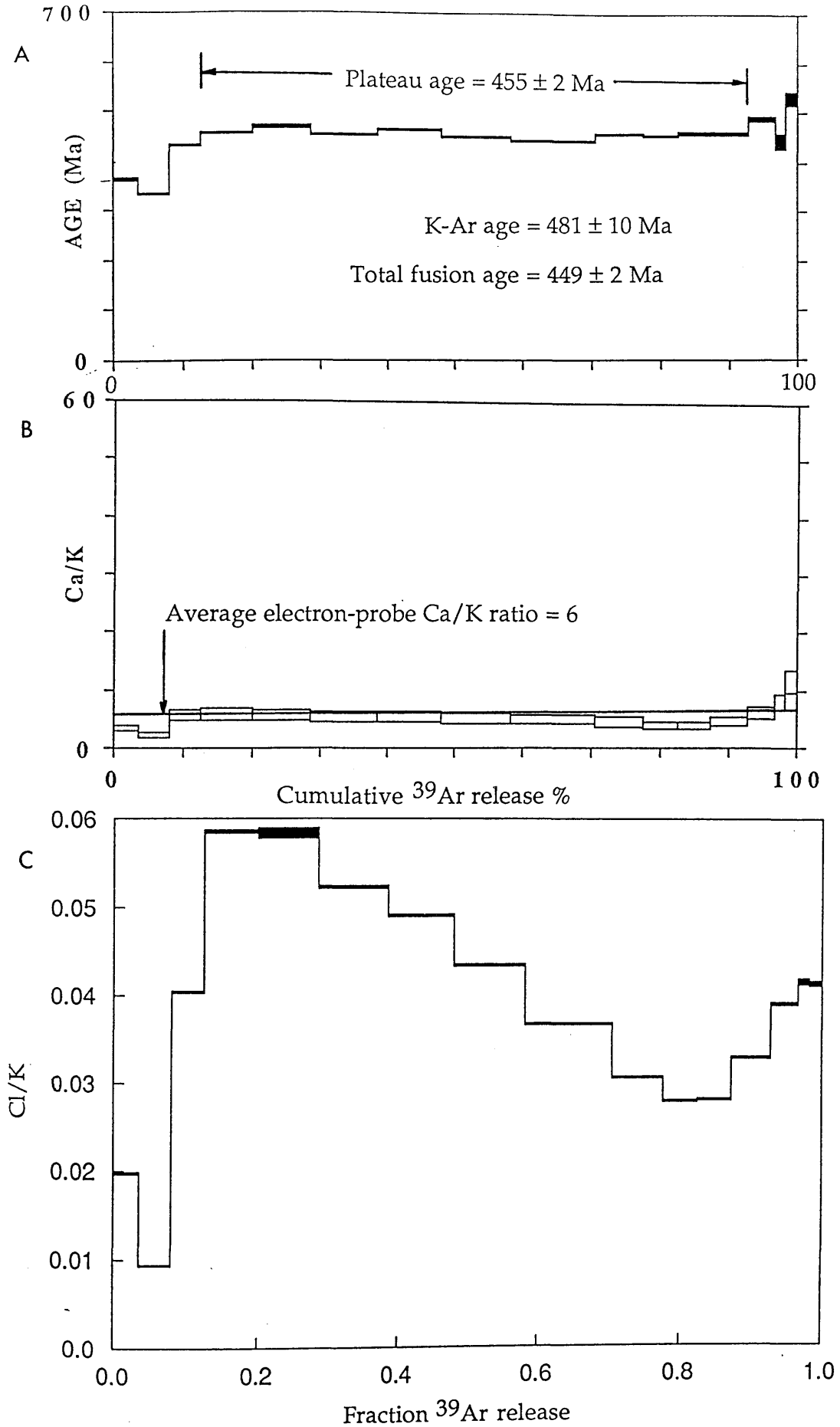

Figure 3.19. WM 228. A) Age spectrum, B) Ca/K release spectrum with the average electron-probe Ca/K ratio indicated, C) Cl/K release spectrum. Note the discrepancy between the K-Ar age and the total fusion age.

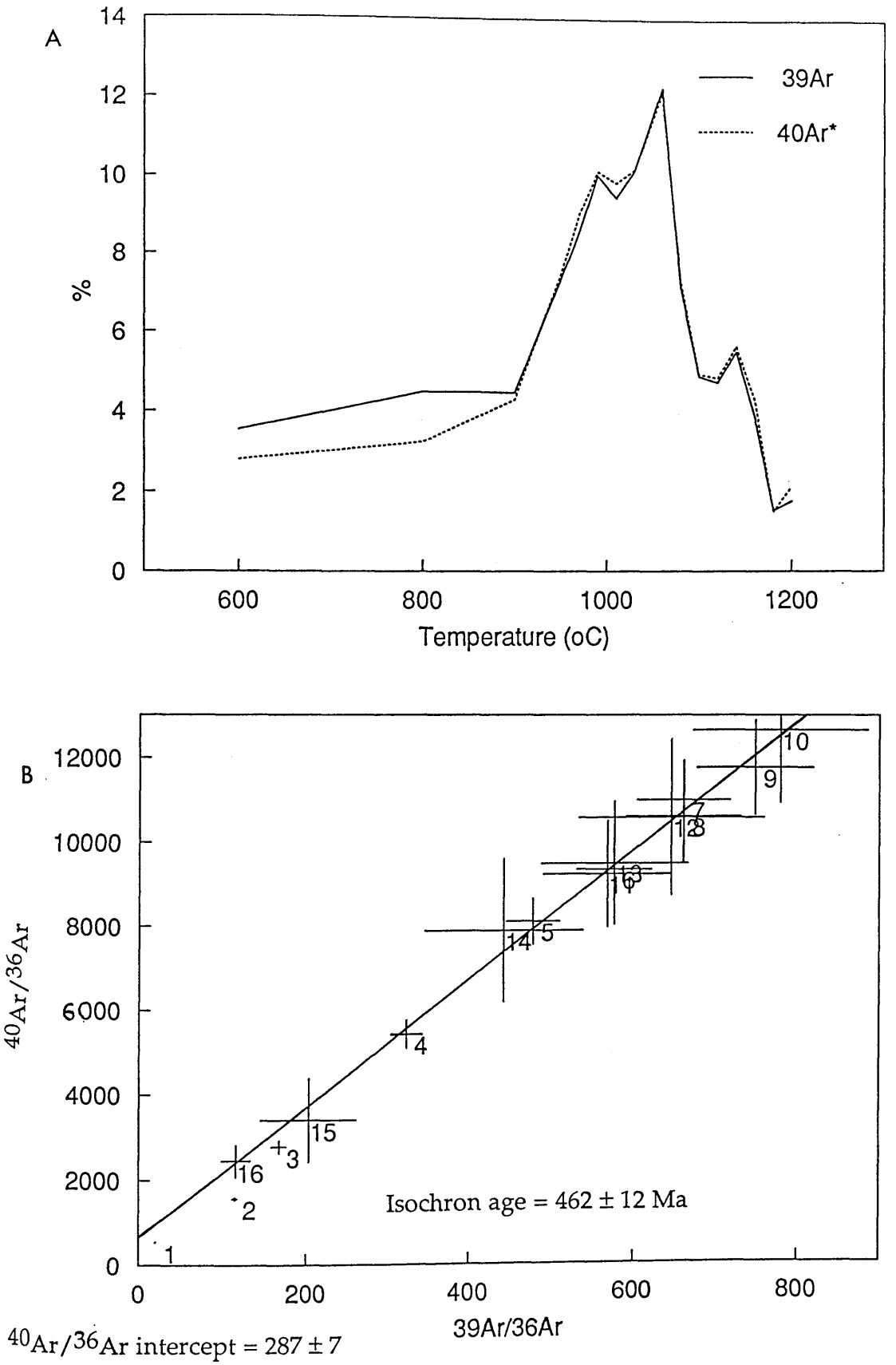

Figure 3.20. WM 228. A) Comparative ^{40}Ar and ^{39}Ar release patterns, B) Isochron diagram.

discrepancy, especially considering the age spectrum is less complicated than for some of the other samples. It is possible that the different aliquots of this sample had different amounts of alteration of the hornblende.

WM 232. K-Ar age = 467±9 Ma, Total fusion age = 460 ±3 Ma.

Seventeen heating steps were obtained from this sample. The overall pattern of the age spectrum, figure 3.21 (a), is one of Ar loss. There is a gradual, stepwise, increase in the ages of steps one to fourteen, with steps thirteen and fourteen giving ages older than the age of the metagabbro-gneiss complex. The last three steps show complicated behaviour, with steps fifteen and seventeen giving younger ages of 426 and 434 Ma and the sixteenth step gives an age older than the metagabbro-gneiss complex of 542 Ma. Two sets of three steps give concordant ages, these are steps seven, eight and nine which give an age of 474±3 Ma and steps ten, eleven and twelve which give an age of 495±3 Ma. These cannot be called plateau ages because too few steps are concordant. The small gas release in step sixteen and its correspondingly anomalous Ca/K and Cl/K ratios suggest that some instrumental error is responsible. The Ca/K release spectrum, figure 3.21 (b), is sympathetic with the age spectrum. The first four steps, forming 11% of the ^{39}Ar release, give Ca/K ratios less than the Ca/K ratio obtained from the electron-probe. The sixteenth step gives a Ca/K ratio higher than the other steps and corresponds to the highest age step. The Cl/K release spectrum, figure 3.21 (c), shows a very high Cl content in the first step, with lower ratios for steps two and three. Steps four to seventeen show consistently low Cl/K ratios, except step sixteen. The % ^{39}Ar and ^{40}Ar release patterns, figure 3.22 (a), indicate that most of

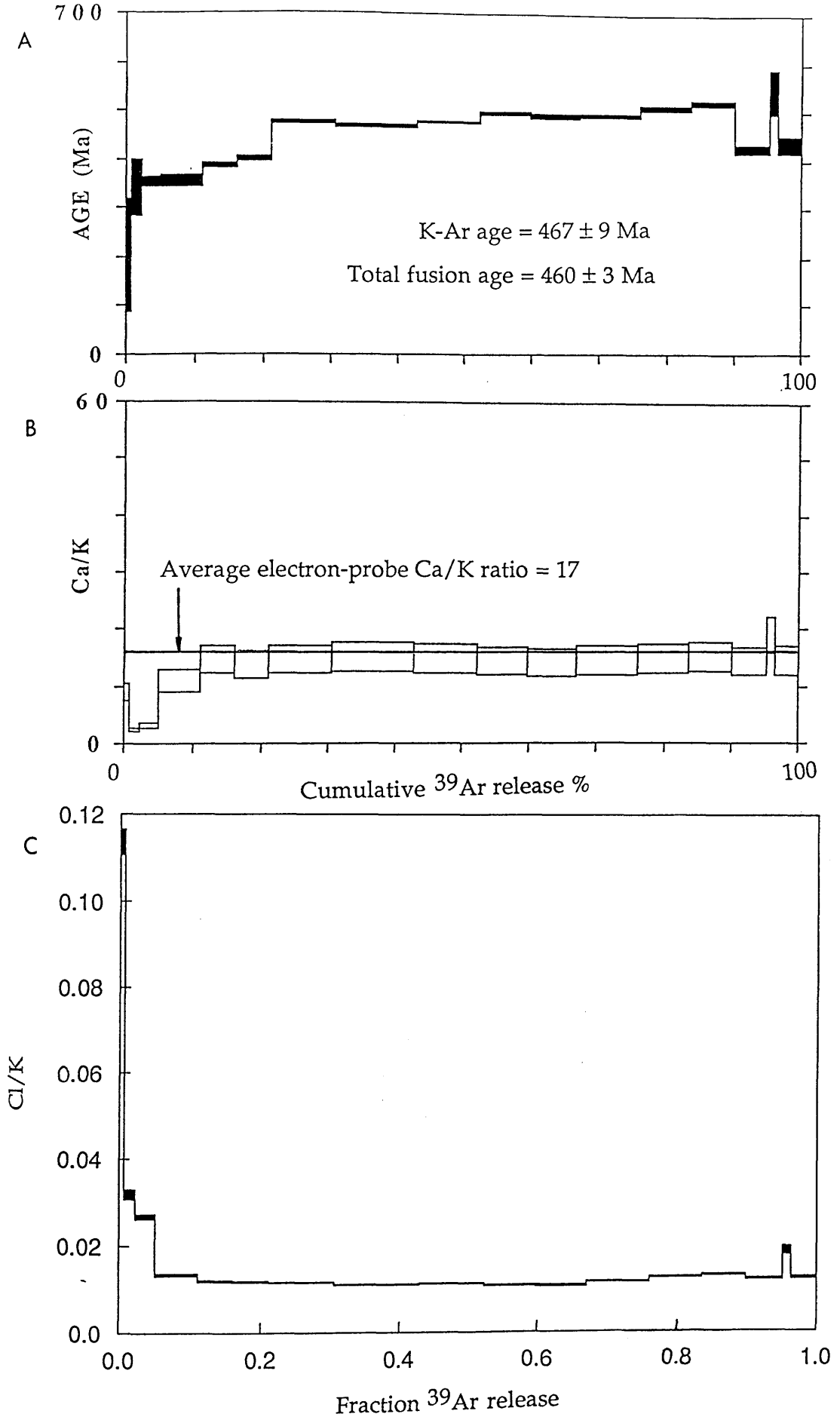

Figure 3.21. WM 232. A) Age spectrum, B) Ca/K release spectrum with the average electron-probe Ca/K ratio indicated, C) Cl/K release spectrum.

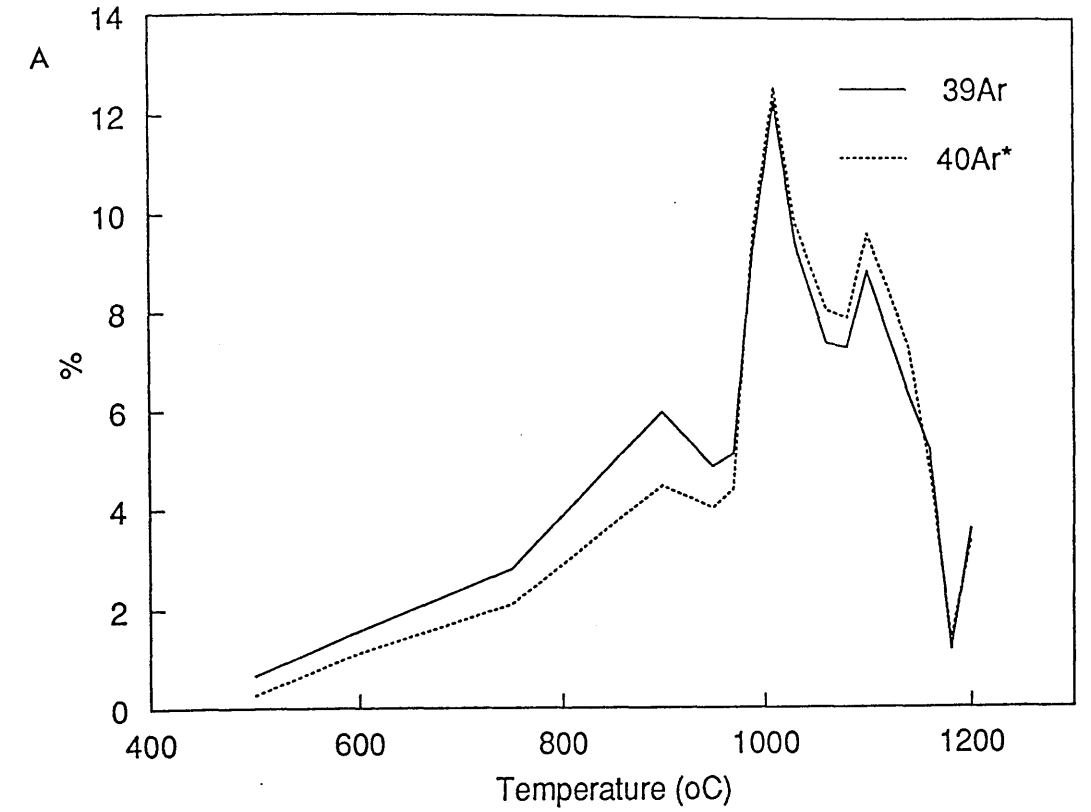

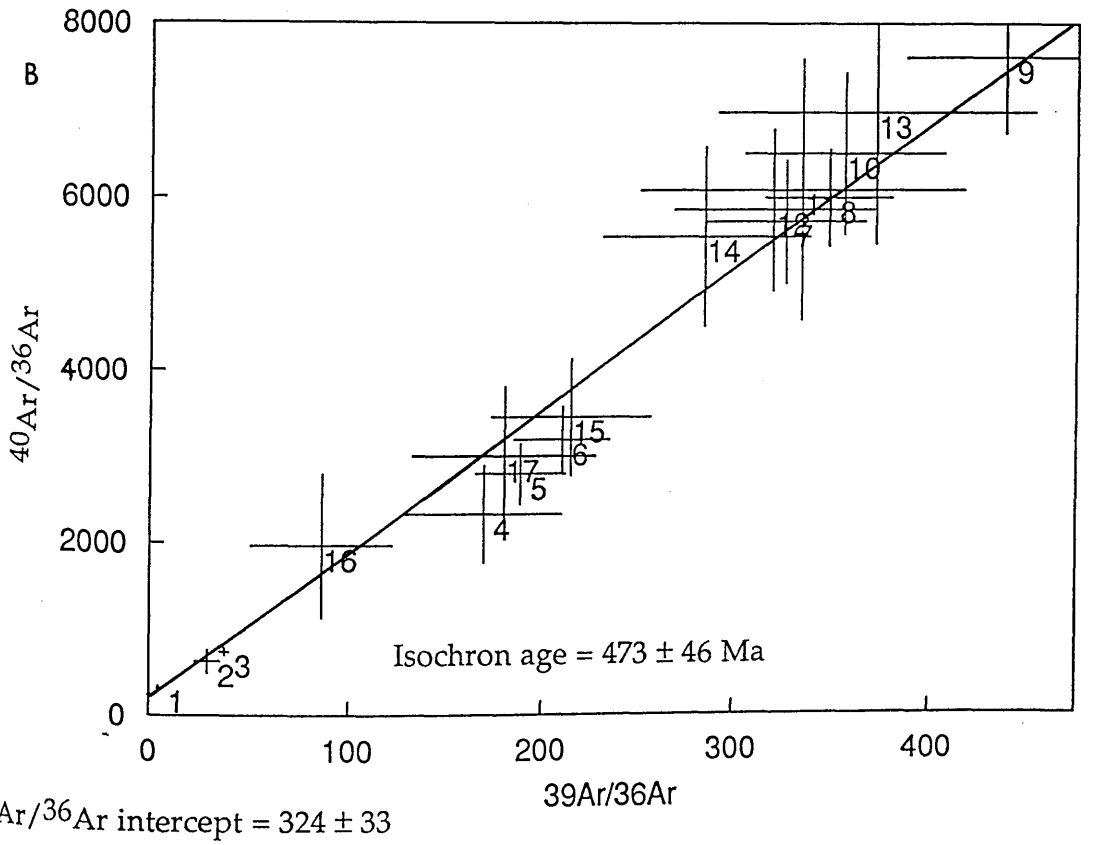

Figure 3.22. WM 232. A) Comparative ^{40}Ar and ^{39}Ar release patterns, B) Isochron diagram.

the gas was released over a broad temperature range, from 800 to 1200°C, but with two peaks at c. 1000 and 1100°C. Figure 3.22 (a) also shows a significant ^{40}Ar deficit in all heating steps up to 970°c and excess ^{40}Ar between 1010 and 1120°c. The ^{40}Ar deficit at low temperatures coincides with the high Cl/K ratios and the low Ca/K ratios. The total fusion age is 459.9±2.9 Ma which is younger than both sets of concordant steps discussed earlier. All the heating steps form an isochron, figure 3.22 (b), with an age of 473.3±46.2 Ma and a $^{40}Ar/^{36}Ar$ intercept ratio of 324±33. The large errors are due to the amount of scatter on the isochron. The total fusion age and the isochron age (because of its large error) are consistent with the K-Ar age of 467±9 Ma.

Although there is considerable variation in the age spectra of these five samples there are some similarities. All of the samples show Ca/K ratios lower than the electron-probe values at the low temperature steps. These low Ca/K ratios are consistent with biotite, the principal alteration product of hornblende, which has been identified in the cleavages of some samples and inferred to be in the cleavages of others. Biotite, especially if it is fine grained, will degas at the low temperature steps. These low temperature, low Ca/K ratio, steps are also deficient in ^{40}Ar compared to ^{39}Ar and this too can be explained by late forming biotite in the hornblende sample. The high Cl/K ratios normally corresponding to these low temperature steps suggests that the biotite alteration occurred in the presence of a brine.

The low Ca/K and high Cl/K ratios could be explicable in terms of recoil of Ca, and to a lesser extent K, occurring at grain boundaries. However, recoil is usually not considered to be significant with the large grain size used in these step-heating experiments, about 250 microns

(McDougall & Harrison 1988). Furthermore, recoil generally has the affect of producing anomalously old ages and these were not recorded.

Above the temperature at which the biotite contamination is degassing some of the samples show step ages of c. 400 to 420 Ma with Ca/K ratios consistent with the hornblende electron-probe data. At increasingly higher temperature steps there is a general rise in the step ages. This type of profile suggests that some Ar loss has occurred out of the hornblende. That the c. 400 Ma age is equivalent to the age of the Lower Devonian Granites strongly suggests that the intrusion of these granites is in some way responsible. At the highest temperature steps some of the samples give ages older than the age of the metagabbro-gneiss complex. It was initially considered, section 3.1.3, that the intrusion of the metagabbro-gneiss complex would have sufficiently heated all the country rocks to have totally reset all the K-Ar 'clocks'. The high temperature heating steps of these samples, recording ages older than the age of the metagabbro-gneiss complex, which have a corresponding apparent excess of ^{40}Ar suggest that the rejuvenation of the minerals was in some cases not total. This excess ^{40}Ar is not thought to have been introduced into the minerals at a later date because, if this were the case, it would be loosely held in locations such as grain margins and so would degas at low, not high, temperatures. These old age steps are therefore interpreted as being due to inherited ^{40}Ar from a pre-metagabbro-gneiss complex period.

There is, then, a general history that can be deduced for the samples from the step-heating data. The intrusion of the metagabbro-gneiss complex caused almost total resetting of the hornblendes, with only a little ^{40}Ar being retained in the most strongly held lattice sites. At some time afterwards, as the hornblendes cooled, they started to retain ^{40}Ar again. The time at which they did this is uncertain and cannot be uniquely defined

from the step-heating data. At c. 400 Ma the intrusion of the Lower Devonian Granites caused partial resetting of the hornblendes. It has been shown earlier that this resetting cannot have been simply a thermal process because of the lack of any relationship between the age and distance to the granite contacts. The high Cl/K ratios of the low temperature, low age steps, are consistent with fluid interaction being involved with this c. 400 Ma resetting event. During this process variable amounts of the hornblende altered to biotite in the presence of fluid. The degree of alteration was most probably controlled by the amount of fluid and its residence time in the amphibolites. The step ages for the degassed biotite are not geologically meaningful. At c. 350 Ma, WM 201 was again almost completely reset by a local thermal event, probably a dyke intrusion. Only one of the heating steps for this sample still records an age older than the Lower Devonian Granites, 415 Ma.

Elias *et al.* (1988) published ^{40}Ar-^{39}Ar step-heating ages on three biotites and one muscovite from the Connemara Schists. Two of the biotites (EL 14 and EL 16) show low age, low temperature steps with an overall pattern that may indicate Ar loss. The third biotite (El 26) yielded a plateau age of 467±3 Ma which is nearly 30 Ma older than the K-Ar age of 439±8 Ma. The muscovite sample (EL 14) yielded a flat age spectrum that gave a plateau of 458±4 Ma identical, within error, to the K-Ar age of 461±9 Ma. These mica ^{40}Ar-^{39}Ar step-heating ages serve to reinforce the conclusion reached in this study that localised partial, resetting of some of the minerals in the Connemara rocks has occurred.

3.4 ^{40}Ar-^{39}Ar total fusion laser-probe ages.

Laser-probe total fusion ^{40}Ar-^{39}Ar ages were determined on hornblende grains from within two thick rock slices of amphibolite from two samples, WM 220 and WM 201. The laser-probe was used to obtain multiple ^{40}Ar-^{39}Ar ages from within single grains because the results from the ^{40}Ar-^{39}Ar incremental step-heating were inconclusive regarding the possible variation in the closure temperatures between samples. Previous studies have revealed patches of variable Ar retentivity from within single hornblende grains (Kelley & Turner 1987) and it has been suggested that this was caused by fine scale exsolution or phyllosilicate inclusions (Blanckenburg & Villa 1988). TEM investigation has revealed both of these features occur within some of the Connemara samples and it is possible that they might occur in all samples. The laser-probe was therefore used to see if there were age variations within grains and to attempt to 'map' any such variations. As with the ^{40}Ar-^{39}Ar incremental step-heating, Ca/K ratios were calculated for each analysis. Unfortunately, accurate Cl/K ratios could not be calculated because during irradiation the samples were screened with Cd plating which inhibits reactions on Cl.

The pulse from the laser-probe produces a single pit of approximately 100 microns diameter and twice as deep. See appendix A.4.4 for analytical details. It was found that this volume of rock did not produce sufficient ^{39}Ar and ^{40}Ar to measure accurately; for that reason several pulses were fired to form overlapping pits. The analysed area was then irregular in shape and about 200 to 300 microns wide. The typical grain size is about 1/2mm in WM 220 and so generally only one or two analyses could be performed on one grain. In WM 201 most of the grains are also about 1/2mm but a few larger grains (up to 5mm) could accommodate more analyses. The multiple pulse procedure makes it more likely that

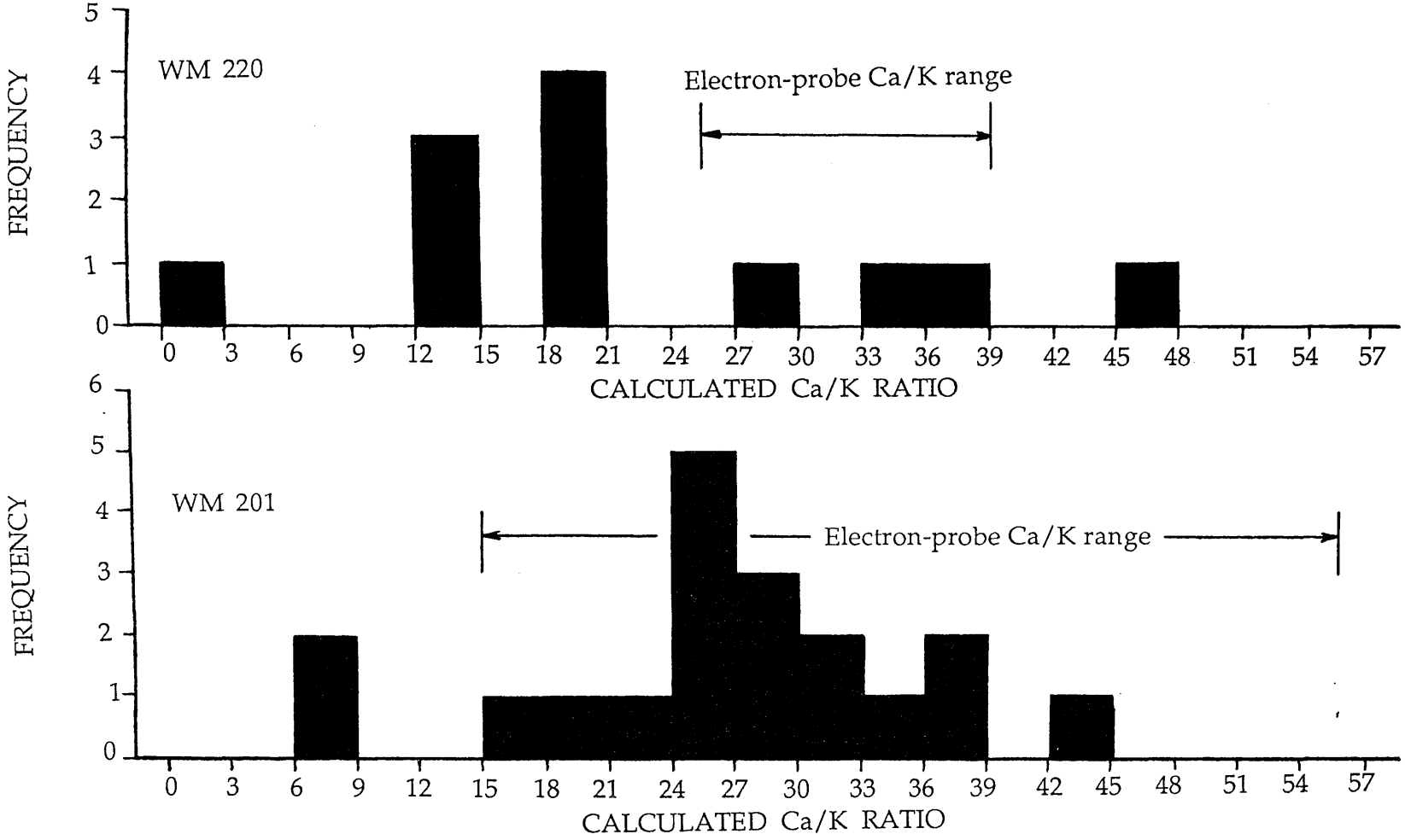

Figure 3.23. Histograms of the Ca/K ratios from WM 201 and WM 220 calculated from laser-probe ^{40}Ar-^{39}Ar isotopic analyses. The range of Ca/K ratios measured directly on these samples during electron-probe analyses are shown for comparison.

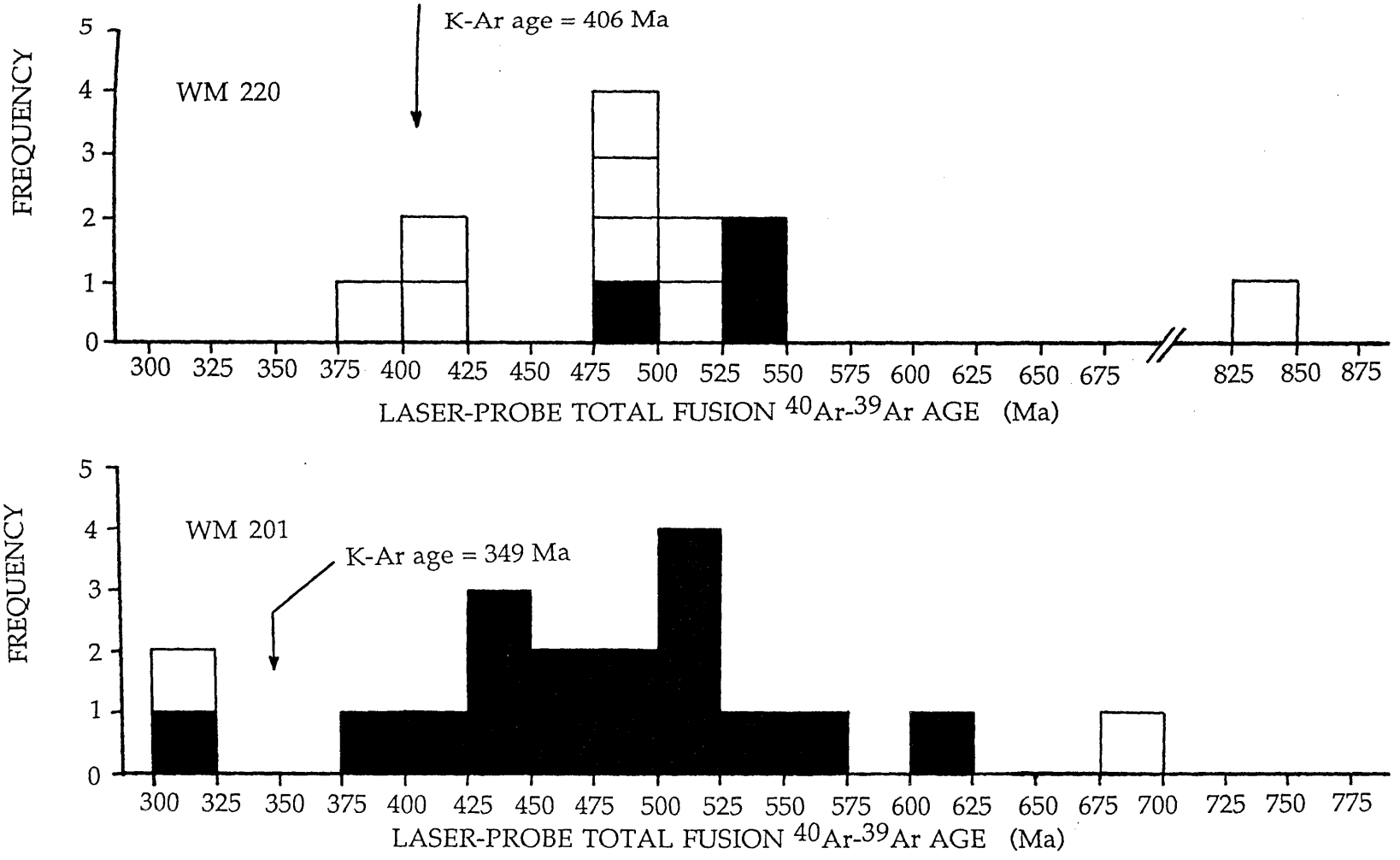

Figure 3.24. Histograms of the laser-probe total-fusion ^{40}Ar-^{39}Ar ages determined on WM 201 and WM 220. The solid squares represent analyses with calculated Ca/K ratios that agreed with electron-probe measurements, the open squares represent analyses with calculated Ca/K ratios that did not agree with the electron-probe measurements. The K-Ar ages for these samples are indicated.

other phases will be analysed along with the hornblende; in particular there is no way of knowing if the deeper pits have penetrated through the hornblende into another mineral species.

The individual results for each analysis are given in appendix A.5.6. The data are displayed graphically as histograms for Ca/K ratios and ^{40}Ar-^{39}Ar laser-probe total fusion ages for both samples in figures 3.23 and 3.24 respectively. Also indicated on the ^{40}Ar-^{39}Ar age histograms are the corresponding K-Ar ages. On the Ca/K ratio histograms the electron-probe Ca/K ratio range is indicated. It is clear that the range of laser-probe ages obtained is very large, in fact the range of these ages for both samples exceeds the total range of hornblende K-Ar ages for all samples. The laser-probe age range for WM 201 is 321 to 675 Ma giving an average of 484 Ma. For WM 220 the age range is 399 to 840 Ma and the average is 509 Ma. Comparison of the calculated Ca/K ratios from the laser-probe analyses with electron-probe values indicate that several of the analyses were apparently contaminated. The contaminant was most likely altered plagioclase which is the second major component of the amphibolite. The Ca/K ratios were used as a guide to indicate which analyses are likely to be of hornblende alone. On this basis seventeen out of nineteen analyses are acceptable for WM 201, but for only three out of twelve analyses are acceptable for WM 220. This difference is related to the comparative grain sizes of the two samples, because WM 201 had some larger grains these could be analysed with less risk of contamination. The acceptable analyses, according to Ca/K ratios, are indicated on the laser-probe age histograms by filled squares, figure 3.24. The average laser-probe ages of all the acceptable analyses are for WM 201, 475 Ma and for WM 220, 523 Ma. It is clear that these average laser-probe ages in no way correspond with the K-Ar ages of 349±8 and 406±8 Ma respectively. The two ages should correspond if

enough laser-probe analyses were performed so that the set of ages is statistically representative of the absolute possible range of ages from the hornblendes in the rock slice, and that the rock slice is representative of the hand specimen. Both of these conditions are thought to have been met. The most likely explanation for this discrepancy is that more of the laser-probe analyses have been contaminated by feldspars than is indicated by the Ca/K ratios. Owing to the variable alteration of the feldspar, particularly to sericite, it is possible that a wide range of Ca/K ratios can be obtained from the feldspar alone. It is, therefore, probable that different proportion of feldspar and hornblende can yield Ca/K ratios indistinguishable from the expected Ca/K ratios from hornblende alone. Other than the Ca/K ratios, no test of sample purity is possible. Simple visual examination is of little value because the analysed material forms a glass as a result of fusion. For that reason there is no way of knowing which analyses are 'good' analyses and which are not. This means that it is not possible to make any conclusions regarding the variability of Ar retention in these hornblendes from the ^{40}Ar-^{39}Ar laser-probe total fusion ages.

3.5 Summary.

A) The lack of any geographical trend to the K-Ar mineral ages and the lack of consistent K-Ar mineral ages from single locations proves that most or all of the K-Ar mineral ages are not simply the result of uplift and cooling of Connemara through invariant, mineral specific, closure temperatures.

B) The apparent correlation between the ranges in the K-Ar mineral ages and the timing of geological events, especially the lowest K-Ar mineral ages coinciding with the age of the Lower Devonian Granites, implies that

some or all of the ages are controlled by the geological events and are not entirely random. Considering A, above, this leads to the view that either the K-Ar ages represent cooling through highly variable, sample specific, closure temperatures, or, they represent 'mixed ages' between a time of initial closure and a later partial resetting event synchronous with the intrusion of the Lower Devonian Granites.

C) The only factors that could possibly have influenced the closure temperatures are the presence of exsolution, inferred to be present in a few hornblendes, and phyllosilicate inclusions, possibly present in many of the hornblendes. It is believed that these factors alone could cause some variation in the K-Ar ages but not to the extent of creating the large range of hornblende ages. These hornblende K-Ar ages are therefore believed to be the result of cooling through variable, *sample* specific, closure temperatures followed by partial resetting during a later event. No known factors control the closure temperatures of the micas and therefore these must represent closure through *mineral* specific closure temperatures followed by partial resetting during a later event.

D) The lack of any obvious relationship between the K-Ar mineral ages and sample proximity with the granite contacts suggests that simple thermal reheating as a result of granite emplacement cannot be the cause of the ages.

E) The correlations between mica K-Ar ages and the degree of co-existing feldspar alteration, together with the high Cl/K ratios of the hornblende alteration product that degasses at low temperatures during ^{40}Ar-^{39}Ar step-heating, suggest some fluid involvement during the resetting event. This is also consistent with the variation in ages from single localities because of the heterogeneous nature of fluid flow in rocks.

CHAPTER FOUR:

HYDROGEN AND OXYGEN STABLE ISOTOPIC RESULTS: IMPLICATIONS FOR RESETTING OF K-Ar SYSTEMS.

4.1. Introduction.

There is much evidence to suggest that significant interaction between the Connemara Schists and one or more fluids has occurred and that this interaction has in some ways affected the K-Ar mineral ages. The principal indications outlined in previous chapters are:

A) Ubiquitous retrogressive alteration of the rocks, with biotite altering to chlorite, plagioclase to sericite and saussurite, less extensive alteration of hornblende to biotite and growth of epidote, section 2.3.

B) Common sealed microcracks with low temperature, hydrous infilling minerals such as calcite, chlorite, epidote and amphibole, table 2.1.

C) Discordant K-Ar mineral ages recorded from samples short distances apart that seem to be best explained in terms of some fluid flow involvement, section 3.1.1.

D) Correlations between biotite and muscovite K-Ar ages with the degree of alteration of co-existing plagioclase, section 3.1.6.

E) Some excess ^{40}Ar, low Ca/K ratios and high Cl/K ratios in low temperature ^{40}Ar-^{39}Ar incremental heating steps of hornblende that correlate with degassing of biotite formed by alteration of the hornblende in the presence of a brine, section 3.3.

As a result of the overall conclusion that some kind of fluid-mineral interaction might have influenced the K-Ar ages, oxygen and hydrogen isotopic analysis was performed on selected biotite, muscovite and hornblende samples in an attempt to characterise the fluid(s) and to identify the process by which the K-Ar ages were reduced. In summary, a clear correlation of hornblende K-Ar ages and hydrogen isotopic ratios, figure 4.1, confirms the influence of fluids on K-Ar mineral ages of some of the hornblendes.

Net oxygen and hydrogen diffusion will occur between a mineral and a fluid if they are out of isotopic equilibrium. The rate at which stable isotopes diffuse is proportional to the temperature and as such there is a characteristic temperature below which diffusion can be said to have effectively ceased in a manner analogous to the Ar closure temperature. Stable isotope closure temperatures have not been so well studied and defined as have radiogenic isotope closure temperatures rather stable isotope workers are more concerned with the effect temperature can have on the fractionation of the stable isotopes between different phases, see section 1.5.2 for a review. Palaeo-temperatures can be calculated from experimentally derived mineral pair fractionation factors such as quartz-magnetite or quartz-muscovite. The advantage of this is that both phases are present in the rock for analysis. Fluid-mineral fractionation factors are essentially the same apart from the fact that the fluid is obviously not available for analysis and consequently a geologically realistic temperature is assumed and the fluid isotopic value calculated. If the temperature used in such a calculation is one derived from the analysis of a mineral pair from the same rock then a degree of internal consistency is forthcoming in the interpretation. It is a procedure such as this, using quartz-epidote and quartz-chlorite mineral pairs, that lead Jenkin (1988) to calculate the

temperature for the fluid involved in the retrogression of the Connemara Schists to be 300 to 350°C, see section 4.2.

4.2 Stable isotopic results and implications for equilibrium fluids.

In the next section the oxygen isotope results of the hornblendes from the amphibolites are discussed. In subsequent sections the hydrogen isotope results of micas from the schists, hornblendes from the amphibolites and then hornblendes from the metagabbro-gneiss complex are discussed. Where possible the isotopic compositions of the equilibrium fluids are calculated and the implications for the timing of mineral-fluid exchange are mentioned. Conclusions regarding the mechanisms by which the K-Ar mineral ages were reduced are left until section 4.3.

At this stage it is worth summarising the conclusions of Jenkin (1988) who undertook a comprehensive stable isotope study of a number of different mineral species from the Connemara rocks. Jenkin (1988) identified two discrete fluids that are of concern to this study, although it is recognised that other fluid flow events must have occurred. The two fluids of interest are:

1) An early, high $\delta^{18}O$ (about +10‰), low δD (about -40‰), high temperature (> 600°C) fluid. This fluid is thought to have been pervasive throughout the Connemara rocks and is assumed to have fully equilibrated

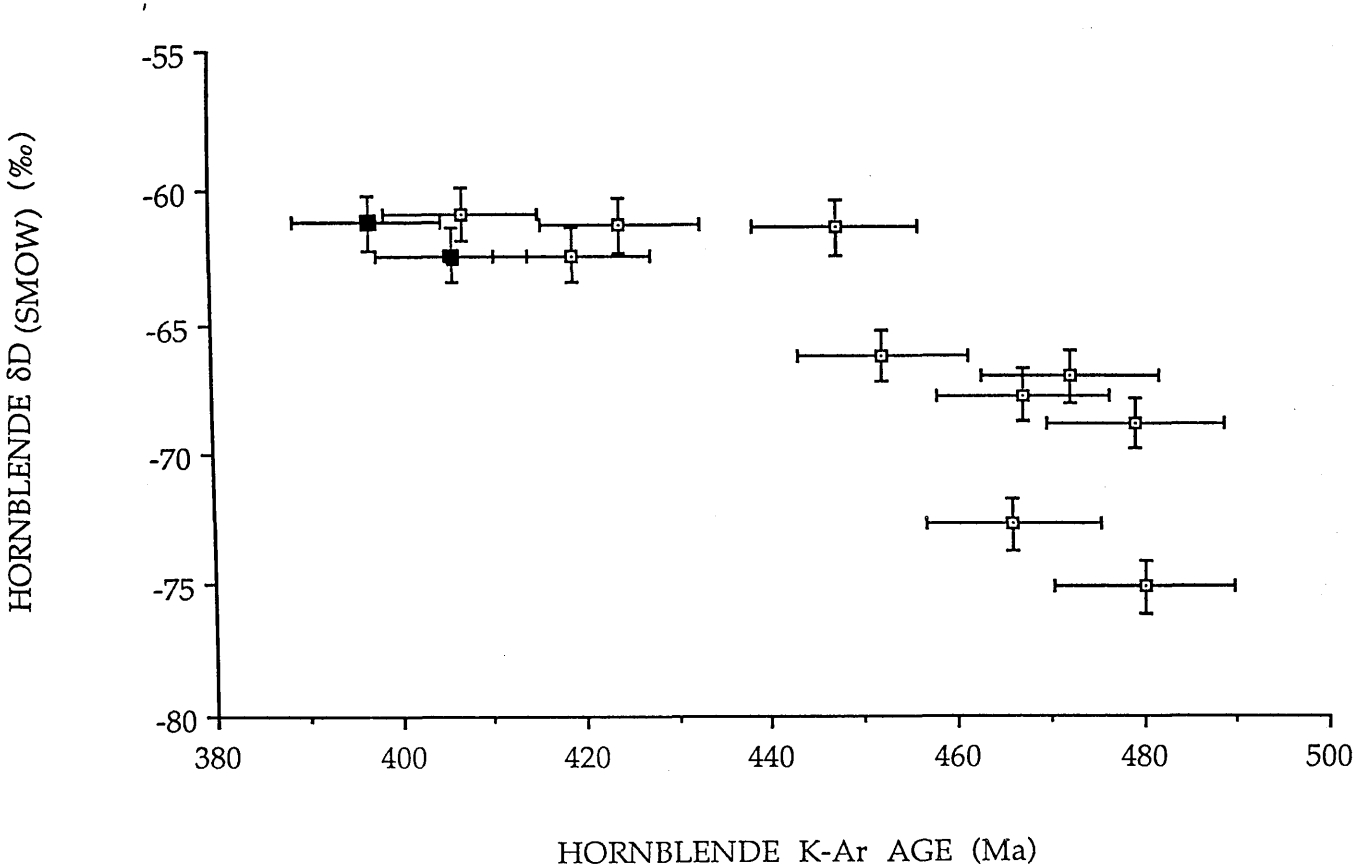

Figure 4.1. Graph showing the relationship between the K-Ar mineral ages and the δD values for samples of amphibolite hornblendes. Note the six samples all with δD values of around -62‰ that exhibit an age range of about 50 Ma. Filled squares mark samples from quarry, figure 2.1.

oxygen and hydrogen isotopes with the rocks. The high temperature of this fluid implies that it is related to the intrusion of the metagabbro-gneiss complex at 490 Ma, because this intrusive event marks the last time such high temperatures are known to have been reached in the Connemara rocks.

2) A later, high δD (about -25‰), low $\delta^{18}O$ (about +5‰), low temperature (300 to 350°C) fluid. This is the fluid that was involved in the retrogressive alteration of the rocks which is evident in nearly all thin sections (see section 2.3 for sample petrography). This fluid was not pervasive throughout the Connemara rocks but must have been channeled to a large extent, as indicated by the variable extent of chloritisation of biotite and sericitisation of plagioclase seen at the outcrop scale. This heterogeneous flow would have caused variable degrees of fluid-mineral contact, which must therefore have resulted in variable degrees of hydrogen isotope exchange. The temperature of this fluid was below the oxygen closure temperature for the minerals in question, therefore no oxygen isotopic exchange occurred between this fluid and the micas or hornblende. Although the flow was channeled, this fluid was extensive throughout Connemara. It has been identified in the Cashel-Recess area, in the Delaney Dome-Ballyconneely Amphibolite area and also in the Galway and Roundstone Granites. This fluid is believed to have been groundwater that was circulated in convection cells following the intrusion of the Lower Devonian Granites at about 400 Ma. On account of the correlation between the age of the Lower Devonian Granites with the youngest mineral K-Ar ages and the conclusion that some fluid was involved in the resetting of those mineral ages (section 3.5) it is believed that this later, low temperature fluid caused the reduction in the K-Ar mineral ages.

These fluids will be referred to frequently throughout the following discussion as the early, high temperature fluid and the later, low temperature fluid.

4.2.1 Oxygen isotopic analysis.

Oxygen isotopic analysis was performed on thirteen hornblendes from the amphibolites from the Connemara Schists. In all cases analyses were performed on aliquots of the same mineral separates used for K-Ar dating. All the analytical procedures are given in appendix A.4.6 and the results are listed in appendix A.5.8.

The $\delta^{18}O$ values range from +5.4 to +10.67‰ relative to SMOW. This range is considered to be large and significant. Jenkin (1988) constructed the following formula, equation 4.1, to calculate the oxygen fractionation factor between hornblende and water from the quartz-water oxygen fractionation data of Bottinga & Javoy (1973) and the quartz-amphibole fractionation data of Javoy (1977). Some caution must be exercised in using this equation because the original data were semi-empirical and there was no laboratory calibration.

$$1000 \ln \alpha_{(\text{hornblende-water})} = 0.95 (10^6 T^{-2}) - 3.4 \qquad \text{(eqn. 4.1)}$$

Jenkin (1988) also constructed curves from the diffusion equations of Crank (1975) to estimate the time taken for 90% oxygen isotope exchange to occur between hornblende and water, at different temperatures, for grains with different effective diffusion dimensions (figure 2.12, Jenkin 1988). From these curves it is apparent that it is unlikely that appreciable oxygen isotope exchange between the water and the hornblendes could have proceeded at temperatures below 600°C. Substituting this temperature

into equation 4.1 the oxygen isotopic fractionation factor between hornblende and water becomes:

$$1000 \ln \alpha \text{ (hornblende-water)} = -2.1 \qquad \text{(eqn. 4.2)}$$

Note that temperatures (T) in these fractionation factor equations are always in degrees Kelvin, although in the text temperatures are discussed in degrees Centigrade, consistent with most geological literature. It follows from equation 4.2 that the $\delta^{18}O$ value of the equilibrium fluid is in the range +7.5 to +12.8‰, relative to SMOW. This may imply that the fluid was isotopically heterogeneous, as was concluded by Jenkin (1988), but alternatively the variation in the mineral $\delta^{18}O$ values might reflect some compositional dependence on the fractionation factor. Some evidence for this comes from the correlation between the Fe_2O_3/FeO ratio and the $\delta^{18}O$ value of the hornblendes, figure 4.2. The Fe_2O_3/FeO ratio most likely reflects original compositional variation in the hornblendes.

Biotite has been inferred to be present in some hornblendes from the petrographic examinations (section 2.3), XRD analyses (section 2.4.1), electron-probe analysis (section 2.4.2), TEM studies (section 2.4.4) and ^{40}Ar-^{39}Ar incremental step-heating experiments (section 3.3). It might be expected that this biotite could be responsible for the range in the hornblende $\delta^{18}O$ values. However, this can not be the case. The maximum amount of biotite in the hornblendes is given by XRD analysis to be around 5%, section 2.4.1. If this biotite were to have an isotopic signature derived from meteoric water, a $\delta^{18}O$ value of about +3‰, then by calculation (see appendix A.4.7) this would cause a shift of only 0.5‰ in the $\delta^{18}O$ value of a hornblende with a $\delta^{18}O$ value of +7‰.

The high temperature at which the oxygen exchange occurred, c. 600°C, implies that this equilibration took place during, or soon after, the

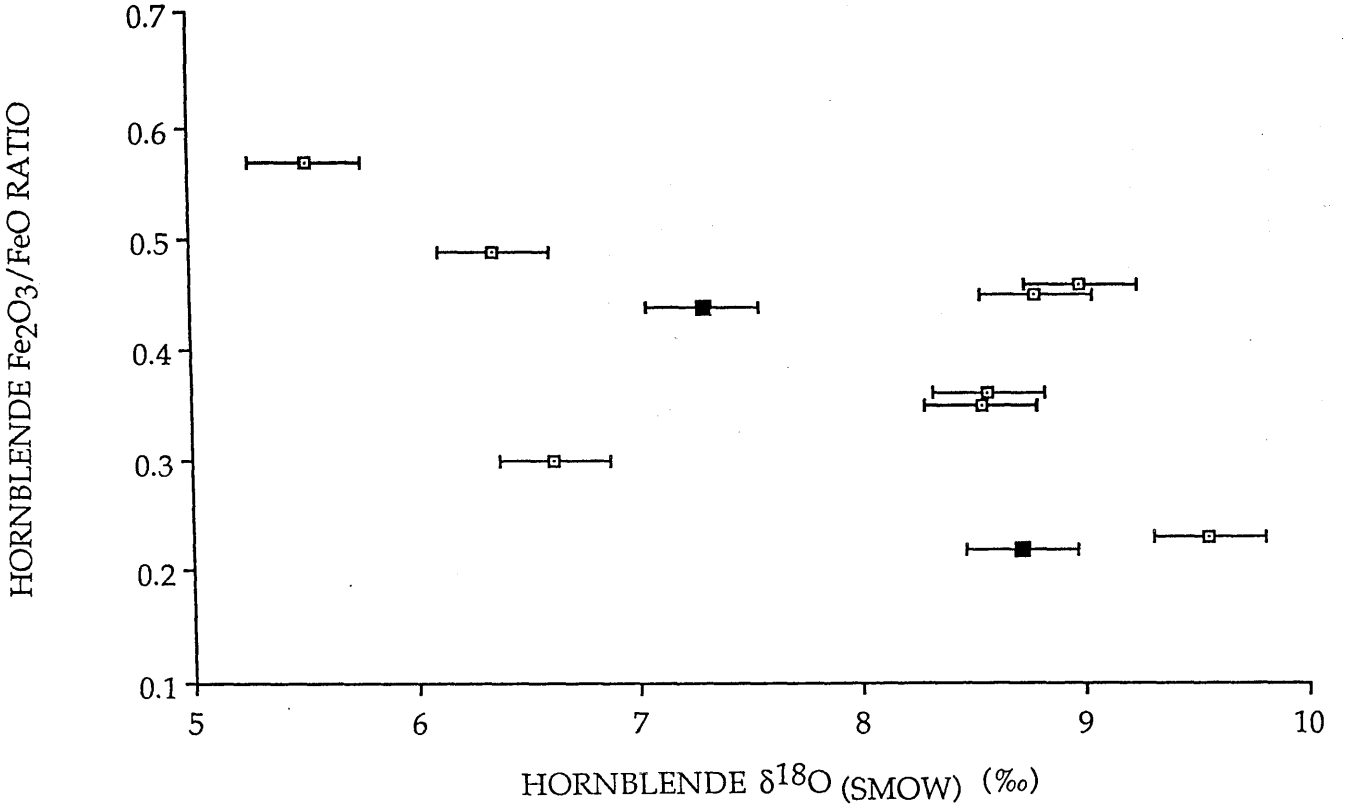

Figure 4.2. Graph showing the relationship between the $\delta^{18}O$ values and the Fe_2O_3/FeO ratios for samples of amphibolite hornblendes. The correlation suggests that the $\delta^{18}O$ values are primary and related to sample composition. Filled squares mark samples from quarry, figure 2.1.

intrusion of the metagabbro-gneiss complex. This is also the last time oxygen isotope re-equilibration could have occurred, because this is the last time the Connemara rocks are known to have been that hot. Consequently no oxygen isotopic exchange occurred between the hornblendes and the later, low temperature fluid. Owing to the fact that it was this later, low temperature, retrogressing fluid that is believed to have been involved in the resetting of the K-Ar mineral ages, section 3.5, the $\delta^{18}O$ values are of no use in identifying the resetting process and therefore they will not be discussed further.

4.2.2 Hydrogen isotopic analysis.

Hydrogen isotopic ratios were determined on seven biotites, six muscovites and fifteen hornblendes from the Connemara Schists and amphibolites and also on four hornblendes from the metagabbro-gneiss complex. In all cases analyses were performed on aliquots of the same mineral separates used for K-Ar dating. During analysis of the isotopic ratio, the absolute abundance of H_2 was measured for each sample, and from this the apparent wt.%. H_2O^+ (structural water content) of the mineral calculated. All the analytical procedures are given in appendix A.4.5 and the results are listed in appendix A.5.7.

Histograms showing the range of measured δD values for muscovite, biotite and hornblende are shown in figure 4.3. It is clear that hornblende exhibits the greatest range in δD values, from -48 to -75‰ relative to SMOW, but that the average hornblende δD value is the same as the average biotite δD value. In contrast muscovite exhibits a larger range in δD values than biotite and has a significantly heavier average δD value. The differences in the average δD values reflects the compositions of the

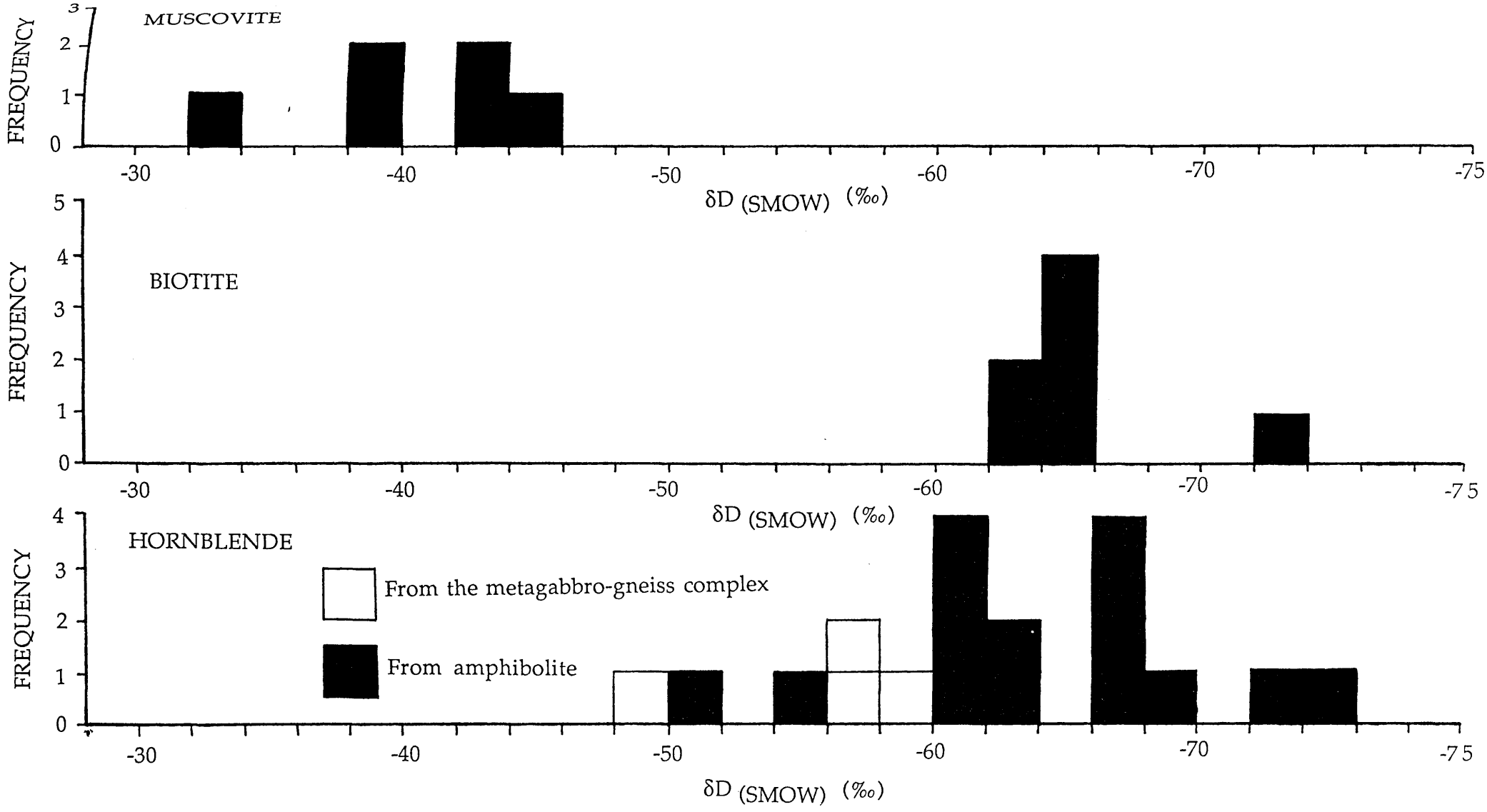

Figure 4.3. Histograms showing the range of δD values measured on biotites, muscovites and hornblendes. See text for details.

different minerals. Although there is much disagreement over the details of compositional control on hydrogen isotopic fractionation (eg. Suzuoki & Epstein 1976, Graham *et al.* 1980) it is generally true that the higher the Fe/Mg ratio of a mineral the lower will be its ability to concentrate deuterium (O' Neil 1986). In the following discussion the hydrogen isotopic results of the micas from the schists will be considered first, then the hornblendes from the amphibolite and lastly the hornblendes from the metagabbro-gneiss complex.

4.2.3 Hydrogen isotopic results of biotite and muscovite from the Connemara Schists.

The biotites show consistent results with six of the seven δD values being the same, within error, at about -65‰. The seventh biotite δD value is somewhat lighter at -72‰ (from WM 231). The muscovites, on the other hand, show greater dispersion in their δD values which cover a range of nearly 12‰ from -33 to -45‰, figure 4.3. Initially it might be thought that the concordance in the biotite δD values and the dispersion in the muscovite δD values would reflect an isotopically heterogeneous fluid equilibrating with chemically similar biotites but chemically variable muscovites. Nonetheless, this is not the case because the mica electron-probe analyses (section 2.4.2) showed that it is the biotites which were compositionally heterogeneous between samples, while the muscovites were not. Suzuoki & Epstein (1976) proposed that the hydrogen isotope fractionation between micas and water obeyed the following rule, which is both composition and temperature dependent:

$$1000 \ln \alpha_{(min\text{-}water)} = -22.4 (10^6 T^{-2}) + (2X_{Al} - 4X_{Mg} - 68X_{Fe}) + 26.3$$

(Eqn. 1.6)

Note that this equation includes the amendment of Kuroda *et al.* (1986) which replaces the original constant of +28.2 by +26.3, this amendment is included wherever calculations have been made using the Suzuoki & Epstein equation in this study. This equation has been used to calculate the δD values of the fluid in equilibration with the micas. These calculated fluid δD values are shown in figure 4.4, together with the corresponding mineral δD values. A temperature of 600°C was used in these calculations. This is equal to the estimated temperature of the early, high temperature fluid. Although the absolute, calculated, fluid δD value depends on the temperature, the difference in equilibrium fluid δD values between samples does not. This means that the degree of overlap between the δD values of the fluid calculated from the biotites and from the muscovites would be the same for any temperature. It is clear from figure 4.4 that this fluid was apparently isotopically heterogeneous with respect to hydrogen isotopes, which implies that the concordance of the biotite δD values was partly fortuitous. Note that this calculation has assumed equilibrium exchange.

Equilibration of hydrogen isotopes between the micas and a fluid could feasibly occur at temperatures as low as 300°C, equal to the temperature of the later fluid. The temperature dependence of the amended Suzuoki & Epstein equation would imply that at 300°C the δD value of the fluid in equilibrium with the micas would be very heavy (about +5 to +10‰) which is geologically unlikely. Jenkin (1988) has questioned the temperature dependence of the amended Suzuoki & Epstein relationship below about 400°C. If there is indeed no temperature

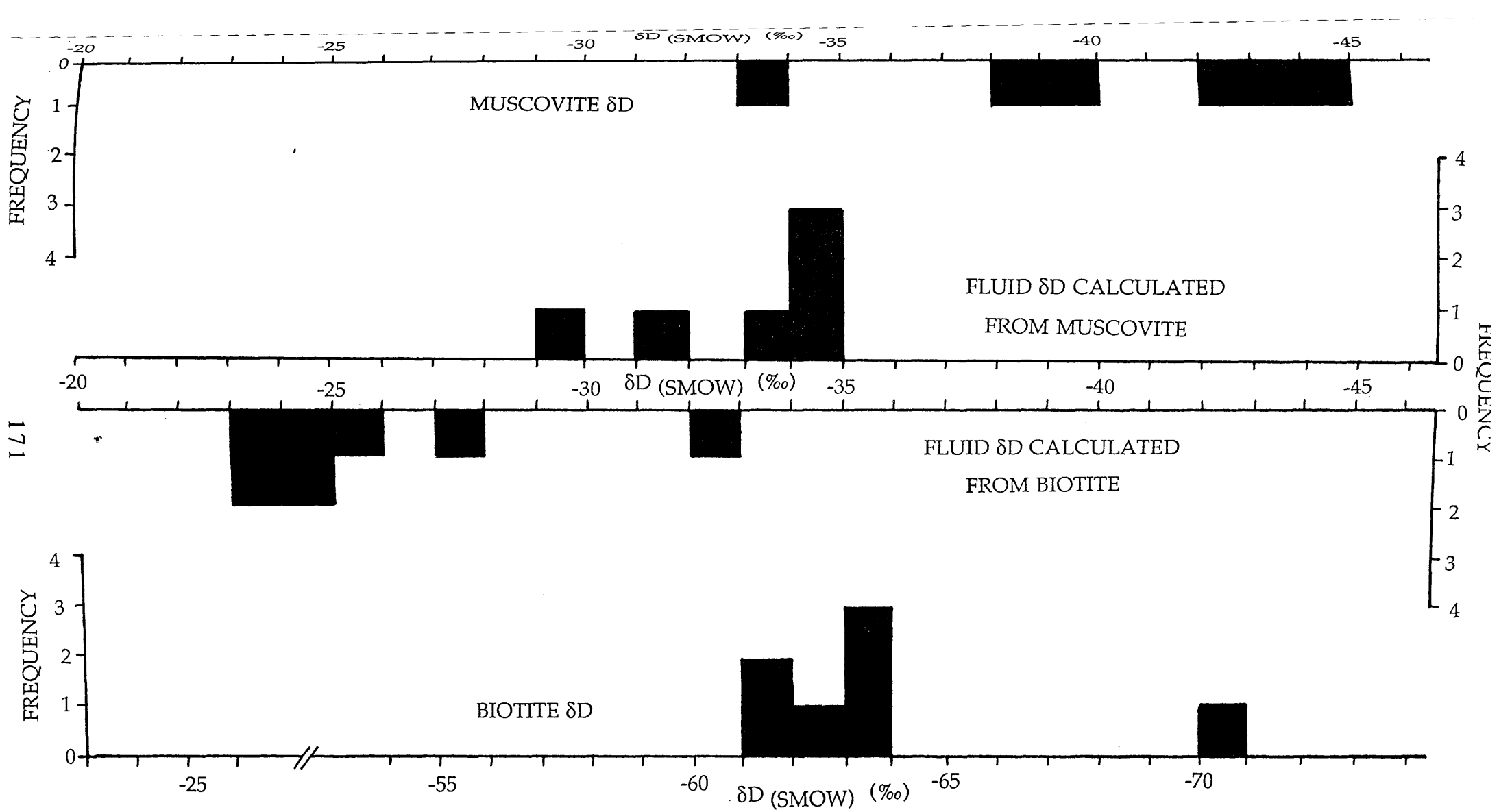

Figure 4.4. Comparison of mica δD values and fluid δD values calculated using the equation of Suzuoki & Epstein (1976). Note the disrupted scale for biotite mineral δD values.

dependence below 400°C then the fluid in equilibrium with the micas would have a δD value in the range -5 to -15‰. If, on the other hand, all the mica δD values represent equilibration with the later, low temperature fluid which had δD values in the -15 to -25‰, then the equilibration temperature according to the amended Suzuoki & Epstein equation would need to be about 500°C which is above the temperature estimate for this fluid. It is apparent that the mica δD values cannot easily be correlated with the estimated fluid δD values by this equation.

The reason for this apparent dichotomy is that it is an over-simplification to use the amended Suzuoki & Epstein equation in this way, that is assuming all the micas equilibrated with the same fluid at the same temperature. This is because the later, low temperature fluid which caused the retrogressive reactions, did not reach and equilibrate with all the mica-bearing rocks. This is indicated by the variable chloritisation of the biotite and sericitisation of the plagioclase. For this reason some of the calculated fluid δD values must represent equilibration with the earlier, high temperature fluid that had a δD value of about -35 to -40‰. Figure 4.4 makes it clear that four of the fluid δD values calculated from muscovite, but none from biotite, fall into this range. All the biotites and the remaining muscovite samples yield fluid δD values that tend to the isotopic composition of the second, lower temperature fluid ie. towards c. -20‰. The difference between the calculated fluid δD values from muscovite and biotite does not simply mean that the later, low temperature fluid did not reach the muscovite bearing rocks, because even in the muscovite sample that yields the heaviest fluid δD value there is sericitisation of the co-existing plagioclase. Two other explanations are likely for this difference. The first is that the hydrogen isotopic exchange is likely to have been more sluggish in the muscovites because the closure

temperature for this reaction is higher than in biotite and close to the estimated temperature of the later, low temperature fluid. The second reason is that because the biotites are more prone to chemical retrogressive reaction than the muscovites, the lighter fluid δD values calculated from biotite do not simply reflect diffusion of the hydrogen in the biotite, but rather chemical reaction (chloritisation). In section 2.4.1 it was shown from XRD examination of the biotite samples that some of them contain chlorite contamination, at most up to 5%. Jenkin (1988) found the δD values of some chlorites to be about -50‰ and he showed that this chlorite grew in the presence of the later, low temperature fluid. Simple calculation (see appendix A.4.7) shows that this chlorite in a biotite with a δD value of -65‰ will shift the bulk δD value to -63‰. This means that it is feasible that the variation in the biotite δD values of ±1.5‰, excepting the one at -72‰, could be accommodated purely by the chlorite inclusions. However, it should be noted that analytical precision may be no better than ±1.5‰. The presence of some chlorite in the biotite is further indicated by the slightly higher than normal water contents for some of the samples, up to 4.42 wt.%. The most water a biotite will need for its structure is about 4.2 wt.%. In the case of the muscovite samples XRD analysis did not reveal any contaminants and so the range in the muscovite δD values is real and not an artifact due to the incorporation of another phase. Consistent with this is the normal water contents of these muscovites, in the range 3.2 to 4.4 wt.%.

In conclusion there were two controls on the mica δD values. The first was a physical control, this was the varied nature of the fluid-rock contact which resulted from the heterogeneous flow of the second, low temperature fluid. The second control was chemical, which made hydrogen isotope exchange more likely in the biotite than muscovite because of its lower hydrogen isotope exchange closure temperature; this exchange was

further enhanced in the biotites by chemical reaction with the later, low temperature fluid (chloritisation). Having established that the mica δD values reflect these two controls little credence can be placed on the fluid δD values calculated from the amended Suzuoki & Epstein equation because of its temperature dependence and the assumption that only equilibrium isotopic exchange occurred. The most general conclusion that can be made is that the biotites that are from rocks which show the greatest extent of hydrous reaction will yield a fluid δD value that most closely reflects the true δD value of the younger, low temperature fluid fluid. These samples also yield the youngest K-Ar ages. On the other hand, the muscovites from the least altered rocks will yield a fluid δD value that most closely reflects the true δD value of the older, high temperature fluid and will give the oldest K-Ar ages. These predictions can be seen to be true from the following table, table 4.1.

Table 4.1. Relationship of biotites from heavily altered rocks and muscovites from little altered rocks with calculated fluid δD values and K-Ar ages. Alteration indices from Table 2.1.

SAMPLE	MINERAL	ALTERATION INDEX	CALCULATED FLUID δD	K-Ar AGE
WM 179	BIOTITE	2	-23.3‰	428 Ma
WM 188	BIOTITE	3	-24.3‰	411 Ma
WM 180	MUSCOVITE	0	-34.9‰	463 Ma
WM 226	MUSCOVITE	0	-34.5‰	461 Ma

4.2.4 Hydrogen isotopic results of hornblende from the amphibolites.

The range in the hornblende δD values from the amphibolites is nearly 30‰ and this is considered to be very large and significant. This

range of δD values for the hornblendes cannot be due to their compositional variations which were indicated by electron-probe analysis, section 2.4.2. Suzuoki & Epstein (1976) proposed that the hydrogen isotope fractionation between amphibole and water followed the same rule (equation 1.6) as for the fractionation between micas and water. This relationship has, however, been demonstrated not to be true for hornblendes by Graham *et al.* (1984) who have shown from experimental evidence that the following, much simpler, relationship holds which is both composition and temperature independent:

$$1000 \ln \alpha_{(\text{min-water})} = -23.1 \pm 2.5 \qquad \text{(Eqn 1.8)}$$

This relationship of Graham *et al.* (1984) implies that if the hornblende δD values are solely the result of complete equilibrium between the hornblendes and one fluid, then this fluid must be isotopically heterogeneous because the dispersion in the fluid δD values is as great as the dispersion in the hornblende δD values. In turn, this would imply that the fluid/rock ratio was small in order that the δD value of the fluid could be significantly shifted during equilibration with the rock. This does not necessarily imply that the fluid was isotopically heterogeneous because the hornblende δD values are not necessarily the result of complete exchange between the hornblendes and one fluid. Indeed the very large range of fluid δD values indicated by the relationship of Graham *et al.* (1984) is thought to be geologically improbable.

A more plausible explanation for the range in the hornblende δD values is that they represent a 'mix' between initial total equilibrium with the early, high temperature fluid and then variable partial re-equilibration of some of the hornblendes with the later, low temperature fluid. This is not consistent with the conclusions of Jenkin (1988) who shows that the samples he analysed did not re-equilibrate with the later, low temperature

fluid. The difference in the findings between the two studies is explained by the fact that the two sets of hornblendes were collected from different regions. Jenkin collected only from around the Cashel-Recess area, whilst the samples analysed in this study come from all over Connemara. In itself, this discrepancy implies that the fluid flow must have been heterogeneous, with short-lived fluid-mineral contact with no isotopic exchange in some places (Cashel-Recess) and longer periods of contact with the fluid that facilitated hydrogen isotope exchange, elsewhere. There are four principal reasons why, in this present study, it is believed that the hornblende δD values are the result of variable partial equilibration with the later, low temperature fluid and are not due to total equilibration with an isotopically heterogeneous earlier fluid.

1) The very large range in the fluid δD values, of about 25‰, implied by the large range in the hornblende δD values is thought to be geologically improbable. Fluid isotopic heterogeneity with respect to hydrogen isotopes is most likely to occur when fluid/rock ratios for hydrogen are small and equilibration is incomplete. In contrast the petrographic evidence (section 2.3) suggests that in the Connemara rocks fluid/rock ratios would have been large.

2) The δD value of the fluid in equilibrium with the hornblende giving the heaviest δD value (-51.5‰) is -28.4‰. This is very close to the δD value of the later, low temperature fluid which was estimated by Jenkin (1988) to be in the range -15 to -25‰, from the δD values of chlorite which grew in the presence of this fluid.

3) Biotite and epidote alteration is known to be present in the cleavages of some of the hornblendes. All the other retrogressive reactions are known to have occurred in the presence of the later, low temperature fluid. It is highly probable, therefore, that the alteration of the hornblende

occurred at this time, and with this fluid, too. It seems intuitively likely that if conditions were suitable for alteration of the hornblende to occur then hydrogen isotopic exchange could proceed also.

4) The hornblende K-Ar ages are most easily explained in terms of a resetting event with fluid involvement. The youngest hornblendes involved in this process give ages of c. 400 Ma which is the age of the Lower Devonian Granites. As these granites are believed to be responsible for the circulation of the later, low temperature fluid it can be concluded that it was this fluid that was involved in the resetting of the hornblende K-Ar ages. This resetting must have involved expulsion of Ar from the hornblendes. It seems highly likely that when the Ar was mobilised, hydrogen isotope exchange could have occurred. This point is discussed more fully in section 4.3.3.

Biotite has been inferred to be present in some hornblendes from the petrographic examinations (section 2.3), XRD analysis (section 2.4.1), electron-probe analysis (section 2.4.2), TEM studies (section 2.4.4) and ^{40}Ar-^{39}Ar incremental step-heating experiments (section 3.3). It might be expected that this biotite would have been responsible for the large range in the hornblende δD values. However, this can not be the case. The maximum amount of biotite in the hornblendes is given by XRD analysis to be about 5%, section 2.4.1. If this biotite were to have an isotopic signature derived from meteoric water, a δD value of about -50‰, then by simple calculation (see appendix A.4.7) this would cause a shift of only 1‰ in the δD value of a hornblende with a δD value of -60‰.

The presence of biotite in the hornblendes is responsible for some, but not all, of the higher than expected water contents, up to 2.7 wt.%. Typically hornblendes contain about 2.1 wt.%. structural water, which is the amount of water required to fill the hydroxyl sites in the hornblende

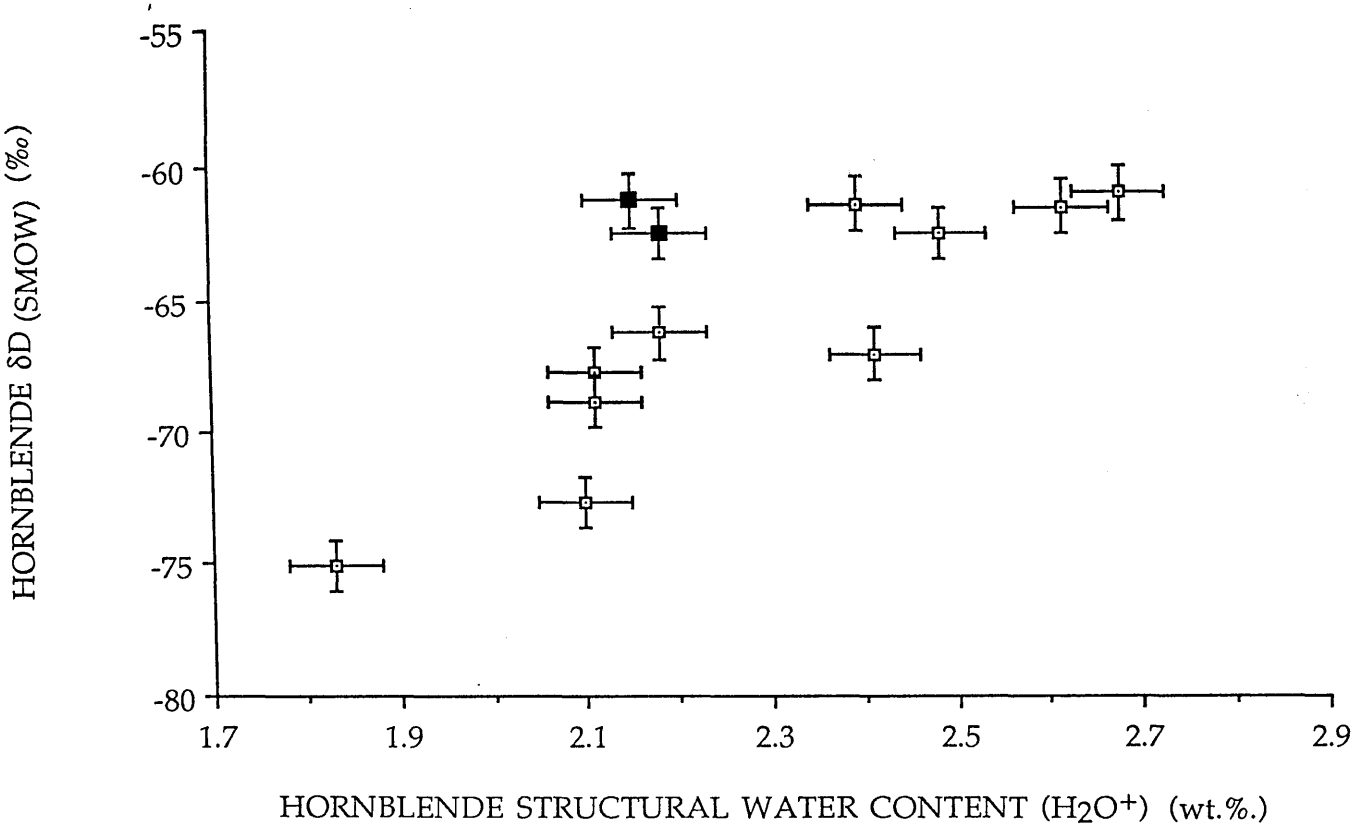

Figure 4.5. Graph showing the relationship between the structural water content (H_2O^+) and the δD values for samples of amphibolite hornblendes. Note the six samples all with H_2O^+ contents of about 2.1 wt.%. that exhibit a variation in δD of about 15‰. Filled squares mark samples from quarry, figure 2.1.

structural formulae based on 22 (O) and 2 (OH). Figure 4.5 shows that the δD values do not form a straight line correlation with apparent water content (H_2O^+) but a 'dog-leg'. Six of the samples show apparent water contents that cluster about 2.1 wt.%. These samples show a large variation in their δD values of 15‰ which must reflect hydrogen isotopic exchange between the fluid and the hornblende hydroxyl groups. A further five samples show water contents in excess of that required by the structural formulae. 'Excess' water has been recorded in many natural amphiboles (Leake 1968 and Leake & Kemp 1975) and some synthetic amphiboles (Kuroda *et al.* 1975) but the structural location of this water has not been identified. Taking the maximum amount of biotite possible in these hornblendes, about 5%, and assuming this biotite has a water content of 5 wt.% and this was incorporated in a typical hornblende with a water content of 2.1 wt.% then by calculation (see appendix A.4.7) this would raise the bulk water content to only 2.3 wt.%, which is below the measured amounts. If, on the other hand, all the 'excess' water were from only 5 % of phyllosilicate inclusions, then these inclusions would have to have a water content of up to 18 wt.%. Only chlorite has a water content approaching this, but chlorite is not compatible with the electron-probe analyses obtained from within hornblende cleavages, table 2.2. For that reason it is concluded that, although some of the 'excess' water comes from the biotite inclusions, in the samples with high measured water contents some of this 'excess' water must be located in the hornblende crystal lattice. It should, however, be noted that the apparent water contents (H_2O^+) were calculated from the amounts of hydrogen liberated during hydrogen isotopic analysis. It may be an incorrect assumption to call the excess, 'excess water', as this hydrogen may not be bound as water in the lattice but may be in the form H^+ or H_3O^+ etc. Therefore, although figure 4.5 refers to H_2O^+ all further discussion will refer to the excess as 'excess' hydrogen.

It can be seen in figure 4.5 that the samples with 'excess' hydrogen show δD values around -62‰, equal to the highest δD of the 'excess' hydrogen-free samples. Although this does not impart any information as to the precise structural location of this 'excess' hydrogen, the clustering of the δD values indicates that the 'excess' hydrogen must be in sites with a hydrogen isotopic fractionation factor equivalent to that of 'normal' hornblende hydroxyl groups.

4.2.5 Hydrogen isotopic results of hornblende from the metagabbro-gneiss complex.

It is shown in figure 4.3, that the δD values of the hornblendes from the metagabbro-gneiss complex lie just within the range of δD values of the hornblendes from the amphibolites, but that the average δD value for the former group is significantly heavier at -55.3‰ compared to -64.3‰ for the latter. The hornblendes from the metagabbro-gneiss complex also have water contents in excess of that required to fill the hydroxyl groups, up to 3 wt.%, similar to the hornblendes from the amphibolites.

Biotite and also chlorite has been identified in some of these hornblendes from the petrographic examinations (section 2.3) and XRD analyses (section 2.4.1). This is unlike the hornblendes from the amphibolites which did not reveal any chlorite in the cleavages, only biotite. The maximum amount of mica in the hornblendes from the metagabbro-gneiss complex is estimated from the XRD analysis to be about 5%. Chlorite can have 12 to 15 wt.% H_2O^+ (Deer *et al.* 1966). By calculation (see appendix A.4.7) only 5% chlorite is required in the hornblende to give a measured bulk water content equal to the highest of 3 wt.%. Therefore, the biotite and chlorite in the metagabbro-gneiss complex hornblendes can

account for all the high water contents and consequently there is no suggestion that 'excess' water (hydrogen) is present within the crystal structure of hornblendes from the metagabbro-gneiss complex, although this has not been ruled out.

Inclusion of the biotite and chlorite mixture cannot explain the range in the measured hornblende δD values. Jenkin (1988) found the δD values of chlorites in the metagabbro-gneiss complex to be about -50‰. By calculation (see appendix A.4.7) if 5% of this chlorite were present in a hornblende with a δD value of -60‰ a shift in the bulk δD of about only 1‰ would result. The range of measured hornblende δD values is therefore real and not the result of the incorporation of another phase.

It should be noted that Jenkin (1988) performed hydrogen isotopic analyses on ten hornblendes from the metagabbro-gneiss complex. The results ranged from -59.2 to -79.8‰ with an average of c. -70‰ and so these are heavier than the analyses presented in this study. The total range of δD values from all the metagabbro-gneiss hornblendes is therefore nearly 30‰. Using the hydrogen isotope fractionation factor of Graham *et al.* (1984), equation 1.8, the δD value of the fluid that would be in equilibrium with these hornblendes would be in the range -60 to -30‰, assuming that the hornblende δD values represent total equilibrium with one fluid. Such an isotopically heterogeneous fluid is considered geologically improbable. Fluid isotopic heterogeneity with respect to hydrogen isotopes is most likely to occur when fluid/rock ratios for hydrogen are small and equilibration is incomplete. In contrast the petrographic evidence (section 2.3) suggests that in the Connemara rocks fluid/rock ratios would have been large.

The hornblendes from the metagabbro-gneiss complex are believed to represent a 'mix' between initial total equilibrium with the early, high

temperature fluid and then variable partial re-equilibration of some of the hornblendes with the later, low temperature fluid. The reasons for this conclusion are the same as those given in the previous section for the range of δD values for hornblendes from the amphibolites. Jenkin (1988) concluded that the metagabbro-gneiss complex hornblendes did not re-equilibrate with the later, low temperature fluid and showed that if the fluid temperature was about 300°C, the time of fluid-mineral contact must be less than 1 Ma. This conclusion, although valid for the hornblendes examined by Jenkin, is not consistent with the hornblende δD values determined in this study. The fluid δD value in equilibrium with the isotopically lightest hornblende analysed, -48‰, from the fractionation factor of Graham *et al.* (1984) would be -25‰, equivalent to Jenkin's estimate for the fluid in which the retrogressive minerals grew, ie the later, low temperature fluid. This difference in the findings between the two studies is explained by the fact that the two sets of hornblendes were collected from different regions of the metagabbro-gneiss complex. Jenkin collected from around the Cashel-Recess area, whilst three of the samples analysed in this study came from the Currywongaun-Doughruagh intrusion and the other two came from close to the contact with the Galway Granite. This implies that the fluid flow must have been heterogeneous, with short-lived fluid-mineral contact in some places (Cashel-Recess) and longer contact times elsewhere. This is consistent with the conclusions drawn from the hydrogen isotopic results of the hornblendes from the amphibolites.

4.3. Disturbance of the K-Ar mineral ages by fluid interaction.

It was concluded in section 3.5 that the reduction in the K-Ar mineral ages likely occurred with some fluid involvement. It has been

shown in the previous sections that different mineral species have responded in different ways to the later, low temperature fluid that is believed to have been involved in the resetting of the K-Ar mineral ages. Accordingly it seems logical to assume that the K-Ar ages would not have been reduced in quite the same manner in each mineral species. For this reason each mineral species will be discussed separately in the following sections.

4.3.1 The reduction in the K-Ar ages of muscovite from the Connemara Schists.

It has been concluded that there is no relationship between the muscovite K-Ar ages and mineral chemistry, section 3.1.4; crystal microstructure, section 3.1.5; mineral grain size, section 3.1.7 or sample elevation, section 3.1.8. Despite this, it has been demonstrated that there is some fluid control over the muscovite K-Ar ages in section 3.1.6 by the correlation between these ages and the degree of alteration of the co-existing feldspar. In section 4.2.3 it was shown that some hydrogen isotope exchange occurred between certain muscovites and the later, low temperature fluid. Nonetheless there is no evidence to suggest that this exchange, itself, could have influenced the K-Ar ages. Furthermore there is no evidence to suggest that any significant chemical reaction occurred between the muscovites and the fluid. With the lack of any other evidence the simplest explanation for the reduction in the muscovite K-Ar ages is that it was caused by heating of the minerals when in contact with the fluid. It has been estimated that the temperature of the later fluid was about 300 to 350°C, section 4.2. This is equal to the Ar closure temperature of muscovite, 350±50°C (Purdy & Jager 1976). Assuming that the Ar opening temperature is effectively equal to the Ar closure temperature, the

variation in the muscovite K-Ar ages is concluded to have been the result of a combination of a) a variation in the supply of fluid to each area of rock and b) the length of time that fluid was in contact with rock. At the time of fluid migration, c. 400 Ma, the Connemara rocks would have been buried under 3 km or more of Silurian rocks, and the region could have been one of high heat flow. This possibility is discussed in detail in section 5.2. Consequently the temperature might have been approaching the Ar closure temperature of the micas, ie. about 300°C. In order for the fluid to then partially reset the muscovite it would have to raise the rock temperature only a few 10's of degrees. As the fluid temperature is thought not to be substantially higher than the rock temperature then the heating effect would be only local and this therefore explains why all the muscovite samples did not experience the resetting process. This implies that the muscovites which were never in contact with the fluid, or were in contact for only a short time, should yield K-Ar ages that are effectively undisturbed. These samples can be identified by their older K-Ar ages and the lack of alteration to the co-existing plagioclase. The geological significance of the undisturbed ages is discussed in chapter five.

4.3.2 The reduction in the K-Ar ages of biotite from the Connemara Schists

It has been concluded that there is no relationship between the biotite K-Ar ages and crystal microstructure, section 3.1.5; mineral grain size, section 3.1.7 or sample elevation, 3.1.8. It has, however, been demonstrated that there is some fluid control over the biotite K-Ar ages in section 3.1.6 by the correlation between these ages and the degree of alteration of the co-existing feldspar. In section 4.2.3 it was shown that some hydrogen isotope exchange occurred between certain biotites and the later,

low temperature fluid and that this exchange was enhanced by the chemical reaction (chloritisation) that also occurred in some samples. There is no evidence to suggest that hydrogen isotopic exchange, where it occurs solely by diffusion and not by reaction, would have influenced the biotite K-Ar ages. There is also no evidence to suggest that the chloritisation process alone caused any significant reduction in the biotite K-Ar ages, because in section 3.1.4 it was shown that there is no correlation between the biotite K-Ar ages and TiO_2 or K_2O, both of which are good indicators of progressive chloritisation. This conclusion is reached despite the fact that both K and Ar are expelled in this reaction. The direction in which the K-Ar age would be shifted depends on which element is lost fastest. There is independent evidence to suggest that, at least initially, K and Ar are lost in equal proportions, causing the age to remain unaltered (Kulp & Engels 1963 and Clauer *et al.* 1982). This must be true for the least altered Connemara samples, but intuitively it seems likely that in the most altered samples, the K-Ar ages would have been somewhat reduced during chloritisation because Ar is generally much more mobile than K.

The estimated temperature of the later fluid, 300 to 350°C, is above the Ar closure temperature of biotite c. 300°C (Harrison *et al.* 1985). It is assumed that the Ar opening temperature is equal to the Ar closure temperature in biotite. Hence, it is concluded that most simple explanation for the reduction in the biotite K-Ar ages is that it has been brought about simply by heating of the minerals when in contact with the fluid, with the effect enhanced during extreme chloritisation of some samples. There are, therefore, two process by which some of the biotite K-Ar ages are believed to have been reduced, with both processes requiring fluid interaction with the biotite. The variation in the biotite K-Ar ages is, therefore, a result of a combination of a) the supply of fluid to each area of rock and, b) the length of time that fluid was present. The argument is the same as for muscovite.

At the time of fluid migration, c. 400 Ma, the Connemara rocks would have been buried under 3 km or more of Silurian rocks, and the region could have been one of high heat flow. This possibility is discussed in detail in section 5.2. Consequently the temperature might have been approaching the Ar closure temperature of the micas, ie. about 300°C. In order for the fluid to then partially reset the biotite it would have to raise the rock temperature only a few 10's of degrees. As the fluid temperature is thought not to be substantially higher than the rock temperature then the heating effect would be only local and this therefore explains why all the biotite samples did not experience the resetting process. This means that the biotites that were never in contact with the fluid, or were in contact for only a short time should yield K-Ar ages that are effectively undisturbed. These samples can be identified by their older K-Ar ages and the lack of alteration to the co-existing plagioclase. The geological significance of the undisturbed ages is discussed in chapter five. The samples that were in contact with the later, low temperature fluid for the longest period would have had their K-Ar reduced to the greatest extent. This is demonstrated by the correlation between the biotite K-Ar ages and the degree of alteration of the co-existing feldspar, section 3.1.6.

4.3.3 The reduction in the K-Ar ages of hornblende from the amphibolites.

It has been concluded that there is no relationship between the K-Ar ages of hornblendes from the amphibolites with either grain size, section 3.1.7 or sample elevation, section 3.1.8. Unlike the micas, there is also no relationship between the hornblende K-Ar age and the degree of rock alteration, section 3.1.6, but there is some indication of a

compositional control on the hornblende ages with a correlation with $Fe^2/(Fe^2+Mg)$, section 3.1.4.

The temperature of the second, retrogressing fluid, 300 to 350°C, is significantly lower than the commonly accepted closure temperature of hornblende, which is c. 550 ± 50°C (Harrison 1981). For that reason, and assuming that the Ar opening temperature is effectively equal to the Ar closure temperature, the temperature of the fluid would be much too low to cause Ar loss from the hornblendes. The evidence accumulated from the hornblendes is not easy to interpret. It is complicated and ambiguous. In an attempt to use and explain all the information, three alternative mechanisms that might explain the reduced ages have been outlined below. Each of these three possibilities details a fluid-mineral interaction mechanism that operates at the grain scale and consequently would occur to differing extents with differing degrees of fluid-mineral contact; this is therefore compatible with the conclusion that the fluid flow was heterogeneous.

Mechanism 1) The closure temperature of the amphibolite hornblendes could be significantly lower than the c. 550 ± 50°C value of Harrison (1981). This could be caused by the compositional variation but more likely as a result of exsolution and phyllosilicate inclusions which are known to be present in two of the samples, and are possibly present in all or some of the others (section 2.4.4). The closure temperature of the amphibolite hornblendes could be as low as, or lower, than the fluid temperature on the evidence of Harrison & Fitz Gerald (1986) who show hornblende closure temperatures as low as 300°C. A detailed account of why exsolution and phyllosilicate inclusions reduce the closure temperature is given in section 3.1.5. If this were the case in the hornblendes from the amphibolites, then simple thermal resetting of the

hornblendes in contact with the fluid might have occurred. This would then imply that the hydrogen isotopic re-equilibrium process was not coupled to the K-Ar mineral age resetting process, although the two process would be continuing side-by-side. In this mechanism the presence of the fluid is only required to supply the heat necessary to raise the mineral temperature above its Ar closure (opening) temperature. Of course in other situations heat could be supplied by simple conduction through the rock mass, without a fluid being present, but this cannot be possible in Connemara because the discordant ages from single locations and the lack of any geographic trend to the K-Ar mineral ages rules out widespread thermal heating to above the Ar closure temperature of micas, ie. about 300 to 350^{o}C (section 3.1.1).

Mechanism 2) Where the fluid and the amphibolite hornblendes were in contact they chemically reacted. The re-crystallisation (re-precipitation) of the hornblende would cause Ar loss from the mineral grains and hydrogen isotopic re-equilibration to occur. The resetting of the hornblende K-Ar ages would not, in this situation, be governed by the Ar closure temperature but rather by the temperature above which chemical reaction between the mineral and the fluid could occur. As with the first possibility the hydrogen isotopic re-equilibrium process would not be coupled to the K-Ar mineral age resetting process although the two processes would be continuing side-by-side. This possibility is not favoured because if all the mineral grains did react with the fluid then oxygen, along with hydrogen, isotopic re-equilibration would have occurred and it has already been concluded (section 4.2.1) that this did not happen to any great extent. The only chemical reaction between the hornblende and the fluid occurred in small zones in the cleavages where the phyllosilicates were precipitated.

Mechanism 3) Where the fluid and the amphibolite hornblendes were in contact they did not chemically react, but the hydrogen isotopic re-equilibration that occurred drove the Ar out of the crystal lattice. This process would imply a direct coupling between the hydrogen isotope exchange and the K-Ar age resetting processes. To the author's knowledge, a mechanism such as this has not been proposed before. The feasibility of such a mechanism is discussed below. Such a mechanism, if physically possible, would proceed when diffusion is facilitated by a reduction in closure temperatures brought about by chemical variations or peculiar crystal microstructures such as the phyllosilicates and exsolution revealed by TEM, section 2.4.4. It can be reasoned that in a 'dry' situation Ar loss from the hornblende would proceed by mechanism 1, but in a 'wet' situation where hydrogen isotope re-equilibration occurs, then Ar loss could proceed by mechanism 3. In other words there could be two relevant closure temperatures for hornblende; a higher temperature 'dry' one and a lower temperature 'wet' one. In the 'dry' situation the Ar loss is passive, ie. it occurs only via random Ar diffusion when the temperature is above the closure temperature. In the 'wet' situation the Ar loss is active, ie. it is coupled to the hydrogen isotopic exchange process. Both the closure temperatures, 'wet' and 'dry', are likely to be sample specific, ie. they could be influenced by crystal chemistry, grain size and lattice defects etc.

From these three mechanisms a model that tries to explain all the information acquired from the hornblendes is constructed below. As a result of the complexity of the data, this model is itself complicated and not easily testable. Accordingly, it is not known if this model is accurate and so it needs to be treated with some caution, but should serve as a starting point for further discussion and research on the systematics of mineral-fluid interaction.

The two potential mechanisms outlined above, one and three, can be distinguished by the requirement for coupling between hydrogen isotopic exchange and K-Ar age resetting in the third mechanism and the lack of such a requirement in the first. Examination of figure 4.6 shows that some relationship does exist between the δD values and the K-Ar ages which lends weight to the overall assumption that the K-Ar ages are fluid controlled. This plot shows that a decline in the K-Ar ages is at first accompanied by increasingly high δD values until samples recording ages of c. 440 Ma. Some samples record a steady decline in ages younger than 440 Ma, but these samples show no change in their δD values which cluster at -62‰. It was shown in section 4.2.4 that these samples, with δD values around -62‰, contain 'excess' hydrogen over and above that required to fill the hornblende hydroxyl groups.

The occupancy of the hornblende 'A' sites by K and Na is given in the structural formulae for each sample, appendix A.5.2. In all cases at least 50% vacancy of the 'A' site exists. The δD values form a 'dog-leg' plot with 'A' site occupancy, figure 4.7. The samples containing 'excess' hydrogen which cluster around -62‰ have the greatest 'A' site vacancy. As these are also the samples with the lowest K-Ar ages it is proposed that the 'excess' hydrogen occupies the vacancy in the 'A' site displacing Ar in the process. Figure 4.8 shows that there is a relationship between the structural water content of amphibolite hornblendes and their 'A' site occupancy. This 'excess' hydrogen cannot occupy the 'A' site as neutral H_2O because this molecule has a significantly different hydrogen isotope fractionation factor to the hornblende hydroxyl groups. Instead the hydrogen must bond to the bridging tetrahedral oxygens in the 'A' site as either H^+ or H_3O^+. The presence of H_3O^+ in the hornblende has been proposed before to explain anomalously high water contents (Hawthorne 1981). It should be noted that the addition of oxygen to the 'A' site with H_3O^+ would not significantly

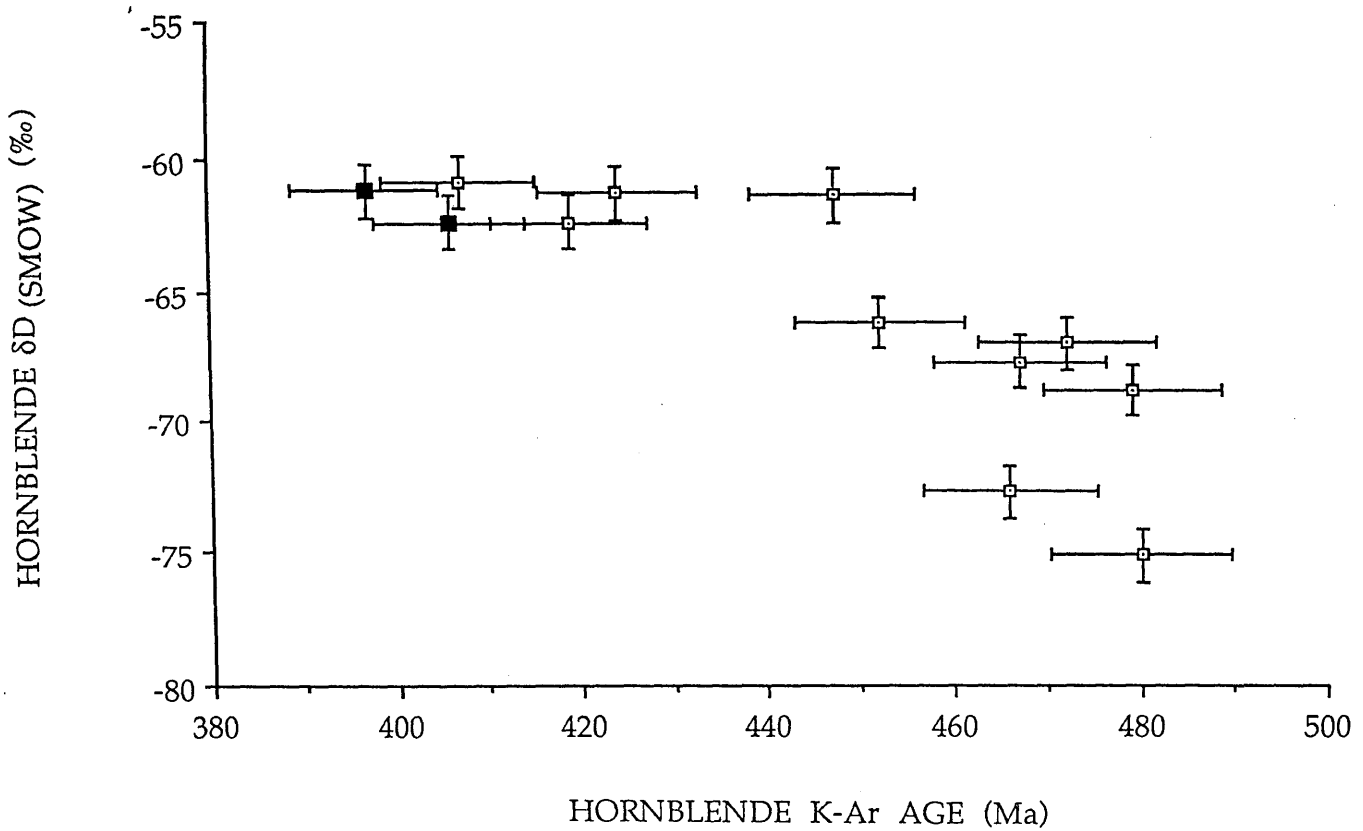

Figure 4.6. (As figure 4.1) Graph showing the relationship between the K-Ar mineral ages and the δD values for samples of amphibolite hornblendes. Filled squares mark samples from quarry, figure 2.1.

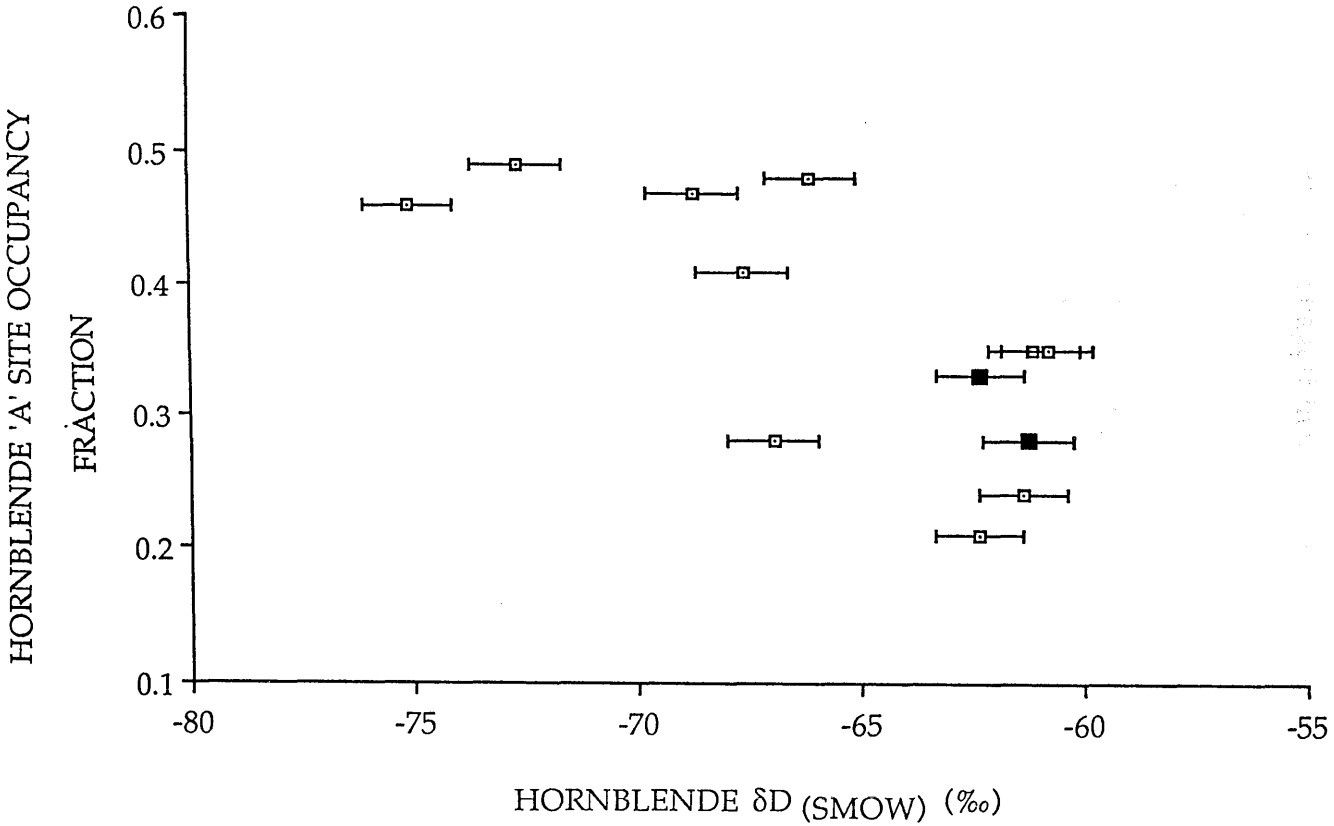

Figure 4.7. Graph showing the relationship between the δD values and the 'A' site occupancy for samples of amphibolite hornblendes. There is a general decrease in the 'A' site occupancy with increasingly heavy δD values. Filled squares mark samples from quarry, figure 2.1.

alter the $\delta^{18}O$ values of the hornblende. Adding 0.7 wt.%. H_3O^+ with a meteoric $\delta^{18}O$ value of -4‰ would cause a shift in the bulk $\delta^{18}O$ value of -0.6‰. The expulsion of Ar from the 'A' site by hydrogen would occur during hydrogen isotope exchange with the fluid and could provide a medium by which mechanism 3 could proceed.

Figures 4.7 and 4.8 suggest that two processes might have occurred which were responsible for the reduced hornblende K-Ar ages. One process reduces the K-Ar ages to no more than 440 Ma but causes a concomitant increase in the δD values without any addition to the hydrogen (water) content of the hornblende. It is suggested that this is mechanism 1, where the K-Ar ages are partially reduced simply by thermal heating of the hornblendes (which have low closure temperatures which result from either exsolution or phyllosilicate inclusions) or by the fluid. The hydrogen isotopes partially re-equilibrate between the mineral and the fluid. In most samples neither the K-Ar ages were totally reset nor the hydrogen isotopes were totally re-equilibrated. This is due to a low supply of fluid to the areas of rock these samples came from. In this process there is no coupling of the K-Ar age resetting process with the hydrogen isotope exchange process.

The second process accounts for the ages lower than 440 Ma. This process involves a significant reduction in the K-Ar age, an increase in the hydrogen (water) content, but no change in the bulk hornblende δD value. It is suggested that this is mechanism 3, where the Ar is actively expelled from the hornblende 'A' site by additional hydrogen bearing molecules. These hydrogen bearing molecules might have accessed the crystal structure along 'pathways' at the margins of phyllosilicates or at exsolution boundaries if they are incoherent. In this process there is coupling of the K-Ar age resetting process with the hydrogen isotope exchange process. It is likely that mechanism 3 occurs after mechanism 1 has proceeded to

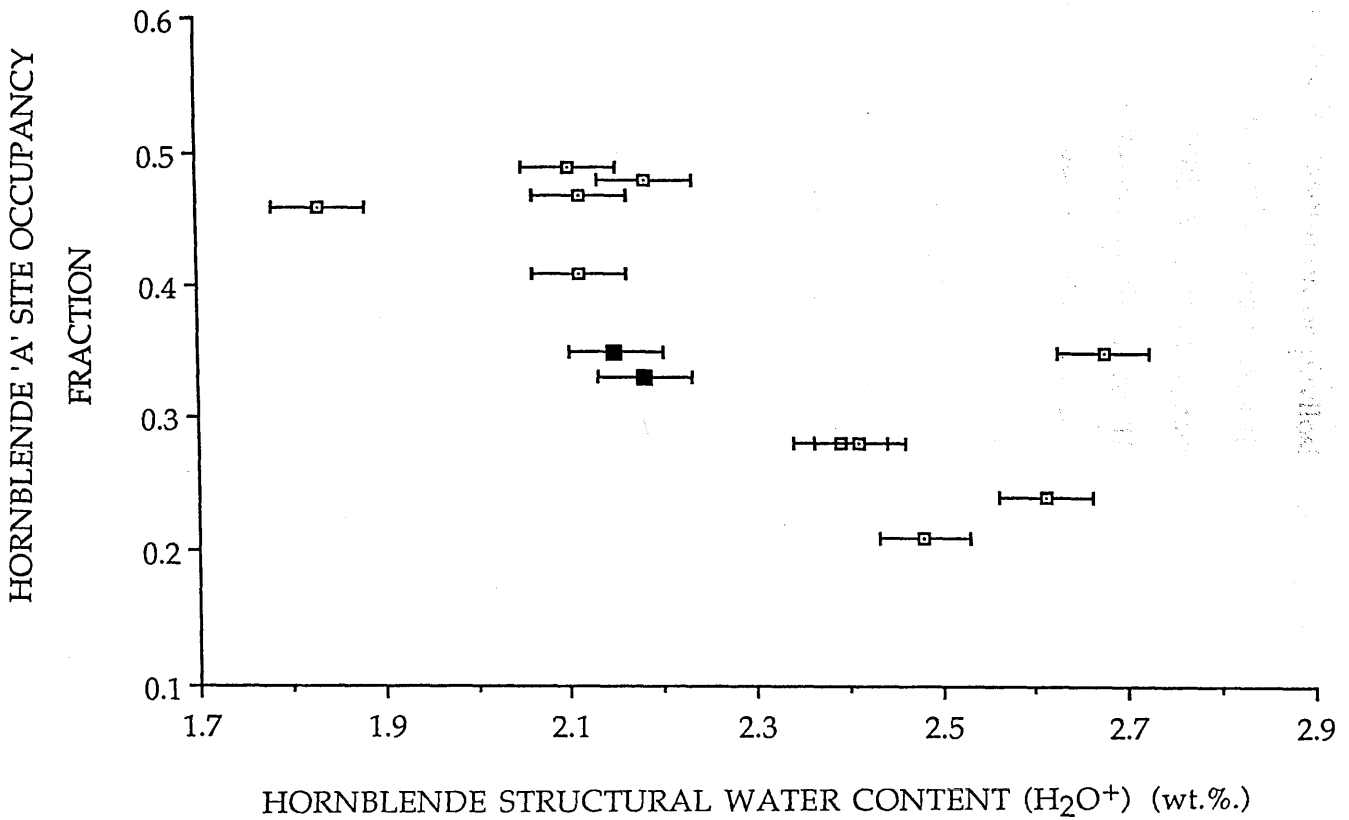

Figure 4.8. Graph showing the relationship between the structural water content (H_2O^+) and the 'A' site occupancy for samples of amphibolite hornblendes. There is a general decrease in the 'A' site occupancy with increasing structural water content. Filled squares mark samples from quarry, figure 2.1.

completion because of the lack of change in the δD values which indicates that total re-equilibration had occurred. Mechanism 3 would only occur when there is an ample supply of fluid to the rock.

In summary, the extent to which the hornblende K-Ar ages became reduced is controlled by a) the degree of complexity of the crystal microstructure ie. exsolution or phyllosilicate inclusions and b) the supply of fluid to the minerals. This means that hornblendes that were never in contact with the fluid, or were in contact for only a short time yielded K-Ar ages that are effectively undisturbed. These samples could be identified by their older K-Ar ages and the lack of crystal heterogeneity, although this would need to be done by TEM investigation. The geological significance of the undisturbed ages is discussed in chapter five. The samples that were in contact with the later fluid for the longest period and had the greatest degree of crystal heterogeneity would have had their K-Ar reduced to the greatest extent.

4.3.4 The reduction in the K-Ar ages of hornblende from the metagabbro-gneiss complex.

In section 3.2 the K-Ar ages of hornblendes from the metagabbro-gneiss complex were presented. These ages show much less dispersion, ranging from 453±9 to 486±10 Ma, than the other mineral groups. Consequently when considering these hornblendes the discussion has to centre on why these hornblendes do not show any significant reduction in their K-Ar ages when most of the hornblendes from the amphibolites and the micas from the Connemara Schists do.

The two youngest K-Ar ages, 453±9 and 457±9 Ma, can be explained by simple thermal resetting from the Galway Granite. These samples are only 200m from the contact, section 3.5. None of the other samples were located so close to the granites and none are believed to have suffered simple thermal resetting.

It has been concluded that there is no relationship between the hornblende K-Ar ages and mineral chemistry, mineral grain size or sample elevation, section 3.2. Unlike the hornblendes from the amphibolites, those from the metagabbro-gneiss complex are not known to exhibit complex microstructures such as exsolution or fine scale phyllosilicate inclusions. Furthermore, although is is known that some hydrogen isotopic exchange occurred between the hornblendes and the fluid there is no evidence of any fluid control on these ages. It is concluded that there is no reason why the closure temperature of these hornblendes should not be close to the normally accepted value of c. 550 ± 50°C (Harrison 1981). Consequently, because the fluid temperature was much less than this, 300 to 350°C no thermal resetting of the hornblendes could occur.

Further evidence that the metagabbro-gneiss complex hornblendes and their Ar closure temperatures are 'normal', ie. about 500 to 550°C comes from the Ballyconneely Amphibolite samples dated by Leake *et al.* (1984), see figure 3.4. These give an average age of 454±11 Ma which is identical, within error, to the 447±4 Ma age of last movement on the Mannin Thrust determined by Tanner *et al.* (1989) at which time they were mylonitised. Only one of these eight samples gives an age (384±12 Ma) that appears to reflect subsequent resetting at the time the Lower Devonian Granites were intruded. This is despite the fact that some of these samples were collected from locations only 2 to 3 km away from the granite contact.

In conclusion the hornblendes from the metagabbro-gneiss complex can be considered 'normal and well behaved', giving the age of initial cooling in contrast to the peculiar behaviour of the hornblendes from the amphibolites.

CHAPTER FIVE:

DISCUSSION AND GEOLOGICAL SYNTHESIS, FURTHER RESEARCH AND IMPLICATIONS FOR OTHER GEOCHRONOLOGICAL STUDIES.

5.1 Geological significance of the K-Ar mineral ages.

It was shown in chapter 4 that the K-Ar mineral ages reflect variable partial resetting with some fluid involvement. Nonetheless, in section 3.1.2 and in figure 3.7, it was shown that there is some correlation between the range of K-Ar mineral ages and major geological events, so that despite the resetting there appears to be some geological significance, to some of the ages at least. The primary conclusion, made in section 3.1.2, is that the intrusion of the metagabbro-gneiss complex at 490 ± 1 Ma would have caused effective total resetting of all the K-Ar 'clocks' in all the mineral species. The lack of any K-Ar mineral ages older than the metagabbro-gneiss complex supports this view. It follows that samples yielding K-Ar ages equal to, within error, 490 Ma cannot have suffered any significant, subsequent, resetting and accordingly these ages must represent rapid cooling of the mineral through their relevant Ar closure temperatures. Only a few hornblende samples yielded K-Ar ages equal to, within error, the age of the metagabbro-gneiss complex.

The second important event that controls the K-Ar mineral ages is the fluid circulation system that operated at c. 400 Ma and which was responsible for the variable partial resetting of the K-Ar mineral ages. It follows that those samples with K-Ar mineral ages of c. 400 Ma must have been effectively totally reset at this time and are therefore geological significant ages whereas the partially reset ages are geologically

meaningless. Samples of hornblende, biotite and muscovite all give ages of c. 400 Ma.

It does not, however, necessarily follow that all the K-Ar mineral ages between 490 and c. 400 Ma have no geological significance. It is very likely that following intrusion of the metagabbro-gneiss complex, not all the Dalradian rocks would have cooled at the same rate and at the same time. This is especially true if cooling was controlled by uplift, and the region broke into different blocks which uplifted at different times, as suggested by Elias *et al.* (1988). In this case some mineral samples, especially those with low closure temperatures, might not have cooled below their relevant closure temperatures until some time after 490 Ma. If these samples did not subsequently become reset by the c. 400 Ma event then they will still record K-Ar ages that are geologically significant closure ages. The problem is how to distinguish between these ages and others which are younger than 490 Ma because they have been partially reset.

5.1.1 The significance of the K-Ar ages of micas from the Connemara Schists.

In section 3.1.6 it was shown that some relationship exists between the mica K-Ar ages and the degree of rock alteration and so it appears that the simplest test for possible resetting of mica K-Ar ages is the alteration of the rock. On this basis all those mica K-Ar ages that are from rock samples with feldspar alteration indexes of 0 or 1 from table 2.1, ie. little or no alteration, are assumed not to have been substantially reset by the fluid and therefore to have geological significant closure ages. The mica samples that are acceptable on this basis are listed in table 5.1 together with their respective K-Ar ages.

The range and averages of the acceptable mica K-Ar ages are compared to the range and averages of all the mica ages, the latter are given in parenthesis. The range of biotite K-Ar ages is 32 Ma, from 426±9 to 458±9 Ma (55 Ma, from 403±8 to 458±9 Ma) with an average of 448 Ma (435 Ma). The range for muscovite is 42 Ma, from 436±9 to 478±10 Ma (70 Ma, from 408±8 to 478 Ma) with an average of 457 Ma (438 Ma).

Table 5.1. Mica samples from rocks with little altered co-existing feldspar (those with feldspar alteration indexes of 0 or 1 in table 2.1), together with the respective K-Ar ages.

BIOTITE		MUSCOVITE	
SAMPLE	AGE (Ma)	SAMPLE	AGE (Ma)
WM 107	447 ± 9	WM 132	436 ± 9
WM 130	450 ± 10	WM 153	453 ± 9
WM 193	458 ± 9	WM 180	463 ± 9
WM 212	426 ± 9	WM 193	478 ± 10
WM 227	454 ± 9	WM 198	458 ± 10
WM 233	453 ± 9	WM 222	464 ± 9
		WM 223	444 ± 9
		WM 226	461 ± 9

It is clear that for both mica species, accepting only the samples from little altered rock, that the range in ages is reduced and the average becomes older. These average, acceptable mica K-Ar ages are thought to be geologically significant and reflect the time the micas cooled below their respective closure temperatures. The sample locations of the little altered rocks are shown on figure 5.1 together with the respective ages. This range in the mica K-Ar ages might be related to tectonic control on the cooling of the rock, this is discussed in section 5.1.4. The average muscovite K-Ar age, 457 Ma, is identical, within error, to the 459±7 Ma Rb-Sr age of the Oughterard Granite (Leake 1978a) while the average biotite K-Ar age, 448

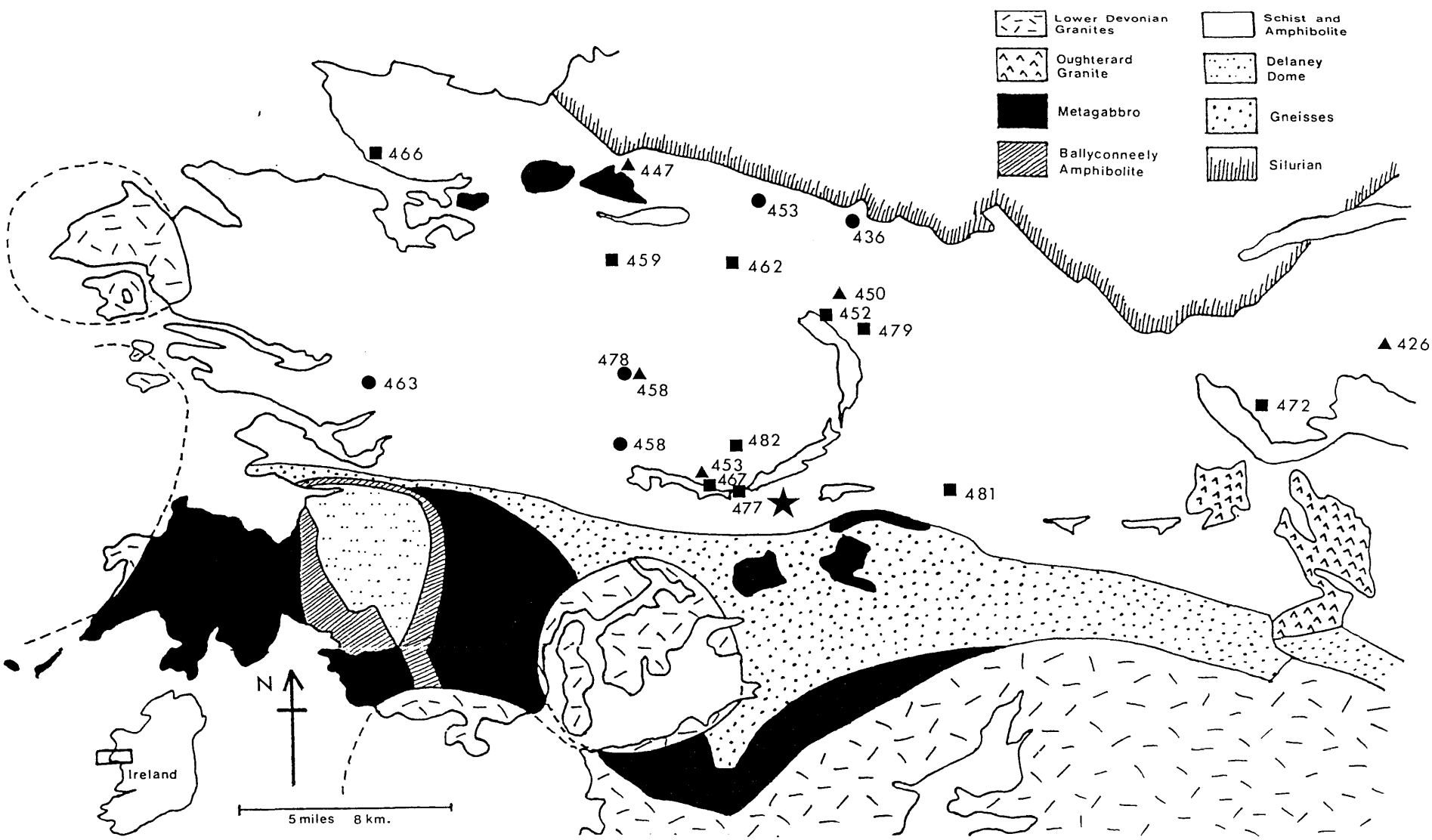

Figure 5.1. Sample locations and ages, in Ma, of those samples which are believed to have yielded undisturbed, geologically significant, cooling ages. The star marks the location of quarry from which the significant ages were, biotite 454 Ma; muscovite, 444, 461 and 464 Ma; hornblende, 481 Ma. Triangles indicate biotite samples, circles indicate muscovite samples and squares indicate hornblende samples.

Ma, is identical, within error, to the 447±4 Ma age of last movement on the Mannin Thrust (Tanner *et al.* 1989). The possible relationship between the mica K-Ar ages and these geological events is discussed in section 5.2.

5.1.2 The significance of the K-Ar ages of hornblende from the amphibolites.

Unlike the micas no relationship was found between the hornblende K-Ar ages and the degree of rock alteration (section 3.1.6). In general the feldspar in the amphibolites is more altered than the feldspar in the schists, section 2.3. This is possibly because the amphibolites are normally found in association with the Lakes Marble Formation and this marble has been shown to be an important aquifer horizon (Yardley 1989). This means that it is likely that most of the samples would have been in contact with the fluid for some time. As crystal microstructure, ie. the presence or absence of phyllosilicate inclusions or exsolution, is important in controlling the closure temperature and the susceptibility of the hornblende to interaction with the fluid the most accurate method to distinguish between samples that are likely to have been reset, from those that have not, is to examine all of them by TEM. To assume that just the hornblende samples that give the older K-Ar ages are little effected by the fluid is not sufficient because this does not take into consideration the highly variable closure temperatures that exist in the hornblendes. Some of the low K-Ar ages would have been caused simply by samples beginning to accumulate Ar later than others without any subsequent resetting, while other low ages are the result of partial resetting.

The lowest published hornblende closure temperature is c. 300°C, ie. equivalent to the closure temperature of biotite (Harrison & Fitz Gerald 1986). Assuming that the lowest closure temperature of any of the Connemara amphibolite hornblendes was not significantly different from this, then all the amphibolite hornblendes must have closed to Ar loss at about the time all the biotites had closed. To a first approximation then, all those amphibolite hornblendes with K-Ar ages older than the average of the acceptable biotite ages (448 Ma) might be considered to have geological significance as closure ages. This is not necessarily true, as they also might be partly reset, but without any further information it is not possible to tell which have, and which have not, been affected. Notwithstanding this uncertainty, all those hornblende K-Ar ages older than 448 Ma are assumed not to have been substantially affected by the c. 400 Ma event. There are eleven such ages which have a range of 30 Ma, from 452±9 to 482±10 Ma. The average of these ages is 469 Ma. The locations of all these samples are shown on figure 5.1 and the range in these hornblende ages is discussed in section 5.1.4 in terms of the likelihood of tectonic control over the cooling history of the rock.

5.1.3 The significance of the K-Ar ages of hornblende from the metagabbro-gneiss complex.

It was concluded in section 3.2 that the hornblende K-Ar ages from the metagabbro-gneiss complex were not significantly disturbed by the resetting event at c. 400 Ma. The two exceptions to this are WM 108 and WM 109 which were collected close to the contact with the Galway Granite. These two samples gave ages of 453±10 and 457±10 Ma respectively, and are believed to be the result of partial thermal resetting. None of the other metagabbro-gneiss hornblendes were affected in this way and consequently

they are believed to yield geologically significant closure ages. There are seven such ages with a range of 15 Ma, from 486 to 471 Ma. This range in the ages is discussed in the next section in terms of the likelihood of tectonic control over the cooling history of the metagabbro-gneiss complex. The average of these hornblende K-Ar ages is 477±10 Ma which, including the errors, is only slightly younger than the age of the metagabbro-gneiss intrusion, dated at 490±1 Ma (Jagger *et al.* 1988).

5.1.4 The possibility of tectonically controlled, variable cooling, in the Connemara rocks.

Elias *et al.* (1988) concluded that the variation in the K-Ar mineral ages they recorded was partly the result of differential uplift and cooling of three 'blocks' separated by the slide zones. In this study it has been shown that the majority of the K-Ar mineral ages are not in fact 'cooling ages' but are the result of partial resetting. Nevertheless, some of these samples are thought to have geologically significant closure ages and these ages, discussed in the previous sections, show some variation for each mineral species.

The range in these mica ages could be the result of diachronous cooling, indicating possible tectonic control on the ages. Alternatively the range of ages could be the result of some slight resetting of the mica K-Ar systems even though little alteration of the rocks has occurred. On the basis of the K-Ar ages alone this possibility cannot be ruled out. Similarly the range of the hornblende K-Ar ages from the metagabbro-gneiss complex samples could be the result of some variation in the time and rate of cooling of these rocks. However, as all these ages, excluding WM 108 and

WM 109 (see previous section), are identical, within error, so any differential in the cooling must have been minimal.

The locations of all the supposedly geologically significant ages are shown on figure 5.1 together with their respective ages. There is a some suggestion that the mica K-Ar mineral ages are slightly younger in the north, with the two lowest mica ages of 426 and 436 Ma close to the Silurian rocks. There is not, however, a proven correlation between mica K-Ar age and location. Elias *et al.* (1988) recorded some young mica and hornblende K-Ar ages from close to the contact with the Silurian rocks. The authors suggested that these ages were connected with an end-Silurian folding event. Such a mechanism however, cannot be responsible for the ages on figure 5.1 because all these ages are believed to be closure ages through cooling, not reset ages. The hornblende samples should not be considered when looking for a correlation between K-Ar ages and location because it has been concluded that a primary control over these ages is their variable closure temperatures. Therefore, although it may be true that the rocks were differentially uplifted and cooled, the variable closure temperatures of the hornblendes would disguise this fact.

In conclusion there is insufficient evidence to prove or disprove any tectonic control over the cooling ages, either by tilting of the whole of Connemara or by splitting of Connemara into separate, uplifting blocks. If differential uplift did occur then the evidence has been obscured by the later disturbance of the K-Ar mineral ages.

5.2 Implications for the geological evolution of Connemara from the K-Ar mineral ages.

In this section the K-Ar mineral ages are discussed in the context of the geological evolution of Connemara. For the purposes of this discussion the intrusion of the metagabbro-gneiss complex is the starting point because this intrusion effectively reset all the K-Ar mineral 'clocks', section 3.1.2. All the K-Ar mineral ages are shown as histograms on figure 5.2, together with the dates of all the major geological events that have occurred in Connemara.

The metagabbro-gneiss complex was intruded into the Connemara Dalradian rocks during the D3 event (Tanner pers. comm., Leake 1989) at 490±1 Ma (Jagger *et al.* 1988). That the initial cooling of the metagabbro-gneiss rocks was rapid is indicated by the coincidence of the Pb-Pb zircon age and the oldest metagabbro-gneiss hornblende K-Ar age (486±10 Ma). The temperature must, therefore, have fallen from c. 1000°C (the likely crystallisation temperature of the zircon) to below about 550°C (the likely closure temperature of the metagabbro hornblendes) in no more than 15 Ma, giving an initial cooling rate of c. 30°C/Ma. The oldest hornblendes from the amphibolites yield ages of c. 480 Ma, equal to, within error, the average age of the hornblendes from the metagabbro-gneiss complex, 477 Ma, and so some of the Dalradian rocks must initially also have cooled rapidly following heating by the intrusion of the metagabbro-gneiss complex. This initial cooling of the Connemara rocks was so rapid because the region was undergoing fast uplift, presumably with very active erosion. Yardley (1987) has shown that the Dalradian rocks were initially at kyanite-staurolite grade, at pressures of about 6 kbar. The uplift accompanied by the intrusion of the metagabbro-gneiss rocks is recorded by the cordierite and andalusite in the leucosomes. The leucosome melts formed at pressures of

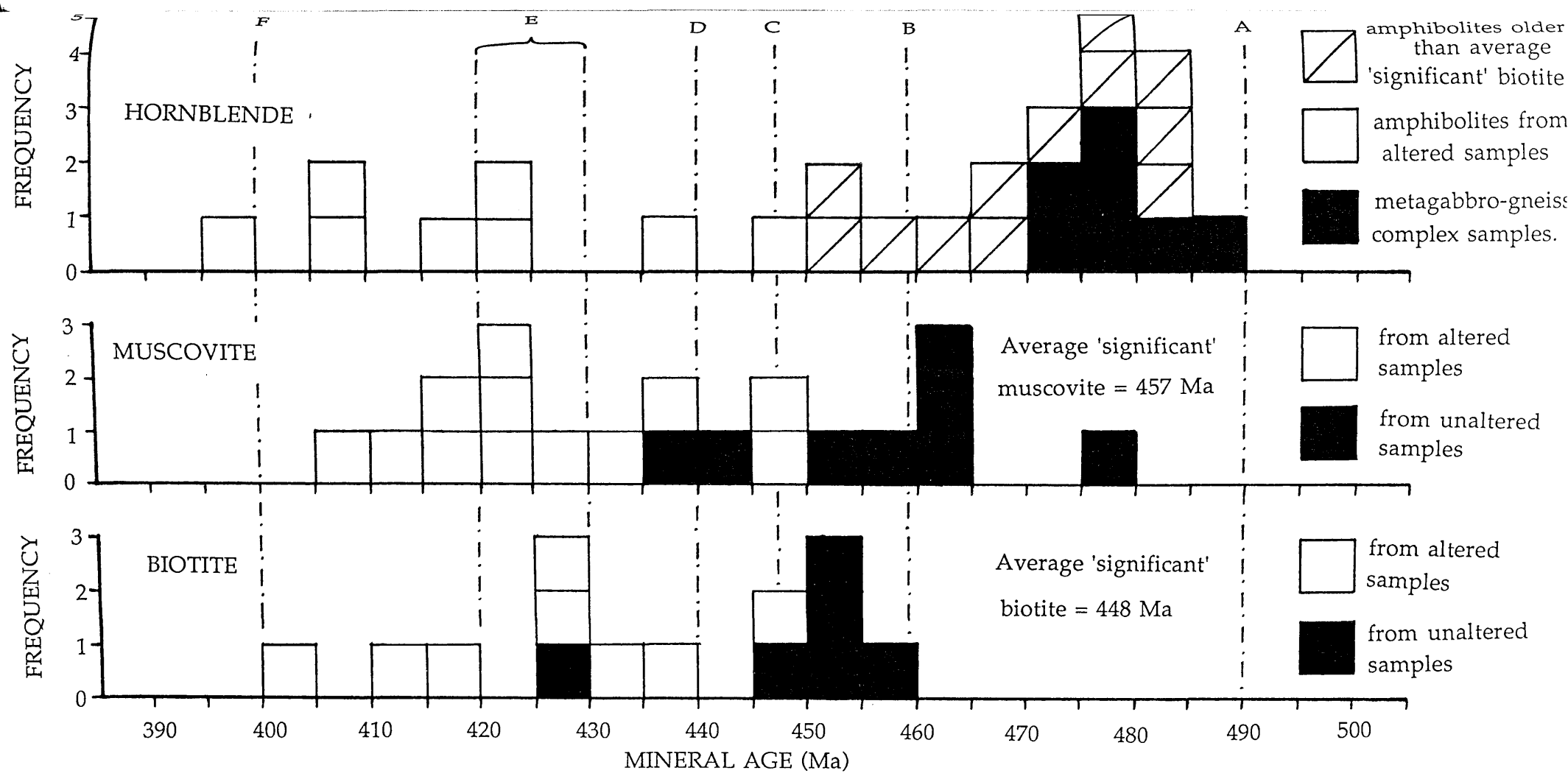

Figure 5.2. Histograms showing the range of all the K-Ar ages for hornblende, muscovite and biotite, except the two hornblende samples which gave ages of c. 350 Ma. Those ages that are believed to be cooling ages, ie. are 'significant' are indicated. The geological events marked are, A = intrusion of the metagabbro-gneiss complex. B = intrusion of the Oughterard Granite. C = last movement on the Mannin Thrust. D = docking of Connemara with the South Mayo Trough. E = submergence and burial in the Silurian. F = intrusion of the Lower Devonian Granites.

about 5.5 kbar (Treloar 1985) but they did not crystallise until pressures had dropped to 3.5 kbar. This cooling and uplift was followed rapidly by the D4 event which created the Connemara Antiform. Morris & Tanner (1977) have shown from palaeomagnetic investigations of the Cashel Hill (part of the metagabbro-gneiss complex) that it was folded into its present position on the southern limb of the antiform before it had cooled below its Curie temperature, which is 550 to 600°C. During the uplift, cooling and D4 event, all the hornblendes from the metagabbro-gneiss complex and some of the hornblendes from the amphibolites cooled below their closure temperatures. No micas (except one muscovite) record K-Ar ages of this age and so it is certain, that at this time, most of the present erosional surface must have been at a temperature below 550°C but above 350°C. Possibly there was some differential uplift of the Dalradian rocks at this time, see the previous section, and that this might explain the one older muscovite age of 478 Ma. Not all the hornblendes from the amphibolites would have closed in this initial uplift and cooling event because of the large dispersion in their closure temperatures, brought about by phyllosilicate inclusions and exsolution in their crystal lattices.

Following the initial uplift and cooling phase there was a c. 20 Ma period of either much slower uplift or a complete hiatus in cooling. Following this time there was a period of renewed, but slower, cooling presumably accompanying uplift. The oldest acceptable muscovite ages are 460 to 465 Ma, table 5.1, slightly younger than this are the oldest acceptable biotite ages of 450 to 460 Ma, table 5.1. This indicates that the present erosional surface passed through 350°C (the Ar closure temperature of muscovite) and then 300°C (the Ar closure temperature of biotite) in about 10 Ma, giving a cooling rate of c. 5°C/Ma. In section 5.1.2 it was explained that by the time all the biotites had closed to Ar diffusion, the amphibolite

hornblendes must have done so also, despite their variable closure temperatures. This second phase of cooling most likely relates to uplift during the ramping of Connemara over the putative Ordovician volcanic Delaney Dome Formation along the Mannin Thrust. The initiation of the ramping of Connemara over the Delaney Dome Formation may well be indicated by the coincidence of the average, acceptable muscovite age of 457 Ma with the age of the Oughterard Granite which is 459±7 Ma (Leake 1978a), figure 5.2. The emplacement of this granite may in part be responsible for the renewed uplift at this time and therefore for the muscovite ages. Last movement along the Mannin Thrust was at 447±4 Ma (Tanner *et al.* 1989) which corresponds to the youngest of the acceptable biotite K-Ar ages. It is therefore concluded that by the time Connemara had been completely ramped over the Delaney Dome Formation all the hornblende, muscovite and biotite minerals were closed to Ar loss. The simple corollary to this, is that all the K-Ar mineral ages younger than 447 Ma must be partially, or totally reset.

Following the ramping along the Mannin Thrust, Connemara docked with the South Mayo Trough. This event occurred at the end of the Ordovician (Taconic) at about 440 Ma (Bluck & Leake 1986). Elias *et al.* (1988) claim that the c. 440 Ma K-Ar mineral ages from Connemara are due to this event. This is not consistent with the conclusion, given above, that all the mineral species would have closed to Ar diffusion by 447 Ma. It is possible that the docking of Connemara with the South Mayo Trough was synchronous with the final stages of ramping over the Delaney Dome Formation in which case the estimate of the time of docking by Bluck & Leake (1986) is about 7 Ma too young.

Subsequent to both the docking with the South Mayo Trough and ramping along the Mannin Thrust cooling ceased and there was a period

of subaerial erosion from the end-Ordovician to the earliest Silurian (Elias *et al.* 1988). By the Upper Llandovery, ie 433 Ma, both the rocks of Connemara and of the South Mayo Trough subsided and the Silurian subaerial basal breccia was succeeded by purple sandstones, marine sandstones, continental edge style turbidites, red shales and then sandstones. This whole succession is over 2 km thick and was laid down by the end of the Wenlockian, ie before 422 Ma. It is suggestive that there is an increase in the frequency of mica K-Ar ages of 420 to 430 Ma, figure 5.2. This feature was also recorded in the data of Elias *et al.* (1988, figure 3). In an ordinary continental shelf or continental edge basin the geothermal gradient would not be sufficiently high for the temperatures to reach the Ar closure temperature of micas (300 to 350°C) at only 2 or 3 km depth. Nonetheless, the Silurian basin may have been a site of higher than normal geothermal gradients because of magmatic activity which is evident in the volcanic rocks extruded at the base of the Silurian succession throughout eastern Connemara. It is suggested that possibly temperatures in the Connemara Dalradian rocks rose to upwards of 300°C at this time so that when the fluid infiltration took place at c. 400 Ma the possibility of fluid interaction with the rock was enhanced. Temperatures could not have been above 300°C because this would have caused resetting of the biotites on a regional scale and this did not occur.

5.2.1 The origin of the c. 400 Ma fluid.

It is believed that the fluid that was responsible for the interaction with the minerals, and consequent reduction in the K-Ar ages, came from the Silurian sediments. Large volumes of water would have been held in the Silurian sediments, this could have been drawn down into the Connemara rocks by the inception of a convection system, driven initially

by the burial heat. Soon after the Silurian burial event ended, the emplacement of the Lower Devonian Granites into the Connemara Dalradian rocks and the metagabbro-gneiss rocks occurred, the heat from these granites would have greatly enhanced the circulation of the fluid.

The reason why the fluid is thought to have come from the Silurian rocks is simply because the fluid must have had an origin external to either the Dalradian rocks or the metagabbro-gneiss complex. Jenkin (1988) used stable isotopic constraints and mass balance calculations to show that the water could not have been derived from the metagabbro-gneiss complex magma or from pore-water within the metasediments. For similar reasons the fluid is very unlikely to originate from the Lower Devonian Granite magmas themselves. Intuitively it seems from the widespread chloritisation in the Connemara schists that large volumes of water flowed through these rocks, it is unlikely that this amount of water could be generated from the granite magmas alone, although some deuteric water would be produce in this manner. The permeability of rocks is the greatest control on the size of a fluid circulation system that can operate within them. Most of Connemara is composed of schists, which have fairly high permeability, and so it is not unreasonable to conclude that a convective hydrothermal system could have extended over the whole of Connemara. Norton & Knight (1977) showed that smaller plutons, of 2 to 3 km diameter, had convective cells up to 6 km wide, ie. 2 to 3 times wider than the pluton. The actual size of the Galway Granite is not known because it extends into Galway Bay, however that part exposed on land is some 40 km long. Using this figure as the size of the granite, which is a conservative estimate, and assuming a 1 : 1 relationship for the pluton : convection cell dimension ratio it is clear that the convective hydrothermal system could easily cover the entire region. The lifetime of such a hydrothermal system must be equal to the time the pluton takes to

crystallise and cool. For a pluton the size of the Galway Granite this may take up to 10 Ma. Nonetheless, from the lack of ages younger than 400 Ma it is suggested that the hydrothermal circulation system in the Connemara rocks around the Lower Devonian Granites lasted for only a few Ma at most.

Mitchell & Mohr (1987) obtained K-Ar ages of biotite-chlorite and feldspar-quartz fractions from ten samples of the Galway Granite. All but one of these fractions, a biotite sample, gave ages substantially younger than the 400 Ma Rb-Sr intrusion age (Leggo *et al.* 1966). The lowest age the authors measured was 253±4 Ma, which came from a biotite-chlorite fraction. This suggests that the chloritisation of the Galway Granite biotite occurred up to 150 Ma after intrusion. On account that no Dalradian rocks yielded K-Ar mineral ages this young, it is suggested that the chloritisation of the Galway Granite must have been a very localised event. The Galway Granite is rich in the radiometric elements K, U and Th (Feely & Madden 1986, 1987 and 1988) and consequently the indigenous heat production and accumulation under thick Carboniferous sediment cover could have kept the biotite in the granite warm enough to prevent closure to Ar diffusion for a long time after crystallisation. It is, however, thought unlikely that this heat production in the granite would be sufficient to power hydrothermal convection cells throughout the whole of the Connemara region after crystallisation of the granite took place. Alternatively the chloritisation of the Galway Granite may in some way be related to the Carboniferous magmatic activity detailed by Mitchell & Mohr (1987).

5.2.2 Post 400 Ma geological events and implications for the K-Ar mineral ages.

It is well established that Connemara suffered several post-400 Ma thermal events. Two of these events are responsible for large dyke swarms and other minor intrusions, these events occurred during the Carboniferous (Mitchell & Mohr 1987) and the Tertiary (Macintyre *et al.* 1975, Mitchell & Mohr 1986). In addition much of western Ireland underwent a Varsican thermal and deformational event. This has been recorded in County Clare and County Limerick and described as post-Westphalian to pre-Upper Permian (Coller 1984). In the Irish Midlands, Lower Carboniferous rocks have undergone greenschist facies metamorphism as a result of Varsican thermal overprinting (Phillips & Sevastopoulo 1986). Mitchell and Mohr (1987) also recognised Varsican thermal overprinting events at c. 300, 245 and 205 Ma in the Carboniferous Logmor Dyke and the Teach Doite dyke swarm in West Connaught from K-Ar whole rock dating. This Varsican event may have had a larger regional effect as witnessed by mineralisation events dated at 285, 250 and 215 Ma in the Caledonian Isle of Man granites (Ineson & Mitchell 1979).

Despite this activity, none of these events are believed to have had any significant influence on the K-Ar mineral ages from the Connemara Dalradian rocks. Any sustained, regional heating episode (greater than 300^{o}C, the Ar closure temperature of biotite) would have resulted in a number of ages below 400 Ma, and these are not found. Only two amphibolite hornblende samples yield K-Ar ages significantly younger than 400 Ma. These samples, WM 183 (334±7 Ma) and WM 201 (349±8 Ma) may have been close to, and heated by, one of the Carboniferous dykes, although none were seen cropping out where the samples were collected. Mitchell & Mohr (1987) dated the Teach Doite dyke swarm at 305 Ma, which

is the whole-rock K-Ar age of their oldest dyke sample. Considering the complete lack of any samples yielding ages between 400 and c. 350 Ma, and the large number of widespread samples dated, it seems unlikely that the heating affect from the dykes can have been anything other than localised, within a few metres of the dykes, otherwise more 300 to 350 ma ages would surely have been recorded in the Connemara Schists and amphibolites.

5.3 Implications for other geochronological studies.

The principal conclusion of this study, namely that some of the K-Ar mineral ages have been significantly reduced by fluid interaction by different mechanisms and to different degrees is, as far as is known, the first time such an explanation has been proposed to interpret K-Ar ages from such a large region. It is important to know if the processes that have occurred in Connemara are unique to Connemara, or if they are typical of, as yet unrecognised, processes that have occurred in many polymetamorphic regions. If the latter case is true, then the implications for other research projects in other areas could be far reaching. Discordant hornblende ages from single exposures are known to occur at locations in the granulite rocks of the Pan-African and Brazilian cratons (T. C. Onstott *pers. comm.*) and these may possibly have resulted from similar processes that operated in Connemara. Another interesting point about these granulites is that one current view about their formation states that the dehydration of the rock was initiated by fluxing of CO_2 rich fluids (see Wickham 1988 for review). Does this imply that any fluid, not just water, could disturb the K-Ar systems in minerals? At present most geochronologists only consider opening and closure of minerals to Ar diffusion in the dry state, and yet in metamorphic terranes most of the geological (metamorphic) events those researchers are trying to date,

proceed with substantial volumes of water flowing through the rocks. It is well recognised that both oxygen and hydrogen isotopes exchange under these conditions and, with oxygen isotopic exchange between hornblende and water, this involves breaking and re-establishing the tetrahedral bonds in the crystal lattice. This study has indicated that, when conditions are suitable for the exchange of stable isotopes, the Ar can be lost out of the mineral grains. This applies particularly to hornblendes with complex crystal microstructures, such as exsolution or phyllosilicate inclusions, which have already been recognised to lower the Ar closure temperature (Harrison & Fitz Gerald 1986, Onstott & Peacock 1987). Certainly the whole concept of Ar loss from minerals during interaction with fluids requires more research and suggestions for particular studies are made in the next section. The geochronologist without access to stable isotope facilities can still perform some experiments, outlined below, that should indicate if his or her samples are likely to have had their K-Ar ages influenced by fluid interaction.

A) The simplest test is to analyse several samples collected from one small locality and check for any dispersion in the resulting ages. If there is any possibility that the ages are varying it is recommended that at every sample locality two or three specimens are taken, a few metres apart, and all are dated to check for age dispersion.

B) It is recognised that dating duplicate and triplicate samples from each exposure greatly increases the laboratory work-load. A quicker, though not a conclusive test, would be to determine the structural water content of all the mineral samples. On the basis of this study, section 4.2.4, any samples, hornblende in particular, with water contents much in excess of that required by the structural formulae can be considered suspect, and other samples from the relevant locality dated.

C) In addition for all hornblende samples the FeO and Fe_2O_3 contents of the minerals should be determined by wet chemical means. There is a suggestion from this work, section 4.3.3, that the 'A' site occupancy affects the closure temperature of hornblendes. The 'A' site occupancy can only be accurately calculated when the FeO/Fe_2O_3 ratio is known. On the basis of this study, those samples with a high proportion of Fe_2O_3 should be considered suspect and other samples from the relevant locality dated.

5.4 Further lines of inquiry.

Several lines of inquiry followed in this study were never fully completed and several new questions have arisen that deserve to be addressed. In the following paragraphs some possible lines for extension and expansion of this study are briefly outlined.

A) The extent and nature of the submicroscopic crystal heterogeneity of the amphibolite hornblendes needs to be fully examined. If at all possible the composition of any phyllosilicate inclusions or exsolved phases needs to be determined and the volume of such features quantified. It would be hoped that the some relationship would exist between the K-Ar age and a quantitative measure of the complexity of the crystal structure. With phyllosilicate inclusions it would be necessary to show if they formed by simple precipitation out of a fluid, or if they formed by actual chemical reaction between the fluid and the hornblende, for in the latter case there is much greater scope for disruption of the K-Ar age. In the case of exsolution it would be necessary to determine if the boundary between the two phases is incoherent or not. If the boundaries were to be incoherent this should significantly lower the effective diffusion

dimension ('a' in the closure temperature equation of Dodson 1973, equation 1.1) of the mineral and therefore reduce its closure temperature. Varying sizes of exsolution lamellae could therefore account for a large dispersion in closure temperatures within one mineral species. In the case of both phyllosilicate inclusions and exsolution lamellae their time of formation should be ascertained. If these features existed prior to the mineral cooling then low closure temperatures would result. If they formed after cooling then Ar loss out of the already closed mineral might occur. The resulting K-Ar ages would not necessarily be the same in both instances. The only way these lattice defects can be imaged is with a TEM, preferably an instrument with a high accelerating voltage (150 to 200 kV) which would allow thicker specimens to appear transparent.

B) Related to the first line of inquiry it could prove interesting to examine some amphibolite hornblende samples on a high resolution TEM (HRTEM). Such an instrument could be used to examine the chain structure of the amphibole. It might be that some of the Connemara amphibolite hornblendes possess a biopyribole structure with more mica chains than normal (cf. Veblen 1981). This could partly explain the high water contents, noting that Veblen & Buseck (1979) measured up to 2 wt.%. structural water (H_2O^+) in jimthompsonite. Although this is purely intuitive, it is likely that biopyribole minerals, because of the higher mica chain content, could have lower closure temperatures than typical amphiboles.

C) More detailed, high resolution laser-probe ^{40}Ar-^{39}Ar profiling of individual hornblende grains might reveal age zoning or patchy Ar retention that could indicate exsolution (cf. Kelley & Turner 1988) and phyllosilicate inclusions and help quantify the effects on the K-Ar ages. It is suggested that for this type of work the largest grains available should be

separated from the rock and analysed individually. This would remove the possibility of incorporating other, non-hornblende, phases in the analyses, such as happened in the course of this study, section 3.4.

D) Prior to the large hornblende grains being irradiated for laser-probe ^{40}Ar-^{39}Ar dating it would be worthwhile if a few of them were examined using an analytical SEM. An attempt was made briefly in this study to do this and it was found, during elemental mapping of some of the grains, that an increase in K concentrations along cleavages was indicated that was consistent with biotite inclusions. The instrument used was a Cambridge Instruments Stereoscan 360 fitted with a Link Analytical Systems energy dispersive X-Ray (EDX) analyser. The SEM investigations were taken no further in this study because, at the time of use, the EDX system had not been calibrated. Further investigation of some of the grains using this type of instrument should show clearly the extent and the nature of any larger (2 to 3 microns) inclusions and exsolution lamellae. It is possible that the resolution could be improved with careful instrument configuration.

F) In conjunction with SEM investigation and laser-probe ^{40}Ar-^{39}Ar dating of some hornblende grains, an ion-probe study could be performed on these grains also. Ion-probe development is reaching the stage where it will be possible to use the instrument to profile across a grain for oxygen, and possibly hydrogen, stable isotopes. It has been concluded in this study, chapter four, that the hornblende grains had partially re-equilibrated hydrogen with the later, low temperature fluid. It is possible that this partial re-equilibration would be manifest as an equilibration front in the grains, giving a zoned nature. If this could be revealed using the ion-probe it would be very interesting to then date the same grain by high resolution, ^{40}Ar-^{39}Ar laser-probe methods. If a pattern of age zoning were

to be found that matched a pattern of stable isotope re-equilibration then this would be very strong evidence to suggests that the loss of Ar is coupled to the stable isotopic exchange process.

G) The most important point that needs to be addressed is whether or not the processes operating in the Connemara rocks are unique to that area or not. It is suggested that similar, comparative studies are conducted in other poly-metamorphic regions and also in other rock types where hydrothermal fluids are known to have flown. Suggested areas are the Alps, the Appalachians (especially in Vermont and New Hampshire where biopyriboles have been discovered, Veblen & Burnham 1978a,b). Also more investigations at locations in the granulite rocks of Africa and Brazil where discordant hornblende ^{40}Ar-^{39}Ar ages have been reported (T. C. Onstott, *pers. comm.*).

H) A final point regarding Connemara. It would be extremely useful to perform seismic and gravity studies over the region in order to establish the extent of any sub-surface granites, of the metagabbro-gneiss complex and also the extent and nature of the Mannin Thrust. Priority should be given to a seismic reflection survey across strike, ie. in a north-south orientation.

APPENDICES

APPENDIX A.1. SAMPLE LOCATIONS.

In the following accounts the six figure grid references are taken from the one inch colour geological map compiled by Leake *et al.* (1981). The locations are marked on the diagrammatic map in figure 2.1.

WM107 Semi-pelitic schist from Kylemore Fm. In the thermal aureole of Doughruagh [755597].

WM 108. Metagabbro from very close (c.100m) to contact with Galway Granite, 5km east of Gowla. From bank of small stream [852386].

WM 109. Metagabbro from stream bank, close to contact with Galway Granite, 1/4km north of WM 108 [852390].

WM 111. Metagabbro from stream bank, close to contact with Galway Granite, 1km north of WM 108 [855401].

WM 119. Large (few cm's) mica books removed from a leucosome in Streamstown Fm. in the migmatite zone. From eastern of two large road cuts by Cashel Cross [822467].

WM124 Orthogneiss from edge of small lough, 2 miles NW of Toombeola [730458].

WM127 Pelitic schist from the Lakes Marble Fm. 1km north of Lehanagh Loughs [871523].

WM128 Amphibolite in Lakes Marble Fm. North end of Lough Inagh [832543].

WM 130. Pelitic schist from Ballynakill Fm. North of Lough Inagh [834551].

WM132 Semi-pelitic schist from the Kylemore Fm. 1km south of Lettershanbally close to Silurian unconformity [835583].

WM134 Bennabeola Quartzite Fm. From the stream running south from Letterbreckaun [852543].

WM135 Meta-gabbro from Dawros, from road cut on road running between Letterfrack and Dawros Bridge [699591].

WM136 Meta-gabbro from Currywongaun, from the western edge just up hill side from road [722597].

WM137 Meta-gabbro from Currywongaun, 1/4km to south east of RC 2092 [723594].

WM138 Meta-gabbro from Doughruagh, from western end of intrusion [745595].

WM 139. Amphibolite from Barnanoruan Fm. Near road leading to Maumeen [894487].

WM146 Amphibolite from Streamstown Fm. Cutting on Ballinafad road 1/2km south of Canal Bridge [802473].

WM148 Pelitic schist from Barnanoruan Fm. From southern ridge from Derryclare running into Glencoaghan [810501].

WM151 Semi-pelitic schist from Streamstown Fm. From riverside running from Bencorr into west side of Lough Inagh [833520].

WM153 Pelitic schist from the Kylemore Fm. Close to Silurian unconformity. 1km south-east of Lough Fee [805595].

WM154 Bennabeola Quartzite Fm. North end of Glencoaghan by stream running down from Bencorr [804517].

WM155 Amphibolite in Streamstown Fm. South end of Glencoaghan, just off the road, 2km north-west of Canal Bridge [793485].

WM157 Bennabeola Quartzite Fm. 2km south-east of Kylemore Lough [792657].

WM158 Siliceous granulite from Streamstown Fm. By small lough at Maumeen [906504].

WM160 Bennabeola Quartzite Fm. Near summit of Benglenisky [767501].

WM165 Amphibolite from Lakes Marble Fm. 1km south-west of summit of Letterbreckaun [846545].

WM167 Amphibolite in Lakes Marble Fm. On footpath 1km south-west of Letterbreckaun [849540].

WM168 Siliceous granulite from Kylemore Fm. From stream, west end of Kylemore Lough [759584].

WM179 Semi-pelitic schist from Streamstown Fm. From road cut 1/2 km south of Streamstown [648527].

WM180 Bennabeola Quartzite Fm. From stream cutting road 1km south of Streamstown [656520].

WM183 Amphibolite from Streamstown Fm. From south edge of lough 2km south of Streamstown [657515].

WM184 Siliceous granulite from Clifden Fm. From a field 1km north of Clifden [657512].

WM188 Pelitic schist from Cashel Fm. North edge of Salt Lake [665498].

WM193 Pelitic schist from Barnanoruan Fm. 1/2km north of Barnanoruan [747513].

WM195 Bennabeola Quartzite Fm. From roadside 1km south of Barnanoruan [751500].

WM196 Cleggan Boulder Bed Fm. Small exposure by bend in road 2km south of Barnanoruan [747494].

WM198 Pelitic schist from the Streamstown Fm. Near Barnanoruan-Clifden-Galway road junction [749491].

WM 200. Metagabbro. From near to summit of Errisbeg [705405].

WM201 Massive amphibolite from Lakes Marble Fm. West end of Ballynahinch Lake [761482].

WM212 Graphitic schist from the Cornamona Fm. 1/2km along the road to Ballydoo Lough from Cornamona [037528].

WM220 Striped amphibolite from Streamstown Fm. in migmatite zone. From eastern of two large road cuts by Cashel Cross [822467].

WM221 Semi-pelitic schist from the Streamstown Fm. in migmatite zone. From eastern of two large road cuts by Cashel Cross [822467].

WM222 Pelitic schist from Streamstown Fm. in migmatite zone. From eastern of two large road cuts by Cashel Cross [822467].

WM223 Pelitic schist from Streamstown Fm. in migmatite zone. From eastern of two large road cuts by Cashel Cross [822467].

WM224 Poorly striped amphibolite from Streamstown Fm. in migmatite zone. From eastern of two large road cuts by Cashel Cross [822467].

WM225 Striped amphibolite from Streamstown Fm. in migmatite zone. From eastern of two large road cuts by Cashel Cross [822467].

WM226 Semi-pelitic schist from Streamstown Fm. in migmatite zone. From eastern of two large road cuts by Cashel Cross [822467].

WM227 Pelitic schist from Streamstown Fm. in migmatite zone. North side of lough at Cashel Cross [822466].

WM228 Banded amphibolite from Streamstown Fm. in migmatite zone. From western of two large road cuts at Cashel Cross [820466].

WM231 Semi-pelitic schist from Streamstown Fm. in migmatite zone from large road cut on the north side of Ballynahinch Lake [782478].

WM232 Massive amphibolite from Streamstown Fm. in migmatite zone from large road cut on the north side of Ballynahinch Lake [782478].

WM233 Pelitic schist from Streamstown Fm. in migmatite zone from large road cut on the north side of Ballynahinch Lake [782478].

WM234 Extensively sheared amphibolite from small track south side of Tully Mountain [661608].

WM235 Amphibolite from large new road cutting on the north side of Derrylea Lough [710498].

WM237 Amphibolite from main road on southwest corner of Lough Shindilla [952456].

WM238 Striped amphibolite from road cutting by two small loughs between Loughs Oorid and Glendollagh [885467].

WM242 Amphibolite from roadside field just uphill from Claggan quarry [018509].

WM244 Striped amphibolite from Lakes Marble Fm. East, 1km, from Streamstown along road on north side of Streamstown Bay [641532].

WM248 Striped amphibolite in Lakes Marble Fm. From small road cutting at the north end of the Inagh Valley [803569].

WM249 Striped amphibolite in Lakes Marble Fm. South shore, west end of Kylemore Lough, near house [764576].

APPENDIX A.2. PETROGRAPHIC DESCRIPTIONS OF SAMPLES.

The following accounts are not intended to be detailed petrographic descriptions of the samples but an extended modal list. The mineral that has been separated from each sample for analysis is mentioned first and its nature described.

WM 107. Semi-pelitic schist from Kylemore Fm. 25% red-brown biotite, up to 0.5mm long, partly chloritised with epidote growth along the cleavages. <10% muscovite. 40% quartz. 25% partly sericitised plagioclase and K-feldspar and occasional garnet (0.2mm).

WM 108. Metagabbro. 50% hornblende. Subhedral grains up to 5mm long. Part alteration to chlorite and epidote. 40% partly sericitised plagioclase (labradorite). 10% quartz. Accessory chlorite, epidote and opaque minerals.

WM 109 Metagabbro. 60% hornblende. Anhedral grains up to 1cm. Some grains strongly corroded and altered to chlorite and epidote and frequent small inclusions of ?quartz. 45% strongly sericitised plagioclase (labradorite). 5% quartz and accessory zircon and opaque minerals.

WM 111 Metagabbro. 50% hornblende. Large grains up to 3cm long. Part alteration to chlorite and epidote. Many inclusions of quartz. 45% slightly sericitised plagioclase (labradorite). 5% quartz and accessory opaque minerals.

WM 119. Large, several cm's, mica books from a large leucosome in the migmatite zone. There is no thin section for this sample. The sample was obtained by 'digging' the mica books out with a pen knife, 2 to 3g of muscovite and biotite obtained this way.

WM 124. Orthogneiss. 30% green pleochroic, subhedral hornblende up to 5mm. The hornblende is partially altered and contains frequent inclusions of quartz and feldspar. 40% heavily sericitised and saussuritised and strained plagioclase. 20% strained and recrystallised quartz. 10% chloritised biotite. Accessory epidote and opaques.

WM 127. Pelitic schist from the Lakes Marble Fm. 30% red-brown biotite, up to 1mm long, partly chloritised with epidote growth in cleavages. 10% muscovite in association with biotite. 20% quartz. 40% slightly sericitised plagioclase and K-feldspar with many inclusions. Accessory zircon and opaques.

WM 128. Amphibolite in Lakes Marble Fm. 40% green, strongly pleochroic, euhedral hornblendes displaying some zoning and occasional twinning. Grains less than 1mm. 10% pale green cummingtonite. 10% heavily chloritised biotite. 20% quartz. 20% sericitised K-feldspar and opaques.

WM130 Pelitic schist from the Ballynakill Fm. 25% red, strongly pleochroic, biotite up to 3mm long. Partly chloritised, slight epidote growth. 10% biotite growing with biotite in 'fish'. 25% quartz, slightly recrystallised. 40% slightly sericitised plagioclase. Accessory garnet, zircon and opaques.

WM 132. Semi-pelitic schist from the Kylemore Fm. 30% pale green, slightly pleochroic, muscovite forming kinked and folded fish up to 5cm. 10% green partly chloritised biotite. 40% quartz. 20% slightly sericitised K-feldspar. Accessory garnet and opaques.

WM 134. Bennabeola Quartzite Fm. Less than 10% pale green, slightly pleochroic muscovite, grains up to 1mm. 85% quartz. 5% sericitised feldspar, zircon, apatite and opaques.

WM 135. Meta-gabbro from Dawros. 40% pale-green, slightly pleochroic, anhedral amphibole. Large 3-4mm grains extensively recrystallised. 60% extensively sericitised and saussuritised plagioclase. Occasional corroded olivine plus accessory sphene, heamatite and opaques.

WM 136. Meta-gabbro from Currywongaun. 10% green-brown, slightly pleochroic, anhedral amphibole. Large 2-3mm grains partly recrystallised. Extensive alteration to epidote and chlorite. 40% sericitised and saussuritised plagioclase. 50% large, strained, partly recrystallised quartz. Accessory zircon and opaques.

WM 137. Meta-gabbro from Currywongaun. 70% pale-green, slightly pleochroic, anhedral amphibole. Large 3-4mm grains extensively recrystallised. 25% sericitised and saussuritised plagioclase, partly recrystallised. Accessory quartz, epidote and opaques.

WM 138. Meta-gabbro from Doughruagh. 20% pale-green, pleochroic, anhedral amphibole. Larger grains extensively recrystallised. 70% sericitised and saussuritised, recrystallised plagioclase. 10% strained quartz.

WM 139. Amphibolite from the Barnanoruan Fm. 40% light green, subhedral, amphibole. Grains up to 2mm long, some twinning. No apparent alteration. 40% partly sericitised plagioclase. 20% quartz. Accessory chloritised biotite and opaque minerals.

WM 146. Amphibolite from Streamstown Fm. 25% green, pleochroic, subhedral hornblende, up to 1mm long. Commonly twinned with frequent inclusions of epidote and quartz. Occasional wide cleavages in the amphibole with a dark alteration product. 40% recrystallised quartz. 35% completely sericitised feldspar. Accessory epidote, apatite, sphene and opaques.

WM 148. Pelitic schist from Barnanoruan Fm. 40% red-brown biotite, up to 1mm long. Frequent pleochroic haloes. Some cleavages seen as wider colourless partings. No chlorite but some epidote growth in the cleavages. 10% muscovite and sillimanite. 30% quartz. 20% partly sericitised and saussuritised plagioclase and K-feldspar. Accessory tourmaline, apatite, epidote and opaques.

WM 151. Semi-pelitic schist from Streamstown Fm. 20% muscovite as 2-3cm fish. 10% completely chloritised biotite grown with muscovite. 40% recrystallised quartz. 30% partly sericitised and saussuritised plagioclase and K-feldspar. Plus calcite and opaques.

WM 154. Bennabeola Quartzite Fm. 10% fine grained, pale green, slightly pleochroic muscovite, less than 1/2mm. 80% quartz. 10% partly sericitised plagioclase and K-feldspar. Accessory haematite, rutile and opaques.

WM 153. Pelitic schist from the Kylemore Fm. 20% pale green, slightly pleochroic muscovite in kinked and folded fish up to 5cm. 10% Fine grained completely chloritised biotite grown around the muscovite fish. 40% partly sericitised plagioclase and K-feldspar. 30% quartz and opaques.

WM 155. Amphibolite in Streamstown Fm. 10% green, pleochroic, subhedral hornblende. Grains up to 2mm. Some wrenching apart of the grains with fractures filled by chlorite. Some grains partly corroded with embayments and inclusions (epidote and quartz) and dark alteration product (?biotite) in cleavages. 60% recrystallised quartz. 30% completely sericitised feldspar. Accessory epidote, chlorite (after biotite) and opaques.

WM 157. Bennabeola Quartzite Fm. Less than 10% very fine grained muscovite, average 0.1mm long. Usually individual grains but some fish development. 80% recrystallised quartz. 10% sericitised and saussuritised K-feldspar, minor opaques.

WM 158. Siliceous granulite from Streamstown Fm. 20% green-brown biotite up to 1mm long. Some chloritisation and epidote growth along the cleavages. 60% quartz, 20% heavily sericitised feldspar. Accessory zircon and opaques.

WM 160. Bennabeola Quartzite Fm. 10% pale green, slightly pleochroic muscovite up to 1mm long. Some grains show mild iron staining. 70% quartz. 20% completely sericitised feldspar. Accessory zircon, haematite and opaques.

WM 165. Amphibolite from Lakes Marble Fm. 40% green, strongly pleochroic, subhedral hornblende. Grains up to 1.5mm. 10% light green, euhedral, cummingtonite, 1mm long. Possibly exsolution of

cummingtonite in hornblende? Frequent pleochroic haloes (zircon) and quartz inclusions. 20% quartz. 30% heavily sericitised feldspar. Accessory zircon and opaques.

WM 167. Amphibolite in Lakes Marble Fm. 65% brown-green, pleochroic, subhedral hornblende. Two generations, large (5cm) twinned, zoned grains recrystallised to give small (<1cm) grains. Abundant zircon and quartz inclusions giving a sieve texture. Streaky birefringence. Some breakdown to give biotite and chlorite. 5% pale green cummingtonite. 20% partly sericitised and saussuritised plagioclase and K-feldspar. 10% quartz. Minor epidote and opaques.

WM 168. Siliceous granulite from Kylemore Fm. 30% muscovite in fish 2-3cm long. 10% biotite completely chloritised grown as individual grains. 50% quartz, 20% partly sericitised plagioclase and K-feldspar. Accessory tourmaline, garnet, zircon, apatite and opaques.

WM 179. Semi-pelitic schist from Streamstown Fm. 25% green-brown biotite up to 2mm long, no apparent chloritisation. <5% muscovite in association with biotite. 40% recrystallised quartz. 30% slightly sericitised plagioclase and K-feldspar. Accessory zircon, epidote and opaques.

WM 180. Bennabeola Quartzite Fm. Less than 10% pale green, slightly pleochroic muscovite, up to 0.2mm long. 80% quartz, 10% sericitised feldspar and accessory haematite and opaques (after biotite?).

WM 183. Amphibolite from Streamstown Fm. 50% pale green, slightly pleochroic hornblende, 10% euhedral cummingtonite, up to 0.3mm. Twinning frequent. Common streaky birefringence. Inclusions of quartz and zircon. 30% heavily sericitised and saussuritised feldspar. 10% quartz, epidote, haematite and opaques. Iron stained veins cut slide

WM 184. Siliceous granulite from Clifden Fm. 15% green-brown strongly pleochroic biotite. Maximum length 1/4mm. Some chloritisation along cleavages. 5% muscovite, length 0.25mm, sometimes intergrown with biotite. 60% strained quartz. 20% partly sericitised plagioclase and K-feldspar, accessory zircon and opaques.

WM 188. Pelitic schist from Cashel Fm. 40% red-brown biotite, up to 3mm long. No obvious chlorite but displays clear zones along cleavages at extinction. Many pleochroic haloes. 20% muscovite and sillimanite

intergrown with biotite. 20% slightly sericitised plagioclase and K-feldspar. 20% quartz and accessory zircon, garnet and opaques.

WM 193. Pelitic schist from Barnanoruan Fm. 30% red-brown biotite, length <0.2mm. Slightly chloritised in places. 10% muscovite up to 4mm. 30% partly re-crystallised and strained quartz. 30% partly sericitised plagioclase and accessory zircon, apatites and opaques.

WM 195. Bennabeola Quartzite Fm. Less than 10% sericite/muscovite less than 0.2mm long. Often growing around the quartz grains. 80% quartz, 10% partly sericitised feldspar and opaques.

WM 196. Cleggan Boulder Bed Fm. 10% green-brown biotite concentrated in fringes around quartzo-feldspathic pebbles (1-2cm). 10% muscovite in association with biotite. 5% sericite/muscovite growing interstitially in pebbles. 60% quartz with sillimanite needle inclusions, 15% plagioclase, K-feldspar and microcline. Accessory zircon and opaques.

WM 198. Pelitic schist from the Streamstown Fm. 60% large (5cm) kinked and strained muscovite grains. Some large partings formed from cleavage. Possible second generation of pale green muscovite across schistosity. 10% chlorite (after biotite). 30% recrystallised quartz. 20% completely sericitised and saussuritised plagioclase and K-feldspar. Accessory epidote and opaques.

WM 200. Metagabbro. 60% hornblende. Euhedral grains up to 1cm long. No obvious alteration of the hornblende, although contains some inclusions. 30% slightly sericitised plagioclase. 5% quartz. 5% opaque minerals (magnetite) and accessory zircon.

WM 201. Massive amphibolite from Lakes Marble Fm. 50% brown-green, strongly pleochroic, euhedral hornblende. Bi-modal size, commonly about 4mm and 0.5mm. Frequent inclusions most commonly seen on larger grains cut normal to the c axis. Twinning common. Zones of alteration along cleavages common. Birefringence and extinction are streaky. 40% completely sericitised and saussuritised feldspar. 10% quartz, sphene and opaques.

WM 212. Graphitic schist from the Cornamona Fm. 40% fine grained muscovite <1/2mm. Possibly two generations of growth. 10% green biotite, partly chloritised grown with muscovite. 20% partly

sericitised and recrystallised feldspar. 30% recrystallised quartz. Minor opaques.

WM 220. Striped amphibolite from Streamstown Fm. 40% green, strongly pleochroic, euhedral hornblende. Elongated crystals 1-2mm long parallel to the striping. Twinning common. Frequently displays streaky birefringence on section cut parallel to c axis. Occasional apatite inclusions. 40% plagioclase and K-feldspar, partially sericitised. 10% quartz and opaques.

WM 221. Semi-pelitic schist from the Streamstown Fm. 30% pale green, faintly pleochroic muscovite, up to 2mm. Often growing as rosettes. 10% chlorite after biotite. 40% recrystallised quartz. 20% partly sericitised and saussuritised plagioclase and K-feldspar and opaques.

WM 222. Pelitic schist from Streamstown Fm. 10% pale green muscovite up to 1mm. 20% chlorite (after biotite) intergrown with 10% sillimanite (fibrolite). 40% heavily sericitised plagioclase and K-feldspar. 20% strained quartz, frequent garnets (0.5mm), calcite and opaques.

WM 223. Pelitic schist from Streamstown Fm. 10% muscovite up to 2mm. 30% heavily chloritised biotite with associated epidote in cleavages. 10% sillimanite mostly as fibrolite. 30% completely sericitised and saussuritised plagioclase and K-feldspar. 20% strained quartz with accessory garnet (1mm), zircon, apatite and opaques.

WM 224. Poorly striped amphibolite from Streamstown Fm. 50% green pleochroic subhedral hornblende. Size up to 2mm. Cleavage poorly displayed. Slight streakiness to birefringence. Some twinning. 30% feldspar, heavily sericitised and saussuritised. 20% quartz, epidote and opaques.

WM 225. Striped amphibolite from Streamstown Fm. 40% green, strongly pleochroic, euhedral hornblende. Grains less than 0.25mm slightly elongated parallel to the striping. Cleavage poorly displayed. 20% plagioclase and K-feldspar, partly sericitised. 20% quartz. 20% chlorite (after biotite), epidote and opaques.

WM 226. Semi-pelitic schist from Streamstown Fm. 20% muscovite up to 5mm long, frequently bent and kinked and show wavy extinction. Intergrown with 20% heavily chloritised biotite and sillimanite (fibrolite) mats. 30% plagioclase and K-feldspar mostly

sericitised and saussuritised. 30% strained quartz. Frequent garnets (0.5mm) and opaques.

WM 227. Pelitic schist from Streamstown Fm. 40% red-brown biotite. Average grain size 0.2mm. Common pleochroic haloes (zircon). Slight chloritisation along cleavages. 30% plagioclase and K-feldspar, partly sericitised. 30% quartz and accessory corroded garnets (3-4mm) and opaques.

WM 228. Banded amphibolite from Streamstown Fm. 30% green-brown, pleochroic, subhedral hornblende. Grains up to 3mm. Twinning occasional. Birefringence slightly streaky. Slight alteration of some larger grains. Inclusions of zircon, sphene, quartz and apatite. 20% diopside (heavily altered) with 10% chlorite (after biotite) and 30% completely sericitised and saussuritised feldspar in bands in-between amphibolite layers. 10% quartz, sphene, epidote and opaques.

WM 231. Semi-pelitic schist from Streamstown Fm. 25% green-brown biotite. Length up to 1mm. Few pleochroic haloes (zircon). Slight chloritisation and epidote growing along cleavages. 35% plagioclase and K-feldspar slightly sericitised. 40% strained quartz and minor opaques.

WM 232. Massive amphibolite from Streamstown Fm. 40% green-brown, pleochroic, euhedral hornblende. Average grain size 1/4mm, slight alignment of larger grains. Birefringence streaky in some grains cut parallel to the c axis. 20% chlorite (after biotite) 30% plagioclase and K-feldspar partially sericitised and saussuritised. 10 % quartz, epidote and opaques.

WM 233. Pelitic schist from Streamstown Fm. 50% green-brown biotite. Average grain length 2mm. Some pleochroic haloes (zircon). Some chlorite layers (after biotite) interleaved with the biotite. 10% muscovite associated with the biotite. 25% plagioclase and K-feldspar, slightly sericitised. 15% quartz and opaques.

WM 234. Extensively sheared amphibolite. 70% light green, pleochroic amphibole. Large (2-3mm) grains are sheared and partly recrystallised. Abundant quartz and feldspar inclusions in the amphibole. Some slight alteration to biotite and chlorite along veins. 20% quartz. 10% heavily sericitised and saussuritised feldspar.

WM 235. Amphibolite from Lakes Marble Fm. 40% green, strongly pleochroic, subhedral hornblende. Grains up to 1/2mm and showing strong alignment. 20% partly chloritised biotite growing in association with the amphibole. 30% partly sericitised and saussuritised plagioclase and K-feldspar. 10% cordierite, quartz, epidote, zircon and opaques.

WM 237. Amphibolite from Lakes Marble Fm. 50% green-brown, pleochroic, equant, euhedral hornblende up to 1/4mm. Apparently fresh. 40% slightly sericitised plagioclase and K-feldspar (mostly altered along veins). 10% slightly strained quartz. Abundant epidote, apatite and opaques.

WM 238. Striped amphibolite from Lakes Marble Fm. 60% green, pleochroic, euhedral hornblende. Large, 5mm, grains recrystallised to small 1/4mm grains. Strong alignment of tabular grains. 20% heavily altered diopside. 20% heavily sericitised and saussuritised feldspar. Accessory biotite, muscovite, epidote and opaques.

WM 242. Amphibolite from Lakes Marble Fm. 50% green-brown, pleochroic, subhedral hornblende. Grains up to 5mm partly recrystallised. 10% completely chloritised biotite. 40% slightly sericitised plagioclase. Accessory epidote, heamatite and opaques.

WM 244. Striped amphibolite from Lakes Marble Fm. 60% green, pleochroic, hornblende. Shows streaky birefringence with epidote in the cleavages. Grains up to 1mm long. 30% heavily sericitised plagioclase. 10% completely chloritised biotite. Accessory epidote and opaques.

WM 248. Striped amphibolite in Lakes Marble Fm. 60% green-brown, pleochroic, euhedral hornblende. Grains up to 1.5mm. 40% partly sericitised plagioclase. Accessory zircon, epidote and opaques.

WM 249. Striped amphibolite in Lakes Marble Fm. 50% green, pleochroic, subhedral, hornblende. Grains up to 1mm. 40% heavily sericitised plagioclase. 10% quartz with accessory zircon and opaques.

APPENDIX A.3. GEOCHEMICAL ANALYSIS METHODS AND PROCEDURES.

A.3.1 MINERAL SEPARATE PREPARATION.

In the field several kilograms of rock were taken from each sample location where possible and, using a hammer, the weathered surfaces were trimmed off. In the laboratory about half the sample was prepared for mineral separation, the remainder used for thin sections, laser probe sections etc. For mineral separation any remaining weathered surfaces were removed and the fresh rock broken down to roughly centimetre cubes with a hydraulic rock splitter. The cubes were then broken down further in a jaw crusher. Maximum mineral separate yield was found to occur when the rock fragments had been reduced to about half the grain size. This was achieved by repeatedly passing the rock fragments from the jaw crusher through a roller mill. After each pass through the roller mill the fragments were sieved, fragments larger than required were passed through the roller mill again. Once all material was smaller than the required mesh size, usually 250 microns, the fine dust was removed by repeated washing in running tap water. The rock fragments were then dried in an oven at 100°C. Once dry the rock fragments were sieved a final time to obtain the required grain size range. Most of the mineral separates prepared were 125 to 250 microns wide/long.

Conventional magnetic and heavy liquid separation techniques were used to obtain the mineral separates. To separate amphibole the heavy liquid used was di-iodomethane and for mica separation bromoform was used, diluted with acetone as required. In a few cases paper shaking was used in the mica separations. This involved placing some of the impure separate on filter paper and shaking in a sideways manner with the paper tilted slightly. The rounder quartz and feldspar grains tend to roll off the paper, while the flat mica grains stick to the rough paper surface. In all cases separates were in excess of 95% pure, most better than 98% pure and many better than 99% pure. It was found to be virtually impossible to completely isolate biotite from chlorite.

Aliquots of the mineral separates were used for: potassium analysis; argon isotope analysis; oxygen isotope analysis; hydrogen isotope analysis;

electron-probe analysis; ion-probe analysis. Various rock slices were used for: optical thin sections; laser-probe sections; TEM sections.

A.3.2 X-RAY DIFFRACTION (XRD) ANALYSIS.

Once mineral separates had been prepared, they were analysed by XRD as a check on their purity. If the separates proved impure they were passed through the mineral separation procedure again. For XRD analysis about 0.2g of material was used. The separate was ground down in a mortar and pestle and the powder spread over one side of double sided 'Sellotape' which in turn was stuck over the window of a standard XRD powder holder which was inserted into the machine.

The XRD machine used was a Philips PW 1120 generator which powered a Philips PW 1050/35 goniometer. The generator was run at 40 kV and 20 mA. The goniometer was geared to run at 1 degree (2Θ) per minute. The goniometer was started at 5^{o} and for most analyses was run through to about 60^{o}.

A.3.3 ELECTRON-PROBE SAMPLE PREPARATION AND ANALYSIS.

All the electron probe chemical determinations given in appendix A.5.1 were obtained from grain mounts. Aliquots of the mineral separates prepared from the whole rock were mounted on normal probe slides using a thermo-epoxy glue. These sections were polished and carbon coated as normal. Up to eight mineral separates were mounted on one probe slide. This method has the advantage that the chemistry of the exact specimen used for dating etc. is obtained. This is important, for the mineral separating procedure concentrates mineral cores preferentially over mineral rims. If the mineral being separated is chemically zoned (perhaps for K and Ar) then the ages obtained from the cores may differ from what would be obtained if complete grains could be used.

The amphibole analyses were performed on the Cambridge Instruments Microscan Mark 5 electron microprobe at the Geology Department, Edinburgh University. The analyses were obtained using the

wavelength dispersive system (WDS). The probe current was 30 mA and the accelerating voltage was 20 kV.

The mica analyses were performed on the Cambridge Instruments Microscan Mark 5 electron microprobe at the Geology Department, Glasgow University. The analyses were obtained using the energy dispersive system (EDS). The EDS X-ray spectrum acquisition and analysis system used was the Link Analytical Systems AN10000. The probe current was 30 mA and the accelerating voltage was 20 kV.

A.3.4 ION-PROBE SAMPLE PREPARATION AND ANALYSIS.

The ion-probe analyses were performed on the Cameca IMS 4f ion-probe at the Geology Dept., Edinburgh University. The samples analysed were prepared as grain mounts in the same manner as described above for electron-probe analysis, except that the mount was a 2.5cm diameter glass disc rather than a normal rectangular electron-probe slide. In addition the grain mounts were gold coated rather than carbon coated. In this way four samples could be mounted onto each glass mount. Five amphibole samples were analysed for major and trace elements in this way. For two of these samples a fresh grain was chosen and step scans were obtained for some major and minor elements, the individual steps were 15 microns.

The amphibole elemental concentrations were determined with the Kakanui and Hoover Dam hornblendes as standards. The elemental count rates were measured by computer controlled 'peak hopping' through all masses with naturally occurring isotopes. Recording times were 4 seconds per mass. The primary beam was $^{16}O^-$ ions with a beam current of 4.5 nA and an accelerating voltage of 10 keV. Corrections had to be made at the vanadium and chromium masses for interference by Mg, Al and MgSi.

A.3.5 TEM SAMPLE PREPARATION AND ANALYSIS.

TEM (Transmission electron microscopy) analysis was performed in the Physics Dept, Glasgow University with the kind approval of Professor Chapman. TEM analysis requires ultra thin sections, only 1 or 2 microns thick, to be transparent to electron beams. The TEM sections were mounted

on thin copper grids with a diameter of 3mm. The TEM sections were prepared from ordinary optical thin sections that had been prepared without a cover slip and using an epoxy resin soluble in chloroform. These optical sections could then be examined to find the most interesting grains for TEM analysis. Once the area of interest had been identified a copper grid was glued over the top using an epoxy that is not soluble in chloroform. Using a sharp scalpel the optical thin section was cut through around the copper grid. The whole optical thin section with glued on copper grid was then immersed in chloroform for about an hour. After this time the optical thin section should have come adrift from its mounting glass, the part glued to the copper grid could then be retrieved.

Once a rock slice has been prepared on a copper grid it is ready for thinning. The thinning was done using an 'Ion Tech Argon Ion Mill', the thinner was run at 6 kilovolts with both upper and lower guns at an incidence angle of 20^{o}, and a 1 mA total current (1/2 mA top and bottom guns). Thinning was continued until a hole had been created in the centre of the sample. This hole should have tapered edges, parts of which should be suitable for analysis. The thinning times for hornblende are long, the argon ion mill thins the hornblende at about 1 micron per hour. Starting with ordinary optical thin sections thinning times ranged from 20 to 40 hours. Once a sample was prepared to this stage a 10 second carbon coat was applied prior to analysis.

It must be stressed that this whole operation is extremely tricky and the success rate was only about 10%. At all stages in this operation it is possible to break the section as it is so thin. Severe problems were encountered with the argon ion thinning process. If large hornblende grains were being prepared the presence of cleavages caused the centre sections of the grains to fall away which meant a suitable taper could not be formed. If small grain size amphibolites were thinned, a similar problem was encountered with entire grains falling away. The thinning operation appears to be more luck than judgement and no obvious recommendations can be made as to which grains are most suitable.

The TEM sections were examined on a JEOL 100C TEM instrument in the Department of Physics, Glasgow University. The machine was run on an accelerating voltage of 100 kV. This enabled magnifications in the range 10 000 to 250 000 times to be achieved. It became apparent that a higher accelerating voltage would really be necessary to allow better

transmission. At 100 kV only the very thinnest parts of the sections could be examined. The instrument had an X-ray camera with which the photomicrographs were taken. Also attached was a Link Systems EDX X-ray acquisition and analysis system. Some attempts were made to obtain spectra for parts of the TEM images; however, this was not very successful for two reasons. Firstly, the system was really designed with a resolution of 10 microns or more while the interesting areas in the TEM sections were 1 micron or less. Secondly, the long ion thinning process meant that the mounting copper grid became eroded and sputtered a fine copper coat over the sample. When the X-ray spectra were obtained most of the diagnostic elements (ie. Ca, Na, K) were swamped by the massive Cu α and Cu β peaks.

APPENDIX A.4. ISOTOPIC ANALYSES METHODS AND PROCEDURES.

A.4.1 K DETERMINATION FOR K-Ar AGE DATING.

Potassium determinations were performed on a flame photometer at SURRC. For mica determinations about 0.01g was required and for amphibole because of the low potassium content between 0.1 and 0.2g was required. This was weighed out into clean Teflon beakers, wrapped in aluminium foil to reduce problems associated with static electricity. The samples were digested overnight, on a hotplate, in a cocktail of sulphuric and hydrofluoric acids. This produced a dry residue which was dissolved in nitric acid, this solution was then added to a Li standard solution and a buffer solution and made up to volume. These solutions were analysed on a Corning EEL 450 flame photometer calibrated with known concentration K standard solutions. Duplicate or triplicate solutions were made up and analysed and the results accepted if they were consistent within 1.5% of the mean. The greatest source of error in this procedure is though to be due to weighing inaccuracies caused by static electricity.

A.4.2 ARGON EXTRACTION AND ANALYSIS FOR K-Ar AGE DATING.

Argon was extracted on the SURRC all-metal 'Ar Line 2' and measured, using an AEI MS10 mass spectrometer operated in the static

mode, against a highly pure and enriched ^{38}Ar spike. The mineral separates were loaded into copper capsules. About 0.1g was required for micas and about 0.3g for amphibole. Nine sample capsules plus one standard were loaded into a vertical sample holder, the 'tree', which connects to the vacuum line. Samples were dropped using a system of magnets into a molybdenum crucible and heated to over 1200°C for 20 minutes using a Radyne radiofrequency induction coil. A known volume of the ^{38}Ar spike was then introduced to the system. The liberated gases were 'cleaned' using a zeolite to trap large molecule gases ie. water, and a titanium sublimation pump to trap other active gases. In principle only the inert gases were then be leaked to the mass spectrometer. The ^{36}Ar, ^{38}Ar and ^{40}Ar isotope peak heights were measured on a chart recorder and a BBC microcomputer programme used to calculate the age, given the potassium content of the sample. In some cases the argon analyses were done in duplicate, but only when spurious ages were obtained from the standard sample on the 'tree'. The lack of duplicates was because of constraints on the time on the argon extraction line.

Errors in the age incorporate errors in the determination of the potassium content and errors in the determination of the argon content of the sample. The errors are calculated automatically by the microcomputer from the following equation:

$$E_t = [\, E_k^2 + (1+(A/R))^2\, E_{40}^2 + E_{38}^2 + (A/R)^2\, E_{36}^2 \,]^{(1/2)}$$

where: E_t is the total error; E_k is the error in the potassium determination, taken to be 1.5% of the mean; A is the % atmospheric ^{40}Ar; R is the % radiogenic ^{40}Ar; E_{40} is the error in the ^{40}Ar determination, taken to be 0.5%; E_{38} is the error in the ^{38}Ar determination, taken to be 0.5%; E_{36} is the error in the ^{36}Ar determination, taken to be 1%.

A.4.3 ^{40}Ar-^{39}Ar INCREMENTAL STEP-HEATING METHODS.

Bulk sample ^{40}Ar-^{39}Ar incremental step-heating experiments were performed on five samples (WM 167, WM 201, WM 225, WM 228 and WM 232) at the Department of Geological and Geophysical Sciences, Princeton University. For irradiation the samples were wrapped in aluminium foil packets and stacked in a 19 by 40 mm aluminium canister. Packets of standard hornblende Mmhb-1 (519.5±2.5 Ma, Alexander *et al.* 1978) were

placed at each end of the five samples to measure the flux gradient. The canister was irradiated at the McMaster Reactor (McMaster University, Canada) for 80 hours. The Mmhb-1 standards indicated that the J value was 0.01817008 ± 0.000097218.

For analysis the samples were transferred from their packets to quartz boats, all five samples were then loaded into the silica-glass extraction line. The furnace section of the line was degassed for 10 hours at 1200°C to remove any adsorbed atmospheric gases. Step-wise degassing of the samples was performed using a Lindberg resistance furnace. The temperature was monitored by two Pt-Rh thermocouples which straddle the furnace tube. These thermocouples are accurate to ±2°C and indicate a thermal gradient across the furnace of 2°C. The samples were maintained at each temperature step for 30 minutes during which time the gas was cleansed on a Ti-sponge getter at 700°C, a Zr-Al getter at 100°C and a liquid nitrogen cold trap. Isotopic analyses were performed on a Varian-MAT GD 150 mass spectrometer. The electromagnet was computer controlled to allow 'peak hopping', by this process the backgrounds and peak heights were measured for atomic masses 36 to 41. These peaks and backgrounds were cycled through 10 times and the results extrapolated back to t=0 (t is time after the gas is admitted to the mass spectrometer) to allow for memory and fractionation effects. The data were corrected for the radioactive decay of ^{36}Cl, ^{37}Ar and ^{39}Ar as well as interference from reactions on Ca.

For a more complete description of the analytical and data correction procedures the reader is directed to Onstott & Peacock (1987) which gives a more detailed account of the operation of the Princeton equipment.

A.4.4 LASER-PROBE ^{40}Ar-^{39}Ar SAMPLE PREPARATION AND ANALYSIS.

Laser-probe ^{40}Ar-^{39}Ar total fusion ages were determined on two samples (WM 201 and WM 220) using the equipment at SURRC. The two samples were whole rock slices cut approximately 1cm^2 and 1mm thick and unmounted. The samples were given a light polish by hand and then cleaned in acetone then distilled water in a sonic bath.

The two samples were irradiated in the Petten nuclear reactor, Netherlands on the 30th August 1989. For irradiation the samples were wrapped in Al foil and placed in an irradiation can. The can was placed in the Petten HF-PIF reactor; row 1, position 4 with cadmium shielding. The irradiation time was 24 hours, with the can being rotated 180^{o} after 12 hours. The can also included the amphibole irradiation standard Hb3gr (1072±11 Ma, Roddick 1983) which later analysis showed to have received a fast fluence of 10^{18} neutrons/cm^{2} and gave a value of J = 0.0038±0.0003.

The samples were analysed over a period from December 1989 to January 1990 at SURRC. The laser-probe system comprises a Spectron Laser Systems Nd YAG continuous laser. The laser has a maximum total output of 130 W, but during analysis was operated at 60 W in short (c.1 second) pulses. The laser beam was directed through the optics of a Leitz Metallux optical microscope to the sample chamber mounted on the microscope stage. The optical microscope was fitted with a video camera allowing the sample to be imaged on a television screen and the laser beam targeted and focussed on the sample. The television also allowed observation of the laser fusion process. Gases liberated from the laser fusion process were passed over a SAES Zr/Al alloy getter for 5 minutes, which adsorbed all active gases. The remaining inert gases were introduced into a Mass Analyser Products 215 mass spectrometer with a second getter. The mass spectrometer electromagnet was computer controlled to allow 'peak hopping', by this process the backgrounds and peak heights were measured for mass to charge 36 to 41. These peaks and backgrounds were cycled through 10 times and the results extrapolated back to t=0 (t is time after the gas is admitted to the mass spectrometer) to allow for memory and fractionation effects. The peak height ratios were measured for a suite of analyses and then these raw data corrected for irradiation-initiated Ar production by reactions on Ca and Cl.

In practise the television monitoring of the sample allows the laser beam to be directed onto target sites with an accuracy of about 10 microns. A 1 second laser pulse will produce a 'pit' about 100 microns in diameter and twice as deep. However, the low K content (about 0.5 wt.% K) of these amphiboles meant that a pit this size yielded insufficient ^{39}Ar and ^{40}Ar for analysis. Consequently, for each analysis between 3 and 7 pits were burned, each overlapping. This necessarily gave a wider and deeper pit, giving lower sample resolution, but the gave the required gas yield. The amphibole grain size (average 0.5mm) ensured that at this pit resolution at

least two ages could be determined for each grain. For sample WM 201 a larger grain (3mm by 4mm) was traversed an gave 9 ages.

A.4.5 HYDROGEN ISOTOPE EXTRACTION AND ANALYSIS METHODS.

Hydrogen extractions were performed on the all glass hydrogen line at SURRC. The hydrogen extraction technique is similar to that described by Godfrey (1962). About 40mg of powdered sample was loaded into a previously degassed platinum crucible and heated at 120°C overnight to release absorbed (H_2O^-) water. The sample vessel was then transferred to the extraction line and the sample heated to about 1400°C for 30 minutes using a Radyne radiofrequency induction coil. During this heating the sample melts totally and liberates hydrogen as free hydrogen and as water vapour. The hydrogen in the water vapour is converted to free hydrogen by reduction with hot uranium. The hydrogen yield is measured on a mercury manometer, from this yield (in micromoles/mg) the wt.% H_2O^+ content of the sample can be calculated by multiplication by a factor of 1.8015. The hydrogen gas was analysed on a VG Micromass 602B mass spectrometer with a modified inlet system against a reference gas that has been calibrated against SLAP and SMOW waters. Duplicate and triplicate sample runs were performed until repeats better than 0.5‰ were obtained.

A.4.6 OXYGEN ISOTOPE EXTRACTION AND ANALYSIS METHODS.

Oxygen was extracted from the samples using the F12 and F6 fluorination lines at SURRC in a process similar to that described by Borthwick & Harmon (1982). For oxygen determinations some 10 to 20mg of powdered sample was used. The oxygen was liberated from the sample by oxidation with Cl F_3 at 680°C overnight. The oxygen thus liberated was reduced to CO_2 by contact with a red hot carbon rod. The yield of CO_2 was measured by a calibrated capacitance manometer. The CO_2 was analysed on a VG-SIRA 10 mass spectrometer against a reference gas that was calibrated against international standard NBS#28. At SURRC repeated analysis of NBS#28 gives a $\delta^{18}O$ of 9.6‰. The samples were run in duplicate or

triplicate until a repeat of ±0.2‰ was obtained. The raw data from the mass spectrometer was corrected to SMOW on the basis of the NBS#28 standard.

A.4.7 CALCULATION OF BULK STABLE ISOTOPIC COMPOSITIONS AND WATER CONTENTS OF MIXTURES OF TWO COMPONENTS.

In chapter four the isotopic composition and the water content of a mixture of two components was frequently referred to. This calculation is basically that of a a mixing curve between two end-members. To calculate the water content of a mixture the equation is:

$$W_{mix} = (W_a \times X_a) + (W_b \times X_b)$$

The equation to calculate the isotopic composition (oxygen or hydrogen) of a mixture is:

$$\delta_{mix} = ((W_a \times X_a \times \delta_a) + (W_b \times X_b \times \delta_b)) / W_{mix}$$

In these equations W is the water content (H_2O^+) in wt.%. X is the weight fraction of the end member and δ is the isotopic composition (oxygen or hydrogen) of the end member. The subscripts mix, a and b refer to the mixture and the two end members respectively.

APPENDIX A.5. CHEMICAL AND ISOTOPIC DATA.

A.5.1 ELECTRON-PROBE ANALYSES.

Amphibole:

The average chemical determination given below is calculated from all the individual analyses for each mineral sample. SD = standard deviation. As FeO is determined by wet chemistry on a bulk sample there is no standard deviation for this oxide.

WM	108	SD	109	SD	111	SD	124	SD
SiO_2	49.58	2.33	47.06	1.55	46.07	1.24	43.76	1.01
TiO_2	0.59	0.34	0.65	0.24	0.94	0.22	1.18	0.29
Al_2O_3	6.87	2.07	9.04	1.34	9.68	1.08	11.57	1.31
FeO	7.84		10.60		10.26		13.24	
Fe_2O_3	2.86	0.78	3.29	0.61	3.71	0.50	2.64	0.64
MnO	0.22	0.13	0.22	0.09	0.33	0.08	0.42	0.08
MgO	16.96	1.63	13.64	1.06	13.10	0.88	11.46	0.85
CaO	10.71	1.52	12.01	0.08	11.81	0.24	11.29	0.18
Na_2O	0.84	0.27	1.16	0.35	1.02	0.27	1.59	0.23
K_2O	0.32	0.21	0.46	0.28	0.71	0.17	0.65	0.09
sum	96.70	0.71	98.10	0.82	97.62	0.67	97.75	0.47
Si	7.13		6.83		6.78		6.51	
Ti	0.06		0.07		0.10		0.13	
Al	1.16		1.55		1.68		2.03	
Fe^2	0.94		1.29		1.25		1.64	
Fe^3	0.31		0.36		0.41		0.29	
Mn	0.03		0.03		0.04		0.05	
Mg	3.63		2.97		2.87		2.54	
Ca	1.65		1.87		1.87		1.80	
Na	0.23		0.33		0.29		0.46	
K	0.06		0.08		0.13		0.12	
sum =23 O	15.33		15.48		15.48		15.62	

WM	128	SD	135	SD	137	SD	138	SD
SiO_2	45.37	1.27	50.02	1.57	49.47	1.16	48.30	0.45
TiO_2	0.51	0.11	0.41	0.17	0.36	0.09	0.87	0.08
Al_2O_3	11.73	1.70	7.25	1.85	7.96	1.33	7.60	0.60
FeO	11.28		11.72		11.84		12.14	
Fe_2O_3	4.01	0.67	0.56	1.35	0.68	0.53	2.26	0.29
MnO	0.26	0.10	0.22	0.10	0.24	0.11	0.21	0.09
MgO	11.68	0.89	15.77	1.49	14.99	0.67	13.93	0.42
CaO	11.35	0.17	11.34	0.37	11.52	0.32	11.38	0.44
Na_2O	2.25	0.38	0.66	0.17	0.61	0.29	0.88	0.26
K_2O	0.26	0.05	0.12	0.07	0.13	0.04	0.38	0.09
sum	98.68	0.68	98.09	0.58	97.81	1.03	97.94	1.02
Si	6.64		7.18		7.13		7.05	
Ti	0.06		0.04		0.04		0.10	
Al	2.02		1.23		1.35		1.31	
Fe^2	1.37		1.40		1.43		1.48	
Fe^3	0.44		0.06		0.07		0.25	
Mn	0.03		0.03		0.03		0.03	
Mg	2.55		3.37		3.22		3.03	
Ca	1.78		1.74		1.78		1.78	
Na	0.64		0.18		0.17		0.25	
K	0.05		0.02		0.02		0.07	
sum	15.64		13.84		15.25		15.36	

WM	139	SD	165	SD	167	SD	183	SD
SiO_2	50.47	2.40	42.45	0.87	46.28	1.48	49.48	0.44
TiO_2	0.39	0.26	0.49	0.08	0.56	0.06	0.40	0.10
Al_2O_3	5.46	2.05	14.07	0.78	10.05	1.65	5.81	0.65
FeO	8.89		14.16		10.70		6.87	
Fe_2O_3	2.01	0.62	3.03	0.80	4.91	0.37	4.45	0.20
MnO	0.34	0.02	0.34	0.02	0.61	0.02	0.26	0.02
MgO	15.83	1.03	9.59	0.61	11.02	0.62	15.40	0.38
CaO	12.40	0.26	10.37	0.22	11.19	0.23	12.04	0.11
Na_2O	0.67	0.27	1.94	0.15	0.97	0.15	0.66	0.11
K_2O	0.47	0.25	0.25	0.04	0.20	0.05	0.12	0.03
sum	97.03	0.40	96.69	0.63	96.49	0.50	96.79	0.25
Si	7.32		6.39		6.90		7.36	
Ti	0.05		0.06		0.06		0.05	
Al	0.94		2.50		1.77		0.99	
Fe^2	1.06		1.77		1.51		0.89	
Fe^3	0.23		0.34		0.38		0.45	
Mn	0.04		0.04		0.08		0.03	
Mg	3.42		2.15		2.45		3.32	
Ca	1.93		1.68		1.79		1.86	
Na	0.19		0.61		0.28		0.19	
K	0.09		0.04		0.04		0.02	
sum	15.30		15.63		15.04		15.19	

WM	201	SD	220	SD	225	SD	228	SD
SiO_2	44.94	0.42	44.47	0.35	43.96	0.30	42.15	0.44
TiO_2	1.33	0.09	0.90	0.05	1.09	0.09	1.10	0.25
Al_2O_3	10.67	0.28	11.31	0.22	11.50	0.24	11.01	0.29
FeO	9.27		9.49		9.99		16.32	
Fe_2O_3	4.63	0.31	4.26	0.10	4.39	0.17	1.65	0.22
MnO	0.22	0.03	0.40	0.18	0.31	0.03	0.92	0.04
MgO	12.03	0.37	12.84	0.59	12.17	0.16	9.16	0.24
CaO	11.76	0.12	10.82	0.12	11.18	0.11	11.80	0.03
Na_2O	1.66	0.06	1.44	0.03	1.39	0.04	1.19	0.04
K_2O	0.58	0.06	0.28	0.02	0.31	0.03	1.58	0.11
sum	97.09	0.22	96.21	0.46	96.29	0.32	96.88	0.22
Si	6.67		6.63		6.49		6.40	
Ti	0.15		0.10		0.12		0.13	
Al	1.87		1.99		2.02		2.00	
Fe^2	1.08		1.17		1.24		2.09	
Fe^3	0.56		0.47		0.49		0.19	
Mn	0.03		0.05		0.04		0.12	
Mg	2.66		2.85		2.71		2.10	
Ca	1.86		1.72		1.79		1.94	
Na	0.48		0.42		0.40		0.35	
K	0.11		0.05		0.07		0.31	
sum	15.56		15.53		15.44		15.66	

WM	232	SD	234	SD	235	SD	237	SD
SiO_2	45.12	0.75	44.07	1.04	42.79	0.36	44.98	0.23
TiO_2	1.06	0.10	0.45	0.08	1.27	0.21	1.75	0.07
Al_2O_3	9.63	0.48	14.14	0.87	10.91	0.31	9.14	0.25
FeO	11.58		9.08		11.86		15.21	
Fe_2O_3	4.04	1.40	4.45	0.20	5.05	0.26	1.74	0.16
MnO	0.37	0.06	0.23	0.03	0.37	0.02	0.29	0.01
MgO	11.84	0.78	11.04	0.45	10.48	0.24	10.44	0.14
CaO	11.15	0.37	11.63	0.21	11.54	0.06	11.54	0.08
Na_2O	1.68	0.13	1.19	0.07	1.50	0.05	1.46	0.06
K_2O	0.52	0.05	0.36	0.01	0.98	0.05	0.95	0.04
sum	96.99	0.27	96.64	0.37	96.52	0.31	97.86	0.32
Si	6.76		6.54		6.51		6.75	
Ti	0.13		0.05		0.15		0.20	
Al	1.67		2.47		1.96		1.62	
Fe^2	1.44		1.11		1.49		1.90	
Fe^3	0.45		0.49		0.57		0.20	
Mn	0.05		0.03		0.05		0.04	
Mg	2.64		2.43		2.31		2.30	
Ca	1.79		1.84		1.88		1.86	
Na	0.49		0.35		0.25		0.45	
K	0.10		0.07		0.19		0.20	
sum	15.45		15.41		15.43		15.58	

WM	238	SD	242	SD	244	SD	248	SD
SiO_2	44.71	0.38	45.70	0.39	45.05	0.57	45.27	1.79
TiO_2	1.02	0.07	1.54	0.04	0.84	0.16	0.56	0.08
Al_2O_3	11.30	0.33	9.08	0.21	10.80	0.34	11.11	0.87
FeO	11.52		10.05		8.91		12.01	
Fe_2O_3	3.43	0.32	5.74	0.23	4.46	0.66	3.92	0.20
MnO	0.29	0.02	0.28	0.02	0.38	0.02	0.59	0.03
MgO	11.38	0.26	11.38	0.18	13.00	0.43	9.12	0.45
CaO	10.84	0.10	11.47	0.10	10.98	0.15	11.01	0.21
Na_2O	1.64	0.08	1.20	0.04	1.28	0.04	1.17	0.07
K_2O	0.45	0.04	0.70	0.04	0.29	0.03	0.21	0.01
sum	96.65	0.13	97.03	0.62	95.99	0.31	94.97	0.37
Si	6.67		6.83		6.65		6.78	
Ti	0.10		0.17		0.09		0.06	
Al	1.98		1.60		1.89		1.96	
Fe^2	1.43		1.24		1.13		1.57	
Fe^3	0.38		0.64		0.47		0.39	
Mn	0.04		0.03		0.05		0.07	
Mg	2.58		2.48		2.88		2.35	
Ca	1.72		1.86		1.75		1.77	
Na	0.46		0.34		0.37		0.34	
K	0.09		0.14		0.06		0.04	
sum	15.51		15.42		15.45		15.36	

WM	249	SD
SiO_2	44.31	1.04
TiO_2	0.43	0.08
Al_2O_3	12.14	0.87
FeO	9.05	
Fe_2O_3	4.42	0.20
MnO	0.24	0.03
MgO	11.14	0.45
CaO	11.64	0.21
Na_2O	1.19	0.07
K_2O	0.37	0.01
sum	94.94	0.37
Si	6.54	
Ti	0.05	
Al	2.42	
Fe^2	1.37	
Fe^3	0.29	
Mn	0.03	
Mg	2.95	
Ca	1.82	
Na	0.34	
K	0.07	
sum	15.89	

Muscovite:

The average chemical determination given below is calculated from all the individual analyses for each mineral sample. SD = standard deviation.

WM	119	SD	127	SD	132	SD	134	SD
SiO_2	45.06	0.72	46.19	0.57	45.47	1.07	46.62	0.81
TiO_2	0.27	0.05	1.33	0.18	0.50	0.13	1.06	0.36
Al_2O_3	35.11	0.69	35.83	1.01	35.56	1.13	34.31	1.29
FeO	3.17	0.15	1.06	0.09	2.59	0.15	1.35	0.08
MnO	0.03	0.02	0.05	0.05	0.02	0.04	0.03	0.03
MgO	0.93	0.06	0.86	0.27	0.72	0.30	1.80	0.53
CaO	0.05	0.05	0.03	0.02	0.04	0.04	0.01	0.03
Na_2O	1.04	0.28	0.86	0.22	1.96	0.46	0.89	0.07
K_2O	10.01	0.19	10.30	0.10	8.74	0.37	10.21	0.12
sum	95.66	1.60	96.63	0.84	95.59	1.19	96.43	0.69
Si	6.04		6.08		6.06		6.16	
Ti	0.03		0.13		0.05		0.11	
Al	5.52		5.52		5.54		5.30	
Fe	0.37		0.12		0.30		0.15	
Mn	0.00		0.01		0.00		0.00	
Mg	0.19		0.17		0.15		0.36	
Ca	0.01		0.00		0.01		0.00	
Na	0.28		0.22		0.52		0.23	
K	1.75		1.77		1.51		1.75	
sum =22 O	14.18		14.02		14.15		14.08	

WM	151	SD	154	SD	157	SD	160	SD
SiO_2	45.79	0.94	46.05	0.83	45.89	0.81	45.44	0.99
TiO_2	0.99	0.14	0.69	0.10	0.64	0.20	0.97	0.16
Al_2O_3	33.49	1.06	32.97	0.99	32.96	0.66	31.75	1.16
FeO	3.81	0.13	3.37	0.24	3.16	0.13	4.04	0.38
MnO	0.01	0.03	0.07	0.08	0.04	0.04	0.00	0.00
MgO	1.07	0.27	1.88	0.25	1.67	0.32	1.69	0.41
CaO	0.03	0.03	0.02	0.02	0.01	0.03	0.00	0.01
Na_2O	0.80	0.19	0.40	0.27	0.58	0.17	0.21	0.16
K_2O	10.23	0.13	10.75	0.08	10.47	0.11	10.63	0.24
sum	96.21	0.65	96.18	0.80	95.42	0.91	94.72	0.82
Si	6.12		6.20		6.25		6.29	
Ti	0.10		0.07		0.06		0.10	
Al	5.26		5.13		5.13		4.96	
Fe	0.43		0.39		0.36		0.47	
Mn	0.00		0.01		0.01		0.00	
Mg	0.22		0.38		0.34		0.35	
Ca	0.01		0.00		0.00		0.00	
Na	0.21		0.11		0.15		0.06	
K	1.78		1.86		1.82		1.87	
sum	14.14		14.15		14.11		14.10	
=22 O								

WM	168	SD	180	SD	188	SD	195	SD
SiO_2	46.04	0.34	46.09	0.98	45.50	0.82	46.12	0.53
TiO_2	0.35	0.11	1.45	0.14	1.18	0.08	0.33	0.15
Al_2O_3	34.95	0.61	31.28	0.94	35.55	1.60	34.82	0.63
FeO	3.09	0.29	4.13	0.38	1.42	0.30	2.01	0.27
MnO	0.03	0.05	0.07	0.07	0.01	0.02	0.03	0.03
MgO	0.71	0.11	1.41	0.36	0.63	0.26	1.14	0.25
CaO	0.02	0.03	0.01	0.02	0.03	0.03	0.01	0.01
Na_2O	1.87	0.24	0.53	0.26	1.07	0.18	0.73	0.20
K_2O	8.84	0.17	10.24	0.23	10.03	0.19	10.36	0.18
sum	95.91	0.73	95.18	0.82	95.41	0.88	95.39	1.00
Si	6.05		6.21		6.02		6.09	
Ti	0.04		0.15		0.12		0.03	
Al	5.55		5.04		5.62		5.54	
Fe	0.35		0.47		0.16		0.23	
Mn	0.00		0.01		0.00		0.01	
Mg	0.15		0.29		0.13		0.23	
Ca	0.00		0.00		0.00		0.00	
Na	0.49		0.14		0.28		0.19	
K	1.52		1.79		1.72		1.78	
sum	14.14		14.09		14.06		14.09	
=22 O								

WM	196	SD	198	SD	221	SD	222	SD
SiO_2	45.41	0.39	45.36	0.72	44.76	0.50	45.31	0.97
TiO_2	1.11	0.17	0.94	0.06	1.14	0.25	0.99	0.17
Al_2O_3	33.73	0.39	32.62	0.50	33.63	0.26	32.95	0.83
FeO	3.47	0.40	4.07	0.27	3.69	0.27	3.63	0.40
MnO	0.03	0.05	0.12	0.05	0.04	0.03	0.05	0.04
MgO	0.87	0.11	1.26	0.14	0.90	0.13	1.00	0.15
CaO	0.04	0.05	0.04	0.03	0.06	0.05	0.08	0.06
Na_2O	0.84	0.24	0.96	0.20	0.81	0.31	0.82	0.24
K_2O	10.17	0.19	9.92	0.14	10.10	0.11	9.95	0.22
sum	95.67	0.33	95.27	1.32	95.26	0.55	94.76	1.22
Si	6.04		6.09		6.01		6.07	
Ti	0.11		0.10		0.12		0.10	
Al	5.41		5.26		5.43		5.34	
Fe	0.40		0.47		0.42		0.42	
Mn	0.00		0.01		0.01		0.01	
Mg	0.17		0.25		0.18		0.21	
Ca	0.01		0.01		0.01		0.01	
Na	0.22		0.26		0.22		0.22	
K	1.77		1.73		1.76		1.75	
sum	14.13		14.18		14.15		14.13	
=22 O								

WM	223	SD	226	SD
SiO_2	44.47	0.24	45.11	0.73
TiO_2	1.49	0.31	0.76	0.15
Al_2O_3	32.90	0.30	34.31	0.91
FeO	3.79	0.31	3.25	0.23
MnO	0.05	0.07	0.04	0.07
MgO	0.92	0.07	0.84	0.10
CaO	0.04	0.03	0.05	0.07
Na_2O	0.65	0.24	1.07	0.33
K_2O	10.16	0.19	9.88	0.14
sum	94.46	0.68	95.16	0.84
Si	6.00		6.05	
Ti	0.15		0.08	
Al	5.37		5.46	
Fe	0.44		0.37	
Mn	0.01		0.00	
Mg	0.19		0.17	
Ca	0.01		0.01	
Na	0.18		0.29	
K	1.79		1.72	
sum	14.14		14.14	
=22 O				

Biotite:

The average chemical determination given below is calculated from all the individual analyses for each mineral sample. SD = standard deviation.

WM	107	SD	119	SD	130	SD	148	SD
SiO_2	34.96	0.40	35.12	0.64	34.41	1.11	34.50	0.23
TiO_2	3.85	0.24	2.45	0.19	2.58	1.03	2.37	0.20
Al_2O_3	17.98	0.45	19.69	0.23	19.99	0.51	19.74	0.24
FeO	20.57	0.29	18.37	0.27	21.75	0.85	21.49	0.83
MnO	0.26	0.09	0.88	0.04	0.14	0.05	0.16	0.06
MgO	7.61	0.16	8.99	0.36	7.90	0.46	7.63	0.13
CaO	0.05	0.05	0.04	0.04	0.07	0.06	0.04	0.04
Na_2O	0.26	0.24	0.58	0.28	0.27	0.20	0.36	0.19
K_2O	9.14	0.08	8.84	0.11	7.77	0.94	8.87	0.36
sum	94.66	0.48	95.09	0.68	94.88	0.94	95.01	0.57
Si	5.34		5.28		5.20		5.23	
Ti	0.45		0.28		0.30		0.28	
Al	3.31		3.58		3.67		3.63	
Fe	2.68		2.37		2.83		2.80	
Mn	0.04		0.11		0.02		0.02	
Mg	1.77		2.06		1.83		1.78	
Ca	0.01		0.01		0.01		0.01	
Na	0.08		0.17		0.08		0.11	
K	1.82		1.74		1.54		1.76	
sum =22 O	15.50		15.60		15.48		15.62	

WM	158	SD	179	SD	184	SD	188	SD
SiO_2	35.62	0.49	35.03	0.51	35.67	0.51	34.60	0.57
TiO_2	2.28	0.09	2.92	0.20	2.78	0.24	3.10	0.57
Al_2O_3	19.38	0.42	17.59	0.36	17.37	0.53	19.66	0.33
FeO	17.35	0.37	23.02	0.57	18.36	0.62	22.14	0.85
MnO	0.47	0.13	0.35	0.04	0.52	0.05	0.09	0.05
MgO	9.41	0.28	7.39	0.32	10.37	0.37	6.42	0.22
CaO	0.08	0.07	0.01	0.01	0.06	0.03	0.03	0.04
Na_2O	0.35	0.23	0.19	0.17	0.39	0.26	0.63	0.25
K_2O	9.25	0.21	9.24	0.34	9.24	0.26	8.64	0.29
sum	94.34	1.11	95.75	0.60	94.76	0.90	95.32	0.76
Si	5.36		5.35		5.38		5.23	
Ti	0.27		0.35		0.33		0.95	
Al	3.54		3.25		3.18		3.62	
Fe	2.24		3.01		2.38		2.90	
Mn	0.06		0.05		0.07		0.01	
Mg	2.17		1.73		2.40		1.50	
Ca	0.01		0.00		0.01		0.00	
Na	0.11		0.06		0.12		0.19	
K	1.83		1.85		1.83		1.73	
sum	15.58		15.63		15.69		15.55	
=22 O								

WM	193	SD	196	SD	212	SD	227	SD
SiO_2	34.67	0.25	35.40	0.86	35.22	0.14	35.78	0.31
TiO_2	3.07	0.58	2.85	0.41	2.76	0.37	2.88	0.25
Al_2O_3	18.56	0.46	18.01	0.50	18.68	0.44	17.38	0.41
FeO	20.29	0.54	17.54	1.55	20.64	0.55	18.94	0.28
MnO	0.35	0.11	0.51	0.05	0.27	0.10	0.38	0.11
MgO	7.92	0.56	10.73	0.73	8.20	0.23	9.39	0.30
CaO	0.01	0.02	0.04	0.06	0.05	0.05	0.06	0.08
Na_2O	0.40	0.21	0.20	0.24	0.61	0.21	0.24	0.30
K_2O	9.29	0.13	8.58	1.16	8.56	0.98	9.15	0.12
sum	94.70	0.68	93.85	0.64	94.98	1.49	94.21	1.14
Si	5.30		5.33		5.32		5.43	
Ti	0.36		0.33		0.32		0.34	
Al	3.43		3.30		3.43		3.20	
Fe	2.66		2.28		2.69		2.47	
Mn	0.05		0.07		0.04		0.05	
Mg	1.85		2.50		1.90		2.19	
Ca	0.00		0.01		0.01		0.01	
Na	0.12		0.06		0.18		0.07	
K	1.86		1.70		1.69		1.82	
sum	15.62		15.57		15.58		15.58	
=22 O								

WM	231	SD	233	SD
SiO_2	35.70	0.47	34.70	0.75
TiO_2	3.92	0.34	3.14	0.34
Al_2O_3	16.86	0.75	17.01	0.34
FeO	20.13	0.66	21.35	1.32
MnO	0.31	0.08	0.29	0.09
MgO	8.96	0.32	8.72	0.67
CaO	0.01	0.02	0.08	0.04
Na_2O	0.32	0.15	0.39	0.23
K_2O	9.32	0.13	8.66	0.99
sum	95.53	0.48	94.29	0.71
Si	5.38		5.34	
Ti	0.46		0.37	
Al	3.08		3.16	
Fe	2.61		2.80	
Mn	0.04		0.04	
Mg	2.07		2.05	
Ca	0.00		0.01	
Na	0.10		0.12	
K	1.84		1.74	
sum	15.59		15.63	
=22 O				

A.5.2 CHEMICAL FORMULAE FOR AMPHIBOLES AND MICAS, NOMENCLATURE OF AMPHIBOLES.

Amphibole formulae:

WM 108 $(Na, K)_{0.20}$ $(Fe^{2}_{0.23}$ $Mn_{0.03}$ $Ca_{1.65}$ $Na_{0.09})$
$(Al_{0.29}$ $Fe^{3}_{0.31}$ $Ti_{0.06}$ $Mg_{3.63}$ $Fe^{2}_{0.71})$ $Si_{7.13}$ $Al_{0.87}$ O_{22} $(OH)_2$

WM 109 $(Na, K)_{0.37}$ $(Fe^{2}_{0.05}$ $Mn_{0.03}$ $Ca_{1.87}$ $Na_{0.05})$
$(Al_{0.38}$ $Fe^{3}_{0.36}$ $Ti_{0.07}$ $Mg_{2.95}$ $Fe^{2}_{1.24})$ $Si_{6.83}$ $Al_{1.17}$ O_{22} $(OH)_2$

WM 111 $(Na, K)_{0.32}$ $(Fe^{2}_{0.01}$ $Mn_{0.04}$ $Ca_{1.85}$ $Na_{0.10})$
$(Al_{0.40}$ $Fe^{3}_{0.41}$ $Ti_{0.10}$ $Mg_{2.85}$ $Fe^{2}_{1.24})$ $Si_{6.73}$ $Al_{1.27}$ O_{22} $(OH)_2$

WM 124 $(Na, K)_{0.51}$ $(Fe^{2}_{0.09}$ $Mn_{0.05}$ $Ca_{1.79}$ $Na_{0.07})$
$(Al_{0.50}$ $Fe^{3}_{0.29}$ $Ti_{0.13}$ $Mg_{2.53}$ $Fe^{2}_{1.55})$ $Si_{6.48}$ $Al_{1.52}$ O_{22} $(OH)_2$

WM 128 $(Na, K)_{0.48}$ $(Mn_{0.03}$ $Ca_{1.77}$ $Na_{0.20})$
$(Al_{0.60}$ $Fe^{3}_{0.44}$ $Ti_{0.06}$ $Mg_{2.53}$ $Fe^{2}_{1.37})$ $Si_{6.59}$ $Al_{1.41}$ O_{22} $(OH)_2$

WM 135 $(Na, K)_{0.20}$ $(Fe^{2}_{0.27}$ $Mn_{0.03}$ $Ca_{1.74})$
$(Al_{0.40}$ $Fe^{3}_{0.06}$ $Ti_{0.04}$ $Mg_{3.37}$ $Fe^{2}_{1.13})$ $Si_{7.17}$ $Al_{0.83}$ O_{22} $(OH)_2$

WM 137 $(Na, K)_{0.19}$ $(Fe^{2}_{0.26}$ $Mn_{0.03}$ $Ca_{1.78})$
$(Al_{0.50}$ $Fe^{3}_{0.07}$ $Ti_{0.04}$ $Mg_{3.22}$ $Fe^{2}_{1.17})$ $Si_{7.12}$ $Al_{0.88}$ O_{22} $(OH)_2$

WM 138 $(Na, K)_{0.28}$ $(Fe^{2}_{0.16}$ $Mn_{0.03}$ $Ca_{1.27}$ $Na_{0.04})$
$(Al_{0.32}$ $Fe^{3}_{0.25}$ $Ti_{0.10}$ $Mg_{3.02}$ $Fe^{2}_{1.32})$ $Si_{7.02}$ $Al_{0.98}$ O_{22} $(OH)_2$

WM 139 $(Na, K)_{0.21}$ $(Mn_{0.01}$ $Ca_{1.92}$ $Na_{0.07})$
$(Al_{0.23}$ $Fe^{3}_{0.23}$ $Ti_{0.04}$ $Mg_{3.41}$ $Fe^{2}_{1.26}$ $Mn_{0.03})$ $Si_{7.30}$ $Al_{0.70}$ O_{22} $(OH)_2$

WM 165 $(Na, K)_{0.47}$ $(Fe^{2}_{0.16}$ $Mn_{0.04}$ $Ca_{1.66}$ $Na_{0.14})$
$(Al_{0.85}$ $Fe^{3}_{0.34}$ $Ti_{0.06}$ $Mg_{2.14}$ $Fe^{2}_{1.61})$ $Si_{6.36}$ $Al_{1.64}$ O_{22} $(OH)_2$

WM 167 $(Na, K)_{0.28}$ $(Mn_{0.08}$ $Ca_{1.78}$ $Na_{0.14})$
$(Al_{0.62}$ $Fe^{3}_{0.38}$ $Ti_{0.06}$ $Mg_{2.43}$ $Fe^{2}_{1.51})$ $Si_{6.86}$ $Al_{1.14}$ O_{22} $(OH)_2$

WM 183 $(Na, K)_{0.11}$ $(Mn_{0.01}$ $Ca_{1.89}$ $Na_{0.10})$
$(Al_{0.24}$ $Fe^{3}_{0.45}$ $Ti_{0.04}$ $Mg_{3.36}$ $Fe^{2}_{0.89}$ $Mn_{0.02})$ $Si_{7.24}$ $Al_{0.76}$ O_{22} $(OH)_2$

WM 201 $(Na, K)_{0.43}$ $(Ca_{1.85}$ $Na_{0.15})$
$(Al_{0.54}$ $Fe^{3}_{0.56}$ $Ti_{0.15}$ $Mg_{2.63}$ $Fe^{2}_{1.08}$ $Mn_{0.03})$ $Si_{6.60}$ $Al_{1.40}$ O_{22} $(OH)_2$

WM 220 $(Na, K)_{0.33}$ $(Fe^{2}_{0.11}$ $Mn_{0.05}$ $Ca_{1.71}$ $Na_{0.13})$
$(Al_{0.54}$ $Fe^{3}_{0.47}$ $Ti_{0.10}$ $Mg_{2.83}$ $Fe^{2}_{1.06})$ $Si_{6.57}$ $Al_{1.43}$ O_{22} $(OH)_2$

WM 225 $(Na, K)_{0.35}$ $(Fe^{2}_{0.07}$ $Mn_{0.04}$ $Ca_{1.78}$ $Na_{0.11})$
$(Al_{0.53}$ $Fe^{3}_{0.49}$ $Ti_{0.12}$ $Mg_{2.69}$ $Fe^{2}_{1.17})$ $Si_{6.52}$ $Al_{1.48}$ O_{22} $(OH)_2$

WM 228 $(Na, K)_{0.66}$ $(Mn_{0.06}$ $Ca_{1.94})$
$(Al_{0.45}$ $Fe^{3}_{0.19}$ $Ti_{0.13}$ $Mg_{2.09}$ $Fe^{2}_{2.09}$ $Mn_{0.05})$ $Si_{6.46}$ $Al_{1.54}$ O_{22} $(OH)_2$

WM 232 $(Na, K)_{0.41}$ $(Fe^{2}_{0.01}$ $Mn_{0.05}$ $Ca_{1.77}$ $Na_{0.17})$

$(Al_{0.38}\ Fe^{3}_{0.45}\ Ti_{0.12}\ Mg_{2.62}\ Fe^{2}_{1.43})\ Si_{6.70}\ Al_{1.30}\ O_{22}\ (OH)_2$

WM 234 $(Na, K)_{0.24}\ (Ca_{1.80}\ Na_{0.17})$

$(Al_{0.90}\ Fe^{3}_{0.49}\ Ti_{0.05}\ Mg_{2.41}\ Fe^{2}_{1.11}\ Mn_{0.03})\ Si_{6.46}\ Al_{1.54}\ O_{22}\ (OH)_2$

WM 235 $(Na, K)_{0.49}\ (Ca_{1.86}\ Na_{0.14})$

$(Al_{0.38}\ Fe^{3}_{0.57}\ Ti_{0.14}\ Mg_{2.35}\ Fe^{2}_{1.49}\ Mn_{0.05})\ Si_{6.44}\ Al_{1.56}\ O_{22}\ (OH)_2$

WM 237 $(Na, K)_{0.46}\ (Mn_{0.01}\ Ca_{1.85}\ Na_{0.14})$

$(Al_{0.34}\ Fe^{3}_{0.20}\ Ti_{0.20}\ Mg_{2.33}\ Fe^{2}_{1.90}\ Mn_{0.03})\ Si_{6.73}\ Al_{1.27}\ O_{22}\ (OH)_2$

WM 238 $(Na, K)_{0.35}\ (Fe^{2}_{0.03}\ Mn_{0.04}\ Ca_{1.72}\ Na_{0.21})$

$(Al_{0.60}\ Fe^{3}_{0.38}\ Ti_{0.11}\ Mg_{2.51}\ Fe^{2}_{1.40})\ Si_{6.63}\ Al_{1.37}\ O_{22}\ (OH)_2$

WM 242 $(Na, K)_{0.28}\ (Ca_{1.81}\ Na_{0.19})$

$(Al_{0.33}\ Fe^{3}_{0.64}\ Ti_{0.17}\ Mg_{2.50}\ Fe^{2}_{1.24}\ Mn_{0.04})\ Si_{6.75}\ Al_{1.25}\ O_{22}\ (OH)_2$

WM 244 $(Na, K)_{0.29}\ (Fe^{2}_{0.08}\ Mn_{0.05}\ Ca_{1.74}\ Na_{0.13})$

$(Al_{0.53}\ Fe^{3}_{0.47}\ Ti_{0.09}\ Mg_{2.86}\ Fe^{2}_{1.05})\ Si_{6.65}\ Al_{1.35}\ O_{22}\ (OH)_2$

WM 248 $(Na, K)_{0.16}\ (Ca_{1.78}\ Na_{0.22})$

$(Al_{0.81}\ Fe^{3}_{0.39}\ Ti_{0.06}\ Mg_{2.05}\ Fe^{2}_{1.57}\ Mn_{0.08})\ Si_{6.83}\ Al_{1.17}\ O_{22}\ (OH)_2$

WM 249 $(Na, K)_{0.31}\ (Mn_{0.02}\ Ca_{1.87}\ Na_{0.11})$

$(Al_{0.79}\ Fe^{3}_{0.29}\ Ti_{0.05}\ Mg_{2.49}\ Fe^{2}_{1.37}\ Mn_{0.01})\ Si_{6.64}\ Al_{1.36}\ O_{22}\ (OH)_2$

Amphibole nomenclature:

Based on the system Leake (1978).

SAMPLE	Mg/Fe	NAME
WM 108	0.63	Magnesio hornblende
WM 109	0.50	Ferro hornblende
WM 111	0.50	Ferro hornblende
WM 124	0.40	Ferro hornblende
WM 128	0.45	Ferro hornblende
WM 135	0.51	Magnesio hornblende
WM 137	0.50	Ferro hornblende
WM 138	0.47	Ferro hornblende
WM 139	0.58	Actinolitic hornblende
WM 165	0.34	Ferro tschermakitic hornblende
WM 167	0.28	Ferro hornblende
WM 183	0.62	Magnesio hornblende
WM 201	0.51	Magnesio hornblende
WM 220	0.51	Magnesio hornblende
WM 225	0.49	Ferro hornblende
WM 228	0.30	Ferro-tschermakitic hornblende
WM 232	0.44	Ferro hornblende

WM 234	0.49	Ferro tschermakitic hornblende
WM 235	0.41	Ferro tschermakitic hornblende
WM 237	0.35	Ferro hornblende
WM 238	0.43	Ferro hornblende
WM 242	0.47	Ferro hornblende
WM 244	0.53	Magnesio hornblende
WM 248	0.36	Ferro hornblende
WM 249	0.44	Ferro hornblende

Muscovite formulae:

WM 119 $(Na, Ca, K)_{2.04}\ (Ti_{0.03}\ Fe_{0.37}\ Mg_{0.19}\ Al_{3.56})$
$(Si_{6.04}\ Al_{1.96}\ O_{20})\ (OH)_4$

WM 127 $(Na, K)_{1.99}\ (Ti_{0.13}\ Fe_{0.12}\ Mn_{0.01}\ Mg_{0.17}\ Al_{3.60})$
$(Si_{6.08}\ Al_{1.92}\ O_{20})\ (OH)_4$

WM 132 $(Na, Ca, K)_{2.04}\ (Ti_{0.05}\ Fe_{0.30}\ Mg_{0.15}\ Al_{3.60})$
$(Si_{6.06}\ Al_{1.94}\ O_{20})\ (OH)_4$

WM 134 $(Na,\ K)_{1.98}\ (Ti_{0.11}\ Fe_{0.15}\ Mg_{0.36}\ Al_{3.46})$
$(Si_{6.16}\ Al_{1.84}\ O_{20})\ (OH)_4$

WM 151 $(Na, Ca, K)_{2.00}\ (Ti_{0.10}\ Fe_{0.43}\ Mg_{0.22}\ Al_{3.38})$
$(Si_{6.12}\ Al_{1.88}\ O_{20})\ (OH)_4$

WM 154 $(Na, K)_{1.97}\ (Ti_{0.07}\ Fe_{0.39}\ Mn_{0.01}\ Mg_{0.38}\ Al_{3.33})$
$(Si_{6.20}\ Al_{1.80}\ O_{20})\ (OH)_4$

WM 157 $(Na, K)_{1.97}\ (Ti_{0.06}\ Fe_{0.36}\ Mn_{0.01}\ Mg_{0.34}\ Al_{3.38})$
$(Si_{6.25}\ Al_{1.75}\ O_{20})\ (OH)_4$

WM 160 $(Na, K)_{1.93}\ (Ti_{0.10}\ Fe_{0.47}\ Mg_{0.35}\ Al_{3.25})$
$(Si_{6.29}\ Al_{1.71}\ O_{20})\ (OH)_4$

WM 168 $(Na, K)_{2.01}\ (Ti_{0.04}\ Fe_{0.35}\ Mg_{0.15}\ Al_{3.60})$
$(Si_{6.05}\ Al_{1.95}\ O_{20})\ (OH)_4$

WM 180 $(Na, K)_{1.93}\ (Ti_{0.15}\ Fe_{0.47}\ Mn_{0.01}\ Mg_{0.29}\ Al_{3.25})$
$(Si_{6.21}\ Al_{1.79}\ O_{20})\ (OH)_4$

WM 188 $(Na, K)_{2.00}\ (Ti_{0.12}\ Fe_{0.16}\ Mg_{0.13}\ Al_{3.64})$
$(Si_{6.02}\ Al_{1.98}\ O_{20})\ (OH)_4$

WM195 $(Na, K)_{1.97}\ (Ti_{0.03}\ Fe_{0.23}\ Mn_{0.01}\ Mg_{0.23}\ Al_{3.63})$
$(Si_{6.09}\ Al_{1.91}\ O_{20})\ (OH)_4$

WM 196 $(Na, Ca, K)_{2.00}\ (Ti_{0.11}\ Fe_{0.40}\ Mg_{0.17}\ Al_{3.45})$
$(Si_{6.04}\ Al_{1.96}\ O_{20})\ (OH)_4$

WM 198 $(Na, Ca, K)_{2.00}\ (Ti_{0.10}\ Fe_{0.47}\ Mn_{0.01}\ Mg_{0.25}\ Al_{3.35})$
$(Si_{6.09}\ Al_{1.91}\ O_{20})\ (OH)_4$

WM 221 $(Na, Ca, K)_{1.99}$ $(Ti_{0.12}$ $Fe_{0.42}$ $Mn_{0.01}$ $Mg_{0.18}$ $Al_{3.44})$ $(Si_{6.01}$ $Al_{1.99}$ $O_{20})$ $(OH)_4$

WM 222 $(Na, Ca, K)_{1.98}$ $(Ti_{0.10}$ $Fe_{0.42}$ $Mn_{0.01}$ $Mg_{0.21}$ $Al_{3.41})$ $(Si_{6.07}$ $Al_{1.93}$ $O_{20})$ $(OH)_4$

WM 223 $(Na, Ca, K)_{1.98}$ $(Ti_{0.15}$ $Fe_{0.44}$ $Mn_{0.01}$ $Mg_{0.19}$ $Al_{3.37})$ $(Si_{6.00}$ $Al_{2.00}$ $O_{20})$ $(OH)_4$

WM 226 $(Na, Ca, K)_{1.92}$ $(Ti_{0.08}$ $Fe_{0.37}$ $Mg_{0.17}$ $Al_{3.51})$ $(Si_{6.05}$ $Al_{1.95}$ $O_{20})$ $(OH)_4$

Biotite formulae:

WM 107 $(Na, Ca, K)_{1.91}$ $(Ti_{0.45}$ $Fe_{2.68}$ $Mn_{0.04}$ $Mg_{1.77}$ $Al_{0.65})$ $(Si_{5.34}$ $Al_{2.66}$ $O_{20})$ $(OH)_4$

WM 119 $(Na, Ca, K)_{1.92}$ $(Ti_{0.28}$ $Fe_{2.37}$ $Mn_{0.11}$ $Mg_{2.06}$ $Al_{0.86})$ $(Si_{5.28}$ $Al_{2.72}$ $O_{20})$ $(OH)_4$

WM 130 $(Na, Ca, K)_{1.63}$ $(Ti_{0.30}$ $Fe_{2.83}$ $Mn_{0.02}$ $Mg_{1.83}$ $Al_{0.87})$ $(Si_{5.20}$ $Al_{2.80}$ $O_{20})$ $(OH)_4$

WM 148 $(Na, Ca, K)_{1.88}$ $(Ti_{0.28}$ $Fe_{2.80}$ $Mn_{0.02}$ $Mg_{1.78}$ $Al_{0.86})$ $(Si_{5.23}$ $Al_{2.77}$ $O_{20})$ $(OH)_4$

WM 158 $(Na, Ca, K)_{1.95}$ $(Ti_{0.27}$ $Fe_{2.24}$ $Mn_{0.06}$ $Mg_{2.17}$ $Al_{0.90})$ $(Si_{5.36}$ $Al_{2.64}$ $O_{20})$ $(OH)_4$

WM 179 $(Na, K)_{1.91}$ $(Ti_{0.35}$ $Fe_{3.01}$ $Mn_{0.05}$ $Mg_{1.73}$ $Al_{0.60})$ $(Si_{5.35}$ $Al_{2.65}$ $O_{20})$ $(OH)_4$

WM 184 $(Na, Ca, K)_{1.96}$ $(Ti_{0.33}$ $Fe_{2.38}$ $Mn_{0.07}$ $Mg_{2.40}$ $Al_{0.56})$ $(Si_{5.38}$ $Al_{2.62}$ $O_{20})$ $(OH)_4$

WM 188 $(Na, K)_{1.92}$ $(Ti_{0.95}$ $Fe_{2.90}$ $Mn_{0.01}$ $Mg_{1.50}$ $Al_{0.85})$ $(Si_{5.23}$ $Al_{2.77}$ $O_{20})$ $(OH)_4$

WM 193 $(Na, K)_{1.98}$ $(Ti_{0.36}$ $Fe_{2.66}$ $Mn_{0.05}$ $Mg_{1.85}$ $Al_{0.73})$ $(Si_{5.30}$ $Al_{2.70}$ $O_{20})$ $(OH)_4$

WM 196 $(Na, Ca, K)_{1.77}$ $(Ti_{0.33}$ $Fe_{2.28}$ $Mn_{0.07}$ $Mg_{2.50}$ $Al_{0.63})$ $(Si_{5.33}$ $Al_{2.67}$ $O_{20})$ $(OH)_4$

WM 212 $(Na, Ca, K)_{1.88}$ $(Ti_{0.32}$ $Fe_{2.69}$ $Mn_{0.04}$ $Mg_{1.90}$ $Al_{0.75})$ $(Si_{5.32}$ $Al_{2.68}$ $O_{20})$ $(OH)_4$

WM 227 $(Na, Ca, K)_{1.90}$ $(Ti_{0.34}$ $Fe_{2.47}$ $Mn_{0.05}$ $Mg_{2.19}$ $Al_{0.63})$ $(Si_{5.43}$ $Al_{2.57}$ $O_{20})$ $(OH)_4$

WM 231 $(Na, K)_{1.95}$ $(Ti_{0.46}$ $Fe_{2.61}$ $Mn_{0.04}$ $Mg_{2.07}$ $Al_{0.46})$ $(Si_{5.38}$ $Al_{2.62}$ $O_{20})$ $(OH)_4$

WM 233 $(Na, Ca, K)_{1.87}$ $(Ti_{0.37}$ $Fe_{2.80}$ $Mn_{0.04}$ $Mg_{2.05}$ $Al_{0.50})$ $(Si_{5.34}$ $Al_{2.66}$ $O_{20})$ $(OH)_4$

A.5.3 ION-PROBE CHEMICAL DETERMINATIONS.

SAMPLE	ION YIELD* $M^{\pm}/Si^{\pm}$	WM 183	WM 201	WM 220	WM 225	WM 232
Oxides in percent.						
SiO_2	1.00	55.0	44.5	50.0	48.7	47.2
TiO_2	2.57	0.45	1.20	0.68	0.89	1.20
Al_2O_3	2.36	6.56	12.2	10.2	10.4	10.2
FeO	0.99	10.0	14.7	12.5	13.4	14.1
MnO	1.10	0.25	0.32	0.42	0.30	0.48
MgO	2.16	13.6	10.5	12.7	12.0	11.8
CaO	3.17	11.4	12.1	10.4	10.9	11.3
Na_2O	0.89	0.63	1.56	1.02	1.04	1.50
K_2O	0.96	0.12	0.57	0.22	0.29	0.51
F	0.0038	0.06	0.13	0.23	0.16	0.22
Trace elements in ppm.						
V	1.70	150.0	356.0	177.0	318.0	142.0
Cr	1.22	793.0	0.0	240.0	168.0	144.0
Sr	2.50	16.0	454.0	33.0	33.0	35.0
Y	3.50	8.2	15.0	44.0	46.0	15.0
Zr	2.20	6.8	34.0	22.0	28.0	17.0
Nb	1.39	1.0	13.0	5.9	4.1	1.6
Ba	1.59	33.0	142.0	5.1	71.0	9.6
La	2.00	2.0	12.0	9.6	9.8	2.8
Ce	1.98	1.7	23.0	36.0	36.0	12.0
Co	0.50	90.0	114.0	114.0	85.0	88.0

* Ion yield count rate of element (M) ratioed to Si.

A.5.4 POTASSIUM, ARGON AND K-Ar AGE DETERMINATIONS.

SAMPLE	MINERAL TYPE	K wt. %.	AV K wt. %	$^{40}Ar^{*}/^{40}Ar_{T}$	^{40}Ar M/g	AGE (Ma)
WM 107	BIOT	6.6885				
WM 107	BIOT	7.0190	6.99	97.76	6.14×10^{-9}	447 ± 9
WM 108	AMPH	0.1951				
WM 108	AMPH	0.2009				
WM 108	AMPH	0.2096	0.20	96.48	1.93×10^{-10}	453 ± 10
WM 109	AMPH	0.3679				
WM 109	AMPH	0.3766				
WM 109	AMPH	0.3799	0.38	82.24	3.38×10^{-10}	457 ± 10
WM 111	AMPH	0.4964				
WM 111	AMPH	0.4903	0.49	91.30	3.85×10^{-10}	480 ± 10
WM 119	MUSC	8.1005				
WM 119	MUSC	8.0008	8.0	96.92	6.96×10^{-9}	438 ± 9
WM 119	BIOT	6.8747				
WM 119	BIOT	6.9761	6.93	93.16	6.10×10^{-9}	447 ± 9
WM 124	AMPH	0.4645				
WM 124	AMPH	0.4487	0.45	88.12	4.58×10^{-10}	476 ± 10
WM 127	MUSC	8.7344				
WM 127	MUSC	8.6827	8.71	99.54	7.13×10^{-9}	420 ± 8
WM 128	AMPH	0.2289				
WM 128	AMPH	0.2345	0.23	90.35	2.05×10^{-10}	452 ± 9
WM 130	BIOT	4.8932				
WM 130	BIOT	4.9081	4.90	96.75	4.34×10^{-9}	450 ± 10
WM 132	MUSC	6.1520				
WM 132	MUSC	6.2080	6.18	99.80	5.28×10^{-9}	436 ± 9
WM 134	MUSC	7.3996				
WM 134	MUSC	7.0091	6.98	97.71	5.70×10^{-9}	418 ± 8
WM 135	AMPH	0.0813				
WM 135	AMPH	0.0712				
WM 135	AMPH	0.0765	0.08	87.26	6.24×10^{-11}	486 ± 10

WM 136	AMPH	0.0882				
WM 136	AMPH	0.0821	0.09	91.98	7.58×10^{-11}	475 ± 10
WM 137	AMPH	0.0918				
WM 137	AMPH	0.0987				
WM 137	AMPH	0.0874	0.09	92.58	8.94×10^{-11}	471 ± 10
WM 138	AMPH	0.2634				
WM 138	AMPH	0.2775	0.27	89.99	2.56×10^{-10}	478 ± 10
WM 139	AMPH	0.5134				
WM 139	AMPH	0.5271	0.52	89.28	4.25×10^{-10}	419 ± 9
WM 146	AMPH	0.8460				
WM 146	AMPH	0.8424	0.84	93.17	8.45×10^{-10}	477 ± 10
WM 148	BIOT	6.4582				
WM 148	BIOT	6.3407	6.40	96.70	5.44×10^{-9}	433 ± 9
WM 151	MUSC	7.9448				
WM 151	MUSC	8.0089	7.98	98.88	6.48×10^{-9}	416 ± 8
WM 153	MUSC	8.1843				
WM 153	MUSC	8.1021	8.14	98.35	7.26×10^{-9}	453 ± 9
WM 154	MUSC	8.8927				
WM 154	MUSC	8.8870	8.89	98.73	7.32×10^{-9}	422 ± 8
WM 155	AMPH	0.7945				
WM 155	AMPH	0.7823	0.79	94.05	7.56×10^{-10}	482 ± 10
WM 157	MUSC	7.9681				
WM 157	MUSC	7.8642	7.92	99.36	6.72×10^{-9}	433 ± 9
WM 158	BIOT	7.3476				
WM 158	BIOT	7.3747	7.36	98.45	6.35×10^{-9}	439 ± 9
WM 160	MUSC	8.9295				
WM 160	MUSC	8.9675				
WM 160	MUSC	8.8201	8.86	99.23	7.04×10^{-9}	408 ± 8
WM 165	AMPH	0.1405				
WM 165	AMPH	0.1396	0.14	83.10	1.37×10^{-10}	479 ± 10
WM 167	AMPH	0.4388				
WM 167	AMPH	0.4377	0.44	92.57	3.64×10^{-10}	424 ± 9

WM 168	MUSC	7.9620				
WM 168	MUSC	7.5938				
WM 168	MUSC	7.2784	7.61	98.23	6.66×10^{-9}	445 ± 9
WM 179	BIOT	7.4743				
WM 179	BIOT	7.5315	7.50	99.08	6.29×10^{-9}	428 ± 9
WM 180	MUSC	8.4923				
WM 180	MUSC	8.3930	8.44	99.80	7.74×10^{-9}	463 ± 9
WM 183	AMPH	0.2077				
WM 183	AMPH	0.2012	0.20	86.66	1.25×10^{-10}	334 ± 7
WM 184	BIOT	7.1693				
WM 184	BIOT	7.1521	7.16	99.55	4.85×10^{-9}	416 ± 8
WM 188	MUSC	7.7706	(125 - 250 microns)			
WM 188	MUSC	7.8817	7.83	98.60	6.49×10^{-9}	425 ± 9
WM 188	MUSC	7.8134	(500 - 2000 microns)			
WM 188	MUSC	7.7956	7.80	98.14	6.73×10^{-9}	431±9
WM 188	BIOT	6.0519				
WM 188	BIOT	6.0524	6.05	98.60	5.31×10^{-9}	411 ± 8
WM 193	BIOT	7.2312				
WM 193	BIOT	7.2693	7.25	99.26	6.23×10^{-9}	458 ± 9
WM 193	MUSC	8.0734				
WM 193	MUSC	8.1674	8.12	98.40	7.45×10^{-9}	478±10
WM 195	MUSC	8.1657				
WM 195	MUSC	8.3686	8.27	99.80	6.81×10^{-9}	422 ± 8
WM 196	BIOT	5.1760	(125 - 250 microns)			
WM 196	BIOT	5.1598	5.17	97.81	4.05×10^{-9}	403 ± 8
WM 196	BIOT	5.2016	(500 - 1000 microns)			
WM 196	BIOT	5.1956	5.20	98.25	4.01×10^{-9}	402±8
WM 196	MUSC	7.9431				
WM 196	MUSC	7.8979	7.92	98.91	6.93×10^{-9}	445 ± 9
WM 198	MUSC	8.2281				
WM 198	MUSC	8.2577	8.24	79.95	7.45×10^{-9}	458 ± 10
WM 200	AMPH	0.3254				
WM 200	AMPH	0.3462	0.34	91.33	5.48×10^{-10}	472 ± 10

WM 201	AMPH	0.4157				
WM 201	AMPH	0.4219	0.42	83.85	2.79×10^{-10}	349 ± 8
WM 212	BIOT	6.2252				
WM 212	BIOT	6.0918	6.16	99.01	5.13×10^{-9}	426 ± 9
WM 220	AMPH	0.2140				
WM 220	AMPH	0.2138	0.21	91.96	1.66×10^{-10}	406 ± 8
WM 221	MUSC	8.1256				
WM 221	MUSC	8.0815	8.10	99.44	6.55×10^{-9}	415 ± 8
WM 222	MUSC	7.8492				
WM 222	MUSC	7.7906	7.82	99.23	7.18×10^{-9}	464 ± 9
WM 223	MUSC	6.5915				
WM 223	MUSC	6.5165	6.55	99.18	5.72×10^{-9}	444 ± 9
WM 224	AMPH	0.2599				
WM 224	AMPH	0.2578	0.26	86.06	2.00×10^{-10}	397 ± 8
WM 225	AMPH	0.7778				
WM 225	AMPH	0.7553	0.77	94.95	6.82×10^{-10}	452 ± 9
WM 226	MUSC	7.6195				
WM 226	MUSC	7.7543	7.69	99.69	7.01×10^{-9}	461 ± 9
WM 227	BIOT	6.8283				
WM 227	BIOT	6.8653	6.85	99.85	6.14×10^{-9}	454 ± 9
WM 228	AMPH	1.0872				
WM 228	AMPH	1.0758	1.08	93.80	1.03×10^{-10}	481 ± 10
WM 231	BIOT	6.6332				
WM 231	BIOT	6.6762	6.65	99.98	5.57×10^{-9}	428 ± 9
WM 232	AMPH	0.4331				
WM 232	AMPH	0.4313	0.43	94.97	4.00×10^{-10}	467 ± 9
WM 233	BIOT	5.8580				
WM 233	BIOT	5.8924	5.88	99.67	5.24×10^{-9}	453 ± 9
WM 234	AMPH	0.2721				
WM 234	AMPH	0.2613	0.27	87.26	2.46×10^{-10}	466 ± 10
WM 235	AMPH	0.8111				
WM 235	AMPH	0.8103	0.81	96.12	7.14×10^{-10}	447 ± 9

WM 237	AMPH	0.7322				
WM 237	AMPH	0.7481	0.74	91.24	5.86×10^{-10}	407 ± 8
WM 238	AMPH	0.3254				
WM 238	AMPH	0.3314	0.33	92.11	3.13×10^{-10}	480 ± 10
WM 242	AMPH	0.6234				
WM 242	AMPH	0.6221	0.62	93.45	5.14×10^{-10}	472 ± 9
WM 244	AMPH	0.3158				
WM 244	AMPH	0.3289	0.32	88.97	3.24×10^{-10}	436 ± 9
WM 248	AMPH	0.2318				
WM 248	AMPH	0.2219				
WM 248	AMPH	0.2171	0.22	90.23	8.65×10^{-10}	462 ± 9
WM 249	AMPH	0.3678				
WM 249	AMPH	0.3812	0.37	91.87	4.56×10^{-10}	459 ± 9

A.5.5 ^{40}Ar-^{39}Ar INCREMENTAL STEP-HEATING RESULTS.

ºC	cum 39	37./39	38./39	$40^{*}./39_K$	40/36	Ma	±
WM 167							
600	0.0193	7.0321	0.4097	56.9197	430.8	504.4	63.8
800	0.0613	4.6286	0.1198	21.9044	849.2	413.9	22.2
950	0.1400	7.9320	0.0614	16.8201	1804.3	409.5	16.3
1000	0.2834	8.3478	0.0330	16.6655	3677.1	442.6	8.8
1050	0.4775	8.2720	0.0257	16.3515	4643.8	442.2	6.9
1100	0.6270	8.0887	0.0287	16.9838	2820.3	440.0	9.3
1150	0.8653	8.9886	0.0344	16.5453	2884.5	430.4	10.3
1200	1.0000	8.8016	0.0364	18.2542	1639.6	433.8	25.2

ºC	cum. 39	37./39	38./39	$40^{*}./39_K$	40/36	Ma	±
WM 201							
600	0.1067	2.8501	0.1265	23.7539	578.5	345.4	3.9
800	0.2697	4.2355	0.0720	14.8303	1137.9	328.1	3.2
900	0.4705	4.3006	0.0914	12.6939	2654.4	336.2	2.5
950	0.5968	9.9399	0.1631	14.8410	2579.5	386.2	2.7

970	0.6800	10.5328	0.1721	13.1224	2624.2	345.9	3.6
990	0.7403	10.3209	0.1675	13.3411	2550.6	350.3	5.7
1010	0.7823	8.7567	0.1454	12.8363	2071.1	328.0	10.5
1030	0.8112	7.9251	0.1417	13.1054	4502.1	362.4	36.5
1060	0.8414	8.6852	0.1633	14.1454	1371.7	331.4	9.4
1090	0.8725	12.4317	0.2512	16.1614	1392.7	374.8	12.6
1120	0.9155	15.4361	0.3176	17.0077	1379.2	391.8	12.5
1150	0.9598	16.2219	0.3347	17.7355	1495.0	414.8	12.2
1170	0.9874	17.4946	0.3238	18.3016	1139.9	397.0	22.5
1200	1.0000	24.3027	0.3225	22.3276	614.7	343.9	71.9

°C	cum. 39	37./39	38./39	$40^{*}./39_{K}$	40/36	Ma	±
WM 225							
600	0.0100	3.5030	0.1750	53.5867	335.7	196.4	65.6
800	0.0289	3.4661	0.0391	28.6096	451.4	296.5	62.8
900	0.0457	4.7846	0.0573	26.3362	515.9	334.5	83.7
950	0.0572	8.3478	0.1071	30.5147	523.9	389.2	48.5
970	0.0685	11.2810	0.1362	28.0043	620.3	423.0	58.8
990	0.0981	13.3042	0.1248	20.1509	941.9	403.8	14.7
1020	0.4427	13.0490	0.0802	17.3003	5062.9	467.7	2.7
1040	0.4776	12.2200	0.0713	20.7442	1176.2	448.1	12.2
1060	0.4942	10.5975	0.0948	23.0868	801.2	422.6	24.9
1080	0.4999	12.5479	0.1014	20.0477	905.6	564.3	78.9
1100	0.5379	13.1812	0.0938	19.9559	1085.3	421.9	19.0
1121	0.6247	13.0781	0.0913	21.2273	2795.1	534.2	9.7
1140	0.7392	12.9279	0.0835	19.9637	2931.2	508.9	12.9
1160	0.9374	12.6128	0.0698	18.2434	3283.6	475.5	5.6
1180	0.9892	12.2931	0.0768	19.4841	1083.9	412.9	17.3
1200	1.0000	11.9603	0.0811	34.5101	520.0	431.9	114.9

°C	cum. 39	37./39	38./39	$40^{*}./39_{K}$	40/36	Ma	±
WM 228							
600	0.0354	1.8929	0.0896	27.0313	542.2	363.7	3.7
800	0.0804	1.2236	0.0425	13.8291	1575.3	334.9	2.4
900	0.1252	3.0819	0.1834	16.6781	2781.8	432.4	3.2
950	0.1988	3.2638	0.2661	16.7516	5455.4	456.3	2.7
970	0.2846	3.1024	0.2654	16.9693	8142.3	469.3	3.6
990	0.3851	2.9432	0.2377	16.2051	9372.8	452.6	2.5

1010	0.4798	2.9231	0.2230	16.6138	11074.0	464.6	2.5
1030	0.5815	2.8017	0.1970	16.0246	10610.9	449.6	2.5
1060	0.7042	2.7000	0.1665	15.7186	11786.3	443.1	2.4
1080	0.7760	2.4715	0.1387	16.2339	12758.0	456.7	2.8
1100	0.8251	2.1461	0.1263	16.2454	9236.3	453.4	3.3
1120	0.8726	2.1168	0.1271	16.3636	10747.2	458.0	3.6
1140	0.9276	2.5900	0.1490	16.4400	9566.5	458.6	3.7
1160	0.9667	3.3728	0.1768	17.8397	7908.2	489.9	5.7
1180	0.9822	4.4321	0.1884	16.7410	3453.7	442.2	15.9
1200	1.0000	6.3220	0.1874	21.3107	2452.6	528.7	15.1

°C	cum. 39	37./39	38./39	$40^{*}./39_{K}$	40/36	Ma	±
WM 232							
500	0.0067	4.8870	0.5164	70.1958	326.5	204.4	115.6
600	0.0224	1.3078	0.1414	21.6107	630.2	341.1	58.5
750	0.0505	1.7505	0.1212	19.7909	745.7	354.3	11.8
900	0.1106	6.0336	0.0606	13.7184	2336.6	355.2	11.4
950	0.1595	8.0549	0.0544	14.7907	2794.0	388.5	5.6
970	0.2111	7.6189	0.0536	15.1402	3227.0	401.9	4.9
990	0.3053	8.0477	0.0528	17.5161	5755.7	475.8	3.7
1010	0.4287	8.2642	0.0503	17.1990	6019.0	469.3	3.1
1030	0.5232	8.1468	0.0511	17.3618	7653.5	477.8	3.2
1060	0.5973	7.9370	0.0493	18.2582	6531.2	496.3	4.1
1080	0.6706	7.7481	0.0489	18.1868	6122.8	493.2	6.3
1100	0.7595	7.9727	0.0528	18.2883	5880.6	494.7	4.8
1120	0.8357	8.1880	0.0570	18.7322	6991.6	508.9	5.6
1140	0.8993	8.2470	0.0591	19.4463	5597.2	520.6	6.6
1160	0.9518	7.9209	0.0554	16.0398	3480.1	426.1	9.4
1180	0.9638	10.4526	0.0849	22.7424	1966.7	542.6	46.2
1200	1.0000	8.0206	0.0565	16.6227	3004.9	434.4	17.3

A.5.6 ^{40}Ar-^{39}Ar LASER-PROBE AGES.

In the following tables all analyses are of hornblende unless otherwise stated. All the following data is in corrected molar amounts. The abundances of K, Ca, and Cl are in E-9 moles whilst ^{36}Ar, ^{40}Ar and $^{40}Ar^*$ are in E-18 moles. The Cl abundances have been calculated from the measured ^{38}Ar, although because of cadmium shielding in the reactor this reaction was muted. The Ca abundances have been calculated from from the $^{36}Ar/^{37}Ar$ and $^{39}Ar/^{37}Ar$ ratios. The K abundances have been calculated from the $^{40}Ar/^{39}Ar$ ratio. The ^{40}Ar column is total ^{40}Ar, while $^{40}Ar^*$ radiogenic ^{40}Ar.

Analyses from WM 201.

No.	Ca	Cl	K	^{36}Ar	^{40}Ar	$^{40}Ar^*$	AGE (Ma)
NO 86	1191	0.68	38.7	0.6064	296.2	117.1	398 ± 36
NO 87	323	-0.92	9.8	0.0189	29.0	23.4	323 ± 145
NO 89	2545	-0.55	87.5	0.1947	343.8	286.3	428 ± 11
NO 90	3844	3.46	148.1	0.6732	800.4	601.4	517 ± 10
NO 92	4901	2.78	131.1	2.1593	1136.8	498.7	488 ± 10
NO 93	4805	1.57	247.4	1.9431	1343.2	769.0	409 ± 7
NO 95	3676	1.11	85.9	0.5436	501.0	340.3	506 ± 31
NO 96	3042	2.13	489.0	1.3717	1569.1	1163.8	321 ± 7
NO 98	4339	3.47	112.9	2.0275	1145.2	546.1	601 ± 26
NO 99	4897	4.3	139.8	0.9832	890.7	600.2	543 ± 20
NO 103	1676	4.24	207.7	2.5669	1912.1	1153.6	675 ± 14
NO 104	3654	-0.66	137.7	0.2627	573.4	495.8	465 ± 18
NO 106	9394	12.8	386.4	4.4501	2831.6	1516.6	502 ± 6
NO 118	1360	-0.41	47.6	0.0158	188.0	183.3	494 ± 43
NO 119	7119	5.05	325.0	1.0176	1380.9	1080.2	434 ± 8
NO 121	3101	3.38	119.3	0.7303	756.7	540.9	569 ± 19
NO 128	1990	-1.3	78.7	0.4041	404.4	285.0	468 ± 20
NO 129	6932	5.71	248.4	1.1733	1328.1	981.4	505 ± 10
NO 132	13430	21.46	763.8	5.4627	4148.9	2534.7	433 ± 7

NO 122*	5295	1.86	123.6	0.7728	836.7	608.3	610 ± 7
NO 131*	6350	0.8	81.8	0.0977	325.9	297.0	469 ± 19
NO 148‡	2773	-0.02	304.6	2.2071	1617.3	965.1	416 ± 8
NO 149‡	5662	-1.1	153.3	1.1626	1170.5	827.0	659 ± 39

* These analyses are from quartz/calcite veins in the rock slice.
‡ These analyses are of quartzo-feldspathic areas.

Analyses from WM 220.

No.	Ca	Cl	K	^{36}Ar	^{40}Ar	$^{40}Ar^{*}$	AGE (Ma)
NO 107	1656	-2.63	44.6	0.0786	215.5	192.3	544 ± 34
NO 109	9721	12.55	805.0	3.2491	3397.5	2437.4	399 ± 5
NO 110	7989	4.77	292.3	0.5722	1305.3	1136.2	498 ± 6
NO 112	11079	17.0	762.8	8.5232	5378.5	2859.9	482 + 5
NO 113	5031	3.2	382.5	4.8767	2911.1	1470.0	493 ± 8
NO 115	4840	3.0	236.2	1.6536	1446.6	957.2	516 ± 11
NO 135	5567	5.86	305.3	1.6279	1697.5	1216.5	509 ± 8
NO 136	7901	7.97	397.2	3.0673	2188.1	1281.7	422 ± 8
NO 138	6169	0.72	158.3	0.7848	2110.1	1621.4	528 ± 8
NO 141	7310	6.1	386.7	2.7603	2239.4	1423.8	495 ± 8
NO 142	8969	7.36	192.7	2.8391	2235.9	1397.0	840 ± 13
NO 144	1572	-8.05	569.1	2.0141	2392.3	1797.1	414 ± 9

A.5.7 HYDROGEN ISOTOPE DETERMINATIONS.

SAMPLE	cm Hg of H_2	$\mu M/\mu Mmg^{-1}$	$\delta D_{(SMOW)}$	wt.% H_2O
Biotite:				
WM 107	24.2	2.45	-65.7	4.42
WM 148	20.6	2.248	-63.6	4.05
WM 179	17.1	2.025	-65.6	3.65
WM 188	24.2	2.44	-65.5	4.42
WM 227	18.9	2.012	-64.0	3.62
WM 231	21.3	1.96	-72.2	3.54
WM 233	19.28	1.92	-63.4	3.48
Muscovite:				
WM 151	14.7	1.78	-42.2	3.21
WM 180	22.65	2.522	-44.6	3.54
WM 188	24.95	2.44	-33.4	4.39
WM 195	43.0	1.953	-39.7	3.52
WM 223	18.1	2.24	-43.6	4.03
WM 226	22.5	2.443	-38.7	4.40
Amphibole:				
WM 111	29.45	1.311	-57.2	2.36
WM 124	18.5	1.334	-67.9	2.40
WM 128	22.6	1.207	-66.2	2.18
WM 135	29.6	1.44	-58.7	2.59
WM 137	35.1	1.485	-57.2	2.68
WM 138	40.0	1.66	-48.0	2.99
WM 139	25.9	1.190	-62.4	2.48
WM 165	20.3	1.172	-68.8	2.11
WM 167	29.0	1.328	-61.3	2.39
WM 183	33.05	1.510	-51.5	2.72
WM 201	31.87	1.358	-55.2	2.54
WM 220	32.04	1.487	-62.4	2.18
WM 224	26.5	1.194	-61.2	2.15
WM 232	29.6	1.325	-67.7	2.11
WM 234	26.8	1.167	-72.7	2.10
WM 235	30.1	1.446	-61.4	2.61

WM 237	34.7	1.484	-60.9	2.67
WM 238	24.25	1.017	-75.1	1.83
WM 242	29.60	1.377	-67.0	2.41

A.5.8 OXYGEN ISOTOPE DETERMINATIONS.

SAMPLE	OXYGEN LINE	CO_2 YIELD	$\delta^{18}O$ (RAW)	$\delta^{18}O$ (SMOW)	$\delta^{18}O$ (SMOW) Av.
Amphibole only:					
WM 124	F12	11.67	-20.719	+10.605	
WM 124	F12	14.27	-16.467	+14.993*	
WM 124	F12	11.84	-20.362	+10.708	+10.67
WM 128	F12	13.29	-22.841	+8.415	
WM 128	F12	11.90	-22.561	+8.704	+8.56
WM 139	F12	12.1	-26.4	+4.68*	
WM 139	F12	13.01	-21.9	+9.31	
WM 139	F12	10.02	-25.412	+5.762*	
WM 139	F12	12.68	-21.233	+10.075	
WM 139	F6	14.14	-21.946	+9.278	+9.55
WM 165	F12	12.12	-21.793	+9.497	
WM 165	F12	12.60	-23.305	+7.936	+8.72
WM 167	F12	14.19	-22.093	+9.187	
WM 167	F12	13.21	-22.52	+8.746	+8.97
WM 183	F6	14.89	-25.62	+5.481	
WM 183	F6	11.38	-25.78	+5.31	+5.40
WM 201	F12	13.60	-24.367	+6.78	
WM 201	F12	12.50	-24.516	+6.69	+6.74
WM 220	F12	12.41	-22.391	+8.81	
WM 220	F12	11.95	-22.542	+8.724	+8.77

WM 225	F12	12.72	-23.870	+7.29	
WM 225	F12	12.84	-23.929	+7.29	+7.29
WM 232	F12	12.41	-22.605	+8.60	
WM 232	F12	11.48	-22.743	+8.46	+8.53
WM 234	F12	13.06	-26.3	+4.785*	
WM 234	F12	6.62	-24.61	+6.521	
WM 234	F6	12.94	-24.716	+6.373	
WM 234	F6	14.69	-24.915	+6.167	+6.35
WM 238	F6	13.28	-24.571	+6.569	
WM 238	F6	12.59	-24.458	+6.67	+6.62
WM 242	F12	11.27	-27.528	+3.52*	
WM 242	F12	13.37	-25.214	+5.91	
WM 242	F6	10.48	-25.797	+5.257	
WM 242	F6	10.29	-25.662	+5.397	+5.52

* These samples have been rejected from calculations and interpretations.

REFERENCES

Alexander, E.C., Mickelson, G.M. & Lanphere, M.A. (1978) MMhb-1: A new ^{40}Ar-^{39}Ar dating standard. *United States Geological Survey, Open File Report,* **78-701,** 6-8.

Anderson, S.L. (1988) Interpretation of K-Ar mineral dates from the Grenville Orogenic Belt. *American Journal of Science,* **288,** 701-734.

Anderton, R. (1982) Dalradian deposition and the late Precambrian-Cambrian history of the N Atlantic region; a review of the early evolution of the Iapetus Ocean. *Journal of the Geological Society of London,* **139,** 421-431.

Armstrong, R.L. (1966) K-Ar dating of plutonic rocks and volcanic rocks in orogenic belts. *In,* Schaeffer, O.A. & Zahringer, J. (eds.) *Potassium-argon dating.* Springer-Verlag.

Badley, M.E. (1976) Stratigraphy, structure and metamorphism of Dalradian rocks of the Maumturk Mountains, Connemara, Ireland. *Journal of the Geological Society of London,* **132,** 509-520.

Bailey, E.B. & Holtedahl, O. (1938) *Northwestern Europe- Caledonides Handbook of Regional Geology.* Leipzig: Akademie Verlag.

Barber, J.P. & Yardley, B.W.D. (1985) Conditions of high grade metamorphism in the Dalradian of Connemara, Ireland. *Journal of the Geological Society of London,* **142,** 87-96.

Berger, G.W. & York, D. (1981) Geothermometry from ^{40}Ar-^{39}Ar dating experiments. *Geochimica et Cosmochimica Acta,* **45,** 795-811.

Berry, R.F. & McDougall, I. (1986) Interpretation of $^{40}Ar/^{39}Ar$ and K-Ar dating evidence from the Aileu Formation, East Timor, Indonesia. *Chemical Geology (Isotope Geoscience Section),* **59,** 43-58.

Blanckenburg, F.V. & Villa, I.M. (1988) Argon retentivity and argon excess in amphiboles from the garbenschists of the western Tauern Window, eastern Alps. *Contributions to Mineralogy and Petrology,* **100,** 1-11.

Blanckenburg, F.v., Villa, I.M., Baur, H., Morteani, G. & Steiger, R.H. (1989) Time calibration of a P-T path from the western Tauern Window, eastern Alps: the problem of closure temperature. *Contributions to Mineralogy and Petrology,* **101**, 1-11.

Bluck, B.J. (1984) Pre-Carboniferous history of the Midland Valley of Scotland. *Transactions of the Royal Society of Edinburgh: Earth Sciences,* **75**, 275-295.

Bluck, B.J. & Leake, B.E. (1986) Late Ordovician to Early Silurian amalgamation of the Dalradian and adjacent Ordovician rocks of the British Isles. *Geology,* **14**, 917-919.

Borthwick, J. & Harmon, R.S. (1982) A note regarding ClF_3 as an alternative to BrF_5 for oxygen isotope analysis. *Geochimica et Cosmochimica Acta,* **46**, 1665-1668.

Bottinga, Y. & Javoy, M. (1973) Comments on oxygen isotope geothermometry. *Earth and Planetary Science Letters,* **20**, 251-265.

Bradshaw, R., Plant, A.G., Burke, K.C. & Leake, B.E. (1969) The Oughterard Granite, Connemara, Co. Galway. *Proceedings of the Royal Irish Acadamy,* **68B**, 39-65.

Brown, E.H. (1971) Phase relations of biotite and stilpnomelane in the greenschist facies. *Contributions to Mineralogy and Petrology,* **31**, 275-299.

Champness, P.E. & Lorimer, G.W. (1976) Exsolution in silicates. *In,* Wenk, H.R. (ed.) *Electron Microscopy in Mineralogy,* 174-205, Springer-Verlag.

Chopin, C. & Maluski, H. (1980) ^{40}Ar-^{39}Ar dating of high pressure metamorphic micas from the Gran Paradiso area (western Alps): Evidence against the blocking temperature concept. *Contributions to Mineralogy and Petrology,* **74**, 109-122.

Clauer, N., O'Neil, J.R. & Courtois-Bonnot, C. (1982) The effect of natural weathering on the chemical and isotopic compositions of biotites. *Geochimica et Cosmochimica Acta,* **46**, 1755-1762.

Clayton, R,N., Goldsmith, J.R., Karel, K.J., Mayeda, T.K. & Newton, R.C. (1975) Limits on the effect of pressure on isotopic fractionation. *Geochimica et Cosmochimica Acta,* **39**, 1197-1201.

Cole, D.R., Ohmoto, H. & Lasaga, A.C. (1983) Isotopic exchange in mineral-fluid systems. I. Theoretical evaluation of oxygen isotopic exchange accompanying surface reactions and diffusion. *Geochimica et Cosmochimica Acta,* **47**, 1681-1693.

Coller, D.W. (1984) Varsican structures in the Upper Palaeozoic rocks of west central Ireland. *In,* Hutton, D.H. & Sanderson, D.J. (eds) *Varsican Tectonics of the North Atlantic Region,* Geological Society of London Special Publication, **14**, 185-194.

Crank, J. (1975) The mathematics of diffusion. *Oxford University Press.*

Dallmeyer, R.D. (1978) ^{40}Ar-^{39}Ar incremental release ages of hornblende and biotite across the Georgia Inner Piedmont: their bearing on late Palaeozoic - early Mesozoic tectonothermal history. *American Journal of Science,* **278**, 124-149.

Deer, W.A., Howie, R.A. & Zussman, J. (1966) An Introduction to the Rock Forming Minerals. *Longmans, Green and Co,* 528pp.

Del Moro, A., Puxeddu, M., Radicati di Brozolo, F. & Villa, I.M. (1982) Rb-Sr and K-Ar ages on minerals at temperatures of 300°c-400°c from deep wells in the Larderello geothermal field (Italy). *Contributions to Mineralogy and Petrology,* **81**, 340-349.

Desmons, J., Hunziker, J.C. & Delaloye, M. (1982) Unconvincing evidence against the blocking temperature concept. Comments on: "^{40}Ar-^{39}Ar dating of high pressure metamorphic micas from the Gran Paradiso area (western Alps): Evidence against the blocking temperature concept." by Chopin, C. & Maluski, H. *Contributions to Mineralogy and Petrology,* 80, 386-390.

Deutsch, A. & Steiger, R.H. (1985) Hornblende K-Ar ages and the climax of Tertiary metamorphism in the Lepontine Alps (south-central Switzerland): an old problem reassessed. *Earth and Planetary Science Letters,* **72**, 175-189.

Dewey, J.F. (1961) A note concerning the age of the metamorphism of the Dalradian rocks of western Ireland. *Geological Magazine,* **98**, 399-405.

Dewey, J.F. (1962) The provinence and emplacement of Upper Arenigian turbidites in County Mayo, Eire. *Geological Magazine,* **99**, 238-252.

Dewey, J.F., McKerrow, W.S. & Moorbath, S. (1970) The relationship between isotopic ages, uplift and sedimentation during Ordovician times in western Ireland. *Scottish Journal Of Geology,* **6**, 133-145.

Dodson, M.H. (1973) Closure temperature in cooling geochronological and petrological systems. *Contributions to Mineralogy and Petrology,* **40**, 259-274.

Elias, E.M. (1985) K-Ar and Rb-Sr isotope studies in Connemara, western Ireland. *Unpublished Ph.D. Thesis, University of Glasgow.*

Elias, E.M., Macintyre, R.M. & Leake, B.E. (1988) The cooling history of Connemara, western Ireland, from K-Ar and Rb-Sr age studies. *Journal of the Geological Society of London,* **145,** 649-660.

Evans, B.W. & Leake, B.E. (1960) The composition and origin of the striped amphibolites of Connemara, Ireland. *Journal of Petrology,* **1**, 337-341.

Farver, J.R. & Giletti, B.J. (1985) Oxygen diffusion in amphiboles. *Geochimica et Cosmochimica Acta,* **49**, 1403-1411.

Faure, G. (1986) Principles of Isotope Geology, 2nd Ed. *John Wiley and Sons.* 589pp.

Feely, M. & Madden, J.S. (1986) A quantitative regional gamma-ray survey on the main Galway Granite, western Ireland. *In,* Andrew, C.J., Crowe, R.W.A., Finaly, S., Pennell, W.M. & Pyne, J.F. (eds), *The Geology and Genesis of Mineral Deposits in Ireland,* Irish Association of Economic Geology, 195-200.

Feely, M. & Madden, J.S. (1987) The spatial distribution of K, U, Th and surface heat production in the Galway Granite, Connemara, western Ireland. *Irish Journal of Earth Sciences,* **8**, 155-164.

Feely, M. & Madden, J.S. (1988) Trace element variation in the leucogranites within the main Galway Granite, Connemara, Ireland. *Mineralogical Magazine,* **52,** 139-146.

Ferguson, C.C. & Al-Ameen, S.I. (1985) Muscovite breakdown and corundum growth at anomalously low f_{H2O}: a study of contact metamorphism and convective luid movement around the Omey granite, Connemara, Ireland. *Mineralogical Magazine,* **49,** 505-514.

Fitch, F.J., Miller, J.A. & Brown, P.E. (1964) Age of Caledonian orogeny and metamorphism in Britain. *Nature,* **203,** 275-278.

Gaber, L.J., Foland, K.A. & Corbato, C.E. (1988) On the significance of argon release from biotite and amphibole during $^{40}Ar/^{39}Ar$ vacuum heating. *Geochimica et Cosmochimica Acta,* **52,** 2457-2465.

Gerling, E.K., Koltsova, T.V., Petrov, B.V. & Zulfikarora, Z.K. (1965) On the suitability of amphiboles for age determinations by the K-Ar method. *Geochemistry International,* **2,** 148-154.

Ghose, S. (1981) Subsolidus reactions and microstructures in amphiboles. *In,* Veblen, D.R. (ed.) *Amphiboles and Other Hydrous Pyriboles-Mineralogy.* Mineralogical Society of America, Reviews in Mineralogy, 9A.

Giletti, B.J. (1974) Diffusion related to geochronology. *In,* Hofmann, A.W., Giletti, B.J., Yoder, H.S. & Yund, R.A. (eds.) *Geochemical Transport and Kinetics.* Carnegie Institute of Washington Publication, **634,** 3-13.

Giletti, B.J. & Yund, R.A. (1984) Oxygen diffusion in quartz. *Journal of Geophysical Research,* **89,** 4039-4046.

Giletti, B.J., Moorbath, S. & Lambert, R. St.J. (1961) A geochronological study of the metamorphic complexes of the Scottish Highlands. *Quarterly Journal of the Geological Society of London,* **117,** 233-272.

Gittos, M.F., Lorimer, G.W. & Champness, P.E. (1974) Precipitation (exsolution) in an amphibole (the hornblende-grunerite system). *Journal of Material Science,* 9, 184-192.

Gittos, M.F., Lorimer, G.W. & Champness, P.E. (1976) The phase distributions in some exsolved amphiboles. *In,* Wenk, H.R. (ed.) *Electron Microscopy in Mineralogy,* 238-248, Springer-Verlag.

Godfrey, J.D. (1962) The deuterium content of hydrous minerals from the east-central Sierra Nevada and Yosemite National Park. *Geochimica et Cosmochimica Acta,* **26,** 1215-1245.

Graham, C.M. & Sheppard, S.M.F. (1980) Experimental hydrogen isotope studies, 2: fractionations in the systems epidote-NaCl-H2O, epidote-CaCl2-H2O and epidote-seawater, and the hydrogen isotope compositions of natural epidotes. *Earth and Planetray Sciences Letters,* **49,** 237-251.

Graham, C.M., Sheppard, S.M.F. & Heaton, T.H.E. (1980) Experimental hydrogen isotope studies-1. Systematics of hydrogen isotope fractionation in the systems epidote-H2O, zoisite-H2O and AlO(OH)-H2O. *Geochemica et Cosmochemica Acta,* **44,** 353-364.

Graham, C.M., Harmon, R.S. & Sheppard, S.M.F. (1984) Experimental hydrogen isotope studies: hydrogen isotope exchange between amphibole and water. *American Mineralogist,* **69,** 128-138.

Graham, J.R. (1987) The nature and field relations of the Ordovician Maumtrasna Formation, County Mayo, Ireland. *Geological Journal,* **22,** 347-369.

Halliday, A.N., Graham, C.M., Aftalion, M. & Dymoke, P. (1989) The depositional age of the Dalradian Supergroup: U-Pb and Sm-Nd isotopic studies of the Tayvallich Volcanics, Scotland. *Journal of the Geological Society of London,* **146,** 3-6.

Hanson, G.N. & Gast, P.W. (1967) Kinetic studies in contact metamorphic zones. *Geochemica et Cosmochemica Acta,* **31,** 1119-1153.

Harris, A.L. & Pitcher, W.S. (1975) The Dalradian Supergroup. *In* Harris, A.L. *et.al.* (eds.) *A correlation of Precambrian rocks in the British Isles,* 52-75. Geological Society of London Special Report, **6.**

Harrison, T.M. (1981) Diffusion of Ar in hornblende. *Contributions to Mineralogy and Petrology,* **78,** 324-331.

Harrison, T.M. (1983) Some observations on the interpretation of ^{40}Ar-^{39}Ar age spectra. *Isotope Geoscience,* **1,** 319-338.

Harrison, T.M. & McDougall, I. (1980) Investigations of an intrusive contact, northwest Nelson, New Zealand-II. Diffusion of radiogenic and excess Ar in hornblende revealed by ^{40}Ar-^{39}Ar age spectrum analysis. *Geochimica et Cosmochimica Acta,* **44,** 2005-2020.

Harrison, T.M. & Fitz Gerald, J.D. (1986) Exsolution in hornblende and it's consequences for ^{40}Ar-^{39}Ar age spectra and closure temperature. *Geochimica et Cosmochimica Acta,* **50,** 247-253.

Harrison, T.M., Duncan, I. & McDougall, I. (1985) Diffusion of Ar in Biotite: Temperature, Pressure and Compositional Effects. *Geochimica et Cosmochimica Acta,* **49,** 2461-2468.

Hart, S.R. (1964) The petrology and isotopic-mineral age relations of a contact zone in the Front Range, Colorado. *The Journal of Geology,* **72,** 493-525.

Hawthorne, H.C. (1981). The crystal chemistry of the amphiboles. *In,* Veblen, D.R. (ed.) *Amphiboles and Other Hydrous Pyriboles-Mineralogy,* Mineralogical Society of America, Reviews in Mineralogy, **9A,** 1-105.

Hutton, D.H.W. & Dewey, J.F. (1986) Palaeozoic terrane accretion in the western Irish Caledonides. *Tectonics,* **5,** 1115-1124.

Ineson, P.R. & Mitchell, J.G. (1979) K-Ar ages from the ore deposits and related rocks of the Isle of Man. *Geological Magazine,* **116,** 117-128.

Jager, E. (1965) Rb-Sr age determination on minerals and rocks from the Alps. *Science Terra,* **10,** 395-406.

Jager, E., Niggli, E. & Wenk, E. (1967) Rb-Sr Altersbestimmungen an Glimmern der Zentralapen. *Beitr Geol Karte Schweiz* **134,** 67.

Jagger, M.D., Max, M.D., Aftalion, M. & Leake, B.E. (1988) U-Pb zircon ages of basic rocks and gneisses intruded into the Dalradian rocks of Cashel, Connemara, western Ireland. *Journal of the Geological Society of London,* **145,** 645-648.

Javoy, M. (1977) Stable isotopes and geothermometry. *Journal of the Geological Society of London,* **133**, 609-636.

Jenkin, G.R.T. (1988) Stable isotope studies in the Caledonides of S.W. Connemara, Ireland. *Unpublished Ph.D. Thesis, University of Glasgow.*

Kanaris-Sotiriou, R. & Angus, N.S. (1976) The Currywongaun-Doughruagh syntectonic intrusion, Connemara, Ireland. *Journal of the Geological Society of London,* **132,** 485-508.

Kelley, S. (1988) The relationship between K-Ar ages, mica grainsizes and movement on the Moine Thrust Zone, NW Highlands, Scotland. *Journal of the Geological Society of London,* **145,** 1-10.

Kelley, S. & Turner, G. (1987) Laser-probe ^{40}Ar-^{39}Ar age profiles across single hornblende grains from the Giants Range Granite, northern Minnesota, USA. (Abstract). *Terra Cognita,* **7**, 285.

Kemp, A.J. & Leake, B.E. (1975) Two hydrous-rich aluminous hornblendes. *Mineralogical Magazine,* **40**, 308-311.

Kennan, P.S. & Murphy, F.C. (1987) Tectonically reset Rb-Sr system during Late Ordovician terrane assembly in Iapetus, western Ireland. *Geology,* **15,** 1155-1158.

Kennan, P.S., Feely, M. & Mohr, P. (1987) The age of the Oughterard Granite, Connemara, Ireland. *Geological Journal,* **22,** 273-280.

Kilburn, C., Pitcher, W.S. & Shackelton, R.M. (1965) The stratigraphy and origin of the Port Askaig Boulder Bed Series (Dalradian). *Geological Journal,* **4,** 343-360.

Krishnaswami, S. & Seidemann, D.E. (1988) Comparative study of ^{222}Rn, ^{40}Ar, ^{39}Ar and ^{37}Ar leakage from rocks and minerals: Implications for the role of nanopores in gas transport through natural silicates. *Geochimica et Cosmochimica Acta,* **52,** 655-658.

Kulp, J.L. & Engels, J. (1963) Discordance in K-Ar and Rb-Sr isotopic ages: *In.* Radiactive Dating, Vienna. *International Atomic Energy Agency,* **440**, 219-138.

Kuroda, Y., Hariya, Y., Suzuoki, T. & Matsuo, S. (1975) Pressure effect on water content of amphiboles. *Geophysical Research Letters,* **2**, 529-531.

Kuroda, Y., Yamada, T., Kobayashi, H., Ohmoto, Y., Yagi, M. & Matsuo, S. (1986) Hydrogen isotope study of the granitic rocks of the Ryoke Belt, Central Japan. *Chemical Geology, (Isotope Geoscience),* **58**, 283-302.

Layer, P.W., Hall, C.M. & York, D. (1987) The derivation of $^{40}Ar/^{39}Ar$ age spectra of single grains of hornblende and biotite by laser step-heating. *Geophysical Research Letters,* **14**, 757-760.

Leake, B.E. (1963) The location of the Southern Uplands Fault in Central Ireland. *Geological Magazine,* **100**, 420-423.

Leake, B.E. (1968) A catalog of analysed calciferous and subcalciferous amphiboles with their associated minerals. *Geological Society of America, Memoir,* **92.**

Leake, B.E. (1969) The origin of the Connemara migmatites of the Cashel District, Connemara, Ireland. *Quartlerly Journal of the Geological Society of London,* **125**, 219-276.

Leake, B.E. (1970) The fragmentation of the Connemara basic and ultrabasic intrusions. *In.* Newall, G & Rast, N. (eds.) *Mechanism of Igneous Intrusion,* Geological Journal Special Issue, **2**, 103-122.

Leake, B.E. (1978a) Granite emplacement: the granites of Ireland and their origin. *In* Bowes, D.R. & Leake, B.E. (eds.) *Crustal evolution in northwestern Britain and adjacent regions.* Geological Journal Special Issue, **10**, 221-248.

Leake, B.E. (compiler for the I.M.A.) (1978b) Nomenclature of amphiboles. *Mineralogical Magazine,* **42**, 533-563.

Leake, B.E. (1989) The metagabbros, orthogneisses and paragneisses of the Connemara complex, western Ireland. *Journal of the Geological Society of London,* **146**, 575-596.

Leake, B.E, Tanner, P.W.G. & Senior, A. (1981) The geology of Connemara (Map, scale 1:63,360), *University of Glasgow.*

Leake, B.E., Tanner, P.W.G., Singh, D. & Halliday, A.N. (1983) Major southward thrusting of the Dalradian rocks of Connemara, western Ireland. *Nature,* **305,** 210-213.

Leake, B.E., Tanner, P.W.G., Macintyre, R.M. & Elias, E. (1984) Tectonic position of the Dalradian rocks of Connemara and its bearing on the evolution of the Midland Valley of Scotland. *Transactions of the Royal Society of Edinburgh: Earth Sciences,* **75,** 165-171.

Leggo, P.J., Compston, W. & Leake, B.E. (1966) The geochronology of the Connemara granites and its bearing on the antiquity of the Dalradian Series. *Quarterly Journal of the Geological Society of London,* **122,** 91-118.

Long, L.E. & Lambert, R.St J. (1963) Rb-Sr isotopic ages from the Moine series. *in,* The British Caledonides. *(eds.)* Johnson, M.R.W. & Stewart, F.H. Edinburgh.

Macintyre, R.M., McMenamin, T. & Preston, J. (1975) K-Ar results from western Ireland and their bearing on the timing and siting of Thulean magmatism. *Scottish Journal of Geology,* **11,** 227-249.

Manning, J.R. (1974) Diffusion kinetics and mechanisms in simple crystals. *In,* Hofmann, A.W., Giletti, B.J., Yoder, H.S. & Yund, R.A. (eds.) *Geochemical Transport and Kinetics.* Carnegie Institute of Washington Publication, **634,** 3-13.

Matsuhisa, Y., Goldsmith, J.R. & Clayton, R.N. (1979) Oxygen isotope fractionation in the system quartz-albite-anorthite-water. *Geochimica et Cosmochimica Acta,* **43,** 1131-1140.

Max, M.D. & Inamadar, D.D. (1983) Detailed compilation magnetic map of Ireland and a summary of its deep geology. *Geological Survey of Ireland Report Series,* **R5 29.**

Max, M.D. & Riddihough, R.P. (1975) Continuation of the Highland Boundary Fault in Ireland. *Geology,* **3,** 206-210.

Max, M.D. & Ryan, P. (1975) The Southern Uplands Fault and its relation to the metamorphic rocks of Connemara. *Geological Magazine,* **112,** 610-612.

Mc Dougall, I. & Harrison, T.M. (1988). Geochronology and Thermochronology by the ^{40}Ar-^{39}Ar method. *Oxford University Press.* 212 pp.

Miller, J.A. & Brown, P.E. (1965) K-Ar age studies in Scotland. *Geological Magazine,* **102,** 106-134.

Mitchell, J.G. & Mohr, P. (1986) K-Ar systematics in Tertiary dolerites from West Connacht, Ireland. *Scottish Journal of Geology,* **22,** 225-240.

Mitchell, J.G. & Mohr, P. (1987) Carboniferous dikes of West Connacht, Ireland. *Transactions of the Royal Society of Edinburgh: Earth Sciences,* **78,** 133-151.

Moorbath, S., Bell, K., Leake, B.E. & McKerrow, W.S. (1968) Geochronological studies in Connemara and Murrisk, western Ireland. *In* Hamilton, E.I. & Farquar, R.H. (eds.) *Radiometric Dating for Geologists,* 259-258. Interscience, London.

Morris, W.A. & Tanner, P.W.G. (1977) The use of palaeomagnetic data to delineate the history of the development of the Connemara Antiform. *Canadian Journal of Earth Sciences,* **13,** 294-304.

Nitsch, K.H. (1970) Experimentelle Bestimmung der oberen Stabilitatsgrenze von Stilpnomelan. *Fortschr Mineral,* **47,** 48-49.

Norton, D. & Knight, J. (1977) Transport phenomena in hydrothermal systems: cooling plutons. *American Journal of Science,* **277,** 937-981.

Norwood, C.B. (1974) Radiogenic Ar diffusion in the biotite micas. *Unpublished Ph.D. Thesis, Brown University, Rhode Island, USA.*

O' Neil, J.R. (1986) Theoretical and experimental aspects of isotope fractionation. *In,* Valley, J.W., Taylor, H.P. & O' Neil, J.R. (eds.) *Stable Isotopes in High Temperature Geological Processes.* Mineralogical Society of America, Reviews in Mineralogy, **16,** 1-40.

O' Nions, R.K.,Smith, D.G.W.,Baadsgaard,H. & Morton, R.D. (1969) Influence of chemical composition on argon retentivity in metamorphic calcic amphiboles from South Norway. *Earth and Planetary Science Letters,* **5,** 339-345.

Onstott, T.C. & Peacock, M.W. (1987) Argon retentivity of hornblendes: A field experiment in a slowly cooled metamorphic terrane. *Geochimica et Cosmochimica Acta,* **51,** 2891-2903.

Pankhurst, R.J. & Pidgeon, R.T. (1976) Inherited isotope systems and the source region pre-history of early Caledonian granites in the Dalradian series of Scotland. *Earth and Planetary Science Letters,* **31,** 55-68.

Parsons, I., Rex, D.C., Guise, P. & Halliday, A.N. (1988) Argon loss by alkali feldspars. *Geochimica et Cosmochimica Acta,* **52,** 1097-1112.

Phillips, D. & Onstott, T.C. (1988) Argon isotopic zoning in mantle phlogopite. *Geology,* **16,** 542-546.

Phillips, W.E.A. & Sevastopoulo, G. (1986) The stratigraphic and structural setting of Irish mineral deposits. *In,* Andrew, C.J., Crowe, R.W.A., Finaly, S., Pennell, W.M. & Pyne, J.F. (eds), *The Geology and Genesis of Mineral Deposits in Ireland,* Irish Association of Economic Geology, 1-30.

Phillips, W.E.A., Graham, J.R. & Simon, J.B. (1983) Pre-Carboniferous evolution of the western continuation, in Ireland, of the Midland Valley of Scotland (abstract). *Transactions of the Royal Society of Edinburgh: Earth Sciences,* **75,** 299.

Pidgeon, R.T. (1969) Zircon U-Pb ages from the Galway granite and the Dalradian Connemara, Ireland. *Scottish Journal of Geology,* **5,** 375-392.

Potts, P.J. (1987) A Handbook of Silicate Rock Analysis. *Blackie & Son.* 622pp.

Purdy, J.W. & Jager, E. (1976) K-Ar ages on rock forming minerals from the Central Alps. *Memorie degli Istituti di Geologia e Mineralogia dell'Universita di Padova,* 30.

Rama, S.N.I. & Hart, S.R. (1965) Excess radiogenic argon in fluid inclusions. *Journal of Geophysical Research,* **70,** 509-511.

Robbins, G.A. (1972) Radiogenic argon diffusion in muscovite under hydrothermal conditions. *Unpublished M.Sc. Thesis, Brown University.*

Roddick, J.C. (1983) High precision intercalibration of ^{40}Ar-^{39}Ar standards. *Geochimica et Cosmochimica Acta,* **47**, 881-898.

Rogers, G., Dempster, T.J., Bluck, B.J. & Tanner, P.W.G. (1989). A high precision U-Pb age for the Ben Vurich granite: Implications for the evolution of the Scottish Dalradian Supergroup. *Journal of the Geological Society of London,* **146**, 789-798.

Ross, J.A. & Sharp, W.D. (1988) The effects of sub-blocking temperature metamorphism on the K-Ar systematics of hornblendes: 40Ar-39Ar dating of polymetamorphic garnet amphibolite from the Franciscan Complex, California. *Contributions to Mineralogy and Petrology,* **100**, 213-221.

Singh, D. (1984) The geochemical study of rocks SW of Clifden, Co. Galway, Connemara, western Ireland. *Unpublished Ph.D. thesis, University of Glasgow.*

Sisson, V.B. & Onstott, T.C. (1986) Dating blueshist metamorphism: A combined $^{40}Ar/^{39}Ar$ and electron microprobe approach. *Geochimica et Cosmochimica Acta,* **50,** 2111-2117.

Steiger, R.H. & Jager, E. (1977) Subcommission on geochronology: Convention on the use of decay constants in geo- and cosmochronology. *Earth and Planetary Science Letters,* **36,** 359-362.

Suzuoki, T. & Epstein, S. (1976) Hydrogen fractionation between OH-bearing minerals and water. *Geochimica et Cosmochimica Acta,* **40**, 1229-1240.

Tanner, P.W.G. & Dempster, T.J. (1988) Comment on "Tectonically reset Rb-Sr system during Late Ordovician terrane assembly in Iapetus, western Ireland." *Geology,* **16**, 762-763.

Tanner, P.W.G., Dempster, T.J. & Dickin, A.P. (1989) Time of docking of the Connemara terrane with the Delaney Dome Formation, western Ireland. *Journal of the Geological Society of London,* **146,** 389-392.

Tanner, P.W.G. & Shackelton, R.M.S. (1979) Structure and stratigraphy of the Daradian rocks of the Bennabeola area, Connemara, Eire. *In* Harris, A.L., Holland, C.H. & Leake, B.E. (eds.) *The Caledonides of*

the British Isles - reviewed. Geological Society of London Special Publication, 8, 243-256.

Treloar, P.J. (1985) Metamorphic conditions in central Connemara, Ireland. *Journal of the Geological Society of London,* **142**, 77-86.

Truesdall, A.H. (1974) Oxygen isotope activities and concentrations in aqueous salt solutions at elevated temperatures: consequences for isotope geochemistry. *Earth and Planetary Science Letters,* **23**, 387-396.

Veblen, D.R. (1981) Non-classical pyriboles and polysomatic reactions in biopyriboles. *In,* Veblen, D.R. (ed.) *Amphiboles and Other Hydrous Pyriboles-Mineralogy,* Mineralogical Society of America, Reviews in Mineralogy, **9A**, 189-236.

Veblen, D.R. & Burnham, C.W. (1978a) New biopyriboles from Chester, Vermont: I. Descriptive Mineralogy. *American Mineralogist,* **63**, 1000-1009.

Veblen, D.R. & Burnham, C.W. (1978b) New biopyriboles from Chester, Vermont: II. The crystal chemistry of jimthompsonite, clinojimthompsonite and chesterite, and the amphibole-mica reaction. *American Mineralogist,* **63**, 1053-1073.

Veblen, D.R. & Buseck, P.R. (1979) Chain-width order and disorder in biopyriboles. *American Mineralogist,* **64**, 687-700.

Verschure, R.H., Andriessen, P.A.M., Boelrijk, N.A.I.M., Hebeda, E.H., Maijer, C., Priem, H.N.A. & Verdurmen, E.A.T. (1980) On the thermal stability of Rb-Sr and K-Ar biotite systems: evidence from coexisting Sveconorwegian (ca 870 Ma) and Caledonian (ca 400 ma) biotites in SW Norway. *Contributions to Mineralogy and Petrology,* **74**, 245-252.

Wagner, G.A., Reimer, G.M. & Jager, E. (1977) Cooling ages derived by apatite fission-track, mica Rb-Sr and K-Ar dating: The uplift and cooling history of the Central Alps. *Memorie degli Istituti di Geologia e Mineralogia dell'Universita di Padova,* **30**, 30-27.

Wickham, S. (1988) Evolution of the lower crust. *Nature,* 333, 119-120.

Yardley, B.W.D. (1976) Deformation and metamorphism of Dalradian rocks and evolution of the Connemara cordillera. *Journal of the Geological Society of London,* **132,** 521-542.

Yardley, B.W.D. (1987) Discussion on geochemistry of Dalradian pelites from Connemara, Ireland: new constraints on kyanite genesis and conditions of metamorphism. *Journal of the Geological Society of London,* **144,** 679-680.

Yardley, B.W.D. (1989) The role of marbles in controlling metamorphic fluid flow in the Connemara Schists, Ireland. (abstract). *EOS,* **70,** 494.

Yardley, B.W.D., Barber, J.P. & Gray, J.R. (1987) The metamorphism of the Dalradian rocks of western Ireland in relation to tectonic setting. *Philisophical Transactions of the Royal Society of London, Series A,* **321,** 243-270.

Yardley, B.W.D., Vine, F.J. & Baldwin, C.T. (1982) The plate tectonic setting of NW Britain and Ireland in late Cambrian and early Ordovician times. *Journal of the Geological Society of London,* **139,** 455-463.

Yund, R.A. & Anderson, T.F. (1978) The effect of fluid pressure on oxygen isotope exchange between feldspar and water. *Geochimica et Cosmochimica Acta,* **42,** 235-239.